# Essays on Climate and Carbon Emissions : The EU Emissions Trading System and Renewable Energies

Mohammadehsan Eslahi

Université de Lille
École Doctorale SESAM
LEM – Lille Économie Management – UMR 9221
IÉSEG School of Management

# Essais sur le climat et les émissions de carbone : le système d'échange de quotas d'émission de l'UE et les énergies renouvelables

Thèse en vue de l'obtention du titre de docteur en sciences économiques

**Mohammadehsan ESLAHI**

Directeur de thèse :

Dr. Paolo MAZZA, HDR

Le 12 Décembre 2022

## Membres de jury

- **Directeur de thèse :**

Dr. Paolo MAZZA, HDR – Professeur, IÉSEG School of Management

- **Rapporteures :**

Dr. Anna CRETI, HDR – Professeur des universités, Paris Dauphine University-PSL

Dr. Maria-Eugenia SANIN, HDR – Maître de conférences, Université d'Évry–Université Paris-Saclay

- **Examinateurs :**

Dr. Jean-Philippe BOUSSEMART*, HDR – Professeur des universités, Université de Lille (*Président du jury)

Dr. Julien CHEVALLIER, HDR – Professeur des universités, Université Paris 8

Dr. Corrado DI MARIA – Professeur, Université d'East Anglia

# Acknowledgements

I would like to express my profound gratitude to my doctoral advisor, Dr. Paolo Mazza, for his availability, enthusiasm, approachability, flexibility and interest in my research career. This dissertation would not have been possible without his constant help, support and expert guidance.

I am extremely grateful to my thesis examination committee members for accepting the invitation to participate in my thesis defense meeting, and the precious time they took to evaluate my research work.

My gratitude also goes to all my university professors and school teachers in Iran and France, who generously provided me with scientific knowledge and expertise, and who taught me invaluable life lessons since I was seven years old. I would like to especially thank Dr. Shiva Zamani from my *alma mater*, Sharif University of Technology, whose constant encouragement and guidance intrigued me, as a math undergraduate student, to pursue graduate studies in Economics. I am also extremely appreciative of the opportunity given to me by Dr. Mohsen Mehrara at the University of Tehran to gain professional teaching experience before embarking on my Ph.D.

I would be remiss not to mention my colleagues, close friends and family members, especially my spouse, parents and young brothers, whose belief in me has kept my spirits and motivation high throughout the Ph.D. journey.

Last but not least, I gratefully acknowledge financial and logistic support from IÉSEG School of Management and the Institut Europlace de Finance (IEF).

To defenders of human rights in my home country. In honor of Woman, Life, Freedom.

# Résumé

La recherche scientifique a montré qu'il existe une relation directe entre le réchauffement climatique et l'émission de carbone et d'autres gaz à effet de serre. En ce qui concerne les pays européens, le développement de la production d'énergie électrique à partir des sources renouvelables et le système d'échange de quotas d'émission de l'Union européenne (EU ETS pour son abréviation en anglais) sont deux outils importants pour réduire les émissions de dioxyde de carbone ($CO_2$) et faire face au changement climatique. L'objectif principal de ce projet de recherche doctoral est d'identifier les facteurs explicatifs des émissions de $CO_2$ et d'explorer comment les principaux outils cités ci-dessus peuvent aider à réduire les émissions au niveau français et européen. La problématique centrale de la thèse consiste en plusieurs sous-questions de recherche, abordées dans quatre articles scientifiques connexes mais toutefois nettement distincts.

Le premier article répond à la question : « Compte tenu d'une augmentation ou d'une diminution de la production d'énergie renouvelable en France, quelle serait l'évolution prévue des émissions dans le secteur de l'électricité ? » et identifie la part optimale de chaque source dans le mix énergétique renouvelable pour minimiser les émissions prévues dans le secteur de l'électricité dans les scénarios de production d'électricité renouvelable plus élevée en France sur la période 2013-2021.

Le deuxième article adopte une approche interdisciplinaire de pointe basée sur l'apprentissage automatique pour caractériser l'impact des conditions climatiques sur les émissions horaires de $CO_2$ dans le système électrique français de janvier 2013 à décembre 2020. Les résultats de cet article devraient apporter une contribution importante à la littérature sur les facteurs déterminants des émissions de $CO_2$ dans le secteur de l'électricité et peuvent donner un aperçu de la sensibilité des émissions liées à l'énergie au changement climatique.

Le troisième article évalue l'efficacité environnementale des trois premières phases (2005-2019) de l'EU ETS pour réduire les émissions de $CO_2$ dans 248 régions socio-économiques des États membres de ce système. Considérant le début de chaque phase comme une intervention, cet article adopte une approche de modélisation prédictive avancée pour construire des émissions de $CO_2$ contrefactuelles pour chaque période post-intervention, et analyse, dans le temps et dans l'espace, l'effet de l'intervention en comparant les émissions réalisées avec des estima-

tions contrefactuelles.

Le quatrième article examine l'impact prédictif des conditions climatiques et de la demande d'électricité sur les prix spot horaires des quotas d'émission au cours des trois premières phases du système d'échange de quotas d'émission de l'Union européenne (2005-2019). Cette étude propose une méthodologie originale pour construire des indices de demande d'électricité et de climat à l'échelle européenne, et caractérise la relation entre ces indices et les prix des quotas d'émission. Cet article contribue à la littérature croissante sur les déterminants structurels des prix du carbone dans l'EU ETS et améliore notre compréhension de l'impact de la variabilité climatique sur la mesure de marché la plus importante pour réduire les émissions de $CO_2$ en Europe.

Dans l'ensemble, cette thèse contribue à la littérature sur l'efficacité environnementale de deux principaux outils pour réduire les émissions de $CO_2$ et faire face au changement climatique, c'est-à-dire la production d'énergie électrique à partir des sources renouvelables et le système d'échange de quotas d'émission de l'Union européenne, ainsi que la littérature sur les facteurs explicatifs de ces émissions en Europe.

# Contents

# List of Figures

# List of Tables

# Notations

**ALE:** Accumulated Local Effects
**$CO_2$:** Carbon Dioxide
**$CO_2$e:** $CO_2$ Equivalent
**CCS:** Carbon Capture and Sequestration
**CRE:** Climate-related Renewable Energy
**CV:** Coefficient of Variation
**EU:** European Union
**EUA:** European Union Allowances
**EU ETS:** European Union Emissions Trading System
**GDP:** Gross Domestic Product
**GHG:** Greenhouse Gas
**GVA:** Gross Value Added
**HER:** Hydro-ecoregions
**kWh:** Kilowatt-hour
**MW:** Megawatt
**NAP:** National Allocation Plan
**NUTS:** Nomenclature of Territorial Units for Statistics
**PV:** Photovoltaic Solar Energy
**RMSE:** Root-Mean-Square Error
**ROR:** Run-of-river Hydroelectricity
**W:** Wind Energy
**XGBoost:** Extreme Gradient Boosting

CHAPTER 1

# General Introduction

Anthropogenic greenhouse gas emissions are the predominant driver of climate change, with carbon dioxide ($CO_2$) emissions bearing the most responsibility for global warming. $CO_2$ emissions from energy use are one of the principal contributors to global climate change and represent almost 75% of all anthropogenic greenhouse gas emissions in the European Union (European Commission, 2021). Such emissions come under the influence of multiple climatic, social and economic factors, and are mainly rooted in the combustion of fossil fuels (e.g. coal, natural gas and petroleum) for electricity production, transportation, industrial manufacturing and agricultural purposes. Addressing climate change thus requires that $CO_2$ reduction and removal measures be taken urgently at national and international level. Carbon pricing (e.g. through carbon taxes and emissions trading systems) and renewable energy development are two major tools for climate change mitigation through reducing sources of carbon emissions.

Many countries worldwide have attempted to enact legislation or devise a mechanism for trading carbon contracts. The main argument for those considerations is that, excessive greenhouse gas emissions and their irreversible consequences for the environment cannot be prevented unless there are powerful (pecuniary) incentives for economic actors to promote emissions reductions. As such, application of the 'polluter pays' principle through putting a price on carbon dioxide ($CO_2$) and other greenhouse gases has found its place in the national and international environmental policies aimed at fighting global warming.

It has long been established by economists that carbon pricing through cap-and-trade systems is one of the most cost-effective ways to decarbonize the economy (Meckling et al., 2017). The European Union Emissions Trading System (hereinafter referred as the EU ETS) is the European Union's major market-based environmental scheme to combat climate change and its impacts under the Kyoto Protocol. Established in 2005, the scheme is the earliest and biggest international carbon market in the world, functioning on a cap-and-trade basis. An annually decreasing cap is set on the total amount of $CO_2$ or the equivalent amount of other notorious greenhouse gases (referred to as $CO_2$ equivalent and denoted by $CO_2e$) that can be emitted by

the installations covered by the system. Within the cap, installations buy emissions allowances (also called emissions certificates, carbon credits or carbon permits). The EU ETS is split into distinct trading periods or phases with their own specificities, of which three had drawn to a close by the end of 2020, and the fourth was well under way at the time of writing this dissertation.

Notwithstanding the fact that all sectors should be held accountable for reducing $CO_2$ emissions, the electricity sector is expected to play the lead role in the decarbonization of economy owing to its more pronounced ability to lower emissions in a cost and time-effective manner (Edenhofer, 2015; Rodrigues et al., 2020; Goh et al., 2018a; Karmellos et al., 2016). This justifies the domination of the EU ETS by firms involved in electricity generation (see Ahamada and Kirat, 2015). Development of renewable energy share of electricity production, leveraging carbon capture and sequestration (CCS) technologies in power plants, and increasing nuclear energy supply are three alternative methods for mitigating $CO_2$ emissions in the electricity sector (Brouwer et al., 2016). Among these options, renewable energy sources have been argued to be the cornerstone of $CO_2$ mitigation in the power sector (Rogelj et al., 2018), not only from an environmental point of view but also in the light of economic, social and political considerations (Waisman et al., 2019). Decarbonizion of the power sector, as a crucial factor in mitigating climate change, is a challenge responding to which requires, in the first place, an in-depth understanding of explanatory factors behind electricity generation-related emissions. Moreover, key questions about the "future" of electricity generation and alternative power generation technologies need to be understood by innovative methods that would possibly allow for a careful evaluation of the "past".

In light of the above considerations, this doctoral project attempts to link three strands of literature on climate change mitigation through reducing sources of carbon emissions. The first and broader strand is that of explanatory factors for greenhouse gas emissions, with a focus on energy-related emissions. More precisely, the present research examines how and to what extent climate impacts on the demand and supply of energy (notably electricity) translate into $CO_2$ emissions in France as well as the EU ETS zone.

The second strand is effectiveness analysis of the EU ETS and renewable energy development, as two main tools for reducing $CO_2$ emissions and dealing with climate change. In order to evaluate the environmental effectiveness of the EU ETS, this work capitalizes on the statistical structure of regional climate-emissions relationships to estimate counterfactual fossil fuel $CO_2$ emissions over the period following the beginning of the first three phases, and examines the impact of the trading scheme by comparing realized monthly emissions with counterfactual estimates across European socio-economic regions. As regards $CO_2$ emissions reduction from renewable energy, the present research characterizes the predictive impact of climate-related renewable electricity generation (i.e. wind, solar photovoltaic, and small-scale run-of-river hy-

droelectric power) on daily $CO_2$ emissions in the French electric power system and identifies, based on a counterfactual analysis, the optimal mix of renewable energy sources for minimizing emissions as well as electricity generation intermittency.

The third strand is that on carbon price drivers in the EU ETS. Although debatable, the price of emissions allowances traded on a carbon market is often used as a measure of the effectiveness of the market. Carbon price provides an economic signal to emitters of $CO_2$, and enables them to decide whether to lower their emissions, or continue emitting and paying for their emissions (World Bank, 2022). In this regard, it is extremely important to understand what drives fluctuations in permit prices. This dissertation aims to contribute to the growing body of literature on the structural determinants of carbon prices in the EU ETS by examining the predictive impact of climate conditions and electricity demand on hourly spot prices of emissions allowances during the first three phases of the scheme.

In summary, the key objective of this dissertation is to empirically disentangle the nexus between climate and carbon emissions in the provision of climate change mitigation policies in France and Europe. This central objective is divided into a number of sub-objectives that are addressed in four individual studies. All these essays were under consideration by peer-reviewed field journals at the the time of writing the dissertation.

The first essay, titled **"Climate-related renewable energy sources and carbon emissions: a machine learning-based investigation of electricity production in France"**, aims to characterize the predictive impact of electricity generation from climate-related renewable energy (CRE) sources (wind, solar photovoltaics, and small-scale run-of-river hydroelectricity) on daily $CO_2$ emissions in the French electric power sector over the 2013-2021 period. The study also identifies the optimal mix of CRE sources for minimizing predicted emissions and electricity generation intermittency under four counterfactual scenarios of increased CRE production in France over the study period.

In an attempt to extend the knowledge about driving factors for $CO_2$ emissions in the electricity sector, the second essay, titled **"Identifying climatic drivers of emissions from electricity production: Insights from a predictive modeling-based approach"**, characterizes climate impacts on hourly $CO_2$ emissions in the French electric power system over the 2013-2020 period.

The third essay, titled **"Mission Accomplished? An ex-post predictive evaluation of the effectiveness of the EU ETS in reducing regional fossil fuel carbon emissions"**, evaluates the effectiveness of the first three phases of the EU ETS in reducing monthly fossil fuel $CO_2$ emissions in European socio-economic regions. The study also examines the predictive usefulness of climate variables as potential drivers of regional fossil fuel $CO_2$ emissions across the EU ETS zone. This essay covers the period from 2005 to 2019, i.e. the first two phases and seven years of the third phase of the EU ETS.

The fourth essay, titled **"Can climate factors and electricity demand predict carbon emissions allowances prices? Evidence from the first three phases of the EU ETS"**, aims to contribute to the literature on determinants of allowances prices in the European carbon market, by examining the predictive impact of climate conditions and electricity demand on hourly spot prices of emissions allowances during the first three phases of the EU ETS. Similar to the third essay, this study covers the period from 2005 to 2019.

From a methodological point of view, the dissertation revolves, on a broad level, around the application of a cutting-edge machine learning algorithm in the energy and climate research– with a clear justification of the choice of methodology in each essay. That being the case, the contributions of the present work go beyond the mere application of machine learning. While adhering to the central theme of the dissertation, each essay addresses an original and clear-cut research problem, which is expected to be of sufficiently immediate interest to a broad range of scholars in the field of energy and environmental economics.

The essays are presented, in the form of complete manuscripts, in separate chapters. The chapters are grouped into two overarching sub-themes: climate and electricity production, and European Union Emissions Trading System. Essay 1 and Essay 2 are associated with the first theme, and address the interplay between climate and carbon emissions in the power sector in relation to renewable electricity production. Essay 3 and Essay 4 belong to the second theme and focus on the leading market-based framework for carbon trading in Europe. The use of hourly, daily and monthly data in different chapters ensures that the dynamics of the interrelation among climate factors, carbon emissions and key climate change mitigation tools at French and European level are investigated across multiple time scales.

The remaining part of the dissertation proceeds as follows. Individual essays are presented in the next four chapters. In light of the fact that the essays share the same predictive modeling technique and interpretation tools, content duplication in the methods section of the chapters was inevitable. Nevertheless, the studies rely on different methodological frameworks and address entirely distinct (yet related) research questions. The concluding part of the dissertation (Chapter 6) reiterates the central research theme, and highlights the significance of the findings and general policy implications.

CHAPTER 2

# Climate and Electricity Production: Renewables and Carbon Emissions

**Article Title:** "Climate-related renewable energy sources and carbon emissions: a machine learning-based investigation of electricity production in France" (Eslahi, 2022a)

**Abstract:** By means of a cutting-edge machine learning-based modeling technique, this study characterizes the predictive impact of electricity generation from climate-related renewable energy (CRE) sources (wind, solar photovoltaics, and small-scale run-of-river hydroelectricity) on $CO_2$ emissions in the French electric power sector over the 2013-2021 period. The results demonstrate that run-of-river hydroelectricity was the most important feature among the three CRE sources for predicting emissions, followed by wind energy. Empirical findings based on a counterfactual analysis also reveal that an increase in the share of energy from CRE sources would be associated with a statistically significant decrease in predicted emissions over the study period. Identification of the optimal mix of CRE sources for minimizing predicted emissions under four counterfactual scenarios of increased CRE production reaffirms the greater relative share of run-of-river hydroelectricity and wind energy within the mix. The findings of this research have two major implications for renewable energy development and management in France. First, they provide fresh quantifiable evidence on the conceptual premise that replacing carbon-intensive energy sources with renewable ones reduces $CO_2$ emissions from electricity generation. Second, they cast a new light on the relative importance of each CRE source with regard to emissions reduction in the electricity sector.

**Keywords:** Climate-related Renewable Energy, $CO_2$ Emissions, Electricity Production, Counterfactual Analysis, Machine Learning

## 2.1 Introduction

Carbon dioxide ($CO_2$) emissions from energy use are one of the principal contributors to global climate change and represent almost 75% of all anthropogenic greenhouse gas emissions in the European Union (European Commission, 2021). Such emissions come under the influence of multiple climatic, social and economic factors, and are mainly rooted in the combustion of fossil fuels for electricity production, transportation, industrial and agricultural purposes. Notwithstanding the fact that all sectors should be held accountable for reducing $CO_2$ emissions, the electricity sector is expected to play the lead role in the decarbonization of economy owing to its more pronounced ability to lower emissions in a cost and time-effective manner (Edenhofer, 2015; Rodrigues et al., 2020; Goh et al., 2018a; Karmellos et al., 2016). Development of renewable energy share of electricity production, leveraging carbon capture and sequestration (CCS) technologies in power plants, and increasing nuclear energy supply are three alternative methods for mitigating $CO_2$ emissions in the electricity sector (Brouwer et al., 2016). Among these options, renewable energy sources have been argued to be the keystone of $CO_2$ mitigation (Rogelj et al., 2018), not only from an environmental point of view but also in the light of economic, social and political considerations (Waisman et al., 2019).

Being a pioneer in the battle against global warming, the European Union already has a significantly lower emissions intensity of electric power generation than other large economies such as the United States, Japan, China, India and Australia (International Energy Agency (IEA), 2020). The French electricity sector is comparatively even more decarbonized (Shirizadeh and Quirion, 2021), largely due to the considerable share of nuclear energy generation.[1] The 2020 report of the electricity transmission system operator of France[2] asserts that, in 2019, emissions from electricity production in the country reached approximately 21.16 million tonnes of $CO_2$ equivalent ($CO_2$e), accounting for 4.8% of total emissions (Réseau de Transport d'Électricité (RTE), 2020).

In alignment with France's carbon neutrality by 2050 objective set by the National Assembly in 2019 under the title "Ecological Emergency and Climate Crisis" (Ministère de la Transition écologique, 2019), $CO_2$ emissions from electricity production need to be further reduced either by retrofitting CCS to existing power plants, building new nuclear reactors or increasing the share of renewable electricity (Débat national sur la transition énergétique, 2013; Shirizadeh and Quirion, 2021). Two analyses conducted by the French Environment and Energy Management Agency (ADEME) have shown that the development of a new generation of nuclear energy would not be economically efficient for the French electricity system, and that in an ideal scenario, electricity generation from renewable sources would constitute the largest share–up to

[1] France has the world's largest share of electricity production by nuclear power, with about 70% of its electricity being generated from nuclear energy (World Nuclear Association, 2022).

[2] RTE–Réseau de Transport d'Électricité (`https://www.rte-france.com/`)

95%–of electricity generation in France over the next few decades (see ADEME, 2015, 2018). It is in this regard that the nexus between $CO_2$ emissions in the electric power sector and various forms of renewable electricity generation needs careful analysis.

Figure 2.1 depicts the share of total electric energy produced by main fuel categories in France from 2013 to 2020. From this figure, two main observations are clear. First, while the share of the fossil fuel mix (i.e. fuel oil, coal and gas in aggregate) in total electricity production has only slightly decreased over this period (from 7.91% in 2013 to 7.51% in 2020), the shares of total electricity production from fuel oil and coal have decreased, respectively, from 0.69% and 3.61% in 2013 to 0.34% and 0.28% in 2020. This decrease has been accompanied by an increase in the share of total electricity production from gas (from 3.61% in 2013 to 6.89% in 2020), indicating a shift in the fossil fuel mix. Second, the share of the wind-solar-hydroelectric energy mix in total electricity production has increased from 17.44% in 2013 to 23.55% in 2020. Accompanied by a decrease in the share of total electricity produced from nuclear energy (from 73.34% in 2013 to 66.99% in 2020), this latter signifies a change in the composition of non-fossil fuel mix, i.e. a gradual transition from nuclear to wind-solar-hydro electricity.[3]

The relationship between $CO_2$ emissions and renewable energy production and consumption has attracted growing interest from scholars in the fields of environmental and energy economics. Adopting a range of conventional methodological approaches to time series and panel data analysis, numerous studies have examined this relationship over different time periods and with different geographical scopes. As suggested by Sharif et al. (2020), existing research in this area can be broadly categorized into five groups according to their findings: studies that indicate a unidirectional causality relationship from renewable energy use to $CO_2$ emissions (Farhani and Shahbaz, 2014; Jaforullah and King, 2015; Özbuğday and Erbas, 2015; Apergis and Payne, 2015; Long et al., 2015; Bilgili et al., 2016; Bulut, 2017; Liu et al., 2017b; Khan et al., 2018; Salazar-Núñez et al., 2021); those arguing that $CO_2$ emissions influence the production and consumption of renewable energy (Sadorsky, 2009; Menyah and Wolde-Rufael, 2010; Shafiei and Salim, 2014; Leitão, 2014; Jebli and Youssef, 2015; Paramati et al., 2017); works suggesting a bidirectional causal association between $CO_2$ emissions and the production and consumption of renewable energy (Apergis et al., 2010; Dogan and Seker, 2016; Dong et al., 2017; Waheed et al., 2018); the ones that imply no causal link between $CO_2$ emissions and the production and consumption of renewable energy (Qi et al., 2014; Bento and Moutinho, 2016; Jebli et al., 2016; Saidi and Mbarek, 2016; Boontome et al., 2017; Jebli and Youssef, 2017; Liu et al., 2017a); and finally studies with mixed or indecisive results on this relationship (Zeb et al., 2014; Apergis and Payne, 2014; Sebri and Ben-Salha, 2014; Ang and Su, 2016; Bélaïd

[3]While there is an ongoing dispute over the optimal relative shares of renewable energy resources and nuclear power in electricity generation in France (Shirizadeh and Quirion, 2021), the share of electricity generation by nuclear power is to be reduced to 50% by 2035 as per government policy (World Nuclear Association, 2022).

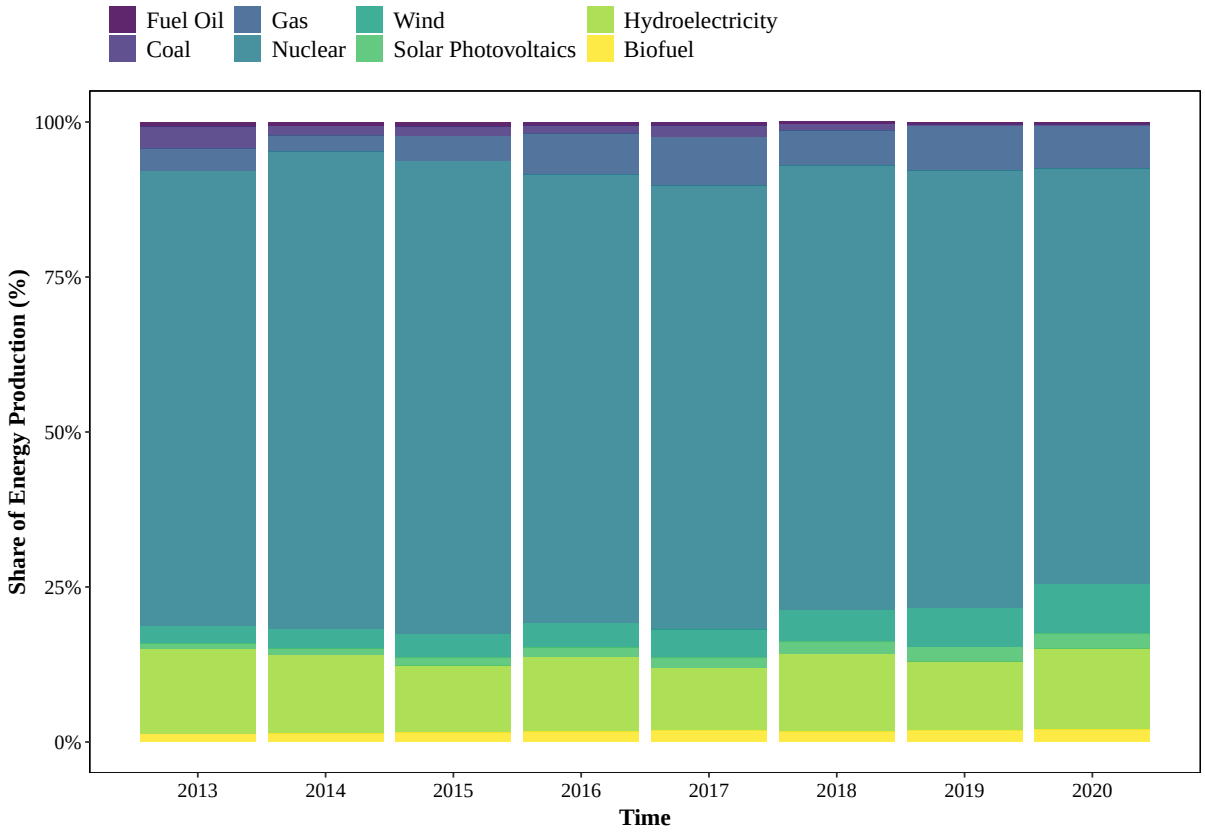


Figure 2.1: Share of total electric energy produced by main fuel categories in France from 2013 to 2020 (Data source: `https://opendata.reseaux-energies.fr/`).

and Youssef, 2017; Sinha et al., 2018; Adams and Nsiah, 2019; Chen et al., 2019; Sharif et al., 2020; Rodrigues et al., 2020).

All the empirical studies listed above have based their analyses upon annual data, with the exception of the work of Sharif et al. (2020), which makes use of monthly data disaggregated from annual series. As emphasized by Adewuyi and Awodumi (2017), this body of literature remains inconclusive on the topic, both at single and multi-country levels. Interestingly enough, some studies with the same geographical scope (i.e. region) and overlapping study periods have yielded inconsistent results (see for example the works of Sebri and Ben-Salha (2014), Dong et al. (2017) and Liu et al. (2017b) on BRICS countries). This highlights the need for the recognition of the specificity of different research settings, and calls for further investigation into the matter, possibly by means of more advanced methodologies that are better fitted to answering the question on the nexus between renewable electricity production and $CO_2$ emissions.

From a methodological point of view, a potential drawback of most existing empirical studies in this area is the fact that they seek (positive or negative) causal links between $CO_2$ emissions and renewable energy production and consumption, while relying on methods and/or measures that are inherently inappropriate for drawing such causal inferences. For instance, commonly used emissions indicators (like the ones used in the present study; see Section 2.2.1)

are typically estimated by considering the contribution of the combustion of carbon-based fuels (such as coal, gas and various fuel oil products) to $CO_2$ emissions, and on the assumption that renewable energy sources (also referred to as clean energy sources) or even biofuels[4] create little to no $CO_2$. Hence, the change in renewable energy production and consumption cannot necessarily be considered to be the "cause" of the change in the values of such emissions variables. Moreover, prior research has often used composite emissions indicators that may embrace, but are not necessarily limited to emissions from electricity production (see for example Apergis et al., 2010; Adams and Nsiah, 2019; Dogan and Seker, 2016). This variable choice could possibly lead to the omitted-variable bias in statistical models, and question the validity of any causal claim about the relationship between $CO_2$ emissions and renewable energy production and consumption.

With reference to the points raised above, it could be argued that most causal claims in this context can be considered indications of correlation, precedence (Leamer, 1985) or temporal relation (Granger and Newbold, 2014) based on a set of theoretical assumptions about the data. One way to overcome this problem of causal interpretation involves the use of advanced predictive modeling techniques to characterize the "predictive impact" (distinguished from causal impact) of renewable energy production on $CO_2$ emissions. Instead of attempting to make a theoretically unsupported causal claim, this alternative approach helps provide answers to questions of great practical importance such as (1) Given an increase or decrease in renewable energy production, what would be the predicted change in emissions in the electricity sector? and (2) Under a higher-renewable-electricity-production scenario, what would be the optimal share of each source in the the renewable energy mix for minimizing predicted emissions in the electricity sector? This proposed predictive framework derives its legitimacy from the fact that an increase in the share of the package of clean energy sources is expected to result in a decrease in the share of high-carbon energy sources as main drivers of $CO_2$ emissions.

On another note, while some existing works have considered the effect of specific types of renewable energy sources like hydroelectricity (Long et al., 2015; Khan et al., 2018) or wind and solar energies (Qi et al., 2014) on $CO_2$ emissions, there has been a general trend towards viewing renewable energy as a single variable and overlooking potential disparities between different types of renewable energy in terms of their impact on $CO_2$ emissions. More importantly, little attention has been paid to the extent to which different renewable energy sources can be influenced by climate change. In order to fill these gaps, the present study distinguishes between constituent sources of the renewable energy block, and focuses further on the role of "climate-related" renewable energy sources in reducing $CO_2$ emissions from electricity pro-

[4]See for example the description of $CO_2$ emissions data from the methodology section of BP Statistical Review of World Energy (https://www.bp.com/en/global/corporate/energy-economics/statistical-review-of-world-energy/using-the-review/methodology.html.html#accordion_carbon)

duction. Consistent with the definition of Engeland et al. (2017), climate-related renewable energy (hereafter referred to as CRE) sources are represented in this paper by wind, solar photovoltaics, and small-scale run-of-river hydroelectricity energy sources. What justifies the appellation "climate-related renewable energy" is the fact that the availability and sporadicity of these resources are dependent on climate factors such as air temperature, wind speed, solar radiation, precipitation, and river runoff. Consequently, among different sources of energy, CRE sources are most affected by climate change.

The main purpose of this work is to characterize the predictive impact of CRE electricity production on $CO_2$ emissions in the French electric power system over the 2013-2021 period. To do so, a machine learning-based empirical modeling framework is employed to first evaluate the importance of different types of CRE electricity production in predicting $CO_2$ emissions, and specify the marginal effect of each CRE source on the predicted outcome of the model. Through a counterfactual analysis, the predictive impact of CRE production potential (as proxied by climate-derived energy indicators) on $CO_2$ emissions is then quantified. This analysis reveals if exploiting the full potential of CRE sources, which is equivalent to an increase in the share of CRE electricity production and a decrease in the share of non-CRE sources, would result in significantly lower predicted emissions over the study period. Finally, four counterfactual scenarios of increased CRE production over the study period are explored, and the optimal mix of CRE sources for minimizing predicted emissions under each scenario is identified. This analysis is complemented by the identification of the optimal CRE mix that would minimize the intermittency of CRE electricity production in France from 2013 to 2021. By limiting the scope of the study to $CO_2$ emissions from electricity production (instead of using composite or total emissions indicators), the present research undermines the possibility of the precedence of emissions over renewable electricity generation. This provides a sound conceptual basis for delineating the predictive effect of CRE electricity production on $CO_2$ emissions.

The contributions of this study to the literature on the relationship between carbon emissions and electricity production from renewable and non-renewable energy sources are manifold. First, while most of the existing studies in this area are based on annual or monthly data, the present research capitalizes on emissions and energy indicators data with a high (i.e. daily) temporal resolution. Indeed, in a similar context to that of the present study, using data with coarse temporal resolution (e.g. annual or monthly) leads to disregard of intra-monthly or intra-annual variability and intermittency of renewable energy sources that depend on climate (see Gernaat et al., 2021). Second, in the attempt to model the relationship between carbon emissions and electricity production from renewable and non-renewable energy sources, this paper considers all categories and subcategories of fuel types. This kind of fine-grained analysis has rarely been undertaken in the energy economics literature. Third, to the best of the author's knowledge, this study is the first to quantify the predictive impact of the (unexploited) CRE

electricity production potential on energy-related $CO_2$ emissions. To this should be added the methodological contributions towards counterfactual estimation of $CO_2$ emissions based on realizable CRE electricity production, particularly in terms of the weighting scheme for energy indicators (see Section 2.2.2.2). Fourth, by decomposing the CRE package into its constituent elements (i.e. wind, solar photovoltaics, and run-of-river hydroelectricity) rather than viewing it as a unified block, the present study is able to determine the optimal share of individual sources within the package that minimizes counterfactual predictions of $CO_2$ emissions under near-feasible to idealistic hypothetical CRE production scenarios. This scenario-based approach has important implications for renewable energy development and management in France, since it provides evidence of the relative importance of each CRE source with regard to emissions reduction in the electricity sector. Finally, in the evaluation of the predictive impact of CRE electricity production on $CO_2$ emissions under the proposed scenarios, this research takes into account the intermittency of CRE sources that is motivated by the natural variability of climate factors. So far, this striking aspect of renewable electricity generation has been largely neglected in the studies on the dynamics between emissions and renewable energies.

The remainder of this paper is structured as follows. Section 2.2 describes data and methodology of the analysis. The results are presented in Section 2.3. A discussion of the study limitations and a few suggestions for future research are provided in Section 2.4. The paper concludes with a summary of the key findings and the empirical contributions made to the existing literature (Section 2.5).

## 2.2 Materials and Methods

### 2.2.1 Data

#### 2.2.1.1 Realized $CO_2$ emissions and electricity production by different fuel types

Consolidated and final half-hourly data on $CO_2$ equivalent emissions from electricity production (g/kWh), and the electrical power production by different fuel types (MW) in France from January 1, 2013 to August 31, 2021 were obtained from the éCO2mix data set, provided by the electricity transmission system operator of France and available on the Open Data Réseaux Énergies (ODRÉ) platform.[5] The emissions indicator represents $CO_2$ emissions released only by the consumption of primary fuel used in power plants, and is calculated based on the relative contribution of fuel oil, coal, gas and biofuel energy sources to $CO_2$ emissions. For the sake of this study and consistent with the nature of emissions data, cross-border physical power exchange (with England, Spain, Italy, Switzerland, Germany and Belgium) and the power con-

[5] `https://opendata.reseaux-energies.fr/`. This platform is a subdivision of the open platform for French public data (`https://www.data.gouv.fr/`)

sumed by pumps in pumped-storage hydroelectricity systems were disregarded. Furthermore, in light of methodological considerations, the analysis was restricted to non-negative values of power production, and negawatts (negative megawatts), if any, were set to zero. The original data were aggregated to average daily values,[6] and all power values in MW were converted to energy values in kWh. Table 2.1 presents the the summary statistics for the original emissions and energy indicators used for empirical modeling (hereafter referred to as "realized" emissions and energy indicators).

Table 2.1: Summary statistics of realized daily emissions and energy indicators over the study period (from January 1, 2013 to August 31, 2021) based on the data provided by the electricity transmission system operator of France. $CO_2$ emissions values are expressed in grams (g). The measurement unit of the electric energy produced by different fuel types is kWh.

| Emissions/Energy Indicator | Mean | Max | Min | SD |
|---|---|---|---|---|
| $CO_2$ Emissions per kWh | 46.45 | 124.06 | 8.56 | 22.84 |
| Fuel Oil (Combustion Turbine) | 674,858 | 20,340,000 | 0 | 1,125,804 |
| Fuel Oil (Cogeneration) | 3,081,020 | 8,260,000 | 725,000 | 1,814,021 |
| Fuel Oil (Other) | 2,527,667 | 59,987,500 | 48,500 | 4,374,613 |
| Coal | 20,267,562 | 137,553,500 | 0 | 24,757,978 |
| Gas (Combustion Turbine) | 649,438 | 11,748,000 | 0 | 1,635,438 |
| Gas (Cogeneration) | 29,434,352 | 78,129,500 | 4,609,500 | 24,688,399 |
| Gas (Combined Cycle Turbine) | 47,794,491 | 138,265,500 | 0 | 40,036,372 |
| Gas (Other) | 1,906,760 | 14,620,500 | 312,000 | 1,687,226 |
| Nuclear | 1,057,000,000 | 1,458,000,000 | 530,400,000 | 166,199,782 |
| Wind | 70,972,076 | 321,939,000 | 3,475,500 | 54,964,062 |
| Solar Photovoltaics | 25,356,374 | 75,390,000 | 1,288,000 | 15,205,422 |
| Hydroelectricity (Run-of-river) | 113,731,842 | 190,018,500 | 34,160,000 | 35,640,184 |
| Hydroelectricity (Lake) | 45,365,080 | 117,566,500 | 6,776,500 | 19,626,978 |
| Hydroelectricity (Pumped-storage) | 16,000,279 | 41,715,000 | 1,621,500 | 7,322,262 |
| Biofuel (Waste) | 11,637,540 | 15,270,000 | 6,078,000 | 1,524,737 |
| Biofuel (Biomass) | 6,151,799 | 11,123,000 | 2,792,000 | 1,572,375 |
| Biofuel (Biogas) | 5,918,516 | 8,558,500 | 2,904,000 | 1,401,570 |

In addition to energy indicators, time-based features (i.e. year and month of the year) were created with integer encoding[7] and included in the empirical model as numerical control vari-

[6]This aggregation is necessary to ensure consistency in sampling frequency across the different data sets used in this study.

[7]The use of integer encoding is permitted since the categories have a natural ordering.

ables to account for possible year and month seasonality information in the data. The ultimate data set used for empirical modeling includes 3165 daily observations (from January 1, 2013 to August 31, 2021) with 19 independent variables (consisting of 17 energy indicators and 2 time-based features), and the natural logarithm[8] of $CO_2$ emissions per kWh of electricity generated as the response variable.

#### 2.2.1.2 CRE electricity production estimates derived from climate variables

Climate variables such as air temperature, wind speed, solar radiation, precipitation, and river runoff can be transformed into potential renewable energy indicators by means of physical or statistical models or a combination of both. Numerical climate models for estimating CRE production potential are useful for delineating important climate-driven changes in the energy sector both in the short and the long term.[9]

By Using a combination of physical and statistical models and considering the available installed energy capacity, the Copernicus Climate Change Service (C3S) at the European Centre for Medium-Range Weather Forecasts (ECMWF)[10] has provided a set of energy indicators for Europe derived from gridded reanalysis data on climate variables (Hersbach et al., 2020). This data set serves as a critical reference for evaluating the quality of climate-to-energy conversion models. The present study makes use of gridded and aggregated data over France on daily onshore wind, solar photovoltaics, and run-of-river hydroelectricity energy indicators from this collection (Ho et al., 2020; Saint-Drenan et al., 2018) for the period between January 1, 2013 and August 31, 2021.

The estimated energy indicators derived from climate variables are used as proxies for energy production "potential", and therefore referred to as "realizable" energy indicators further on in this paper. Indeed, they are assumed to represent the level of CRE electricity production that could be attained given the climate conditions of the study area (represented by the set of grid points within the area) over the period of interest.[11] Table 2.2 presents the the summary statistics for these energy indicators.

Figure 2.2 compares the distributions of original and estimated CRE indicators over the study period. A comparison of the respective medians in each panel of Figure 2.2 demonstrates a difference between the location of realized and realizable energy indicators. The significance of this location shift is further assessed using a non-parametric statistical test.

The results of the paired Wilcoxon signed-rank test (Wilcoxon, 1992; Conover, 1999) in-

[8]This transformation is necessary for empirical modeling purposes, i.e. to avoid potential negative predicted values of the response variable. Predicted emissions are back-transformed for the presentation and visualization of results.

[9]See Engeland et al. (2017) for a review of the foundations of such models, and a summary of the studies on the nexus between climate variability and renewable electricity production.

[10]`https://cds.climate.copernicus.eu/`

[11]This assumption, however, is subject to some limitations that are discussed in more detail in Section 2.4.

Table 2.2: Summary statistics of realizable daily climate-related renewable energy indicators over the study period (from January 1, 2013 to August 31, 2021) based on the data provided by the Copernicus climate change service (C3S). The realizable electric energy which could be generated by each fuel type is expressed in kWh.

| Energy Indicator | Mean | Max | Min | SD |
|---|---|---|---|---|
| Wind | 76,968,009 | 342,734,701 | 4,364,166 | 58,676,724 |
| Solar Photovoltaics | 29,833,555 | 58,314,090 | 1,865,264 | 13,638,494 |
| Hydroelectricity (Run-of-river) | 116,866,214 | 184,264,440 | 42,334,890 | 32,351,424 |

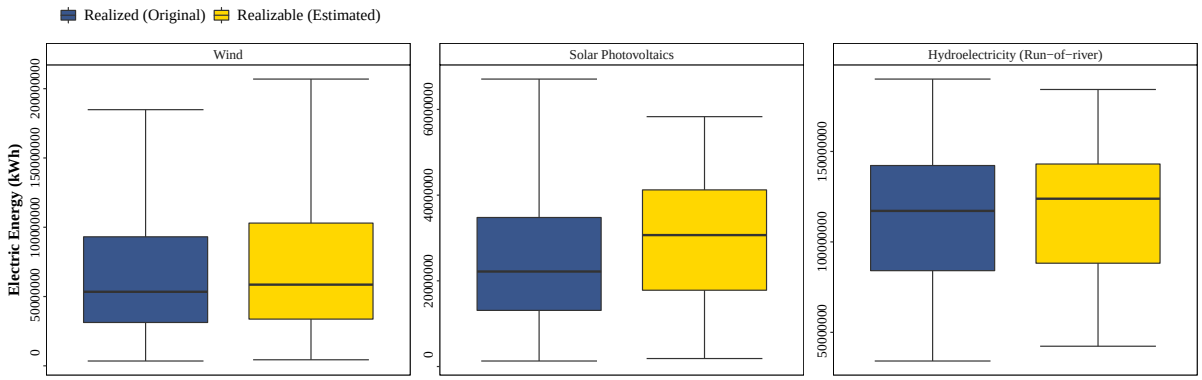


Figure 2.2: Compact box plots of realized (original) and realizable (estimated) CRE indicators over the study period. Note: The upper (lower) whisker extends from the hinge to the largest (smallest) value no further than 1.5 times the interquartile range. Data points beyond the whiskers are removed from the plot for the sake of better visualization.

dicate that the median of the population of differences between estimated (model-derived) and original CRE indicators is greater than zero in all three cases ($p < 0.01$). From an empirical point of view, it thus seems perfectly legitimate to consider the so-called realizable energy indicators derived from climate variables as proxies for the CRE electricity production potential.

## 2.2.2 Methodology

### 2.2.2.1 Empirical modeling of $CO_2$ emissions from electricity production based on various fuel types

In order to empirically model (learn) the relationship between $CO_2$ emissions and the electric energy produced by different fuel types over the study period, stochastic Extreme Gradient Boosting (XGBoost) algorithm of Chen and Guestrin (2016) has been utilized.[12] XGBoost is

[12]As with any other predictive model, XGBoost does not in itself imply "causal" relationships between variables. In this regard, by no means does the present modeling framework suggest that a change in low-carbon (in particular CRE) electricity production directly causes a change in $CO_2$ emissions. Indeed, in the calculation of emissions indicator in the éCO2mix data set, the contribution of low-carbon energy sources (nuclear, wind, solar photovoltaics, and hydroelectricity) has been considered equal to zero. Hence, such sources cannot directly "drive" emissions by definition. That being said, an increase in the share of nuclear and renewable energy sources inevitably translates into a decrease in the share of high-carbon energy sources as main drivers of $CO_2$ emissions.

a cutting-edge, speedy and highly performant decision-tree-based ensemble machine learning algorithm that can provide accurate predictions of a response variable by integrating the estimates obtained from a number of base models (trees). This predictive tool can model complex nonlinear relationships without assumptions about the data distribution, and is unsusceptible to multicollinearity. In its most general form, the tree ensemble model of the XGBoost algorithm that uses $K$ trained trees to predict the value of the response variable for a given data set with $N$ data points and $p$ features (predictors) $\{(x_i, y_i) \,|\, i = 1, ...N, x_i \in \mathbb{R}^p, y_i \in \mathbb{R}\}$ can be expressed as

$$\hat{y}_i = \hat{f}(x_i) = \sum_{k=1}^{K} g_k(x_i) \quad g_k \in \mathscr{F} \tag{2.1}$$

where $\mathscr{F} = \{g(x) = w_{q(x)}\}\,(q : \mathbb{R}^p \to J, w \in \mathbb{R}^J)$ is the space of regression trees, $q$ is the structure of each individual (independent) tree that maps an observation to the corresponding leaf score $w$, and $J$ is the total number of leaves in the tree (Chen and Guestrin, 2016).

Each regression tree starts with a root node and is grown to a specific depth (i.e. the longest path from the root node to a leaf) by repeatedly splitting the training data based on all or some of the features in the feature space. This process results in a tree with a root node, a number of internal nodes (each of which split data points by one feature), and some leaves to which prediction scores (weights) are assigned. The ultimate predicted value of the response variable for a given observation is obtained by taking the sum of all the scores in the relevant leaves of individual trees. As proposed by Chen and Guestrin (2016), the choice of splitting points and the assignment of prediction scores in XGBoost are done by means of an improved and more regularized version of gradient boosting technique, in such a way as to minimize loss of an objective function that is composed of training loss and regularization (to avoid overfitting). Mathematically speaking, the tree building algorithm is reliant upon the minimization of

$$\mathscr{L} = \sum_{i=1}^{N} L(\hat{y}_i, y_i) + \sum_{k=1}^{K} \Omega(g_k) \tag{2.2}$$

where

$$\Omega(g_k) = \gamma J_k + \frac{1}{2}\lambda \sum_{j=1}^{J_k} w_{j,k}^2$$

Here, $L$ is a loss (cost) function (i.e. squared error, by default) and measures the difference between original values of the response variable $y_i$ and the predicted values $\hat{y}_i$ (Chen and Guestrin, 2016). $J_k$ and $w_{j,k}$ are the number of leaves and the prediction score assigned to the

In this regard, a change in low-carbon electricity production is expected to be associated with a change in emissions. This is exactly where an empirical modeling framework like the one used here proves useful to characterize the "predictive" relationship between $CO_2$ emissions and electricity production from different fuel types (including low-carbon ones).

$j$-th leaf of the $k$-th regression tree, respectively. The parameter $\gamma$ is the minimum loss reduction required to further split the leaf node, and $\lambda$ is the L2 regularization on the prediction scores. These two, along with a number of tree-related parameters (together called hyperparameters of the model), cannot be estimated from data and need to be specified a priori.

In order to further minimize overfitting[13] and find the best model specification, the present study combines extensive grid search hyperparameter tuning with repeated n-fold cross-validation ($n = 5$ with 5 repetitions). The metric used to evaluate the model performance for each hyperparameter configuration is the root-mean-square error (RMSE). There are 2592 variations in the hyperparameter search space and each variation is evaluated using repeated 5-fold cross validation with 5 repetitions, resulting in a total number of $2592 \times 25$ tree ensemble models to be trained and evaluated. The hyperparameter configuration that results in the minimum average RMSE across all folds is selected as the best tune. Possible hyperparameter values are determined mainly on the basis of recommendations of Boehmke and Greenwell (2019) and Thakur (2020). Table 2.3 presents the hyperparameter configurations used for evaluating tree ensemble models.

Table 2.3: Hyperparameter configurations used for evaluating tree ensemble models

| Hyperparameter | Range | Default Value | Selected Values for Tuning |
|---|---|---|---|
| $\gamma$ | [0,∞) | 0 | {0.1,1,10} |
| $\eta$ | [0,1] | 0.3 | {0.05,0.1,0.2,0.3} |
| Maximum Depth | {1..∞} | 6 | {3..8} |
| Minimum Child Weight | [0,∞) | 1 | {7,10,20} |
| Column Sample by Tree | (0,1] | 1 | $\{\frac{6}{19}, \frac{10}{19}, \frac{14}{19}\}$ |
| Sub-sample | (0,1] | 1 | {0.3,0.5} |

Here, $\eta$ is the learning rate (also called shrinkage parameter), which shrinks prediction scores to prevent overfitting. $\gamma$ is the minimum loss reduction required to make a further split on a node of a given tree. Increasing $\gamma$ leads to a more conservative algorithm. The maximum depth parameter controls the number of terminal nodes in a a tree, and increasing its value makes the model more complex and more prone to overfitting. Minimum child weight determines the minimum sum of instance weight (hessian) required in a child node of a tree. A higher minimum child weight provides more conservative results. The column sample by tree parameter controls the fraction of columns (features) used for constructing each tree. Sub-sampling of columns takes place once for every tree constructed. Using values less than 1 for this parameter

[13] Although this study takes preventative measures to reduce overfitting, the reader's attention is drawn to the fact that overfitting should not, in principle, be cause for concern in the context of modern machine-learning models such as decision trees and ensemble methods. Belkin et al. (2019) show that modern (and complex) algorithms with near-perfect fit in training may still exhibit strong performance on unseen data.

leads to a more conservative algorithm. The sub-sample parameter determines what fraction of data should be used to build trees in every boosting iteration. Using values less than 1 for this parameter leads to "stochastic" boosting, distinguished from "regular" boosting (which makes use of all points to grow a tree). In this analysis, the number of trees used for boosting is set to 50 and 100. In addition, the hyperparameter $\lambda$ is kept at the default value of 1.

It should be noted that the utilized algorithm is safeguarded against likely temporal auto-correlation in the data for two reasons. First, the data are divided, in a random manner, into training and validation data sets during the repeated 5-fold cross-validation process. Second, using stochastic boosting (as opposed to regular boosting) makes the algorithm randomly select (without replacement) a proportion of the training data at each iteration. Therefore, the likelihood of neighboring observations being used by the algorithm at each iteration is very negligible.

Once the the model with the best tune is obtained from hyperparameter optimization, the "importance" of CRE sources in predicting emissions is calculated using the permutation feature importance algorithm with the RMSE ratio as the importance measure (Breiman, 2001; Fisher et al., 2019; Molnar, 2020), and 1000 repetitions. Permutation with repetition is performed with the aim of constructing the null distribution of importance measures. In its simplified form, the feature importance measure of a feature $p$ can be mathematically expressed as

$$\text{Feature Importance}_p = \frac{\text{RMSE}(y_i, \hat{f}(x_i^{perm:p}))}{\text{RMSE}(y_i, \hat{f}(x_i))} \quad (x_i \in \mathbb{R}^p; y_i \in \mathbb{R}) \tag{2.3}$$

where $x_i^{perm:p}$ is the $i^{\text{th}}$ instance with the $p^{\text{th}}$ feature replaced by a randomly sampled value, without replacement, from another instance. Being based on resampling without replacement, the permutation feature importance algorithm of Fisher et al. (2019) allows for conducting a permutation test with the null hypothesis that the importance of feature $p$ is 1:

$$H_0 : \text{Feature Importance}_p = 1 \tag{2.4}$$

If the $p^{\text{th}}$ feature is not important in the prediction, one should expect that the values for its feature importance measure be around 1. In point of fact, the proposed permutation test provides a framework for computing confidence intervals and p-values from resampling without replacement, and allows for determining statistical significance of a feature's importance.

As a complement to the features' importance evaluation, the influence of CRE electricity production on the prediction of the tree ensemble model is evaluated and visualized using mean-centered accumulated local effects (ALE) (Apley and Zhu, 2020). In machine learning, the ALE of a feature at a certain value is interpreted as the main effect of the feature at that value compared to the average prediction of the data (Molnar, 2020). By aggregating the calculated

effects at different values, ALE plots–as unbiased alternatives to partial dependence plots–are hence able to show the (possibly nonlinear) relationship between the response variable and a given input feature. In mathematical terms, the mean-centered[14] ALE of a continuous feature $p$ at a given value $x$ is estimated as

$$\hat{f}_{p,ALE}(x) = \hat{\tilde{f}}_{p,ALE}(x) - \frac{1}{N}\sum_{i=1}^{N}\hat{\tilde{f}}_{p,ALE}(x_p^{(i)}) \tag{2.5}$$

where

$$\hat{\tilde{f}}_{p,ALE}(x) = \sum_{l=1}^{l_p(x)}\frac{1}{n_p(l)}\sum_{i:x_p^{(i)}\in N_p(l)}\left[\hat{f}(z_{l,p}, x_{\setminus p}^{(i)}) - \hat{f}(z_{l-1,p}, x_{\setminus p}^{(i)})\right]$$

To estimate $\hat{\tilde{f}}_{p,ALE}(x)$, the distribution of the feature of interest $p$ is divided into a number of intervals (grids) denoted by $N_p(l)$, with $n_p(l)$ being the number of feature points that lie within the interval $N_p(l)$. The inner sum adds up the "effects" of all data points within such an interval (i.e. the differences in predictions, if the value of the feature of interest is replaced with the starting and end points of the given interval, namely $z_{l-1,p}$ and $z_{l,p}$). This sum is then divided by the number of feature points in this interval to obtain the average difference of the predictions for this interval. Finally, the outer sum accumulates the average effects across all intervals up to and including the interval $l_p(x)$ to which $x$ belongs (Apley and Zhu, 2020; Molnar, 2020). In order to define the aforementioned intervals, the present study makes use of the percentiles of the distribution of features. A distinct advantage of this choice is that each interval will contain the same number of data points. However, in this approach the length of intervals used for the calculation of ALE may not be the same.

#### 2.2.2.2 Counterfactual estimation of $CO_2$ emissions based on realizable CRE electricity production

Once the predictive relationship between $CO_2$ emissions and electricity production from different fuel types is learned by the empirical model, original (realized) electricity production indicators are replaced with new conjectural values, and predictions of counterfactual emissions are generated from the model. The objective of this section is to describe a hypothetical yet achievable scenario, in which the maximum possible electric energy is generated from climate variables of the study area at a given time point, and the share of energy from non-CRE sources is reduced on a pro rata basis. Analyzing such a scenario is the first step towards quantifying the effect of increased share of CRE electricity production on predicted $CO_2$ emissions.

On a given day $t$, if the realizable value of a CRE source is greater than its corresponding

[14] Mean-centering the ALE plot makes the average effect over the data be zero.

realized value, the former is used as the new energy indicator and the difference between the realizable and realized values is regarded as the "unexploited" electricity production potential. Otherwise, the indicator is kept at the realized value, assuming that the potential for CRE electricity production has already been fully exploited. New counterfactual shares of CRE sources in the total electricity production are calculated based on the new energy indicators. In the next step, new counterfactual shares of non-CRE sources are calculated in such a way as to keep the total electricity production at the original level. This method of share reallocation guarantees a pro rata contribution of each non-CRE source to electricity production in the new setting. In other words, an increase in the share of the CRE package is counterbalanced by a proportional decrease in the share of each source in the non-CRE package.[15] In formal notation,

$$\text{Share}_{i,t}^{(\text{new})} = \text{Share}_{i,t}^{(\text{old})} \times \frac{1 - \sum_j \text{Share}_{j,t}^{(\text{new})}}{\sum_i \text{Share}_{i,t}^{(\text{old})}} \tag{2.6}$$

where

$$\begin{aligned}
\text{Share}_{i,t}^{(\text{old})} &= \frac{\text{Energy}_{i,t}^{(\text{old})}}{\sum_{\mathscr{S}} \text{Energy}_t}, \\
\text{Share}_{j,t}^{(\text{new})} &= \frac{\text{Energy}_{j,t}^{(\text{new})}}{\sum_{\mathscr{S}} \text{Energy}_t}, \\
\text{Energy}_{j,t}^{(\text{new})} &= \max\left(\text{Energy}_{j,t}^{(\text{realized})}, \text{Energy}_{j,t}^{(\text{realizable})}\right)
\end{aligned}$$

The superscripts (new) and (old) characterize new conjectural and original (realized) values, respectively. In addition, $i \in \mathscr{S} \setminus \{\text{W}, \text{PV}, \text{ROR}\}$, $j \in \{\text{W}, \text{PV}, \text{ROR}\}$, and $\mathscr{S}$ is the set of all energy indicators. W, PV and ROR denote wind, solar photovoltaics and run-of-river hydroelectricity, respectively. For non-CRE sources, new energy indicators are then calculated by multiplying their corresponding new share by the original sum of electricity production by different fuel types:

$$\text{Energy}_{i,t}^{(\text{new})} = \text{Share}_{i,t}^{(\text{new})} \times \sum_{\mathscr{S}} \text{Energy}_t \tag{2.7}$$

To test whether there is statistically significant difference between the locations of counterfactual and observed emissions in this scenario, the non-parametric Wilcoxon signed-rank test is used. The null hypothesis of this test is that the median difference between pairs of counterfactual and observed emissions is greater than or equal to zero. The rejection of the null hypothesis leads to the conclusion that, with the same level of total electricity production, increasing the

[15] While in this proposed framework the relative share of nuclear energy (as the main source of electricity in France) in the non-CRE package remains unaltered (with a still higher share of other sources in the non-CRE package), policy concerns are mainly included in the direct substitution of CRE sources for nuclear energy and the likely exclusion of nuclear power plants in the future.

share of energy from CRE sources (i.e. exploiting their full potential) decreases $CO_2$ emissions from electricity production.

#### 2.2.2.3 Characterizing the optimal mix of CRE sources for minimizing predicted $CO_2$ emissions under different production scenarios

In another attempt to specify the effect of CRE electricity production on predicted $CO_2$ emissions, different CRE production scenarios–from near-realistic to ambitious–are investigated and the optimal mix of CRE sources for minimizing emissions under each scenario is identified. Such scenarios would have been realized had the CRE electricity capacity been higher over the study period. Indeed, this analysis provides an overview of the relative importance of each CRE source (wind, solar photovoltaics and run-of-river hydroelectricity) within the CRE package with regard to the reduction of predicted $CO_2$ emissions.

With this aim and following the methodology of François et al. (2016), new CRE indicator daily series from Section 2.2.2.2 are normalized so that the mean production of each source equals the mean total daily electricity production over the study period (the same notation as above):

$$\text{Energy}_{j,t}^{(\text{normalized})} = \frac{\text{Energy}_{j,t}^{(\text{new})}}{\langle \text{Energy}_{j,t} \rangle} \times \langle \sum_{\mathscr{S}} \text{Energy}_t \rangle \tag{2.8}$$

where $\langle\rangle$ is the temporal mean operator. In this framework, a CRE mix electricity production can be described as a weighted sum of the three normalized CRE indicator series:

$$\text{Energy}_{CRE,t}(\zeta) = \zeta \sum_j \alpha_j \text{Energy}_{j,t}^{(\text{normalized})} \quad (\alpha_j \geq 0, \sum_j \alpha_j = 1) \tag{2.9}$$

where $\alpha_j$ is the share of the $j$-th CRE source in the CRE mix (package), and $\zeta$ is the ratio between the average energy produced by the CRE energy mix and the average total electricity production over the study period:

$$\zeta = \frac{\langle \text{Energy}_{CRE,t} \rangle}{\langle \sum_{\mathscr{S}} \text{Energy}_t \rangle} \tag{2.10}$$

If $\zeta = 1$, the mean daily CRE electricity production equals the mean daily total electricity production (i.e. the CRE electricity production is, on average, equal to the total electricity production over the study period). If $\zeta < 1$, a fraction of the total electricity production can, on average, be fulfilled by the CRE mix over the entire period. For the sake of this study, four hy-

pothetical CRE electricity production scenarios with $\zeta = 0.25, 0.5, 0.75$ and 1 are considered.[16] For each scenario, all different combinations of wind, solar photovoltaics and run-of-river hydroelectricity in the CRE mix (with each share $\alpha_j$ ranging from 0 to 1 in increments of 0.05) are used to construct new CRE indicators. This results in 231 unique configurations of the CRE mix for each value of $\zeta$. Under a specific scenario and for each configuration, the shares of non-CRE sources are reallocated following the same approach as described in Section 2.2.2.2, and the empirical model introduced in Section 2.2.2.1 is utilized for generating predictions of counterfactual emissions. For a given scenario, the configuration that minimizes predicted mean daily $CO_2$ emissions over the study period is selected as the optimal CRE mix for emissions reduction.

Moreover, in order to account for the intermittency of CRE electricity production that is driven by the natural variability of climate factors (Seyedhashemi et al., 2021), the coefficient of variation (i.e. the ratio of the standard deviation to the mean) of the normalized daily CRE mix is calculated for each of the above-mentioned 231 configurations. The configuration that minimizes the coefficient of variation (hereafter denoted as CV) over the study period is selected as the optimal CRE mix for reducing intermittency. This additional analysis is offered to compare the optimal mix of CRE sources for minimizing $CO_2$ emissions under different production scenarios and the optimal mix of CRE sources for reducing problems of intermittency.[17]

All the analyses and data visualization in this study have been carried out in R software environment (R Core Team, 2020; Kuhn, 2008; Molnar et al., 2018; Hamilton and Ferry, 2018).

## 2.3 Results

### 2.3.1 Influence of CRE electricity production on the prediction of $CO_2$ emissions

Among all hyperparameter configurations for evaluating the tree ensemble models (see Section 2.2.2.1), the configuration with the hyperparameter values shown in Table 2.4 proved to minimize average RMSE across all folds (average RMSE$= 0.062$; average $R^2 = 0.986$), hence selected as the best tune.

The model with this optimal hyperparameter configuration was used as the base model for statistical analyses and prediction purposes of this study. The results of the permutation feature importance algorithm for the three CRE indicators based on the best empirical model are

[16] To be as realistic as possible, the present study sets the upper bound of $\zeta$ to 1. This means that scenarios with mean daily CRE electricity production exceeding the original mean daily total electricity production over the study period are not considered.

[17] The CV depends only on the shares of wind, solar photovoltaics and run-of-river hydroelectricity in the CRE mix, and is independent of the production scenario. Consequently, the optimal CRE mix for reducing intermittency is calculated once, regardless of the value of $\zeta$.

Table 2.4: Optimal hyperparameter configuration of the tree ensemble model

| Hyperparameter | Best Tune |
|---|---|
| $\gamma$ | 0.1 |
| $\eta$ | 0.1 |
| Maximum Depth | 7 |
| Minimum Child Weight | 10 |
| Column Sample by Tree | $\frac{14}{19}$ |
| Sub-sample | 0.5 |
| Number of Trees | 100 |

presented in Table 2.5. Here, the importance of each feature is measured by calculating the increase in the model's prediction error (in terms of the RMSE ratio) at each repetition, when the values of that feature are shuffled (Molnar, 2020). A given CRE indicator is "important" for the prediction of emissions, if permuting its values increases the model RMSE (i.e. the model is reliant on the feature for the prediction). The CRE indicator is unimportant if permuting its values leaves the model RMSE unaltered (i.e. the feature is ignored by the model for the prediction).

Table 2.5: Permutation feature importance of CRE sources in predicting $CO_2$ emissions (number of repetitions = 1000).

| Feature | Importance (RMSE Ratio) | | |
|---|---|---|---|
| | 5th Percentile | Median | 95th Percentile |
| Wind | 1.171104 | 1.181664 | 1.192710 |
| Solar Photovoltaics | 1.007700 | 1.009709 | 1.011769 |
| Hydroelectricity (Run-of-river) | 1.252940 | 1.268573 | 1.282155 |

For all CRE indicators, the value 1 is outside the 90% confidence interval for feature importance estimates. This concludes that wind, solar photovoltaics and run-of-river hydroelectricity features are all important for the prediction of emissions resulting from the generation of electrical power at the 0.1 significance level (see Equation 2.4). Among the three CRE indicators, run-of-river hydroelectricity proves to be the most important feature for predicting emissions, followed by wind energy. The importance of solar photovoltaics feature is only marginal, since the 5th, 50th and 95th percentiles of the distribution of RMSE ratio for this feature are close to 1. This finding acts as an early indicator of the level of importance of each CRE source for emissions reduction in France.

The influence of each CRE source on the prediction of emissions by the best model is further

assessed by calculating ALE values. Figure 2.3 presents ALE plots of wind, solar photovoltaics and run-of-river hydroelectricity features. In basic terms, multiple panels of this figure illustrate how the model predictions change–compared to the average prediction of the data–for different values of each CRE indicator.

As a first observation, the ALE curve is monotonically non-increasing for all CRE indicators.[18] This means that the prediction decreases or remains constant, compared to the average prediction, with increasing CRE electricity production–a finding consistent with expectations that renewable energy sources can contribute to the reduction of carbon emissions.[19] For wind, solar photovoltaics and run-of-river hydroelectricity features, the prediction of $CO_2$ emissions remains approximately constant in intervals below the 30th, 70th and 13th percentile (corresponding to 34898000, 31780500, and 66610500 kWh of electrical energy produced), and above 99th, 92nd and 98th percentile (corresponding to 256266500, 50565500, and 178323000 kWh of electrical energy produced), respectively. Compared to the case of wind and run-of-river hydroelectricity features, the ALE function of the solar photovoltaics feature is constant on larger intervals. Furthermore, the range of change in the ALE of solar photovoltaics (i.e. as the feature increases from the its minimum value to the maximum value) is relatively smaller than those of wind and run-of-river hydroelectricity features (0.009 for solar photovoltaics, compared to 0.076 for wind and 0.075 for run-of-river hydroelectricity). This is another important finding in the understanding of the significance of each CRE source for reducing emissions that are associated with the generation of electrical power.

### 2.3.2 Estimated counterfactual $CO_2$ emissions based on realizable CRE electricity production

Using new conjectural energy indicators constructed from realizable CRE electricity production (see Section 2.2.2.2), the best model can generate counterfactual estimates of $CO_2$ emissions, i.e. emissions that would have been realized provided that the full potential of CRE sources for electricity production had been exploited. Figure 2.4 compares observed (realized) and estimated counterfactual daily emissions based on new energy indicators in France from January

[18] Although interval-wise effects are accumulated to construct a smooth ALE curve, the effects are estimated locally using different data points. Therefore, one should be cautious when interpreting the effect across intervals (Molnar, 2020).

[19] Special caution must be taken when evaluating and interpreting the predictive impact of individual low-carbon power generation technologies on $CO_2$ emissions in the electricity sector. A climate-driven increase (decrease) in the share of a given CRE source may not necessarily be counterbalanced by a decrease (increase) in the share of high-carbon energy sources (coal, fuel oil, gas and biofuel). For instance, an increase (decrease) in the share of solar photovoltaics due to greater (smaller) availability of solar resources may be offset by a decrease (increase) in the share of other non-polluting energy sources (e.g. nuclear, hydroelectricity, etc.) and not necessarily fossil-fuel fired electricity generation, hence leaving emission levels unaltered. A full discussion of the elasticity of inter-fuel substitution between different CRE sources, between nuclear and CRE sources, and between different fossil fuels and CRE sources lies beyond the scope of this study.

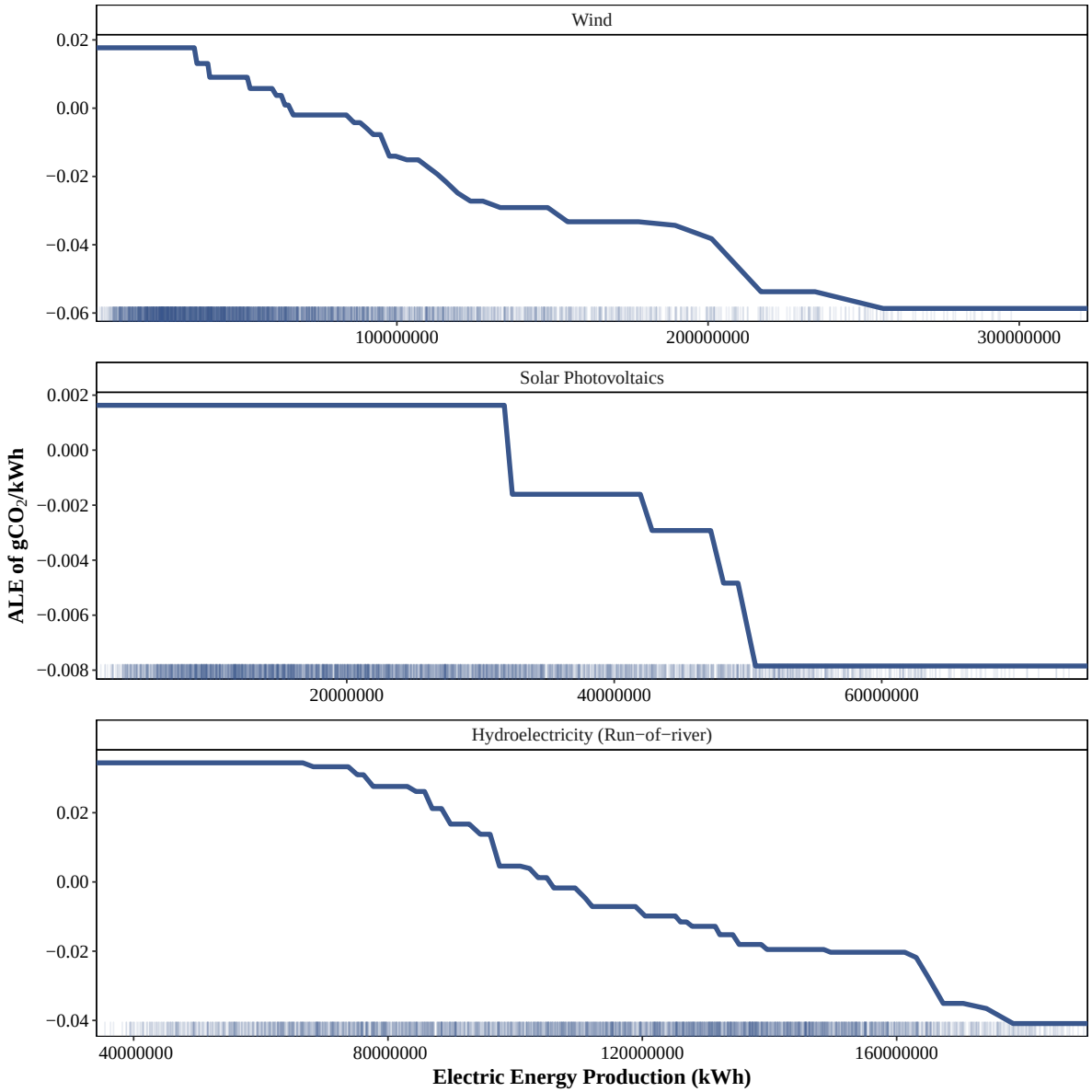


Figure 2.3: Mean-centered accumulated local effects (ALE) of CRE sources in predicting $CO_2$ emissions over the study period. The distribution of data points for each feature is displayed on the margin of horizontal axis.

1, 2013 to August 31, 2021.

The percentage difference between estimated counterfactual and observed daily emissions (calculated as [estimated counterfactual emissions−observed emissions)/observed emissions] $\times 100$) ranges from $-20.15$ to 19.91, with the average percentage difference being $-1.13$. This result highlights that exploiting the full potential of climate variables for electricity production would have, on average, resulted in 1.13% reduction in predicted $CO_2$ emissions in France over the study period. The distribution of the difference between estimated counterfactual and observed emissions over the entire study period is illustrated in Figure 2.5.

The null hypothesis of the non-parametric Wilcoxon signed-rank test (i.e. the median dif-

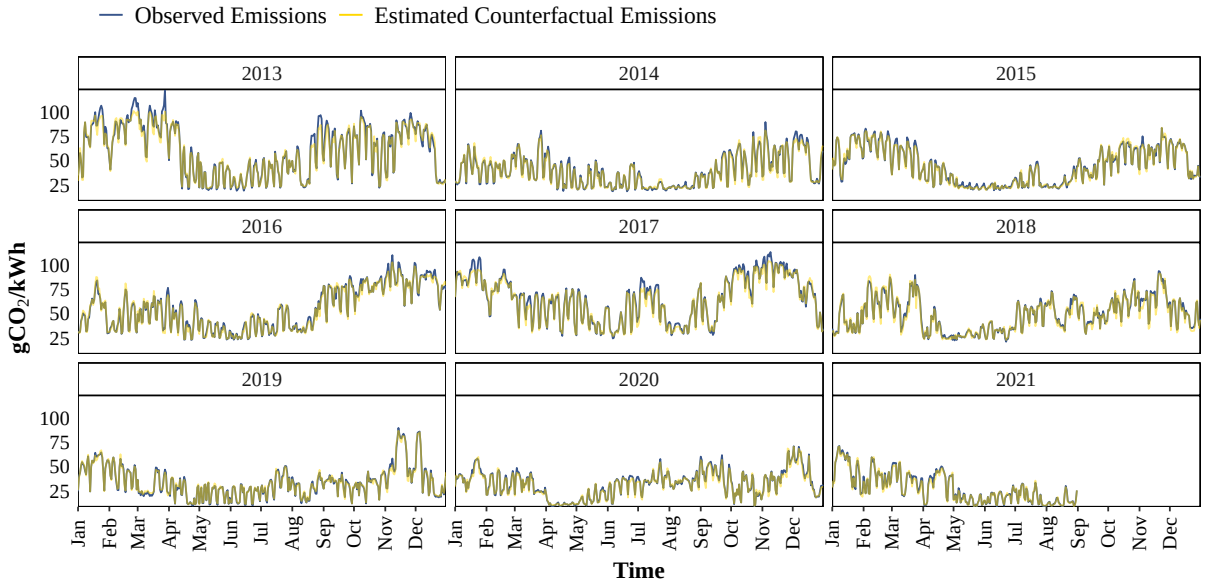


Figure 2.4: Observed (realized) and estimated counterfactual daily emissions based on realizable CRE electricity production over the study period. For visualization purposes, data for each year are presented in a separate panel.

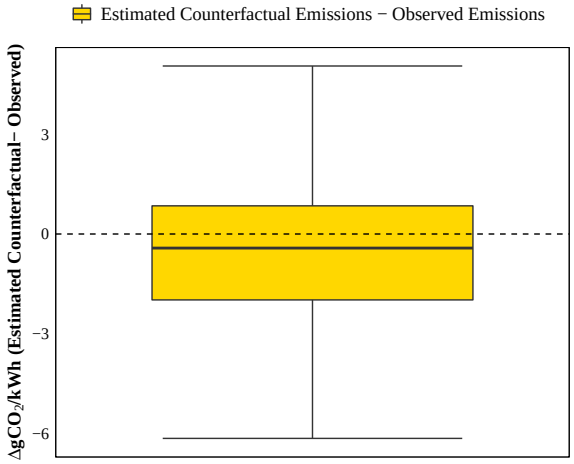


Figure 2.5: Box plot of the difference between estimated counterfactual emissions (based on realizable CRE electricity production) and observed emissions over the study period. Note: The upper (lower) whisker extends from the hinge to the largest (smallest) value no further than 1.5 times the interquartile range. Data points beyond the whiskers are removed from the plot for the sake of better visualization.

ference between pairs of counterfactual and observed emissions is greater than or equal to zero) is rejected at the 0.01 significance level, indicating that an increase in the share of energy from CRE sources (under a scenario where the maximum possible electric energy is generated from climate variables) would have been associated with a statistically significant decrease in $CO_2$ emissions from electricity production over the study period.

### 2.3.3 Optimal mix of CRE sources for minimizing predicted $CO_2$ emissions under different production scenarios

This section presents the results of the analysis of the four electricity production scenarios outlined in Section 2.2.2.3. Under each scenario, counterfactual estimates of $CO_2$ emissions (generated by the base empirical model) are compared with observed emissions.

The first scenario corresponds to the situation where the mean daily CRE electricity production equals 25% of the mean electricity production over the study period ($\zeta = 0.25$). The empirical $\zeta$ based on the realized and realizable CRE electricity production (as defined in Sections 2.2.1.1 and 2.2.1.2) over the study period is 0.144 and 0.158, respectively. In other words, the CRE electricity production satisfied, on average, 14.4% of the total electricity production over the study period in reality. Had the full potential of CRE sources been exploited over the same period, this ratio would have risen to 15.8%. From these observations, it is clear that the first scenario is the most realistic and feasible among the four proposed scenarios. Figure 2.6 compares observed (realized) and estimated counterfactual daily emissions under the first scenario from January 1, 2013 to August 31, 2021.

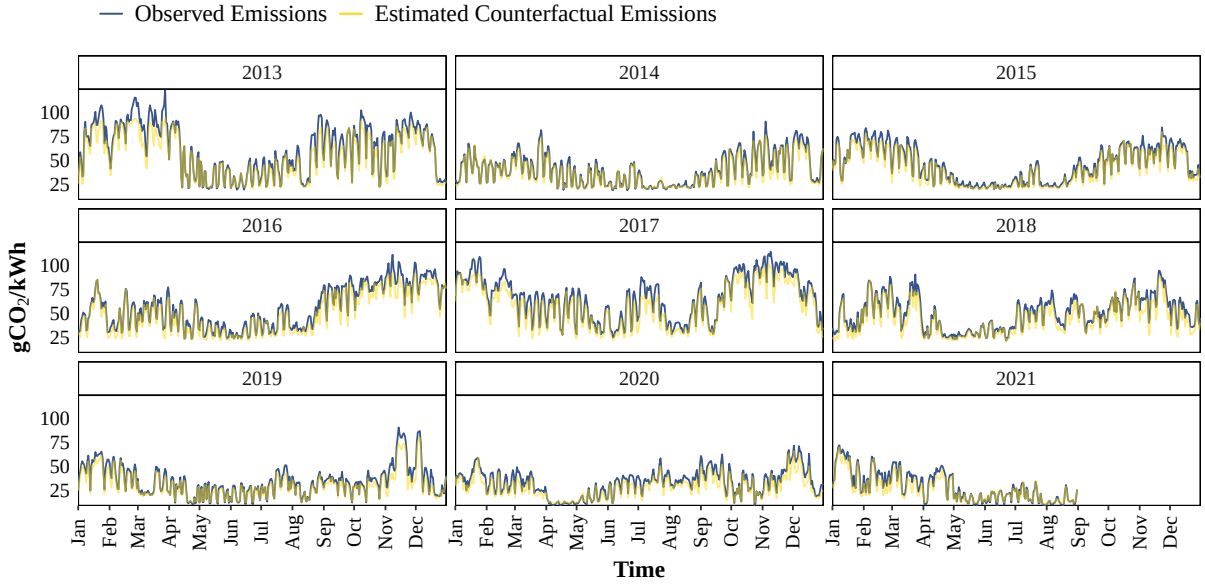


Figure 2.6: Observed (realized) and estimated counterfactual daily emissions over the study period under the first production scenario ($\zeta = 0.25$). For visualization purposes, data for each year are presented in a separate panel.

The percentage difference between estimated counterfactual and observed daily emissions for $\zeta = 0.25$ ranges from $-36.07$ to 35.69, with the average percentage difference being $-9.56$. This suggests that, under the first hypothetical CRE electricity production scenario, daily $CO_2$ emissions would have, on average, decreased by 9.56%.

The second scenario corresponds to the situation where the mean daily CRE electricity production equals 50% of the mean electricity production over the study period ($\zeta = 0.5$). Figure 2.7 compares observed (realized) and estimated counterfactual daily emissions under the second scenario from January 1, 2013 to August 31, 2021.

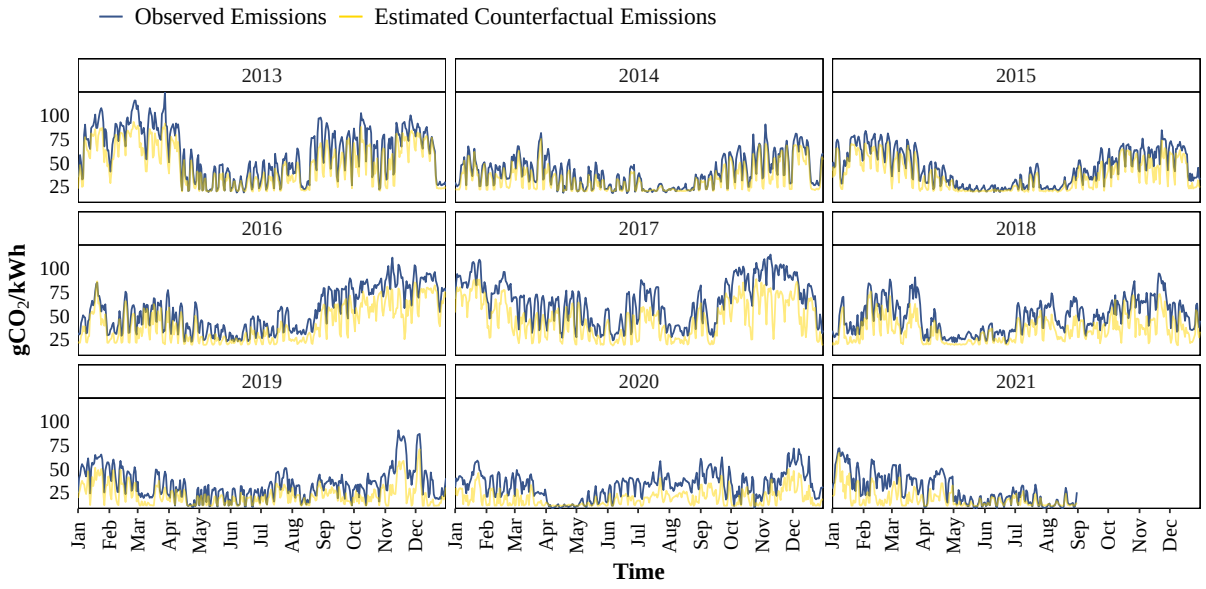


Figure 2.7: Observed (realized) and estimated counterfactual daily emissions over the study period under the second production scenario ($\zeta = 0.5$). For visualization purposes, data for each year are presented in a separate panel.

The percentage difference between estimated counterfactual and observed daily emissions for $\zeta = 0.5$ ranges from $-78.34$ to 36.25, with the average percentage difference being $-24.93$. This suggests that, under the second hypothetical CRE electricity production scenario, daily $CO_2$ emissions would have, on average, decreased by 24.93%.

The third scenario corresponds to the situation where the mean daily CRE electricity production equals 75% of the mean electricity production over the study period ($\zeta = 0.75$). Figure 2.8 compares observed (realized) and estimated counterfactual daily emissions under the third scenario from January 1, 2013 to August 31, 2021.

The percentage difference between estimated counterfactual and observed daily emissions for $\zeta = 0.75$ ranges from $-83.03$ to 32.32, with the average percentage difference being $-36.92$. This suggests that, under the second hypothetical CRE electricity production scenario, daily $CO_2$ emissions would have, on average, decreased by 36.92%.

The fourth and last scenario corresponds to the situation where the mean daily CRE elec-

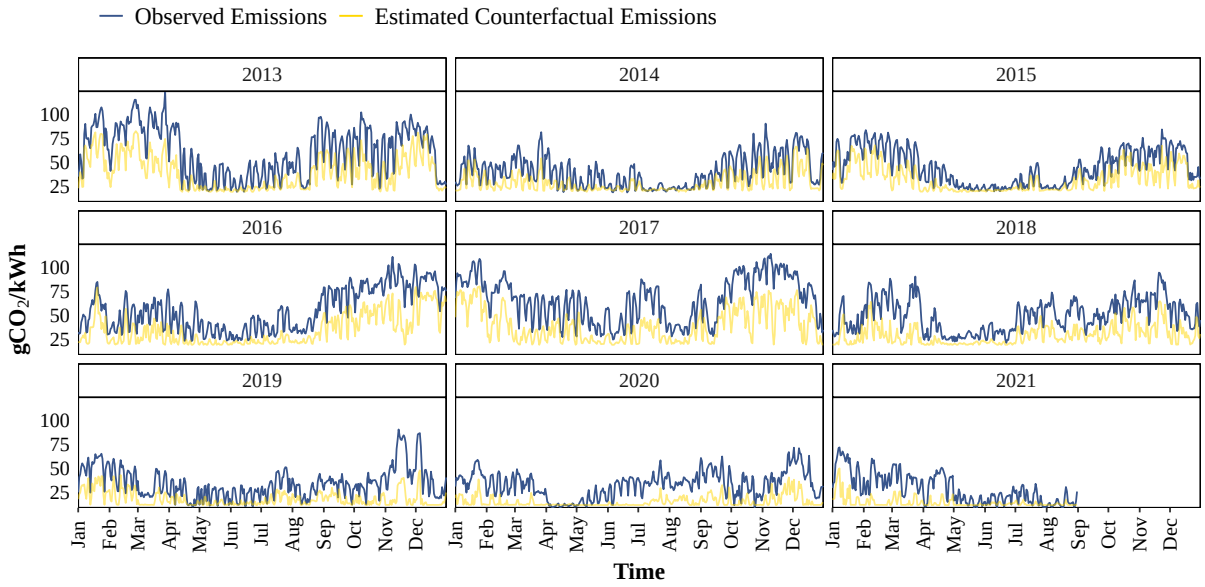


Figure 2.8: Observed (realized) and estimated counterfactual daily emissions over the study period under the third production scenario ($\zeta = 0.75$). For visualization purposes, data for each year are presented in a separate panel.

tricity production equals the mean daily total electricity production ($\zeta = 1$). This scenario is the most ambitious among the four proposed scenarios. Figure 2.9 compares observed (realized) and estimated counterfactual daily emissions under the fourth scenario from January 1, 2013 to August 31, 2021.

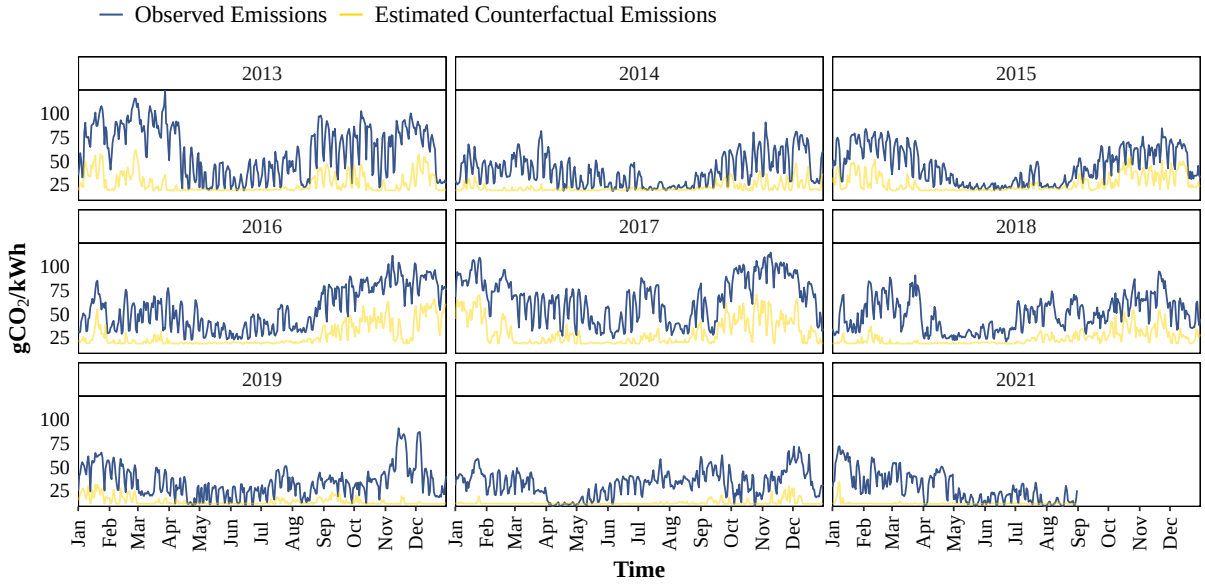


Figure 2.9: Observed (realized) and estimated counterfactual daily emissions over the study period under the fourth production scenario ($\zeta = 1$). For visualization purposes, data for each year are presented in a separate panel.

The percentage difference between estimated counterfactual and observed daily emissions for $\zeta = 1$ ranges from $-87.06$ to 32.32, with the average percentage difference being $-47$.

This suggests that, under the fourth hypothetical CRE electricity production scenario, daily $CO_2$ emissions would have, on average, decreased by 47%.

The distributions of the difference between estimated counterfactual and observed emissions under the four proposed scenarios over the entire study period are illustrated in Figure 2.10.

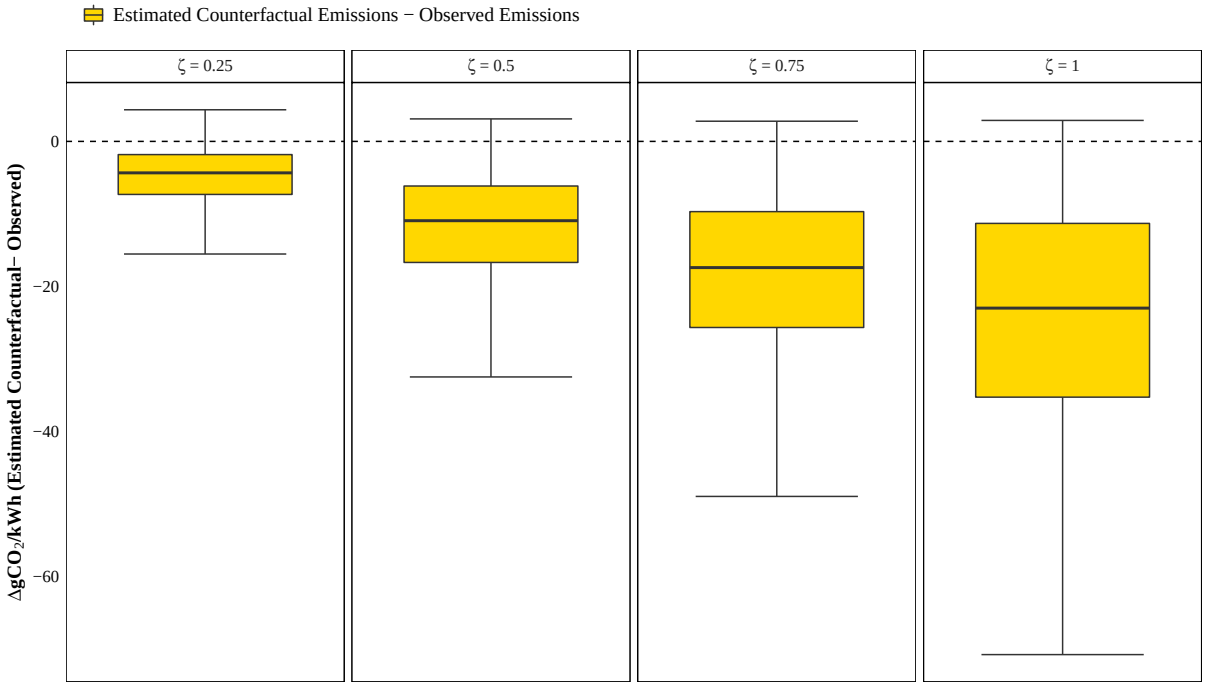


Figure 2.10: Box plot of the difference between estimated counterfactual emissions under different production scenarios ($\zeta = 0.25, 0.5, 0.75$ and 1), and observed emissions over the study period. Note: The upper (lower) whisker extends from the hinge to the largest (smallest) value no further than 1.5 times the interquartile range. Data points beyond the whiskers are removed from the plot for the sake of better visualization.

The null hypothesis of the non-parametric Wilcoxon signed-rank test (i.e. the median difference between pairs of counterfactual and observed emissions is greater than or equal to zero) is rejected at the 0.01 significance level for all the proposed scenarios. The results confirm that an increase in the ratio of mean daily CRE electricity production to mean total electricity production, would have been associated with a statistically significant decrease in predicted $CO_2$ emissions in France from 2013 to 2021. From a practical and economic standpoint, this means that increasing the share of CRE electricity production and decreasing the share of non-CRE sources, while retaining the same level of total production, would have significantly reduced emissions over the study period.

In the next step and in order to characterize the relative importance of each CRE source for reducing predicted $CO_2$ emissions from electricity production, the optimal CRE mix for emissions reduction under each proposed scenario is identified. Figure 2.11 depicts the predicted mean daily $CO_2$ emissions over the study period in the CRE mix space. The share of each source in the CRE package ranges from 0 to 1 in increments of 0.05, with the sum of shares

being equal to 1.

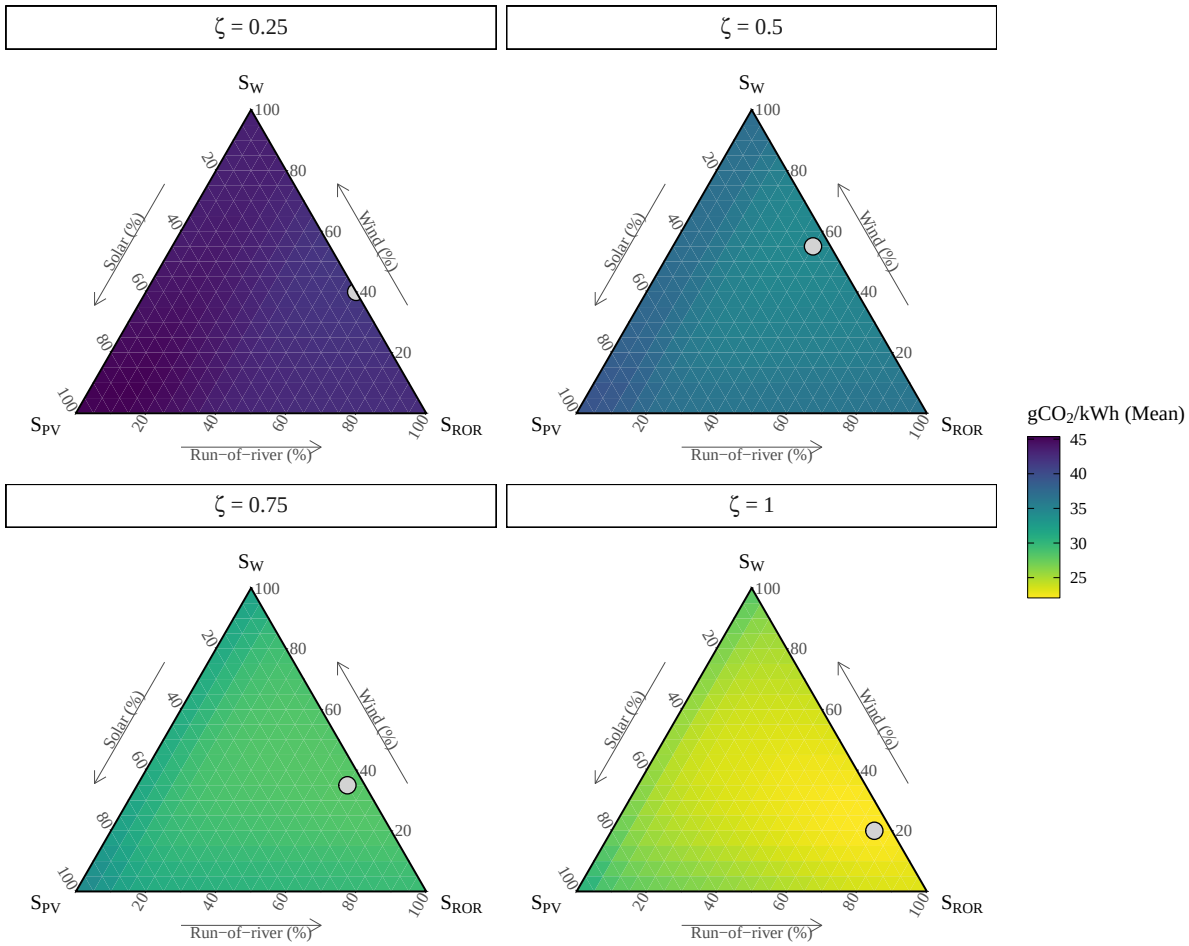


Figure 2.11: Ternary graphs of the mean daily $CO_2$ emissions over the study period for different shares of wind, solar photovoltaics and run-of-river hydroelectricity in the CRE mix under different production scenarios ($\zeta = 0.25, 0.5, 0.75$ and 1). The optimal CRE mix for emissions reduction is marked with a circle on each graph.

Table 2.6 presents the optimal CRE mix for emissions reduction under the four proposed scenarios ($\zeta = 0.25, 0.5, 0.75$ and 1), and the corresponding predicted mean daily $CO_2$ emissions for each mix. These results offer additional evidence that run-of-river hydroelectricity is the most important source for reducing energy-related $CO_2$ emissions in France, with up to 75% share in the optimal CRE mix. The only exception is when $\zeta = 0.5$, where the share of run-of-river hydroelectricity is less than the share of wind in the optimal CRE mix. Solar photovoltaics has the smallest share of CRE sources in the optimal mix under all proposed scenarios.

These results should be considered in comparison with realized and realizable mean shares of the three sources in the CRE mix. The empirical mean shares of wind, solar photovoltaics and run-of-river hydroelectricity in the CRE mix based on the realized electricity production

Table 2.6: Optimal CRE mix for emissions reduction under the four proposed scenarios, and the corresponding predicted mean daily $CO_2$ emissions.

| Scenario | Optimal CRE Mix | | | $gCO_2$/kWh (Mean) |
|---|---|---|---|---|
| | $S_W$ | $S_{PV}$ | $S_{ROR}$ | |
| $\zeta = 0.25$ | 40% | 0% | 60% | 41.56 |
| $\zeta = 0.5$ | 55% | 5% | 40% | 34.47 |
| $\zeta = 0.75$ | 35% | 5% | 60% | 28.15 |
| $\zeta = 1$ | 20% | 5% | 75% | 22.10 |

(as defined in Section 2.2.1.1) are 31.11%, 13.06% and 55.82%, respectively, with the corresponding mean daily $CO_2$ emissions being 46.44 $gCO_2$/kWh. In a similar vein, the empirical mean shares of wind, solar photovoltaics and run-of-river hydroelectricity in the CRE mix based on the realizable electricity production (as defined in section 2.2.1.2) are 31.84%, 14.98% and 53.17%, respectively, with the corresponding predicted mean daily $CO_2$ emissions being 45.7 $gCO_2$/kWh. From this comparison, two key findings emerge: (1) an increase in the share of CRE electricity production is associated with a decrease in average emissions from electricity generation, and (2) in both real and hypothetical contexts, the shares of different sources are not uniformly distributed within the CRE package.

To characterize the relative importance of each source for reducing the intermittency of CRE electricity production, the optimal CRE mix that minimizes CV over the study period is identified. This allows for comparison between the optimal CRE mix for emissions reduction under different scenarios and the optimal CRE mix for reducing intermittency. Indeed, the configurations that result in the minimum mean daily $CO_2$ emissions under the proposed scenarios do not necessarily result in low intermittency and high reliability of CRE electricity production over the study period. Figure 2.12 depicts the CV in the CRE mix space based on the normalized CRE indicator series over the study period. The share of each source in the CRE package ranges from 0 to 1 in increments of 0.05, with the sum of shares being equal to 1.

The shares of wind, solar photovoltaics, and run-of-river hydroelectricity in the optimal CRE mix for reducing the intermittency are 15%, 30% and 55%, respectively, with the corresponding CV being 0.22.[20] This CRE mix would result in the mean daily $CO_2$ emissions of 42.47, 35.5, 28.96 and 23 $gCO_2$/kWh under the first, second, third and fourth proposed scenario, respectively. Comparing these values with the optimal values in Table 2.6, it can be deduced that the optimal CRE mix for reducing intermittency is associated with slightly larger emissions than those of the optimal CRE mix for emissions reduction under the proposed scenarios.

These findings are important for two reasons. First, while the share of wind is larger than

[20]The empirical CV of the CRE package based on the realized and realizable CRE electricity production (as defined in Sections 2.2.1.1 and 2.2.1.2) are 0.31 and 0.30, respectively.

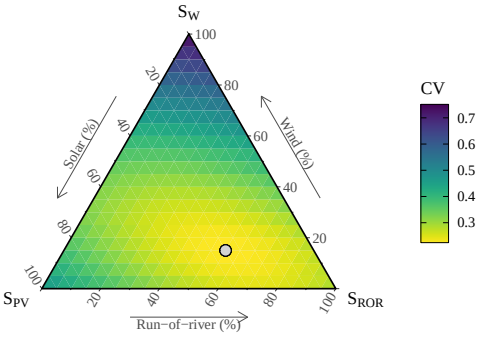


Figure 2.12: The coefficient of variation (CV) of the normalized daily CRE mix over the study period. The optimal CRE mix reducing intermittency is marked with a circle on the graph.

that of solar photovoltaics in the optimal CRE mix for emissions reduction under all the proposed scenarios, solar photovoltaics proves to have a larger share than wind in the optimal CRE mix for reducing intermittency. Second, among the three sources, run-of-river hydroelectricity has the largest share in the optimal CRE mix as it was the case for the optimal CRE mix for emissions reduction under three (out of four) proposed scenarios. The results of the present study can complement those of François et al. (2016), who determined the optimal CRE mix for maximizing energy penetration in France over the $1980-2012$ period ($S_W = 15\%$, $S_{PV} = 45\%$, $S_{ROR} = 40\%$, with the corresponding CV being 0.28). While beyond the scope of this paper, disentangling the complexities in finding the optimal balance among emissions reduction, intermittency reduction and energy penetration maximization might prove an important area for further investigation.

## 2.4 Discussion

On the part of European countries, the development of electricity generation from renewable sources and the European Union Emissions Trading Scheme (EU ETS)–the mainspring of the European Union's policy to reduce $CO_2$ emissions–are two important tools to address climate change. Nevertheless, complex interactions between these instruments, and in particular, the potential dampening effects of renewable electricity growth on emissions allowances prices, have raised considerable doubts on the feasibility of combining different targets and policies to effectively reduce carbon emissions (see del Río (2017) and Möst and Fichtner (2010)). A multidisciplinary economic analysis of this interaction by del Río (2017) indicates that most of the concerns on this matter are not supported by economic theory, and that the combination of the EU ETS and renewable energy-based electricity development should be favored. Notwithstanding, after several years of research, there is still no firm consensus on the environmental

viability of combining emissions trading systems and renewable energy expansion. According to a recent theoretical study, in the long run, emissions trading systems may impede the expansion of renewable energy capacity rather than promoting it (Bersani et al., 2022). In this regard, a venue for future research includes (1) replicating the findings of the present research in other Member States of the EU ETS, and (2) empirically investigating the interaction between the EU ETS and the development of different types of CRE electricity production in Europe, especially by focusing on the economic value of renewable energy-induced emissions reduction considering the EU ETS allowance prices and potential carbon leakage.[21]

As with the majority of studies, the findings of this research have to be considered in the light of some limitations. The first limitation concerns the choice of proxies for CRE electricity production potential. It could be argued that in the process of estimating counterfactual $CO_2$ emissions, the construction of new CRE indicators relies only on the realizable CRE indicators that are greater than their corresponding realized values (see Section 2.2.2.2). In statistical terms, only "overestimated" CRE electricity production derived from climate variables is retained and "underestimated" values are disregarded. The assumption here is that, if the realized energy indicators are greater than the indicators estimated by the climate-to-energy model, the potential for CRE electricity production has already been fully exploited and there is therefore no point in utilizing the climate-derived energy indicators in such a case. In justification of this assumption, an argument can be made that in 63.06%, 68.53% and 62.27% of daily observations, the so-called realizable indicators are greater than their corresponding realized values for wind, solar photovoltaics, and run-of-river hydroelectricity, respectively. Moreover, for wind, solar photovoltaics, and run-of-river hydroelectricity, the normalized root-mean-square deviation (defined as the square root of the quadratic mean of the differences between realizable and realized values, divided by the range of realized values) that is associated with "overestimation" instances is, respectively, 1.6, 1.45 and 1.32 times greater than the normalized root-mean-square deviation associated with "underestimation" instances for the same energy source. Unless the models behind the data described in Section 2.2.1.2 are prone to systematic overestimation, one possible conclusion that can be drawn from these results is that the transformation of gridded climate variables into energy indicators would provide more of a reference to assess the "potential" of CRE sources than an estimation of the level of energy generation practically achieved. This assumption is the primary limitation to the interpretation of the results presented in Section 2.3.2. Nevertheless, in the absence of better alternatives, climate-to-energy conversion models are the only tools available to measure the (unexploited) potential for electricity production from CRE sources.

Another limitation of the present study includes the non-consideration of within-country

[21] As a relevant work in this area, see the study of Beltrami et al. (2021) that has examined the value of carbon emission reduction induced by renewable energy production in Italy.

(i.e. regional) dynamics between carbon emissions and electricity production from renewable energy sources. This limitation is mainly rooted in the lack of data at the regional level on $CO_2$ emissions from electricity production at daily time scale. Upon availability of more spatially-fine-grained data on emissions and climate-derived energy indicators, future studies could explore such regional dynamics. To provide a starting point for discussion and further research, Figure 2.13 illustrates the average share of daily electricity production from wind, solar and hydroelectric sources (run-of-river, lake and pumped-storage) by administrative region in metropolitan France over the study period. As shown in this figure, the share of wind and solar photovoltaics energy in electricity production is higher in northern and southern (coastal) regions, respectively. As expected, hydropower generation is more pronounced in mountainous regions, with the Auvergne-Rhône-Alpes region having a high average share of 44.55% in total electricity production in France over the study period.

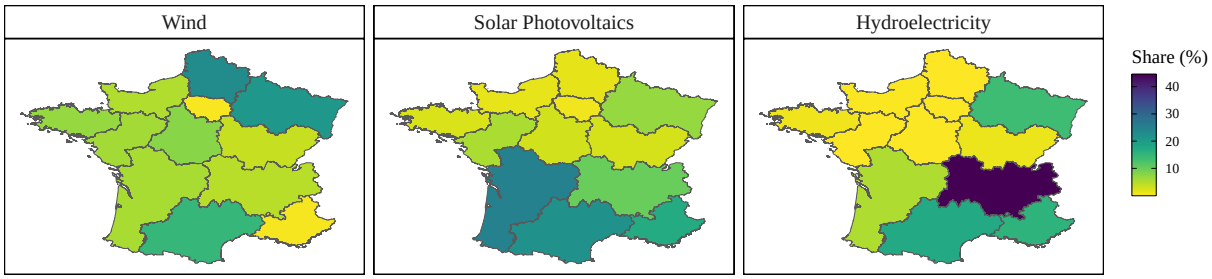


Figure 2.13: Average share of daily electricity production from wind, solar and hydroelectric sources (run-of-river, lake and pumped-storage) by region in metropolitan France over the study period.

Additionally, neither energy storage and residual load variability nor the economic and social cost of increasing the share of renewable energy vis-à-vis emissions reduction is considered in this paper. The study of Shirizadeh and Quirion (2021) has evaluated the relative contribution of renewable (wind, solar photovoltaics, run-of-river and lake hydroelectric) energy production, nuclear power and CCS technologies to the cost-optimal electricity mix in France, taking into account the social cost of carbon. The authors have found that a cost-optimal power mix consists of approximately 75% electricity production by renewable energy sources, and the remaining 25% is shared among nuclear power and fossil fuels, with or without CCS technologies. In a subsequent study, Shirizadeh et al. (2022) have examined the robustness of a renewable power system for France to key technology cost uncertainties by considering several cost scenarios. They have found that, although the cost-optimal electricity mix in France heavily depends on assumptions about technology costs, investments in the development of renewable energy should be prioritized even if those underlying cost assumptions prove to be wrong.[22] These findings, together with the results of the present study, may be important for policy and subsequent re-

[22] Also see the study of Chu and Hawkes (2020) that has proposed a multi-objective optimization model to find the optimal mix of CRE sources in global electricity systems, considering cost, residual load variability, and portfolio output variability.

search.

Last but not least, it is worth noting that the principal outcomes of this explorative study are based on historical data and a counterfactual analysis of the nexus between CRE electricity production and $CO_2$ emissions in France. Hence, one should be careful when interpreting or extrapolating these results to other settings and/or time periods. For instance, in the majority of proposed scenarios, run-of-river hydroelectricity is identified as the CRE source of greater relative importance for reducing counterfactual predictions of $CO_2$ emissions over the 2013-2021 period. However, the soundness of increased investment in the development of run-of-river hydroelectric power facilities (either by increasing the number of run-of-river power plants or improving the efficiency of installed power plants) to cut $CO_2$ emissions in the future is subject to the extent that France's run-of-river hydropower potential is affected by climate change, on top of cost considerations. A study based on the climate change projections and a set of scenario assumptions for future water use in Europe (Lehner et al., 2005) confirms that run-of-river hydropower potential (as measured by river discharges) will remain rather stable in the case of France for the time slices for the 2020s and 2070s. With the help of newly-developed climate projections, further research on this direction is warranted.

## 2.5 Conclusion

As a path forward to combat global climate change, the development of renewable energy share of electricity production remains the cornerstone of $CO_2$ emissions reduction in the electric power sector. Considering the dependence of the availability and sporadicity of climate-related renewable energy (CRE) sources (wind, solar photovoltaics, and small-scale run-of-river hydroelectricity) on climate factors, the relationship between $CO_2$ emissions and electricity production from these sources merits careful analysis. By means of a cutting-edge decision-tree-based modeling technique, this study characterized the relationship between daily CRE electricity production and energy-related $CO_2$ emissions in France and offered a framework for counterfactual analysis of such relationship over the 2013-2021 period.

The empirical analysis was undertaken in three steps. In the first step, the importance of CRE electricity production in predicting $CO_2$ emissions was assessed by means of the permutation feature importance algorithm. Furthermore, the nonlinear relationship between realized electricity production from CRE sources and predicted emissions was identified through accumulated local effects (ALE) plots. From the results, run-of-river hydroelectricity proved to be the most important feature among the three CRE sources for predicting emissions, followed by wind energy. Solar photovoltaics was shown to be of marginal importance in respect of predicting emissions. Next, the predictive impact of CRE electricity production potential (as proxied by climate-derived energy indicators) on $CO_2$ emissions was quantified. The results demonstrated that an increase in the share of energy from CRE sources–under a scenario where the

maximum possible electric energy is generated from climate variables–would have been associated with a statistically significant decrease in $CO_2$ emissions from electricity production over the study period. Ultimately, four hypothetical CRE production scenarios were considered and the optimal mix of CRE sources for minimizing emissions under each scenario was determined. The findings confirmed greater relative importance of run-of-river hydroelectricity and wind energy within the CRE package with regard to the reduction of predicted $CO_2$ emissions. This step was complemented by the identification of optimal CRE mix for reducing intermittency of CRE electricity production. This complementary analysis found further evidence for a higher share of run-of-river hydroelectricity in the CRE mix.

The findings of this research, while exploratory, can have important implications for renewable energy development and management in France, since they provide some support for the conceptual premise that replacing carbon-intensive energy sources with renewable ones reduces carbon emissions from electricity generation. Additionally, the findings cast a new light on the relative importance of each CRE source with regard to emissions and intermittency reduction in the electricity sector. Together these results might prove enlightening for policymakers who decide which renewable energy infrastructure investments should be given priority.

CHAPTER 3

# Climate and Electricity Production: Climatic Predictors of Carbon Emissions

**Article Title:** "Identifying climatic drivers of emissions from electricity production: Insights from a predictive modeling-based approach" (Eslahi, 2022b)

**Abstract:** This research sets out a state-of-the-art interdisciplinary machine learning-based framework for characterizing the impact of climate conditions on hourly $CO_2$ emissions in the French electric power system from January 2013 to December 2020. The results indicate that, while controlling for the effect of time, 86.43% of the variation in $CO_2$ emissions from electricity production can be explained by climatic predictors. Air temperature and relative humidity are identified as the most and least important factors, respectively, for the prediction of emissions in France. The study also found that the predictive relationship between most climate variables and $CO_2$ emissions from electricity generation was nonlinear in nature over the study period. The findings of this research should make an important contribution to the literature on driving factors for $CO_2$ emissions in the electricity sector, and can provide insight into the sensitivity of power-related emissions to climate change.

**Keywords:** Electricity Production, $CO_2$ Emissions, Climate, Predictive Modeling

## 3.1 Introduction

Anthropogenic greenhouse gas emissions are the predominant driver of climate change, with carbon dioxide ($CO_2$) emissions bearing the most responsibility for global warming. Addressing climate change thus requires that $CO_2$ reduction and removal measures be taken urgently at national and international level. Owing to its ability to foster decarbonization of the economy in a faster and less costly manner than other energy supply and end-use sectors (Karmellos et al., 2016; Goh et al., 2018b; Rodrigues et al., 2020), the electricity sector is expected to provide one of the most significant contributions to climate change mitigation and be the keystone of the European Union's environmental policy to reach a state of net-zero greenhouse gas emissions by 2050 (European Environment Agency , 2022). As emphasized by the European Environment Agency, the carbon intensity of electricity production is nevertheless not uniform in the European Union (EU), and differs significantly from one Member State to the other, depending mainly on the national electricity mixes.

As a global pioneer in the fight against climate change, France has had time-honored aspirations for transforming its economy towards carbon neutrality. The electricity sector in France has one of the lowest carbon intensities in the EU, mostly due to the dominance of nuclear power. The share of electricity generated from nuclear sources in France reaches more than two thirds of the total electricity production–a larger share than any other country, making France the world's largest net exporter of electricity as well (World Nuclear Association, 2022). Notwithstanding, the French power sector was to blame for emitting 21.16 million tonnes of $CO_2$ equivalent ($CO_2$e) in 2019, corresponding to 4.8% of the country's total emissions (Réseau de Transport d'Électricité (RTE), 2020). As per France's commitment to going carbon neutral by 2050, enacted under the title "Ecological Emergency and Climate Crisis" by the National Assembly in 2019 (Ministère de la Transition écologique, 2019), electricity generation-related $CO_2$ emissions has to be further minimized either by leveraging carbon capture and storage (CCS) technologies in existing fossil-fuel-fired power plants, or through an increase in the share of low and zero-carbon electricity production (Débat national sur la transition énergétique, 2013; Shirizadeh and Quirion, 2021). The latter takes the form of the development of renewable electricity production and/or augmentation of the nuclear energy supply.[1] In the provision of climate change mitigation, the effective implementation of measures to reduce greenhouse gas emissions from the electricity sector necessitates in any case an in-depth understanding of po-

[1]There is ongoing debate about the proper balance between nuclear and renewable energy in France. Two studies of the French Agency for Ecological Transition (`https://www.ademe.fr/`) on evolutionary trajectories of the electricity mix (ADEME, 2018) and the viability of a 100% renewable electricity mix (ADEME, 2015) have shown that the development of the next generation of nuclear power plants would not be economically viable for the electricity sector in France, and that in an ideal case, renewable electricity generation holds up to 95% of the total electricity generation in the decades to follow. The French government policy aims to reduce nuclear share of electricity generation to 50% by 2035 (World Nuclear Association, 2022).

tential determinants of such emissions.

$CO_2$ emissions from electricity production come, by and large, under the influence of factors such as fuel structure, generation efficiency and technology, economic growth,[2] and climate conditions (Christiansen et al., 2005; Alberola et al., 2008; Karmellos et al., 2016; Goh et al., 2018b; Rodrigues et al., 2020). Climatic factors have a major double impact on $CO_2$ emissions in the electricity sector for the reason that they affect both the demand and supply of (renewable and non-renewable) electricity. Indeed, the electricity sector not only is a contributor to climate change, but also one of the most vulnerable economic sectors to changes in climate variables (Ebinger and Vergara, 2011; Schaeffer et al., 2012; Yalew et al., 2020). Although the demand for electricity is closely linked with economic activity and development, it also depends on non-economic factors, notably climate variables (Moral-Carcedo and Vicéns-Otero, 2005). On the demand side, climate variations (e.g. alteration in temperature) influence electricity demand by affecting heating and cooling requirements (Yalew et al., 2020; Yao, 2021). On the supply side, renewable energy sources such as wind, photovoltaic solar and hydroelectric powers are directly impacted by climate change to varying degrees on account of changes and variability in wind speed, solar radiation, and precipitation (Crook et al., 2011; Schaeffer et al., 2012; Bartos and Chester, 2015; Owusu and Asumadu-Sarkodie, 2016; Yalew et al., 2020; Gernaat et al., 2021). In an assessment of the sensitivity of European power systems to energy scenarios and climate change projections, Bloomfield et al. (2021) have shown that sub-continental renewable supply is significantly influenced by physical climate change, regardless of the choice of power system pathway. Moreover, fossil fuel, nuclear and biofuel plants undergo climate-related impacts on cooling and power generation efficiency (Yalew et al., 2020), mostly due to changes and variability in temperature, atmospheric pressure, and relative humidity (Arrieta and Lora, 2005; Ebinger and Vergara, 2011).

A large and growing body of literature has examined climate impacts on electricity demand and renewable or non-renewable power generation (see among others Van Vliet et al., 2012; Behrens et al., 2017; Perera et al., 2020; Yalew et al., 2020; Gernaat et al., 2021).[3] Despite this, quantifications of climate impacts on emissions from electricity production remain scarce (but see Tarroja et al., 2016; Qin et al., 2020). Most studies on the drivers of $CO_2$ emissions from electricity production in Europe and worldwide have typically focused on fuel mix, generation efficiency and socio-economic factors (see Karmellos et al., 2016; Ang and Su, 2016; Goh et al., 2018b; Rodrigues et al., 2020; Scarlat et al., 2022), and have tended to overlook the significance of climatic factors with respect to electricity generation-related emissions, as well as the poten-

[2]Despite the 15% increase in France's gross domestic product (GDP) per capita from 2000 to 2019, along with the 11% population growth over the same period, emissions from electricity production decreased by 29% over that decade, indicating a decoupling of economic growth and electricity generation-related $CO_2$ emissions in France (International Energy Agency, 2021).

[3]For an extensive literature review on this topic, see Ebinger and Vergara (2011), Gerlak et al. (2018) and Solaun and Cerdá (2019).

tial interconnectedness of climatic and non-climatic determinants of such emissions. Hence, there is still a major gap in our understanding of how and to what extent climate impacts on the demand and supply of electricity translate into greenhouse gas emissions in the electricity sector.

Interestingly, a strand of literature dealing with the empirical study of the European Union Emissions Trading System (EU ETS),[4] has recognized climate variables (e.g. air temperature, rainfall and wind speed), among other factors (e.g. energy prices and fuel switching), as explanatory factors for the carbon price (see Mansanet-Bataller et al., 2007; Alberola et al., 2008; Benz and Trück, 2009; Keppler and Mansanet-Bataller, 2010; Hintermann, 2010; Bredin and Muckley, 2011; Lutz et al., 2013; Rickels et al., 2015; Batten et al., 2021) without an explicit assessment of the (climatic) explicative factors behind $CO_2$ emissions themselves.[5] In view of the fact that the EU ETS is dominated by firms involved in electricity generation (Ahamada and Kirat, 2015), comprehensive examination of climatic predictors of electricity sector emissions in the EU Member States will not only advance the debate on climate change mitigation in the power sector but also benefit the literature on the functioning of the EU ETS, notably research on carbon price drivers in this emissions trading system.

The main purpose of the present work is to investigate the observed association between hourly $CO_2$ emissions in the French electric power system and a comprehensive set of climate factors over the 2013-2020 period. To do so, the study adopts an innovative interdisciplinary approach to constructing electric power-weighted climate indices from gridded climate variables and regional power indicators, based on the principal mechanism through which each climate variable can affect $CO_2$ emissions in the electricity sector. A non-parametric regression predictive modeling framework is then used to empirically learn the relationship between the obtained climate indices and $CO_2$ emissions from electricity production. Finally, the learning model is analyzed using post hoc interpretation methods, with the aim of extracting various forms of information on the relationship between electricity generation-related emissions and their climatic predictors.

For the sake of this analysis, six climate variables are identified as potential drivers of emissions from electricity production because of their influence on electricity production and consumption: air temperature, solar radiation, relative humidity, wind speed, total precipitation, and surface air pressure. Air temperature, solar radiation, wind speed and total precipitation are expected to serve as a determinant of electricity generation-related emissions as they may affect (if not always exclusively) electricity consumption, photovoltaic solar power generation, wind

[4]The EU ETS is the leading market-based measure, functioning on a cap and trade basis, to reduce $CO_2$ emissions in the European Union under the Kyoto Protocol.

[5]One exception is the study of Gloaguen and Alberola (2013), which has examined the factors behind $CO_2$ emissions during the first two phases of the EU ETS. While acknowledging the potential effect of climate conditions on emissions, the paper has not, however, included any climate variable in its econometric analysis due to lack of data, and the temporal scale of observations.

power generation and hydroelectric power generation, respectively. Relative humidity and surface air pressure are candidate predictors for emissions from electricity production, as they can influence generation cycle and cooling system efficiency of thermal and nuclear power plants.[6]

There are several important areas where this study makes an original contribution to research on determinants of $CO_2$ emissions from electricity production. First, in order to identify as fully as possible the effects of climate conditions on $CO_2$ emissions in the electricity sector, the present research gathers the most extensive set to date of climate variables linked with electricity generation-related emissions. To this should be added the rather incomparable granularity and scope of the data used for analysis. On the one hand, the use of high-resolution gridded data on climate variables over the geographical area of metropolitan France opens up the possibility to construct composite indices that could represent climate conditions in the country in the most comprehensive manner possible. On the other hand, the use of hourly emissions and climate data for a span of 8 years (i.e. 2013-2020) assists in our enhanced understanding of determinants of intra-day $CO_2$ emissions in the French electricity sector. In addition, using a relatively large data set ensures adequate sample representativeness and maximized performance of the machine learning algorithm used for empirical modeling.

Second, this work offers a novel methodological contribution, on a well-grounded interdisciplinary basis, to the construction of national climate indices. The suggested framework not only accommodates intra-country spatial climate heterogeneity but also takes into account the potential mechanism through which climate variables may have an impact on emissions in the electricity sector. The proposed approach to climate index construction may as well be applied in other areas of climate economics research and be used, with slight modifications, for purposes other than characterization of the relationship between climate variables and electricity generation-related $CO_2$ emissions.

Third, by employing a powerful tree-based ensemble learning algorithm in tandem with cutting-edge interpretation methods, this study is able to (1) measure the significance of every single climate index for explaining $CO_2$ emissions from electricity production, and rank those indices based on their importance in estimating the predictive model; (2) characterize and quantify complex, nonlinear relationships between electricity sector emissions and their climatic

[6]The more efficient the conversion of fossil fuels and biofuels to electricity, the less fuel is required to generate the same amount of electricity. This translates into fewer $CO_2$ emissions per unit of electricity generated. As regards nuclear power generation, efficiency consequences for emissions are less clear-cut. From a technical standpoint, nuclear power plants resemble standard thermal power plants, with the exception that they use nuclear fission (instead of fossil fuel or biofuel combustion) as the heat source. Therefore, relative humidity and surface air pressure are expected to exert a similar effect (if any) on thermal and nuclear power plants. Increase (decrease) in the efficiency of nuclear power plants leads to increase (decrease) in the amount of electric power produced for each unit of thermal power. Under the plausible assumption that in the short-run, increase (decrease) in nuclear electricity production per unit of thermal power is, at least partly, counterbalanced by decrease (increase) in the use of fossil fuels and/or biofuels for electricity generation, $CO_2$ emissions per unit of electricity generated are expected to have an inverse relationship with the the efficiency of nuclear power plants.

predictors, and show for the first time how the effects of such predictors on emissions change throughout the complete range of values of the predictors while controlling for various types of time properties; and (3) explore potential interactions between different climate factors in respect of their predictive impact on $CO_2$ emissions from electricity production, and examine both pure main and second-order effects of climatic predictors. When quantifying climate change impacts as complex as those in the electric power sector, it might not be enough to focus solely on a single climate change variable at a time. In this regard, analyzing interactive effects of multiple climate factors can be a major elementary step towards a more complete understanding of the sensitivity of electricity sector emissions to climate change and variability.

The remaining part of the paper proceeds as follows. Section 3.2 is concerned with the presentation of the data and methodology used for this study. The research methodology is divided into three parts: the construction of electric power-weighted national climate indicators, the empirical modeling of $CO_2$ emissions from electricity production based on climate indices, and the characterization of the predictive impact of climate indices on such emissions. Section 3.3 presents the findings of the research, focusing on the three key elements of methodology. Section 3.4 includes a discussion of some significant and unexpected results, identifies potential limitations and weaknesses of the study, and makes suggestions for further research. Finally, Section 3.5 gives a brief summary of the main findings and reiterates the importance of the topic for policy and subsequent research.

## 3.2 Materials and Methods

### 3.2.1 Data

For the purpose of analysis, data on $CO_2$ emissions from electricity production, electric power consumption and output, and climate variables are collected from publicly-available open data sources. The two latter sets of data are utilized for building national electric power-weighted climate indices that serve as the main explanatory variables in the model. The temporal scope of the study extends from January 1, 2013 (00:00) to December 31, 2020 (23:00). The ultimate sample used for empirical analysis consists of 70128 hourly observations of one dependent ($CO_2$ emissions from electricity production) and 10 independent variables (6 electric power-weighted climate indices and 4 time-based predictors[7], namely hour of the day, day of the week, month of the year and year).

[7]In addition to electric power-weighted climate indices, numerical time-based predictors are created and included in the analysis as independent variables to account for possible seasonality in time series data. See Section 3.2.2.2 for more details about the function of time-based predictors.

#### 3.2.1.1 $CO_2$ emissions from electricity production

Estimates of $CO_2$ emissions resulting from the generation of electrical power in France, expressed in grams of $CO_2$e per kWh generated, are obtained from the national éCO2mix data set of RTE (Réseau de Transport d'Électricité[8]), available on the Open Data Réseaux Énergies (ODRÉ) platform[9]. The emission indicator in this data set illustrates $CO_2$ equivalent emissions produced by the consumption of primary fuel (fuel oil, coal, gas and biofuel) in power plants located in France, and does not include exchanges of energy at interconnections (i.e. electricity imports or exports). The original quarter-hourly national emissions estimates are aggregated into hourly means, so that they match the temporal frequency of climate variables (and consequently climate indices). Additionally, hourly emissions estimates are natural log-transformed to avoid possibly negative predicted values of the dependent variable in the empirical modeling process (see Section 3.2.2.2).

#### 3.2.1.2 Electricity consumption and power generation by energy source

Consolidated and definitive data on electricity consumption and power generation by energy source in metropolitan regions of France, expressed in megawatts (MW), are sourced from the RTE's regional éCO2mix data set, available on the open data platform described in Section 3.2.1.1. Given the nature of the proposed methodology for the construction of national climate indices (see Section 3.2.2.1), negative values of power production (aka negawatts), if any, are set to zero. The original half-hourly power values are aggregated into total hourly sums, so as to guarantee consistency between the temporal frequency of the electric power indicators and climate variables. For the sake of consistency with the nature of emissions data, neither inter-regional exchange and cross-border trading of electric power[10] nor regional energy storage potential are considered in the present study.

#### 3.2.1.3 Climate variables

Gridded ($0.25^\circ \times 0.25^\circ$) hourly historical data on climate variables over the area of metropolitan France from January 1, 2013 (00:00) to December 31, 2020 (23:00) are obtained from the ERA5 climate dataset (Hersbach et al., 2020). ERA5 is the latest climate reanalysis produced by the Copernicus Climate Change Service (C3S) at the European Centre for Medium-Range Weather Forecasts (ECMWF), and provides the most comprehensive picture currently possible of the past global climate and weather by combining observations with past short-range forecasts obtained from advanced weather forecasting models (ECMWF, 2020b). Data on air

[8]The electricity transmission system operator of France

[9]`https://opendata.reseaux-energies.fr/`. ODRÉ is a subdivision of the open platform for French public data (`https://www.data.gouv.fr/`)

[10]Cross-border power trading takes place between France and England, Spain, Italy, Switzerland, Luxembourg, Germany and Belgium.

temperature at 2m above the surface (K),[11] total sky direct solar radiation[12] at surface ($Jm^{-2}$), total precipitation (m) and surface air pressure (Pa) are directly available from the C3S. For a given grid point, wind speed ($ms^{-1}$) is calculated from the eastward (u) and northward (v) wind components at the height of 100m.[13] Relative humidity (%) values are computed from the 2m air and dew point[14] temperatures (K) using the August-Roche-Magnus approximation (Alduchov and Eskridge, 1996). The original dataset represents the mean area average of climate variables over each grid at a given time point (hour).

## 3.2.2 Methodology

### 3.2.2.1 Construction of electric power-weighted climate indices

To construct nation-wide indices that could represent climate conditions across France in the most comprehensive and relevant manner possible, the study relies on the European Hydro-ecoregion regionalization framework from hydrology and environmental science (Wasson et al., 2002, 2007). European Hydro-ecoregions (abbreviated hereafter as HER) by definition are geographical regions that have similar climatological, topographic, geological and lithological characteristics (Wasson et al., 2007). Europe (including Eastern Thrace) covers 133 HERs that are further categorized, according to several climatic factors, into 9 homogeneous climate regions (also known as climate classes): Alpin Mountain, Boreal, Continental Cold, Hyper Mediterranean, Mediterranean, Oceanic, Temperate, Temperate Mountain, and Temperate Warm. Metropolitan France embraces 33 HERs and 7 of these climate classes (Figure 3.1).

HERs are grouped into climate classes so as to minimize (maximize) intra-class (inter-class) variations in respect of climate conditions (see Wasson et al., 2007). On this point, the underlying assumption of the index construction method put forward by the present study is that the climate variables used for analysis, namely air temperature, solar radiation, relative humidity, wind speed, total precipitation and surface air pressure, show slight variation within each climate class. In light of this assumption, at a given point in time (hour), the mean area average of a given climate variable over all the HERs belonging to the same climate class is well representative of the overall value of the variable across the relevant HERs at that time point.

To begin the process of index construction, climate conditions over mainland France at each hour are aggregated by climate class by taking average of the (hourly) values of climate variables at the grid points lying within the geographical area of respective climate classes. For

[11] For ease of interpretability, temperatures are converted from kelvin to degrees Celsius before being used for regression predictive modeling.

[12] Solar photovoltaic panels are most productive when exposed to direct (as opposed to diffuse) solar radiation.

[13] The average hub height of modern land-based wind turbines used for wind power generation is close to 100m (Wiser et al., 2020).

[14] The dew point is the temperature at which air is saturated with water vapor (at constant pressure and water content), resulting in the formation of dew.

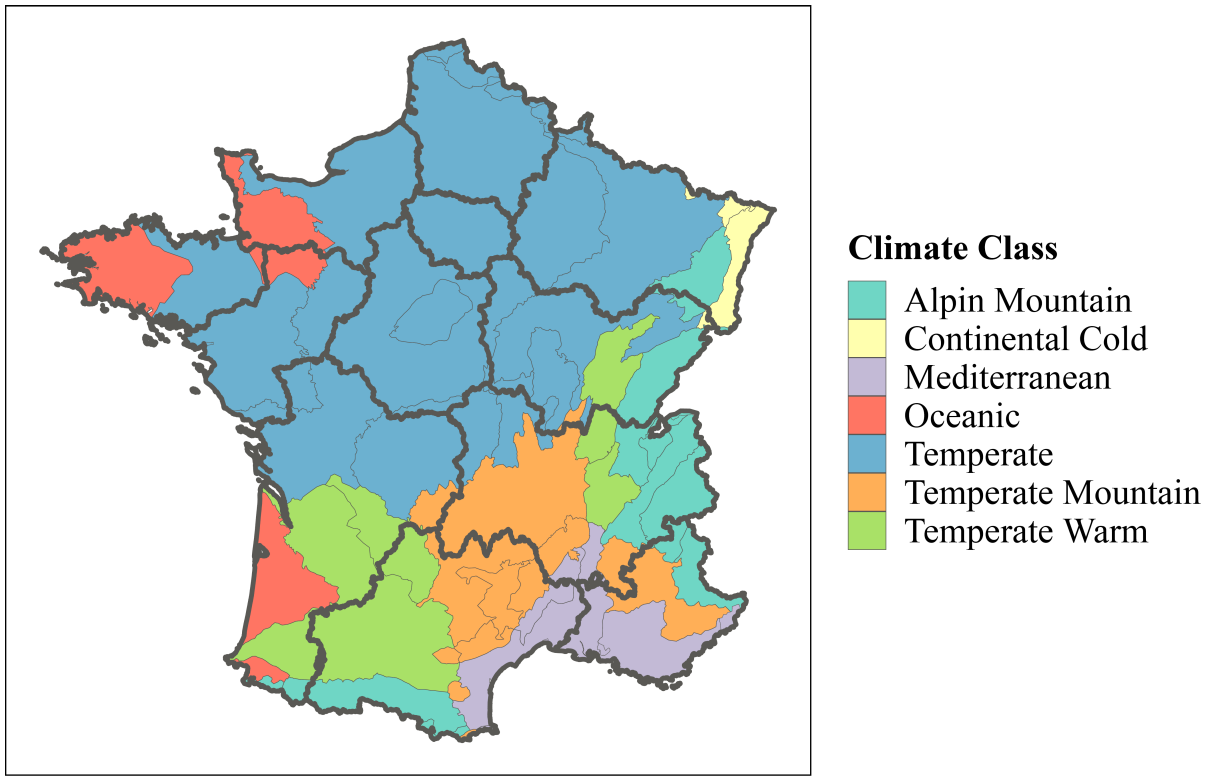


Figure 3.1: Hydro-ecoregions (HERs) and their corresponding climate classes across France, intersected with metropolitan (administrative) regions excluding Corse. HERs and the 12 metropolitan regions are delineated by thin light and thick dark lines, respectively. Data used for plotting Hydro-ecoregions and administrative regions are sourced from Wasson et al. (2007) and OpenStreetMap France (`https://www.openstreetmap.fr/donnees/`), respectively.

each climate variable and at each time point (hour), the resulting 7 aggregate climate indicators are then combined into a single nation-wide climate index by means of an original weighting scheme based on the regional share of electricity consumption and power production by different energy sources. This weighting scheme relies on the evaluation of the importance that should be given to each climate class as regards the potential effect of regional climate conditions on national $CO_2$ emissions. The idea is that the primary mechanism through which climate variables can affect $CO_2$ emissions in the electricity sector is the alteration of electricity demand and power generation by renewable and nonrenewable energy resources. Consequently, the relative share of each homogeneous climate region in national electricity consumption and production is the perfect candidate for measuring the relevance of climate conditions in climate classes to countrywide emissions indicators. The set of climate variables used for analysis and their corresponding relevant power indicators are presented in Table 3.1.

In mathematical terms, for a climate variable $v$, the electric power-weighted index at a given hour $t$ is defined as the convex combination

$$\text{Climate Index}_v^{(t)} = \sum_r \left( \text{Power Share}_{r,v}^{(t)} \times \text{Climate Indicator}_{r,v}^{(t)} \right) \tag{3.1}$$

Table 3.1: List of climate variables identified as potential predictors of $CO_2$ emissions from electricity production, along with their corresponding relevant power indicators used for the construction of electric power-weighted climate indices. In the case of relative humidity and surface air pressure, total electricity production from fossil fuels, nuclear power and biofuels is used as the relevant power indicator.

| Climate Variable | Relevant Power Indicator(s) |
|---|---|
| Air Temperature | Electricity Consumption |
| Solar Radiation | Photovoltaic Solar Power |
| Relative Humidity | Fossil Fuel, Nuclear and Biofuel Powers |
| Wind Speed | Wind Power |
| Total Precipitation | Hydroelectric (Run-of-river, Lake and Pumped-storage) Power |
| Surface Air Pressure | Fossil Fuel, Nuclear and Biofuel Powers |

where the summation index $r$ runs over the 7 homogeneous climate regions in France. The weighting coefficients in Equation 3.1 estimate the relative share of the homogeneous climate regions in the national consumption or production of the power indicator corresponding to the climate variable of interest at the given time point. These coefficients are obtained by first calculating the proportion of area of metropolitan (administrative) region[15] that is covered by each homogeneous climate regions. For each hour, the obtained area shares are multiplied by the relative share of the corresponding metropolitan regions in the national consumption or production of the power indicator bearing upon a given climate variable. The sum of the obtained multiplicative terms over all metropolitan regions provides the desired weighting coefficient for each climate class:

$$\text{Power Share}_{r,v}^{(t)} = \sum_{s} \left( \text{Area Share}_{r,s} \times \text{Power Share}_{s,v}^{(t)} \right) \tag{3.2}$$

where

$$\text{Area Share}_{r,s} = \frac{\text{Area}_{s \cap r}}{\text{Area}_{s}} \quad \text{and} \quad \text{Power Share}_{s,v}^{(t)} = \frac{\text{Power Indicator}_{s,v}^{(t)}}{\sum_{s} \text{Power Indicator}_{s,v}^{(t)}}$$

The subscript $s$ denotes the metropolitan regions, $\text{Area}_s$ is the surface area of the $s^{\text{th}}$ metropolitan region (in $\text{km}^2$), and $\text{Area}_{s \cap r}$ is the total area of the metropolitan region $s$ that belongs to the climate class $r$ (in $\text{km}^2$). For a given climate variable $v$, $\text{Power Indicator}_{s,v}^{(t)}$ represents the $s^{\text{th}}$ metropolitan region's relevant power indicator (in MW) at time $t$. Power shares are obtained by

[15]Mainland France is divided into 13 metropolitan regions: Auvergne-Rhône-Alpes, Bourgogne-Franche-Comté, Bretagne, Centre-Val de Loire, Corse, Grand Est, Hauts-de-France, Île-de-France, Normandie, Nouvelle-Aquitaine, Occitanie, Pays de la Loire, Provence-Alpes-Côte d'Azur. The island of Corsica (Corse in French) is excluded from the analysis due to the unavailability of data on electricity consumption and power production by different energy sources.

calculating the proportion of the regional power indicator values out of the total power indicator values across all metropolitan regions.

Table 3.2 presents the summary statistics of the constructed electric power-weighted climate indices and $CO_2$ emissions indicator, i.e. the variables included in the empirical model (see Section 3.2.2.2).

Table 3.2: Summary statistics of the explanatory and explained variables (excluding time-based predictors) over the study period–from January 1, 2013 (00:00) to December 31, 2020 (23:00). The total number of observations is 70128.

| Variable | Mean | Max | Min | SD |
|---|---|---|---|---|
| $CO_2$e Emissions per kWh (g) | 44.70 | 138.50 | 7.00 | 22.73 |
| Air Temperature Index (°C) | 11.89 | 35.72 | -8.63 | 6.93 |
| Solar Radiation Index ($Jm^{-2}$) | 373664 | 2812771 | 0 | 583154 |
| Relative Humidity Index (%) | 93.49 | 99.51 | 71.42 | 4.61 |
| Wind Speed Index ($ms^{-1}$) | 5.83 | 17.43 | 1.06 | 2.06 |
| Total Precipitation Index (m) | $1.19 \times 10^{-4}$ | $1.97 \times 10^{-3}$ | 0 | $1.85 \times 10^{-4}$ |
| Surface Air Pressure Index (Pa) | 98020 | 100514 | 94293 | 813.09 |

#### 3.2.2.2 Empirical modeling of $CO_2$ emissions from electricity production based on climate indices

The relationship between climate indices and $CO_2$ emissions from electricity production is quantified using the Extreme Gradient Boosting (XGBoost) algorithm. XGBoost is a pioneering, highly efficient gradient boosting-based tree ensemble machine learning algorithm that can be used for regression predictive modeling purposes. The algorithm is capable of estimating the (possibly complex nonlinear) relationship between independent and dependent variables by combining the prediction results obtained from several regression trees (for complete details about the algorithm, see Chen and Guestrin, 2016). As is the case with any tree-based algorithm, multicollinearity does not affect the prediction performance of XGBoost. Furthermore, the algorithm does not require input normalization and functions perfectly with skewed distributions, noisy data and outliers.

The regression analysis is conducted using log-transformed $CO_2$ emissions indicator as the dependent variable and 10 independent variables, namely electric power-weighted air temperature, solar radiation, relative humidity, wind speed, total precipitation and surface air pressure indices, together with 4 time-based predictors created with integer encoding: hour of the day, day of the week, month of the year and year). It can be imagined that the learning algorithm could use time-based predictors to help tease out time-of-year, time-of-month or time-of-day

type seasonality information. As with other predictive modeling techniques, the proposed empirical modeling framework does not, in and of itself, establish any direct cause-effect relationship between variables. To be more precise, the utilized approach does not maintain that a change in climate indices directly causes a change in $CO_2$ emissions in the electricity sector. Instead, it evaluates the association, if any, between a change in climate indices and the change in emissions from electricity production. The nature of the weighting scheme for the construction of climate indices (see Section 3.2.2.1) provides a sound conceptual basis for evaluating the predictive relationship between these indices and the target variable.[16]

Chen and Guestrin (2016) define the tree ensemble model of the XGBoost algorithm that uses $K$ additive trained trees to predict the outcome for a dataset with $N$ data points and $p$ explanatory variables $\{(x_i, y_i) \,|\, i = 1, ...N, x_i \in \mathbb{R}^p, y_i \in \mathbb{R}\}$ as

$$\hat{y}_i = \hat{f}(x_i) = \sum_{k=1}^{K} g_k(x_i) \quad g_k \in \mathscr{G} \tag{3.3}$$

where $\mathscr{G} = \{g(x) = w_{q(x)}\}\,(q : \mathbb{R}^p \to J, w \in \mathbb{R}^J)$ is the space of regression trees, $q(x)$ is a function that directs and assigns every data point to the $q(x)$-th leaf of the tree, $w_{q(x)}$ is the weight on the $q(x)$-th leaf, assigned to every data point belonging that leaf, and $J$ is the total number of leaves in the tree. Each $g_k$ features an independent tree structure $q$ and leaf weights $w$ (Chen and Guestrin, 2016).

Every regression tree $g_k$ grows from an initial (root) node and expands to a maximum depth (i.e. the maximum number of nodes allowed from the root to the farthest leaf of a tree) specified outside of the training process. Each internal node of a tree partitions the training data by one of the predictors, and prediction weights are assigned to the new leaves. The tree is eventually pruned with the aim of removing nodes with negative gains. The tree building algorithm (i.e. split finding and assignment of prediction scores) is dependent upon the optimization of an objective function that consists of a training loss and a regularization term to avoid overfitting:

$$Obj = \sum_{i=1}^{N} L(\hat{y}_i, y_i) + \sum_{k=1}^{K} \Omega(g_k) \tag{3.4}$$

where

$$\Omega(g_k) = \gamma J_k + \frac{1}{2}\lambda \sum_{j=1}^{J_k} w_{j,k}^2$$

[16]It should be noted that low-carbon energy sources (nuclear, wind, solar photovoltaics, and hydroelectricity) make, by definition, no contribution to the calculation of emissions indicator in the éCO2mix dataset. In this regard, a climate-driven change in electricity generation from these sources is not directly linked with a change in $CO_2$ emissions. Nonetheless, a climate-induced increase (decrease) in the share of clean (nuclear and renewable) energy sources in electricity production is expected to translate into a decrease (increase) in the share of high-carbon energy sources (coal, fuel oil, gas and biofuel) as major determinants of $CO_2$ emissions.

where $J_k$ is the number of leaves pertaining to the $k$-th regression tree, and $w_{j,k}$ is the prediction weight assigned to the $j$-th leaf of that tree. $L$ is a convex differentiable function (squared error, by default) that measures how the model fits on the training data, $\Omega$ measures the complexity of trees by penalizing large weights and large number of leaves. This latter term helps addressing the bias–variance trade-off. The parameter $\gamma$ is the minimum loss reduction required to make a further partition on a leaf node of the tree, and $\lambda$ is the L2 regularization term on the prediction weights. As is the case with the maximum depth, $\gamma$ and $\lambda$ are not internal to the model, so their values cannot be directly estimated from data. These configuration variables and a few other parameters (together referred to as the model hyperparameters) control the learning process and their values are determined through the hyperparameter tuning process. As argued by Chen and Guestrin (2016), the regularized objective function in Equation 3.4 cannot be minimized using conventional optimization methods. Instead, it is optimized using a modified version of the gradient boosting algorithm in such a way that each added tree improves the model by correcting the errors of the previous one:

$$Obj^{(t)} = \sum_{i=1}^{N} L(y_i, \hat{y}_i^{(t-1)} + g_t(x_i)) + \Omega(g_t) \tag{3.5}$$

where $\hat{y}_i^{(t-1)}$ is the predicted outcome for the $i$-th data point at the $t$-th boosting iteration (refer to Chen and Guestrin, 2016, for complete details on the gradient tree boosting algorithm).

As a complement to the algorithm's principal regularization on the number of leaves and the magnitude of leaf weights, additional measures are adopted to prevent overfitting.[17] First, the learning process is slowed down using the shrinkage technique introduced by Friedman (2002). The shrinkage hyperparameter $\eta$ scales newly added weights after each step of tree boosting, hence reducing the influence of individual trees and leaving space for future trees to improve the model (Chen and Guestrin, 2016). Second, the utilization of stochastic boosting (as an alternative to regular boosting) requires that the algorithm randomly sub-sample, without replacement, rows of the training dataset at every boosting iteration. Third, owing to column sub-sampling, only a proportion of predictors (columns) are used for the construction of each tree. Finally, and most importantly, hyperparameter tuning is carried out using exhaustive grid search with repeated 5-fold cross-validation (number of repetitions=5). For a given hyperparameter configuration, the mean model performance, as measured by root-mean-square error (RMSE), across all folds and all repeats is calculated and the configuration resulting in the minimum average RMSE is chosen as the optimal combination of hyperparameters. The grid search is performed over the parameter values specified in Table 3.3, with the values of the two

[17] While robust measures are taken in the present research to prevent overfitting, the reader should bear in mind that overfitting does not necessarily translate into poor generalization of modern machine-learning methods such as tree-based ensemble algorithms. Belkin et al. (2019) provide empirical evidence on good generalization behavior of overfitted boosted decision trees.

remaining hyperparameters, namely the number of trees used for boosting and $\lambda$, being kept at 100 and 1, respectively. The choice of possible hyperparameter values is made principally according to the suggestions of Boehmke and Greenwell (2019) and Thakur (2020).

Table 3.3: Hyperparameter configurations used for evaluating tree ensemble models.

| Hyperparameter | Range | Default Value | Selected Values for Tuning |
|---|---|---|---|
| $\gamma$ | [0,∞) | 0 | $\{0.1, 1, 10\}$ |
| $\eta$ | [0,1] | 0.3 | $\{0.05, 0.1, 0.2, 0.3\}$ |
| Maximum Depth | $\{1..\infty\}$ | 6 | $\{3..8\}$ |
| Minimum Child Weight | [0,∞) | 1 | $\{7, 10, 20\}$ |
| Column Sample by Tree | (0,1] | 1 | $\{\frac{3}{10}, \frac{5}{10}, \frac{7}{10}\}$ |
| Sub-sample | (0,1] | 1 | {0.3,0.5} |

A lower value of the shrinkage factor $\eta$ makes the model more robust to overfitting. Likewise, decreasing the the maximum depth results in a less complex model that is less likely to overfit. The larger gamma and minimum child weight (minimum sum of hessians needed in a leaf node) are, the more conservative the algorithm will be. Given that there are 1296 configurations in the hyperparameter search space, a total number of $1296 \times 5 \times 5$ tree ensemble models are trained and assessed during the cross-validation process.

Thanks to the usage of row sub-sampling and data splitting techniques during the model training and cross-validation resampling procedures, the probability of a contiguous time series being used is very low, making the utilized algorithm circumvent possible serial correlation. That having been said, the inclusion of numerical time-based predictors (hour of the day, day of the week, month of the year and year) in the machine learning model building guarantees that additional information pertaining to the temporal aspect of the data (such as possible seasonality) is accounted for.

#### 3.2.2.3 Characterizing the predictive impact of climate indices on $CO_2$ emissions from electricity production

The predictive relationship between climate indices and $CO_2$ emissions from electricity production is described in two major steps. First, the statistical significance of each climate index for the prediction of $CO_2$ emissions is assessed through the model-agnostic permutation feature importance algorithm (Breiman, 2001; Fisher et al., 2019). The significance (importance) of a given climate index is evaluated by calculating the increase in model's prediction error (measured by an error function such as RMSE) when the index values are shuffled and the existing association between the index and the original values of the dependent variable ($CO_2$ emissions)

is broken.[18]

The permutation feature importance algorithm takes the trained tree ensemble model $\hat{f}$ with the optimal combination of hyperparameters, the data points $\{(x_i, y_i) \,|\, i = 1, ...N, x_i \in \mathbb{R}^p, y_i \in \mathbb{R}\}$, and a loss (error) function $L$ such as RMSE as inputs, and calculates, in a first step, the original model error $L(y_i, \hat{f}(x_i))$. Next, for each climate index $p$ and at each repetition, the algorithm permutates the variable of interest while retaining the original values of all other explanatory variables. This permutation results in new feature vectors $x_i^{perm:p}$ that are then used to compute the model error $L(y_i, \hat{f}(x_i^{perm:p})$ based on the predictions of the permuted data. Finally, the feature importance measure of the climate index $p$ (denoted by $\text{FI}_p$) is computed as the ratio $L(y_i, \hat{f}(x_i^{perm:p})/L(y_i, \hat{f}(x_i))$.

To construct the null distribution of importance measures and allow for a permutation null hypothesis testing ($H_0 : \text{FI}_p = 1$), the algorithm is repeated a sufficiently large number of times (1000 times in the present study). The larger the increase in model's prediction error (loss) after shuffling an explanatory variable, the more important that variable is for predicting the outcome. Conversely, if permuting the values of a given explanatroy variable leaves the prediction error unchanged, it could be concluded that the predictive model takes little account of the variable for making predictions (Molnar, 2020). More concretely, the climate index $p$ is important, at the significance level $\alpha$, for predicting $CO_2$ emissions, if $\text{FI}_p$ does not contain 1 in its $(1-\alpha)$ confidence interval.

As a second step to characterize the predictive impact of climate indices on $CO_2$ emissions from electricity production, the main effects of individual indices and their second-order interaction effects are estimated and visualized using the accumulated local effects (ALE) approach (Apley and Zhu, 2020). ALE is a model-agnostic, computationally fast, post hoc interpretation method that describes the pure (possibly nonlinear) effect of each explanatory variable on the target variable by blocking the effects of other variables. Unlike other machine learning interpretation methods (e.g. partial dependence plots), ALE is unbiased with correlated predictors as it uses the conditional distribution of features (Molnar, 2020). Nevertheless, if explanatory variables are highly correlated, ALE curves require careful interpretation (see Section 3.4).

For a single numerical explanatory variable, ALE values are estimated as follows. First, the variable of interest is split into multiple intervals. For the sake of the present analysis, the (unique) percentiles of the distribution of variables are used to define such intervals.[19] Next, for

[18]This permutation also breaks the existing association between the index and other explanatory variables. Consequently, the permutation feature importance algorithm takes into consideration all possible interactions among explanatory variables. The disadvantage is that the importance of any interaction between a pair of variables is included in the feature importance of both variables. In addition, in the presence of a strong correlation between explanatory variables, the algorithm can be biased by unrealistic data points. For detailed description of advantages and disadvantages of this algorithm, please refer to Molnar (2020).

[19]There is no hard-and-fast rule for choosing the number of intervals. A small number of intervals results in not very accurate ALE estimates, whereas if the number is too large, ALE curves can become unstable and shaky (Molnar, 2020). Using percentiles for defining the ALE evaluation intervals warrants that the same number of data

the data points in a given interval, the difference in the model's prediction is calculated when the values of the variable concerned are replaced with the upper and lower bounds of the interval. These differences are then accumulated over the conditional distribution across all intervals and centered (so that mean effect over the data is zero), resulting in the ALE curve (Apley and Zhu, 2020; Molnar, 2020). Each point on the curve thus represents the difference with average model's prediction. Formally speaking, for a given numerical predictor $p$, the mean-centered accumulated local effect at a certain value $x$ is estimated as

$$\hat{f}_{p,ALE}(x) = \hat{\tilde{f}}_{p,ALE}(x) - \frac{1}{N}\sum_{l=1}^{L} n_p(l)\hat{\tilde{f}}_{p,ALE}(z_{l,p}) \tag{3.6}$$

where

$$\hat{\tilde{f}}_{p,ALE}(x) = \sum_{l=1}^{l_p(x)} \frac{1}{n_p(l)} \sum_{i:x_p^{(i)} \in N_p(l)} \left[\hat{f}(z_{l,p}, x_{\setminus p}^{(i)}) - \hat{f}(z_{l-1,p}, x_{\setminus p}^{(i)})\right]$$

Here, $N$ is the total number of data points, $L$ is the number of evaluation intervals, $N_p(l)$ signifies the $l^{\text{th}}$ interval (aka neighborhood) among the intervals into which the distribution of the predictor $p$ is split, and $n_p(l)$ is the number of data points whose value of the predictor $p$ lies within the interval $N_p(l)$. Lower and upper limits of the interval are represented by $z_{l-1,p}$ and $z_{l,p}$, respectively. In the estimation of the the uncentered ALE ($\hat{\tilde{f}}_{p,ALE}(x)$), the outer sum runs from the first interval up to and including the interval $l_p(x)$ to which the value $x$ belongs. The ALE value obtained from Equation 3.6 can be interpreted as the main (first-order) effect of the climate index $p$ at a certain value $x$ compared to the average prediction of $CO_2$ emissions over the data.

Using the same notation as before, the second-order (interaction) effect of two predictors $p$ and $q$ at a certain value $(x_p, x_q)$ is estimated as

$$\hat{f}_{\{p,q\},ALE}(x_p, x_q) = \hat{\tilde{f}}_{\{p,q\},ALE}(x_p, x_q) - \frac{1}{N}\sum_{l=1}^{L}\sum_{m=1}^{L} n_{\{p,q\}}(l,m)\hat{\tilde{f}}_{\{p,q\},ALE}(z_{l,p}, z_{m,q}) \tag{3.7}$$

points lies in each of the intervals. This choice however has a disadvantage in that the length of intervals may be very different. Therefore, caution is needed in interpreting interval-wise effects in the case of skewed distributions.

where

$$\hat{\tilde{f}}_{\{p,q\},ALE}(x_p,x_q) = \hat{g}_{\{p,q\},ALE}(x_p,x_q) - \sum_{l=1}^{l_p(x_p)} \frac{1}{n_p(l)} \sum_{m=1}^{L} n_{p,q}(l,m) \left[\hat{g}_{\{p,q\},ALE}(z_{l,p},z_{m,q}) - \hat{g}_{\{p,q\},ALE}(z_{l-1,p},z_{m,q})\right] - \sum_{m=1}^{l_q(x_q)} \frac{1}{n_q(m)} \sum_{l=1}^{L} n_{p,q}(l,m) \left[\hat{g}_{\{p,q\},ALE}(z_{l,p},z_{m,q}) - \hat{g}_{\{p,q\},ALE}(z_{l,p},z_{m-1,q})\right]$$

The uncentered effect $\hat{g}_{\{p,q\},ALE}(x_p,x_q)$ defined in Equation 3.7 is estimated by

$$\hat{g}_{\{p,q\},ALE}(x_p,x_q) = \sum_{l=1}^{l_p(x_p)} \sum_{m=1}^{l_q(x_q)} \frac{1}{n_{\{p,q\}}(l,m)} \sum_{i:x^{(i)}_{\{p,q\}} \in N_{\{p,q\}}(l,m)} \left\{ \hat{f}(z_{l,p},z_{m,q},x^{(i)}_{\setminus\{p,q\}}) - \hat{f}(z_{l-1,p},z_{m,q},x^{(i)}_{\setminus\{p,q\}}) - \left[\hat{f}(z_{l,p},z_{m-1,q},x^{(i)}_{\setminus\{p,q\}}) - \hat{f}(z_{l-1,p},z_{m-1,q},x^{(i)}_{\setminus\{p,q\}})\right] \right\} \tag{3.8}$$

The calculation principles remain the same as for estimating the main effect of a single predictor, except that instead of one-dimensional intervals, rectangular cells are utilized to accumulate the effects in two dimensions[20] (Molnar, 2020). The method of estimation of second-order ALE values is adjusted to take account of the overall mean effect, as well as the main effects of both predictors. Indeed, the estimated ALE value for two explanatory variables can be interpreted as the the additional interaction effect of the variables after the main effects of the variables are accounted for (see Apley and Zhu, 2020; Molnar, 2020, for complete details on the estimation of first and second-order ALE). The notation and concepts used in the estimation of first and second-order ALE are schematically illustrated in Figure 3.2.

Before proceeding to the analysis results, it would be well to remark that data preparation, empirical modeling, statistical computing and graphics in the present study are carried out in R software environment (R Core Team, 2020; Kuhn, 2008; Molnar et al., 2018).

## 3.3 Results

The first step to characterize the relationship between climate indices and $CO_2$ emissions from electricity production is to find the model architecture with the maximized performance on the given data set. This is achieved through cross-validation and hyperparameter tuning. Exhaus-

[20]Unlike percentile-based first-order ALE estimation which guarantees the same number of data points in all evaluation intervals (note that the intervals may still have very different lengths), second-order ALE estimation inevitably uses a different number of data points to calculate the local effect in each rectangular cell. As a consequence, estimates have a different accuracy across the feature space–although they are still the best attainable estimates of second-order effect (Molnar, 2020)

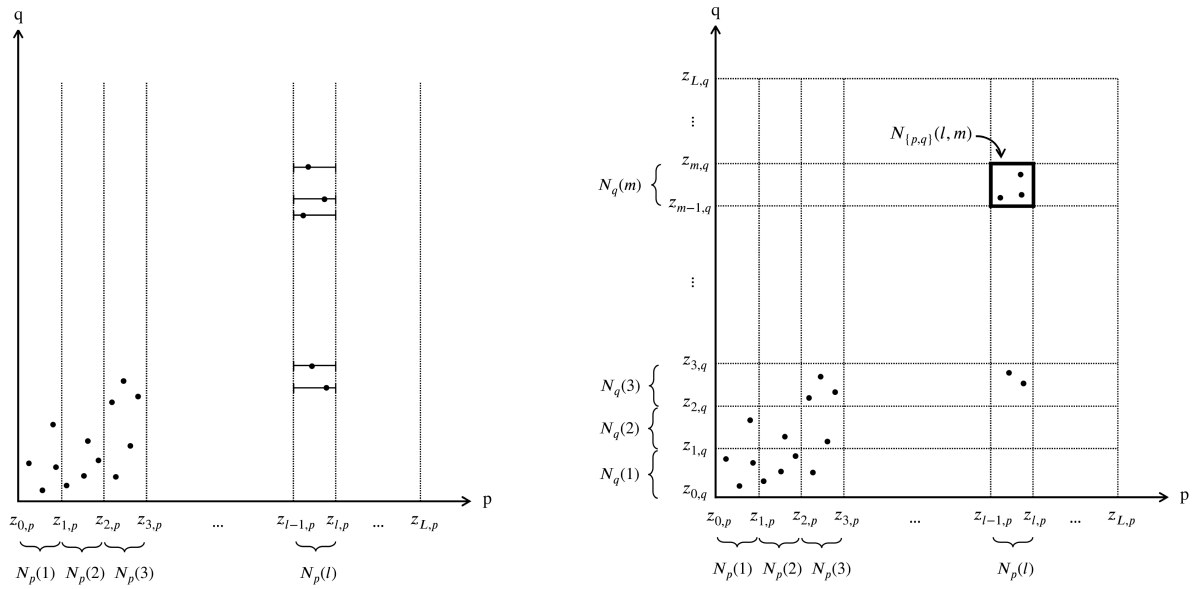


Figure 3.2: Simplified schematic illustration of the notation and concepts utilized for computing the first-order ALE of the $p^{th}$ predictor for a model with two predictors $p$ and $q$ (left), and the second-order ALE of the $p^{th}$ and $q^{th}$ predictors (right). Illustrations are reproduced from Apley and Zhu (2020).

tive grid search through the specified subset of the hyperparameter space with 1296 unique configurations (see Section 3.2.2.2) results in the following optimal hyperparameters for the learning algorithm, pertaining to minimum average RMSE across all folds: $\gamma = 0.1$; $\eta = 0.2$; Maximum Depth $= 8$; Minimum Child Weight $= 10$; Column Sample by Tree $= 0.7$ and Sub-sample $= 0.5$. The average RMSE and $R^2$ across all folds for the best model are 0.2043 and 0.8643, respectively.

Once the the model with the best tune is obtained from hyperparameter optimization, the statistical significance of each climate index for the prediction of $CO_2$ emissions is evaluated using the permutation feature importance algorithm. Figure 3.3 presents permutation feature importance measures (based on 1000 repetitions) for the six climate indices. It can be seen from this figure that the 90% confidence intervals for feature importance estimates do not contain 1, hence leading to the rejection of the null hypothesis ($H_0 : \text{FI}_p = 1$) at the 0.1 significance level. This compressed global insight into the model's behavior substantiates that all of the six climate factors identified as potential drivers of $CO_2$ emissions in the electricity sector are indeed relied upon as important features for predicting emissions. Different indices, however, do not bear equal importance for the prediction. The air temperature index proves to be the most important predictor of $CO_2$ emissions in the French electric sector (median importance$= 1.726$), followed by the wind speed index (median importance$= 1.63$). On the other side, the relative humidity and total precipitation indices are of the least importance for the prediction of electricity generation-related $CO_2$ emissions, with median importance of 1.162 and 1.195, respectively. Unsurprisingly and in support of the great attention given to air temperature as a

key determinant of energy-related emissions in the existing literature, the air temperature index has been identified as the most relied-upon feature for the prediction of $CO_2$ emissions from electricity production in France from 2013 to 2020. As to the comparatively low importance of the relative humidity and surface air pressure indices for the prediction of $CO_2$ emissions in the electricity sector,[21] the findings of this evaluation accords with evidence from previous observations (e.g. Arrieta and Lora, 2005; Bull et al., 2007; Ebinger and Vergara, 2011; González-Díaz et al., 2017) that climate impacts on the efficiency of fossil-fuel-fired, nuclear, and biomass-fired power plants tend to be relatively small. In any case, the results indicate that surface air pressure bears more importance, in comparison with relative humidity, for the prediction of emissions.

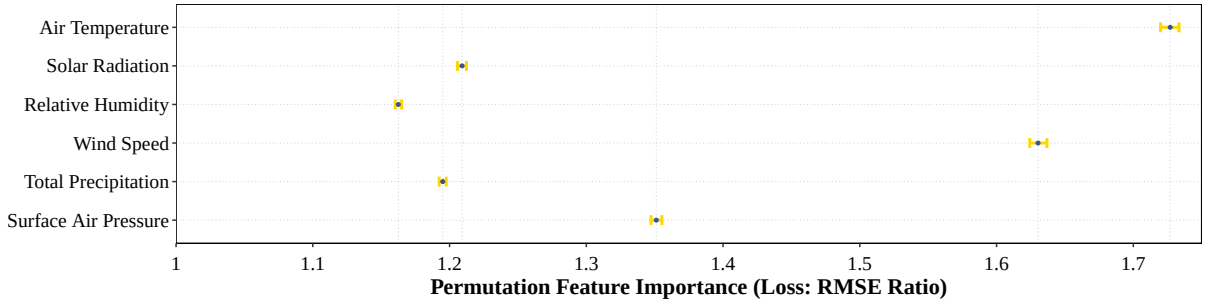


Figure 3.3: Permutation feature importance measures (RMSE ratios) for the six electric power-weighted climate indices. I-shaped bars represent 5% to 95% inter-quantile ranges of importance values from 1000 repetitions. The solid dot within the interval signifies median importance.

Evaluation of the predictive impact of climate indices on $CO_2$ emissions from electricity production is accompanied by the estimation and visualization of first-order (main) and second-order (interaction) effects of indices. Figure 3.4 illustrates first-order (main) ALE plots of different electric power-weighted climate indices. The line graph in each individual panel of this figure represents the change in predicted emissions when the selected index has the given value, compared to the average model prediction. From Figure 3.4, it is apparent that there exists a nonlinear predictive relationship between climate indices and $CO_2$ emissions from electricity generation in France over the study period.

As would be expected, the ALE of $CO_2$ emissions exhibits a U-shaped response to the electricity demand-weighted air temperature index. The main effect of air temperature is persistently higher than average prediction of the data at values below 7.40°C (corresponding to the $29^{th}$ percentile of index values) and above 24.03 °C (corresponding to the $94^{th}$ percentile). When the value of the air temperature index is between 7.40°C and 24.03 °C (corresponding to the 29%-94% inter-quantile range), the model prediction is lower than the average predic-

[21]The average annual share of the aggregate of fossil fuel, nuclear and biofuel powers (i.e. relevant power indicators for relative humidity and surface air pressure) in total electricity production in France over the 2013-2020 period was 81.61%. If relative humidity and surface air pressure exerted considerable influence on the generation cycle and cooling efficiency of these types of power plants, the learning model would rely heavily on the relative humidity and surface air pressure indices for the prediction of emissions in the electricity sector.

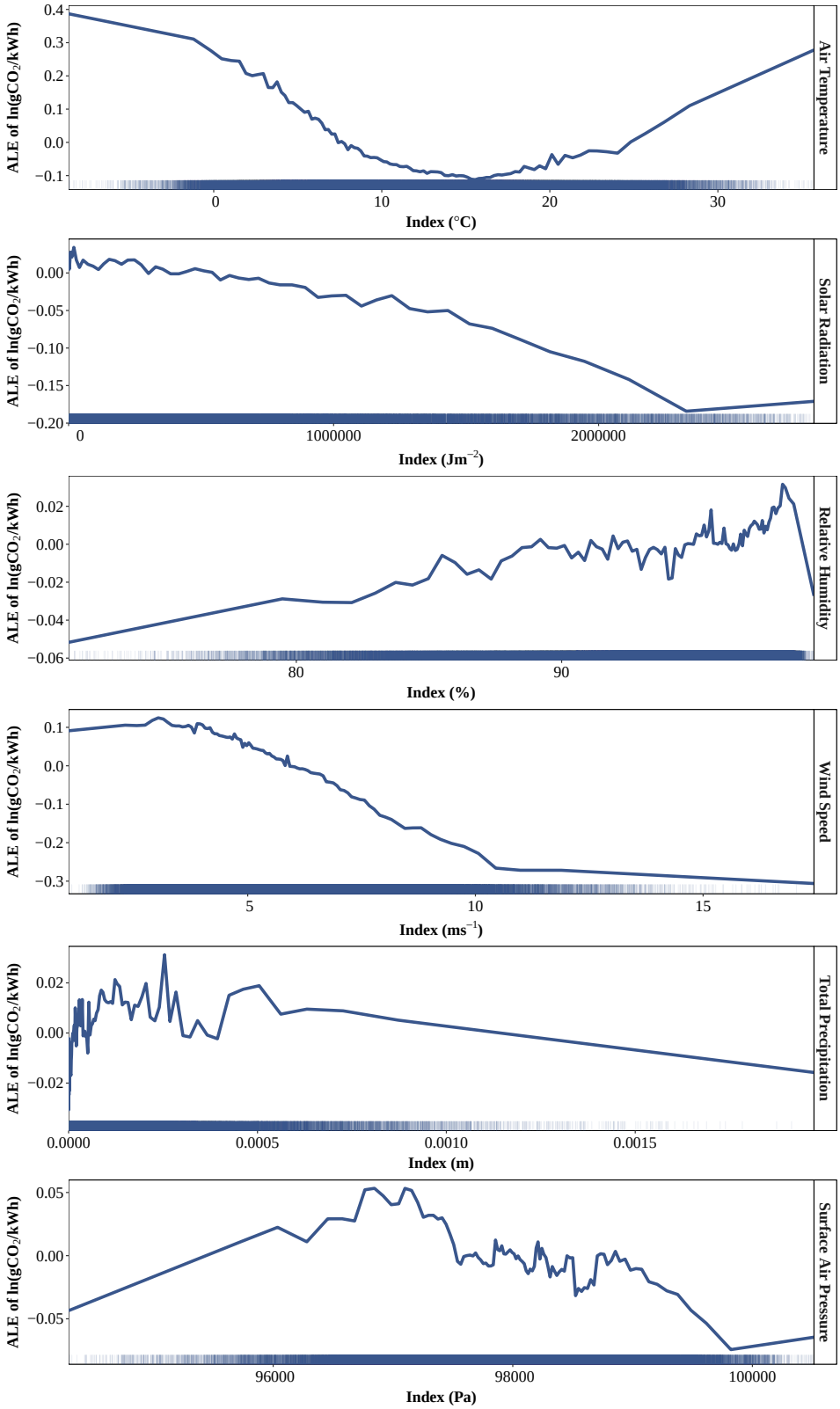


Figure 3.4: First-order (main) mean-centered accumulated local effects (ALE) of electric power-weighted climate indices on the prediction of $CO_2$ emissions from electricity production over the study period (2013-2020). The distribution of data points for each index is displayed on the margin of horizontal axis.

tion, and the global minimum feature effect pertains to 15.56°C (corresponding to the 69$^{th}$ percentile), where the model prediction is lower by 0.11 compared to the average prediction. These findings broadly support the work of other studies linking electricity demand and air temperature.[22] In accordance with the present results, previous studies have demonstrated that there exists a U-shaped relationship between electricity consumption and air temperature, with the vertex point ranging between 11.5°C and 16°C depending on the region under study (see Moral-Carcedo and Vicéns-Otero, 2005; Bessec and Fouquau, 2008; Lee and Chiu, 2011).

Moving to the second panel of Figure 3.4, it can be seen that the average prediction decreases in general with increasing solar radiation, albeit in a non-monotonic fashion. Above the index value of 572,707 Jm$^{-2}$ (corresponding to the 74$^{th}$ percentile), the pure effect of solar radiation on the prediction of emissions is negative in all intervals. At index values below 572,707 Jm$^{-2}$, model predictions in the majority of intervals are marginally greater than average prediction. This result is in agreement with expectations that higher photovoltaic solar power potential–resulting from high solar radiation–can be associated with the reduction of carbon emissions in the electricity sector.

Up to the index value of 94.64% (corresponding to the 46$^{th}$ percentile) for relative humidity, model predictions are lower than average predictions in the vast majority of intervals, although the ALE curve does not exhibit a monotonic behavior across such intervals. At index values from 94.64% to 98.74% (corresponding to the 46%-99% inter-quantile range), the estimated pure effect of relative humidity on the prediction of $CO_2$ emissions is positive in most intervals. These results seem to corroborate the hypothesis that the cooling efficiency of thermal and nuclear power plants decreases with increasing atmospheric humidity (Wilbanks et al., 2008), potentially leading to higher emissions from electricity production. Interestingly, however, the ALE of $CO_2$ emissions drops significantly at the relative humidity index values above 98.74%. One plausible explanation for this observation is that, at extremely high relative humidity values, the reduced efficiency of nuclear and fossil fuel-fired power generation (which could lead to increased emissions) is offset by an increase in net river runoffs due to high humidity, even when precipitation is unchanged (Milly et al., 2005; Ebinger and Vergara, 2011). This could have major impacts on the availability of hydropower resources and the amount of electricity generation from hydropower plants–as a replacement for fossil fuels' electricity production, hence making the main effect of relative humidity on $CO_2$ emissions be negative at the extreme right tail of the distribution.

The ALE curve of wind speed reveals an overall decreasing (yet non-monotonic) behavior starting from the index value of about 3.03 ms$^{-1}$ (corresponding to the 5$^{th}$ percentile). This speed is within the typical cut-in speed range for modern land-based wind turbines (3-5 ms$^{-1}$),

[22] As argued by Ampudia et al. (2022), in the short run and given production rigidities, higher demand for electricity is expected to translate directly into an increase in emissions.

i.e. the speed at which turbines start to rotate and generate electricity. At wind speed values above 5.92 $ms^{-1}$ (corresponding to the $59^{th}$ percentile), the model prediction is consistently lower than the average prediction in all evaluation intervals. This confirms the concept that increased wind power potential (owing to higher wind speeds) is generally associated with an increase in the share of wind energy and decrease in $CO_2$ emissions from electricity production.

As regards total precipitation, no evidence is found for persistent below-average (above-average) predictions in upper (lower) percentiles of the distribution. Up to the index value of $1.19 \times 10^{-5}$ m (corresponding to the $31^{st}$ percentile), the main effect of total precipitation on emissions is negative in all intervals. From $1.19 \times 10^{-5}$ m to $8.71 \times 10^{-4}$ (corresponding to the 31%-98% inter-quantile range), the feature effects take positive and negative values around zero, with more intervals bearing positive ALE values. At extremely high index values (above around $1.12 \times 10^{-3}$ m, corresponding to the $99^{th}$ percentile), however, the model predicts lower values of $CO_2$ emissions with respect to the average prediction. These findings suggest that, except in the case of heavy precipitation, increase in precipitation–isolated of all other climate factors–may not always be associated with a decrease in $CO_2$ emissions from electricity production at hourly scale.

Finally, the ALE curve shown in the bottom panel of Figure 3.4 indicates a quasi inverted-U-shaped relationship between predicted emissions (relative to the average prediction) and the surface air pressure index. The main feature effect of surface air pressure is negative in the first percentile (below the index value of 95719 Pa) and in the overwhelming majority of intervals pertaining to index values above 98027 Pa (corresponding to the $48^{th}$ percentile). For the intervals in which the surface pressure index value is within the 1%-48% inter-quantile range (between 95719 Pa and 98027 Pa), ALE estimates are mostly positive, and the peak of the curve is attained at the $8^{th}$ percentile. Owing to the fact that empirical research to date has not yet determined the magnitude and extent of air pressure influence on net power plant efficiency (see Loew et al., 2020), these exploratory findings are to be further scrutinised before they can provide immediately dependable conclusions about the nature and mechanisms of surface air pressure effect on $CO_2$ emissions from electricity production.

Analysis of the combined effects of multiple climate factors on the prediction of $CO_2$ emissions is made possible by the estimation and visualization of second-order accumulated local effects. Second-order ALE plots cast light on possible hidden information that first-order plots fail to capture. Figure 3.5 presents second-order (interaction) effects of different pairs of electric power-weighted climate indices. In the estimation of second-order ALE, the main effect of each index (as shown in first-order ALE plots, Figure 3.4) is already taken into account, and the plot shows only the additional interaction effect of the two predictors on the outcome.

Figure 3.5 reveals a noteworthy interaction between some pairs of climate indices. What

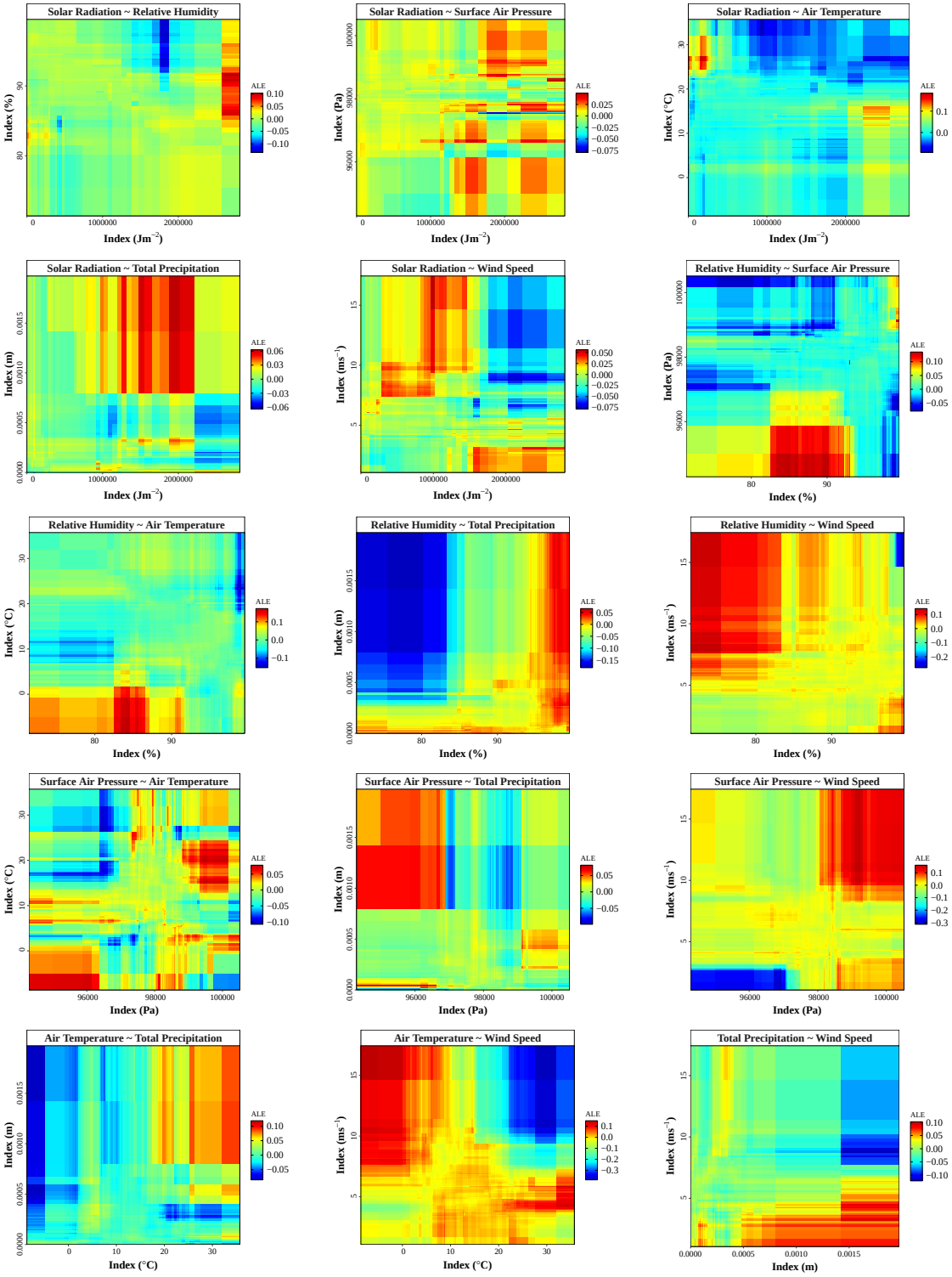


Figure 3.5: Second-order (interaction) mean-centered accumulated local effects (ALE) and partial dependence plots support (for cells outside the data distribution) of all pairs of electric power-weighted climate indices in predicting $CO_2$ emissions from electricity production over the study period (2013-2020). The horizontal (vertical) axis in each subplot (panel) represents the first (second) climate index appearing in the title of the subplot.

stands out in this figure is the interaction of relative humidity and surface air pressure with total precipitation and wind speed, as well as the interaction between air temperature and wind speed.

Below the index value of around 85% (corresponding to the $7^{\text{th}}$ percentile) for relative humidity, and above the index value of around $3 \times 10^{-4}$ m (corresponding to the $87^{\text{th}}$ percentile) for total precipitation, predictions are remarkably lower than average, when the main effects are already taken into consideration. When relative humidity is above 95% (corresponding to the median), the additional interaction effect of relative humidity and total precipitation is positive. When total precipitation is below around 85% (corresponding to the $7^{\text{th}}$ percentile) and wind speed is above around 7.5 $\text{ms}^{-1}$ (corresponding to the $81^{\text{st}}$ percentile), a notable additional positive effect on predicted emissions is observed. In summary, a climate with low relative humidity and high precipitation decreases predicted $CO_2$ emissions, whereas arid and windy climate increases the prediction when the main effects of the corresponding indices are accounted for.

Up to the index value of around 96500 Pa (corresponding to the $4^{\text{th}}$ percentile) and for total precipitation values above $8 \times 10^{-4}$ m (corresponding to the $98^{\text{th}}$ percentile), predictions are noticeably higher than average when the main effects are already considered. Simply put, high levels of precipitation together with low-to-moderate atmospheric pressure have an additional positive effect on predicted $CO_2$ emissions from electricity production. Apropos the interaction between the surface air pressure and wind speed indices, an additional negative effect on predicted emissions is observed when surface air pressure is below around 97000 Pa (corresponding to the $10^{\text{th}}$ percentile) and wind speed is below around 3 $\text{ms}^{-1}$ (corresponding to the $5^{\text{th}}$ percentile). An additional positive effect on the prediction can be clearly observed when surface air pressure is above around 98000 Pa (corresponding to the $46^{\text{th}}$ percentile) and wind speed is above around 7.5 $\text{ms}^{-1}$ (corresponding to the $81^{\text{st}}$ percentile). The latter result is interesting, since the individual first-order (main) effects of surface air pressure and wind speed are mostly negative in medium-to-high-pressure and high-wind conditions, respectively (see Figure 3.4). In essence, in low wind speeds and low pressures, the combined effect of surface air pressure and wind speed on predicted emissions is smaller than the sum of the main effects, whereas in medium-to-high-pressure and windy climate conditions, the combined effect of the two climate factors is larger than the sum of the main effects.

At temperatures below 3°C (corresponding to the $9^{\text{th}}$ percentile of index values) and wind speeds above around 7.5 $\text{ms}^{-1}$ (corresponding to the $81^{\text{st}}$ percentile), model predictions are remarkably higher than average when the main effects are already taken into account. When temperature is above around 23°C (corresponding to the $93^{\text{rd}}$ percentile) and wind speed is above around 10 $\text{ms}^{-1}$ (corresponding to the $96^{\text{th}}$ percentile), an additional negative effect on predicted emissions can be observed. Put simply, at high (low) temperatures and high wind speeds, the combined effect of air temperature and wind speed on $CO_2$ emissions from electricity production is noticeably smaller (larger) than the sum of the main effects.

A closer examination of the remaining subplots of Figure 3.5 suggests the existence of some notable interaction between other pairs of climate indices (e.g., solar radiation and air temperature; solar radiation and total precipitation; relative humidity and surface air pressure; total precipitation and wind speed) as well. At temperatures above around 23°C (corresponding to the 93$^{\text{rd}}$ percentile of index values) and solar radiations above around 950,000 Jm$^{-2}$ (corresponding to the 84$^{\text{th}}$ percentile of index values), an additional negative effect on predicted emissions from electricity production is observed. It should be reminded that the main effects of air temperature and solar radiation indicate an increase in predicted emissions in hot hours and a decrease in predicted emissions in sunny hours, compared to the average prediction and isolated from other climate factors. In hot and sunny climate, the combined effect of air temperature and solar radiation is therefore not the sum of the main effects, but smaller than the sum. Additionally, above the index value of around $7 \times 10^{-4}$ m (corresponding to the 97$^{\text{th}}$ percentile) for total precipitation and for solar radiation values between $1.3 \times 10^{6}$ and $2.2 \times 10^{6}$ Jm$^{-2}$ (corresponding to the 90%-98% inter-quantile range), predictions are remarkably higher than average, when the main effects are already taken into consideration. Besides, below the index value of around 96000 Pa (corresponding to the 2$^{\text{nd}}$ percentile) for surface air pressure and for relative humidity values between 82% and 92% (corresponding to the 3%-28% inter-quantile range), model predictions are remarkably higher than average, when the main effects are already taken into consideration. In low humidity and low air pressure, the combined effect of relative humidity and surface air pressure is larger than the sum of the main effects. Ultimately, when total precipitation is above around $1.12 \times 10^{-3}$ m (corresponding to the 99$^{\text{th}}$ percentile), predictions are remarkably higher (lower) than average in low (high) percentiles of the wind speed index (i.e. below around 4 ms$^{-1}$, corresponding to the 18$^{\text{th}}$ percentile, and above around 7.5 ms$^{-1}$, corresponding to the 81$^{\text{st}}$ percentile), when the main effects are already taken into account. For the sake of brevity, and in order to avoid repetition of the data included in the figure, modest, ambivalent or less pronounced interactions between climate indices are not described here.

## 3.4 Discussion

Unlike many other models, decision tree ensembles (e.g. Extreme Gradient Boosting) are able to learn from data even when explanatory variables are highly (or perfectly) correlated. Correspondingly, the permutation feature importance algorithm and accumulated local effects (ALE) can very well handle correlated predictors. Notwithstanding, a strong correlation between explanatory variables calls for careful interpretation of feature importance and ALE estimates. According to Molnar (2020), highly correlated predictors can bias feature importance estimates by introducing unrealistic (unlikely) data instances. In addition, the permutation feature importance algorithm may underestimate the importance of each of the two correlated variables by dividing the importance between them. In analyzing first-order ALE estimates, one should note

that an interpretation of the effect across intervals (i.e. comparison of changes in the main effect of a variable–relative to the average prediction–at different values, assuming that the values of other variables are fixed) is not allowed if predictors are strongly correlated[23] (Molnar, 2020). Since the effects are calculated per interval using different data points, the interpretation of ALE estimates should be local, especially if predictors are strongly correlated.

Pairwise correlation analysis of the electric power-weighted climate indices reveals a weak (yet significantly different from zero, due to large sample size) linear correlation between all distinct pairs of predictors (magnitude of Pearson correlation coefficients $< 0.4$), with the exception of solar radiation-relative humidity ($r = -0.77$), air temperature-relative humidity ($r = -0.67$), solar radiation-air temperature ($r = 0.56$) and total precipitation-surface air pressure ($r = -0.51$). Given this, a perhaps more meaningful and practical measure of the strength of association between variables (also known as effect size) is the coefficient of determination ($R^2$) from a linear model trained on each pair of indices, which explains the proportion of variation in one climate index accounted by its association with another index. Figure 3.6 presents a pairwise scatter plot, along with density plots of the electric power-weighted climate indices and a pairwise linear model-based variance explained, evaluating how changes in one variable affect the changes in another variable. The proportion of the variation in any climate index that is predictable from another index does not exceed 0.59 (the value obtained for solar radiation and relative humidity). Even though the results indicate no association of practical importance between any pair of explanatory variables used to build the modeling framework, caution is advised when interpreting the permutation feature importance and the ALE curve of relative humidity, solar radiation, air temperature, surface air pressure and total precipitation.

Although this study is, to the best of the author's knowledge, the most comprehensive account to date of climatic factors behind $CO_2$ emissions in the French electricity sector, it does suffer from a number of limitations. Firstly, in order to simplify the interpretation process, the weighting scheme used in the construction of electric power-weighted climate indices (Section 3.2.2.1) considers only the "principal" mechanism through which climate variables can affect $CO_2$ emissions in the electricity sector. For instance, the present approach presumes that air temperature induces changes in emissions from electricity production via affecting electricity demand, and therefore bases the construction of climate indices on the relative share of the homogeneous climate regions in the national electricity consumption. This, however, is not the sole mechanism through which air temperature can exert its emission-altering effect. Air temperature may as well have an influence on renewable and non-renewable electricity generation. Higher air temperatures can reduce water storage and power output of hydroelectric facilities

[23]The rationale behind such constraint derives from the fact that, if two predictors are highly correlated, analyzing the effect of changing both predictors jointly should be favored over the analysis of the individual effect of each predictor separately. This disadvantage is, however, a general problem of using strongly correlated explanatory variables for empirical modeling, and is not specific to the interpretation of ALE estimates.

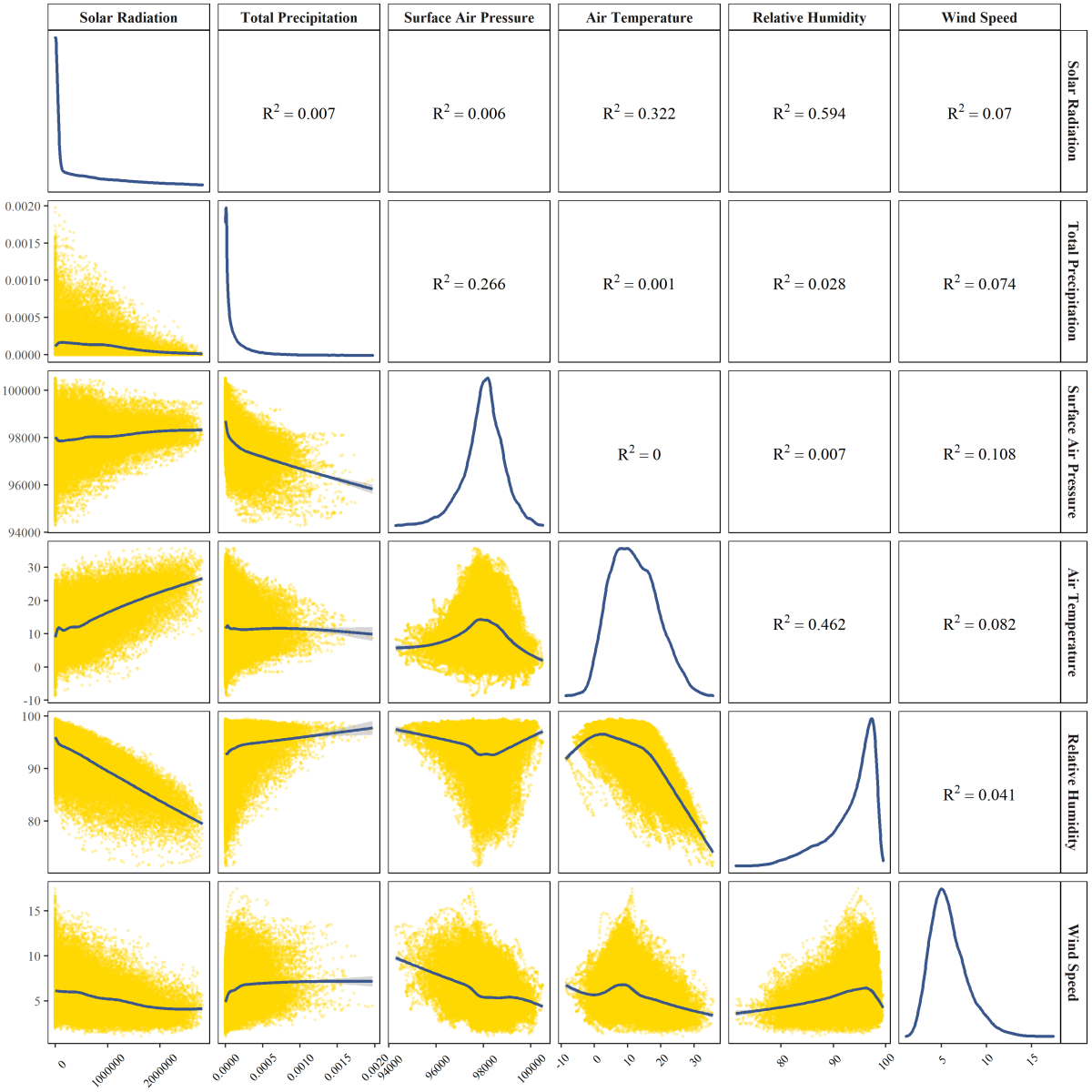


Figure 3.6: Pairwise scatter plot of electric power-weighted climate indices, accompanied by smoothed conditional means using generalized additive model with integrated smoothness as the smoothing method (lower triangular portion of matrix); Density plots of climate indices (main diagonal of matrix); Pairwise coefficient of determination ($R^2$), or the proportion of variation in an index that is predictable from another index (upper triangular portion of matrix).

(via increasing surface water evaporation), decrease the power output of wind turbines (by causing a slight decline in air density), and negatively affect the efficiency and power output of solar photovoltaic cells (see Solaun and Cerdá, 2019, for an extensive account of climate change impacts on renewable energy generation). Furthermore, air temperature is significantly and positively correlated with surface water temperature (Seyedhashemi et al., 2022)–a variable that is directly linked with cooling and generation cycle efficiency of fossil-fuel-fired, nuclear, and biomass-fired plants (Ebinger and Vergara, 2011; Van Vliet et al., 2012). The non-uniqueness of

the impact mechanism is not limited to air temperature. Wind speed and total precipitation may also influence seemingly-irrelevant power indicators. In addition to affecting the supply of wind power, changes in wind speed can have minor implications for solar photovoltaic power generation (Solaun and Cerdá, 2019). Regional precipitation levels affect water availability–a variable of special significance for thermoelectric power generation potential (Van Vliet et al., 2012), and can reduce the efficiency of solar photovoltaic cells as well (Solaun and Cerdá, 2019). This very limitation of the weighting scheme comes in the shape of the trade-off between the comprehensiveness (complexity) of constructed climate indices and the interpretability of results. In future investigations, it might be possible to incorporate all potential impact mechanisms pertaining to each climate variable into the design and construction of electric power-weighted national climate indicators.

Secondly, a central assumption of the proposed weighting scheme is that electricity consumption and power generation by different energy sources are uniformly distributed over metropolitan regions. In other words, it is assumed that the share of any given segment of a metropolitan region in the regional electricity consumption and production is proportional to the geographical area of the segment. While this assumption may not be perfectly realistic from an empirical point of view, it is an unavoidable part of the proposed weighting scheme for two interconnected reasons. First, homogeneous climate regions extend over multiple metropolitan regions of France, and no climate class is exclusive to one metropolitan region. Second, power indicators data are not available at a more granular level than metropolitan regions, making it impossible to intersect climate classes with metropolitan regions in a more accurate manner–in the sense of the contribution that each metropolitan region makes to a climate class's electricity consumption and production. That said, this limitation applies only to 75% of metropolitan regions, and does not concern three regions (Hauts-de-France, Île-de-France, and Centre-Val de Loire) whose entire geographical areas are covered by a single climate class (i.e. Temperate).

On another note, an arguable weakness of the proposed weighting scheme is the tacit assumption that a climate-driven increase (decrease) in the share of a given low-carbon power generation technology (nuclear, wind, solar photovoltaics, and hydroelectricity) is inevitably counterbalanced by a decrease (increase) in the share of high-carbon energy sources (coal, fuel oil, gas and biofuel) as major drivers of $CO_2$ emissions in the electricity sector. While this assumption holds at an upper level (i.e. when considering nuclear, wind, solar photovoltaics, and hydroelectricity as a "whole package" of clean energy sources, distinguished from the set of polluting energy sources such as coal, fuel oil, gas and biofuel), it may not hold for individual low-carbon power generation technologies. For example, an increase (decrease) in the share of wind energy due to greater (smaller) availability of wind resources may be offset by a decrease (increase) in the share of other non-polluting energy sources (e.g. nuclear, hydroelectricity, etc.)

and not necessarily fossil-fuel fired electricity generation.[24] Future research should therefore concentrate on the investigation of the short and long-run elasticity of inter-fuel substitution between different (intermittent) renewable energy sources, between nuclear and renewable energies, and between different fossil fuels and nuclear/renewable resources (see Kumar et al., 2015; Percebois and Pommeret, 2019; Kim, 2019, as some relevant works in this area) to devise a more refined method for estimating climate impacts on $CO_2$ emissions in the French electricity industry.

Analysis of simultaneous effects of different pairs of electric power-weighted climate indices on predicted emissions from electricity production is a major step towards a deeper understanding of the emission sensitivity of the French power system to changing climate conditions, and should make an important contribution to the literature on explanatory factors for such emissions. Nevertheless, several questions remain unanswered at present as to the theoretical and technical basis for why any two climate factors should have extra, non-additive effects on $CO_2$ emissions in the electricity sector. A full discussion of the amalgamated "mechanism of action" of multiple climate factors in re emissions from electricity generation lies beyond the scope of this study and is left for future work. Additionally, the implications of the findings of the current study for climate-energy research and policy need to be further explored in light of climate uncertainty and future, potentially renewable-intensive, power system planning (i.e. energy scenarios). Comprehensive uncertainty quantification and sensitivity analysis of emissions in the French power system vis-à-vis climate change and variability are high on the agenda for future research.

In the provision of climate-related renewable energy production, as a substitute for nuclear and carbon emitting electricity generation, the current study has found that wind speed is the most important climatic predictor of $CO_2$ emissions in the French electricity sector. Comparatively, solar radiation and total precipitation (in decreasing order of importance) are less relied upon by the model for the prediction of emissions. Alterations to the share of electricity generation from renewable energy sources is assumed by the present study to be the sole mechanism through which wind speed, solar radiation and total precipitation may exert an influence on predicted electricity generation-related $CO_2$ emissions. In this regard, higher importance of the wind speed index than the solar radiation index for the prediction of emissions may be explained by the larger share of wind electricity generation compared to that of solar photovoltaic energy in France. The average annual share of wind and solar photovoltaic power in total electricity production in France over the 2013-2020 period was 4.71% and 1.67%, respectively. What is

[24]It should however be noted that, baseload power plants such as nuclear and large coal-fired facilities–that do not change their power output rapidly–cannot be relied upon as backup power-generating sources for intermittent renewable power generation. Immediate changes in the availability of electricity from climate-related renewable energy sources (wind, solar photovoltaics, and small-scale run-of-river hydroelectricity) can be counterbalanced by open-cycle gas (or diesel) turbines, pumped-storage hydroelectricity and storage systems.

surprising, however, is that the total precipitation index–the climate variable linked with hydropower generation with the average annual share of 11.99% in total electricity production in France between 2013 and 2020, bears the lowest importance–in permutation feature importance sense–for the prediction of emissions over the study period.

There are several possible explanations for this result. First, among different types of hydroelectric power generation, small-scale run-of-river hydroelectricity[25] has the least operational flexibility and is most vulnerable to climatic variations (see Ebinger and Vergara, 2011). The availability of water resources for hydropower generation in run-of-river plants comes under the major influence of several meteorological variables (e.g. type of precipitation, precipitation intensity, precipitation duration, soil temperature, soil moisture and relative humidity), and total precipitation (representing the *accumulated amount* of liquid and frozen water that falls to the surface in a given hour) is only partly responsible for changes in runoff. Second, climate impacts on a hydropower generation are ultimately dependent upon the complexity of the hydropower system, itself being identified with the relevance of hydropower generation for the whole power system in the specific region under study (i.e. whether hydroelectricity is complementary to (as is the case for France) or complemented by other power sources), as well as geographical dispersion and the level of integration of hydropower through transmission capacity (Ebinger and Vergara, 2011). That being so, a change in pertinent climate factors (such as total precipitation) does not necessarily translate into an immediate change in the share of hydropower of total electricity generation, and hence a change in $CO_2$ emissions in the power sector. On a related note, the generalizability of the results obtained from this analysis to contexts with different hydropower system complexity is subject to limitation. Third, overall climate impacts on hydropower generation have been estimated to be smaller compared to other renewable energy technologies (e.g. wind and solar energy), but local impacts are most likely greater (Solaun and Cerdá, 2019). Consequently, it seems possible that aggregating regional-level total precipitation values into countrywide indicators smooths potentially significant local effects and undermines the importance of the total precipitation index for predicting $CO_2$ emissions in the electricity sector. Given these considerations, there is abundant room for further progress in characterizing the predictive impact of hydropower generation-related climate variables on emissions in the electricity sector in France and other regions of the world.

## 3.5 Conclusion

It is well established from a variety of studies, that decarbonizion of the electricity sector has to be at the heart of any national and international effort to combat climate change. Central

[25] According to the 2021 Electricity Balance published by RTE, in 2020, run-of-river hydroelectricity accounted for 50.28% (31.43 TWh) of total hydroelectric power generated in France (62.5 TWh) (RTE-Réseau de Transport d'Électricité, 2021).

to the debate on electricity generation-related $CO_2$ emissions is the assessment of explicative factors behind emissions in the electric power sector. Such as assessment is indeed indispensable for identifying the most cost-effective policy measures to lessen the negative environmental impacts of electricity generation. Climate conditions are certainly among the most important potential determinants of emissions in the power sector, due to their impact on demand and supply of electricity from renewable and non-renewable sources. Notwithstanding this, far too little attention has been paid to understanding and quantifying the relationship between climate variables and emissions from electricity production. Disentangling the effects of different climatic drivers on emissions in the power sector is, from a policy standpoint, a prerequisite for a precise analysis of electricity generation options for sustainable energy transition.

The present research was designed to examine the relevance of climate conditions as a determinant of $CO_2$ emissions from electricity production in France. Relying on hourly data on electricity generation-induced emissions, multiple regional power indicators and an extensive set of climate variables over the 2013-2020 period, the paper provided a data-driven framework for characterization and quantification of the complex relationship between climate factors and $CO_2$ emissions in the French electric power sector. The study's methodological contribution lies in formulating an interdisciplinary approach to the construction of aggregate climate indices from gridded climate data, as a viable alternative to population-weighted indices traditionally used for modeling climate impacts on energy systems and markets. It is expected that the application of this novel approach in energy and climate research will reveal new, possibly overlooked aspects of climate-driven changes in electricity sector emissions across Europe, and result, on a broader level, in new perspectives on the dynamic between spatio-temporal climate variability and climate change mitigation efforts in the power sector.

The empirical findings suggest that climate variables, namely air temperature, solar radiation, relative humidity, wind speed, total precipitation, and surface air pressure are all of predictive importance–although not equally–as for the estimation of $CO_2$ emissions from electricity production in France. Along with the quantification of nonlinear main effects of different climate variables on emissions, the study has discovered and explored several noteworthy interaction effects. In spite of its limitations, this work certainly adds to our understanding of the sensitivity of power sector $CO_2$ emissions to variations in climate variables. Last but not least, the reader should bear in mind that this study was exploratory in nature. An in-depth discussion of the mechanisms underlying the relationships between electricity generation-related $CO_2$ emissions and single or pairs of climate variables, as well as verification of whether or not such relationships are causal lie beyond the scope of this paper and are left for future reseach.

CHAPTER 4

# European Union Emissions Trading System: Effectiveness Assessment

**Article Title:** "Mission Accomplished? An ex-post predictive evaluation of the effectiveness of the EU ETS in reducing regional fossil fuel carbon emissions" (Eslahi, 2022c)

**Abstract:** This study evaluates the effectiveness of the first three phases (2005-2019) of the European Union Emissions Trading System (EU ETS) in reducing fossil fuel $CO_2$ emissions in 248 socio-economic regions from 25 EU ETS Member States. Considering the beginning of each phase as an intervention, the paper adopts an advanced predictive modeling framework to build counterfactual fossil fuel $CO_2$ emissions for each post-intervention period, and analyzes, in time and space, the intervention effect by comparing actual emissions with counterfactual estimates. The results of the temporal analysis indicate a significant overall emissions reduction in the second and third phases and 8 (out of 36) months of the first phase. The spatial analysis has found evidence for significant emissions reduction in 84, 209 and 226 regions in the first, second and third phase, respectively. The results also demonstrate that 66 European regions went through significant emissions reduction in all three phases.

**Keywords:** The EU ETS, Fossil Fuel $CO_2$ Emissions, Climate Variables, Predictive Modeling, Spatio-temporal Analysis, Counterfactual Inference

## 4.1 Introduction

According to the statistical office of the European Union,[1] carbon dioxide ($CO_2$) emissions from fossil fuel combustion account for about 80% of all European Union greenhouse gas (GHG) emissions that originate in human activity. Fossil fuel $CO_2$ emission is produced as a result of burning non-renewable energy sources such as coal, natural gas and petroleum products mainly for the purpose of generating electric power, transportation and industrial manufacturing, and is influenced by several factors including climate conditions and economic indicators.

Economists have long held that carbon pricing through cap-and-trade systems is one of the most cost-effective ways to decarbonize the economy (Meckling et al., 2017). As the pioneering and second biggest carbon market across the globe (preceded by China's Emissions Trading Scheme, introduced in July 2021), the European Union Emissions Trading System (abbreviated as the EU ETS) is the keystone of the EU's policy to fight climate change and its central tool for reducing $CO_2$ and other greenhouse gas emissions under the 1997 Kyoto Protocol's commitment periods (European Comission, 2021b).

The EU ETS covers $CO_2$ emissions from the most polluting industrial sectors, accounting for up to 70% of each member state's emissions (Ellerman and Buchner, 2008). Since its launch, the EU ETS has split into a number of trading periods or phases, each characterized by specific features and legislation. The first trading period (denoted here as "Phase I") started in January 2005 and ended in December 2007. The second phase (hereinafter referred to as "Phase II") extended across a period of five years from the beginning of 2008 to the end of 2012. The third phase (referred to as "Phase III" in the present work) started in January of 2013 and continued until the end of December 2020. At the time of writing this paper, the system was in its fourth phase, which started in January 2021 and was planned to continue until the end of December 2030.

A growing body of literature has examined the effectiveness of different phases of the EU ETS in reducing $CO_2$ emissions at sector, firm, country and EU levels, but with no decisive results (see Laing et al., 2013). While some works have evaluated the effectiveness of the EU ETS over the time periods covering more than one phase, extensive large-scale empirical assessments of the effectiveness of all the first three phases remain scarce. In addition, there is still a major gap in the regional scale spatio-temporal understanding of the impact of the EU ETS on realized $CO_2$ emissions. One purpose of this study is to fill this gap and examine whether the first three phases of the EU ETS were effective in reducing monthly emissions across socio-economic regions in the EU ETS zone. Relying on high-resolution fine-grained data on realized fossil fuel $CO_2$ emissions and their potential climatic predictors at regional level, the present study employs a cutting edge predictive modeling technique to build counterfactual emissions

[1] `https://ec.europa.eu/eurostat`

and compare them with actual emissions.

On a different note, notable but scant among studies on the EU ETS are those investigating the explanatory factors for $CO_2$ emissions (see Gloaguen and Alberola, 2013; Ellerman and McGuinness, 2008; Anderson and Di Maria, 2011; de Perthuis et al., 2010). Climate conditions and weather variables are among the least studied of such factors, mainly due to lack of access to data at European level. Available studies have mostly focused on a limited set of climate variables such as temperature, rainfall and wind speed, and mainly utilized coarse-grained (e.g. country-level) climate proxies (see Anderson and Di Maria, 2011; Benz and Trück, 2009). This could seem to be a naive approach in terms of disregarding a sometimes significant intra-country climate variability. Moreover, despite the existence of theoretical grounds for the impact of climate factors on $CO_2$ emissions, there is only little understanding of the extent to which such factors can prove to be useful for predicting emissions in practice. A second objective of the present work is thus to evaluate the usefulness of all potential climate variables (including understudied ones like solar radiation, cloud cover, surface pressure and relative humidity) in predicting carbon emissions at regional level, where spatial variation in climate variables is much less pronounced.

This research contributes to the existing literature on the EU ETS in multiple ways. First, to date no study has investigated the environmental effectiveness of this trading scheme by means of a climate-based counterfactual analysis of $CO_2$ emissions in the geographical scope of the EU ETS. Causal inference based on counterfactuals is indeed known in impact evaluation studies in economics (see among others Ellerman and Buchner, 2008; Declercq et al., 2011; Anderson and Di Maria, 2011). The selection of appropriate comparison groups or predictor series that are themselves not affected by the corresponding intervention (e.g. policy) is often the most challenging step in any counterfactual analysis. Instead of relying on conventional methodological approaches, the present work offers an innovative and intuitive machine learning-based approach to counterfactual estimation of $CO_2$ emissions based on multiple climate variables that are theoretically expected to exert an influence on carbon emissions, but themselves are not influenced by the EU ETS. Such an approach can make a contribution of wide interest to academic research on the predictors of $CO_2$ emissions, while fulfilling the main objective of evaluating the environmental effectiveness of the EU ETS. Second, to the best of the author's knowledge, no previous research on the explanatory factors for $CO_2$ emissions has used data sets of comparable quality to the emissions and climate data used in the present work. Thanks to these data, the drawing of causal inferences about the impact of the EU ETS on fossil fuel $CO_2$ emissions has been made feasible at the finest possible temporal (monthly) and spatial (regional) scales. Third, this study makes use of the most comprehensive set of potential climatic predictors of $CO_2$ emissions to develop a counterfactual for assessing the environmental impact of the EU ETS. Indeed, the predictive impact of some climate factors such as solar

radiation, cloud cover, surface pressure and relative humidity on fossil fuel $CO_2$ emissions in Europe is explored for the first time in the literature. Finally, the region-based spatio-temporal analysis proposed in the present study may complement existing firm, sector, country and EU-level analyses of the effectiveness of the EU ETS in reducing anthropogenic emissions of $CO_2$ throughout its first three phases.

The remainder of this paper is structured as follows. Section 4.2 reviews existing research on the effectiveness evaluation of the EU ETS, and lays the foundations of the proposed methodology. Section 4.3 introduces the potential climatic predictors of regional fossil fuel $CO_2$ emissions that are used for constructing counterfactual emissions. The research setting, data and methodology of the empirical analysis are described in Section 4.4, followed by the presentation of results in Section 4.5. The paper concludes with a discussion of some limitations and venues for future research (Sections 4.6 and 4.7).

## 4.2 Evaluation of the effectiveness of the EU ETS

When it comes to the effectiveness assessment of carbon markets, carbon price is regularly the touchstone of choice where low prices are, explicitly or implicitly, associated with ineffectiveness (Bayer and Aklin, 2020). However, it has been argued that carbon abatement is justifiable even if market prices are low, and that the EU ETS may effectively reduce emissions in spite of low prices (Bayer and Aklin, 2020). Indeed, the primary measure of the performance of any emissions trading scheme should be the extent of emissions reduction (Ellerman et al., 2016), and the EU ETS is no exception. Evaluating the effectiveness of the EU ETS should therefore not be based on market prices but rather an assessment of whether the policy caused emissions to diminish (Bayer and Aklin, 2020). From a methodological point of view, the difficulty of such an evaluation relies on the fact that actual emissions under the EU ETS need to be compared to unobservable or counterfactual emissions that would have been realized if the EU ETS had not been in place (see Bayer and Aklin, 2020; Grubb et al., 2012; Ellerman et al., 2010; Helm and Sprinz, 2000).

In general, counterfactual approaches to causal inference can be classified into experimental (e.g. randomized controlled trial), non-experimental (e.g. logically-constructed counterfactual) and quasi-experimental (e.g. difference in differences, (propensity score-based) matching, instrumental variables estimation, regression discontinuity and statistically-created counterfactual) research designs. Previous studies on the effectiveness of the EU ETS in reducing carbon emissions have used a variety of non-experimental and quasi-experimental approaches. Table 4.1 provides a summary of these studies.

As argued by Ellerman and Buchner (2008), non-experimental studies in this context (i.e. those relying on baselines or logically-constructed counterfactuals) mainly suffer from potential bias in and imperfect comparability of data across Europe. On the other hand, classical quasi-

| Reference | Study Period | Geographical Scope | Method | Comparison/Control Group | Outcome of Interest | Finding(s) |
|---|---|---|---|---|---|---|
| Anderson and Di Maria (2011) | 2005-2007 | 25 EU Member States | Dynamic panel data modeling | Baseline emissions estimated based on industrial economic activity levels, energy prices and weather effects (heating degree days, cooling degree days and precipitation) | Industrial $CO_2$ emissions | 2.8% net $CO_2$ emissions reduction over the study period |
| Bayer and Aklin (2020) | 2008-2016 | 25 EU Member States | Generalized synthetic control | Non-ETS sectors | Sector-level $CO_2$ emissions | 3.8% $CO_2$ emissions reduction compared to the total emissions over the study period |
| Bel and Joseph (2015) | 2005-2012 | 25 EU Member States | Dynamic panel data modeling | - | National installation-level GHG emissions from electricity and industry sectors | 11.47% and 13.84% of total GHG reduction over the study period |
| Dechezleprêtre et al. (2018) | 2005-2012 | France, the Netherlands, Norway and the United Kingdom | difference in differences | - | Installation-level carbon emissions | 6% carbon emissions reduction from 2005 to 2007 and 15% reduction from 2008 to 2012 |
| Egenhofer et al. (2011) | 2005-2009 | 25 EU Member States | Comparison of emissions reduction with business-as-usual (BAU) emissions | BAU emissions projected from the 2000-2004 period (proposed by Ellerman et al., 2010) | Sector-level $CO_2$ emissions | 1% average annual intensity improvement from 2005 to 2007 and 3.35% intensity improvement from 2008 to 2009 |
| Ellerman and Buchner (2008) | 2005-2006 | 25 EU Member States | Comparison with baseline emissions | Baseline emissions estimated based on indicators of economic activity | Installation-level $CO_2$ emissions | 3% $CO_2$ emissions reduction over the study period |
| Ellerman et al. (2016) | 2004-2014 | 25 EU Member States | Comparison with long-term perspective on ETS sector emissions | - | Sector-level $CO_2$ emissions | 2.1% average annual $CO_2$ emissions reduction in ETS sectors from 2004 to 2014 |
| Gloaguen and Alberola (2013) | 2005-2012 | 21 EU Member States | Dynamic panel data modeling | BAU emissions based on manufacturing activity, development of renewable energies, energy efficiency, carbon price, and energy ratio | Country-level $CO_2$ emissions of all ETS sectors | 7.3% $CO_2$ emissions reduction over the study period |
| Jaraite-Kažukauske and Di Maria (2016) | 2003-2010 | Lithuania | Matching | Non-ETS firms | Firm-level $CO_2$ emissions | No significant $CO_2$ emissions reduction |
| Ellerman and McGuinness (2008) | 2005-2006 | The United Kingdom | Panel data modeling | Counterfactual emissions based on individual units' planned generation and availability | Plant-level $CO_2$ emissions from combined cycle gas turbine and coal power plants | Between 13 million and 21 million tons of $CO_2$ emissions reduction in 2005 and from 14 to 21 million tons of reduction in 2006 as a result of fuel-switching |
| Petrick and Wagner (2014) | 2005-2010 | Germany | Difference in differences | Non-ETS firms | Plant-level $CO_2$ emissions from manufacturing firms | No significant emissions reduction from 2005 to 2007, 20% emissions reduction between 2007 and 2010 |
| Wagner et al. (2014) | 2005-2010 | France | Propensity score-based difference in differences | Non-ETS firms | Plant-level $CO_2$ emissions from manufacturing firms | An average of 15-20% emissions reduction from 2007 to 2010; no significant reduction from 2005 to 2007 |
| Klemetsen et al. (2016) | 2001-2013 | Norway | Propensity score-based difference in differences | Non-ETS firms | Plant-level $CO_2$, $N_2O$ and PFCs (measured in $CO_2$ equivalents) emissions | A weak tendency of emissions reduction from 2008 to 2012 |
| Abrell et al. (2011) | 2005-2008 | 21 EU Member States | Dynamic panel modeling with propensity score matching | Non-ETS firms | Firm-level $CO_2$ emissions growth rate | 3% emissions reduction in 2007-2008 relative to 2005-2006 |
| Gretszel et al. (2020) | 2005-2018 | 22 EU Member States | Generalized method of moments (GMM) | Benchmark variant | Installation-level $CO_2$ emissions | Significant emissions reduction especially in low-polluting economies |

Table 4.1: Summary of the literature on the effectiveness of the EU ETS in reducing carbon emissions. Contents of this table were partially adapted from Rafaty et al. (2020) and Green (2021).

experimental methods such as (propensity score-based) matching and difference in differences are either reliant upon strong assumptions (e.g. conditional independence assumption), or limited in terms of explaining the time evolution of the intervention effect (Brodersen et al., 2015). From these premises, it could be argued that statistically-created counterfactual designs have the edge over other quasi-experimental approaches.

An effective statistical technique for creating counterfactuals is to amalgamate a collection of potential predictor series into a synthetic control (Brodersen et al., 2015; Abadie et al., 2010; Abadie and Gardeazabal, 2003). Two major sources of information that can be exploited for the construction of a credible synthetic control are the behavior of the target variable before the intervention and that of other series that could predict the outcome variable in the pre-intervention period (Brodersen et al., 2015). On condition that such control series are themselves uninfluenced by the intervention and that the relationship between them and the treated series remains stationary over time (Brodersen et al., 2015), any model that captures the relationship between the response variable and its predictors prior to the intervention can be used for predicting the outcome variable in the post-intervention period based on the behavior of the predictor series after the intervention. The assumptions that have been made here are intertwined. In the absence of any evidence that the predictor series are affected by the intervention, it is reasonable to presume an unvarying relationship between the target series and the control series before and after the intervention (Brodersen et al., 2015). Selecting a proper set of series to be used as contemporaneous controls is thus the most challenging aspect of such a scheme.

Perhaps the most relevant research of this type within the framework of the effectiveness evaluation of the EU ETS is the study of Bayer and Aklin (2020), which makes use of emissions series of non-ETS sectors across the EU (i.e. sectors that are not covered by the EU ETS) as synthetic control group units to estimate counterfactual emissions. Naturally, taking non-ETS sectors or firms as a comparison or control group rests on the fundamental assumption that such sectors (or firms) are not subject to any type of parallel carbon constraint regulations that may have been put in place simultaneously with the EU ETS (see Jaraite-Kažukauske and Di Maria, 2016). Nonetheless, this assumption may not be correct for all non-participant sectors (or firms) at European level. For instance, according to the French Environment and Energy Management Agency (ADEME), in parallel with the EU ETS, alternative domestic mechanisms have been established in France to cut emissions from sectors not concerned by the emissions trading system (ADEME, 2021). More importantly, since 2008, most sectors not included in the EU ETS have been targeted by the Effort Sharing regulation set by the EU,[2] with the aim of meeting an emissions reduction target of 30% in the affected sectors by 2030. Therefore, at least in theory, non-ETS sectors (or firms) may not be the most appropriate control units in a European-scale study.

[2] `https://ec.europa.eu/clima/policies/effort_en`

Instead of using external units as control groups to build counterfactual emissions in the target unit, the present study capitalizes on endogenic factors in each region (which are themselves unaffected by carbon reduction policies) to estimate counterfactuals. Considering the beginning of each phase of the EU ETS as an intervention, this paper proposes a regression-like setting where advanced tree-based ensemble models are trained in the pre-intervention period to learn the relationship between the outcome variable and a number of predictors on a regional scale. Those models are then applied to the post-intervention period to predict the outcome based on the predictor series. Those predictions provide the counterfactual estimates of regional fossil fuel $CO_2$ emissions. In contrast to the methods proposed by Abadie et al. (2010) and Abadie and Gardeazabal (2003), the approach adopted here does not impose any restrictions (such as convexity condition) on how potential predictor series should be combined, and exploits predictors exclusively in respect of how well they predict the outcome of interest in the pre-intervention period. The predictive modeling framework put forward in the current study must be differentiated from a forecasting scheme. Instead of using historical data as input to establish a forecast of the variable of interest (here emissions) within a given time horizon in the future, the proposed framework focuses on learning how emissions can be explained as a function of climate variables to make counterfactual predictions. It then capitalizes on disparities between actual and counterfactual emissions, which are interpreted as the casual impact of the EU ETS on fossil fuel $CO_2$ emissions.

In essence, the methodology of this research follows a similar logic to the method put forward by Brodersen et al. (2015). The key difference between the two methods is that the present study employs a tree-based ensemble machine learning algorithm, namely Extreme Gradient Boosting (XGBoost) in lieu of Bayesian structural equation modeling (SEM) to estimate counterfactuals. The rational behind this choice of method is that SEM-type modeling techniques typically require strict assumptions about the relationship between variables–a feature that makes such tools wholly appropriate for systematic theory-building and hypothesis testing while limiting their predictive power (Edelsbrunner and Schneider, 2013). Since one of the main objectives of the present paper is to examine the predictive usefulness of climate variables as potential drivers of regional fossil fuel $CO_2$ emissions based on the fewest theoretical assumptions about the data, an XGBoost-supported predictive modeling framework seems more relevant to this research design.

## 4.3 Potential predictors of regional fossil fuel $CO_2$ emissions

Energy production and consumption originating from fossil fuels are a major determinant of $CO_2$ emissions (Ang, 2007; Apergis and Payne, 2009; Iwata et al., 2012; Shafiei and Salim, 2014). In Europe, power generation remains the primary source of greenhouse gas emissions, with $CO_2$ being by a great amount the most dominant greenhouse gas emitted (European En-

vironment Agency, 2020). While the power sector falls under the jurisdiction of the EU ETS as the mainspring of the EU's policy to reduce $CO_2$ emissions, the development of energy generation from renewable sources (such as wind, solar and hydro power) has attracted increasing attention as a complementary tool to address climate change. Since increasing the share of energy from renewable sources is expected to reduce carbon emissions (Dogan and Seker, 2016; Bento and Moutinho, 2016), special attention should be given to the role of renewable energy production and consumption in any study on the predictors of fossil fuel $CO_2$ emissions.

Power generation services are, by and large, influenced by climate conditions on the production or consumption side (Yalew et al., 2020). Such influence serves as a connecting link between climate variables and emissions of carbon dioxide. As an example, the share of power produced by carbon-free sources like hydro power, wind and solar energy is directly affected by climate variables like rainfalls, wind speed and sunlight (Chevallier, 2013; Bartos and Chester, 2015; Gernaat et al., 2021). Furthermore, changes in climate variables (e.g. air temperature, and less substantial, wind speed) can be associated with alteration in energy consumption, and eventually affect $CO_2$ emissions (Perera et al., 2020; Chèze et al., 2020). When it comes to causal inference based on counterfactuals, climate variables are arguably among the most suitable predictors of regional fossil fuel carbon emissions since they are related to the outcome of interest and conceivably unaffected by policy interventions such as the launch of emissions trading systems.

For the sake of this study, seven climate variables with a potential predictive impact on emissions via affecting nonrenewable and renewable energy systems are identified: air temperature, solar radiation, total cloud cover, total precipitation, surface air pressure, relative humidity and wind speed. To the best of the author's knowledge, this is the most comprehensive set to date of climate variables studied in the context of the relationship between climate and carbon markets. In the following, the association between each climate variable and energy production and consumption is described.

**Air Temperature:** Existing research points to a close relationship between air temperature and energy demand and production in general (See for example Cruz Rios et al. (2017) for a list of studies on the relationship between temperature and demand for energy in different countries, and Benz and Trück (2009)). An increase in air temperature is positively (negatively) related to the need for cooling (heating) (Ebinger and Vergara, 2011). Since cooling demand is primarily satisfied by air conditioning systems that are powered by electricity, air temperature rise may translate into a shift in energy delivery from fossil fuels used for heating to electric power (Pryor et al., 2014). Such an alteration in energy consumption presumably has an effect on $CO_2$ emissions. Nevertheless, the extent of this influence eventually depends on the sources of primary energy (renewable or non-renewable) used for electricity generation. On another note, rising temperatures can negatively affect the efficiency of thermal power plants and solar

photovoltaic panels, hence leading to increased emissions (Ebinger and Vergara, 2011).

**Solar Radiation:** The amount of solar radiation that reaches the surface of the Earth is directly related to solar energy generation as a non-polluting substitute for fossil fuels. The two main types of solar energy technologies, namely solar thermal generation and solar photovoltaic generation, are both reliant upon direct sunlight[3] to generate heat and electricity. In addition, increase or reduction in solar radiation may affect some end-uses of energy (Ebinger and Vergara, 2011).

**Total Cloud Cover:** Solar energy systems are largely reliant on direct radiation, and cloudiness diminishes the effect of direct solar radiation on solar panels (Chrobak et al., 2016). A change in total cloud cover (i.e. the proportion of the sky covered by cloud) influences solar power production as well as demand for cooling (Ebinger and Vergara, 2011). It should be noted that different cloud types can have a slightly different impact on solar radiation. However, since multiple cloud genera can often be seen in the sky at the same time, the interpretation of the interrelation between cloud genera and solar radiation is complex and not always possible (Matuszko, 2012). Hence, for the sake of this study, the effect of cloud genera on the association between cloud cover and solar power production is disregarded.

**Total Precipitation:** $CO_2$ production depends on precipitation, mainly due to the fact that the amount of accumulated liquid and frozen water (i.e. rain and snow) that falls to the surface is inextricably linked with the generation of hydro power as the most widely-used renewable energy (Benz and Trück, 2009; Wei et al., 2020). On another note, an increase in total precipitation increases water availability for cooling purposes, and a drop in precipitation levels is associated with reduced cloud cover with positive implications for solar energy production (Ebinger and Vergara, 2011).

**Surface Air Pressure** and **Relative Humidity:** The pressure of the atmosphere at the surface, and the moisture content of the atmosphere (relative to air temperature) have major implications for fossil-fuel-fired power production (Ebinger and Vergara, 2011; Loew et al., 2020). Such impacts are mainly related to the efficiency of power generation cycle and cooling requirements (Wilbanks et al., 2008).

**Wind Speed:** Wind energy is one of the most important renewable energy sources with considerable potential owing to its economic and environmental cost advantages over fossil fuel plants (Wilbanks et al., 2008). Wind speed is a major parameter that affects wind power production (either positively or negatively) (Ebinger and Vergara, 2011). In this regard, wind speed affects the share of non-$CO_2$ power generating sources and thus emissions levels (Benz and Trück, 2009).

From a theoretical standpoint, all of the above-mentioned climate variables fulfill the condi-

[3]The sunlight that reaches the Earth's surface is either direct or diffuse (scattered) radiation. Solar thermal plants require direct radiation to operate effectively (Breeze, 2019). Similarly, solar photovoltaic plants are most productive when exposed to direct sunlight. Therefore, in the present work diffuse solar radiation is disregarded.

tions for serving as synthetic control series in the present analysis; they are themselves uninfluenced by the beginning of each EU ETS phase (intervention),[4] and the nature of their relationship with the outcome variable remains unaltered before and after each intervention. From an empirical point of view, however, it is not expected that the entire set of climate variables will prove equally decisive in predicting the fossil fuel $CO_2$ emissions at a regional level in all statistical units of study. This is exactly why an empirical assessment of the predictive usefulness of each variable for estimating counterfactual emissions in each socio-economic region proves useful.

Much research in the energy economics literature has related economic activity to carbon emissions (see for example Moutinho et al. (2017) for a list of studies on the relationship between economic growth and emissions, and Benz and Trück (2009)). The global financial crisis of 2007-2008 is a case in point during which $CO_2$ emissions declined in response to a decrease in economic activity (Sadorsky, 2020). A similar pattern could be observed during the COVID-19 pandemic, which led to a decrease in global $CO_2$ emissions in 2020 as a result of the disruption in economic activities (Liu et al., 2020). Therefore, when drawing causal inference based on counterfactual emissions, economic activity needs to be controlled for to avoid confounding. In this regard, total regional gross value added (GVA) is included as a control variable in the analyses conducted in this study. Being a proxy of the economic productivity of a region or an economic sector, GVA measures the value of output subtracting the value of the goods and services consumed as inputs (OECD, 2008). At the regional level, GVA is favored over gross domestic product (GDP) since it excludes taxes or subsidies on products that are difficult to ascribe to local units (Eurostat, 2008).

## 4.4 Materials and Methods

### 4.4.1 Research setting

The study area covers economic regions of the EU ETS Member States at the second level of Nomenclature of Territorial Units for Statistics (NUTS). The NUTS classification is a referencing system that splits the economic territory of the European Union and the United Kingdom[5]

[4]It may be argued that air temperature can be affected by the intervention, even though indirectly. Indeed, owing to the causal structure between $CO_2$ emissions and air temperature (i.e. increase in global mean surface temperature due to anthropogenic carbon emissions, as shown by a large body of research on climate change), a likely reduction in emissions caused by the intervention may make an alteration to air temperature. To rule out the possibility of incorrectly estimating the true intervention effect due to such possibility, air temperature trend in all the regions under study was analyzed and tested for the presence of any structural break at intervention periods (see Section 4.4.3.2). This additional analysis found no evidence of air temperature being affected by the intervention.

[5]This classification does not cover members of the European Free Trade Association including Iceland, Liechtenstein and Norway (that joined the EU ETS from Phase II). However, a similar classification system is used to code the statistical regions of these countries (see `https://ec.europa.eu/eurostat/web/nuts/statistical-regions-outside-eu`).

into three levels of nested regions with the aim of collecting, processing and coordinating official statistics, conducting socio-economic analyses and formulating regional policies.[6] In the present work, NUTS level 2 regions (hereafter referred to simply as NUTS regions) are selected as units of analysis. These are basic socio-economic regions in which regional policies are applicable. Level 3 regions (small regions for particular analyses) were too fine-scale to be matched with the fossil fuel $CO_2$ emissions and climate data used in this study. In consideration of the method of attributing gridded data to each region (see section 4.4.2), the first level regions were also unsuitable for this analysis; they were rather coarse-scale in the sense that they could introduce significant variations in climate conditions and hence reduce the credibility of counterfactual construction.

The original NUTS 2021 classification includes 283 regions at the second level. Owing to their gridded nature, the data on fossil fuel $CO_2$ emissions and climate variables (see section 4.4.2) provided the most flexibility in terms of determining the geographical scope of the study. However, the availability of data on regional economic activity, and the late joining of some countries in the EU ETS[7] set a limit on the ultimate number of NUTS regions that could be retained for the analysis of all the three phases. The eventual sample consisted of a total number of 248 NUTS regions from 25 countries that were members of the EU ETS from the first phase: 24 EU Member States plus the United Kingdom.

## 4.4.2 Data

### 4.4.2.1 Fossil fuel $CO_2$ emissions

Monthly high-resolution ($1\times1$ degree) fossil fuel $CO_2$ emissions data over the study area were downloaded from the Open-source Data Inventory for Anthropogenic $CO_2$ (ODIAC) (Oda et al., 2018). The year 2020 version of ODIAC (ODIAC2020) (Oda and Maksyutov, 2015) emanates from the latest fossil fuel $CO_2$ emissions estimates provided by the Carbon Dioxide Information Analysis Center (CDIAC) (Gilfillan and Marland, 2020), and covers the period from January 2000 to December 2019. Capitalizing on manifold spatial proxies such as satellite remote sensing of night lights, ODIAC provides one of the most granular and objective historical data on fossil fuel $CO_2$ emissions–an attribute that makes such data the ideal candidate for this region-based study. Emissions are expressed in the unit $gC/m^2/day$ (monthly mean). For the sake of consistency with the spatial resolution of climate variables, the data (i.e. raster layer) were disaggregated, using the *raster* R package (Hijmans, 2020), to smaller $0.25\times0.25$ degree cells with the exact same values as the original cells. This adjustment allowed for an orderly intersection

[6] See `https://ec.europa.eu/eurostat/web/nuts/background` for more information.

[7] Bulgaria and Romania joined the European Union and the EU ETS in 2007. Hence, they were not participants in the majority of Phase I. Croatia became a European Union's member state in July 2013, i.e. it was entirely absent in the first two phases of the EU ETS. Finally, Iceland, Liechtenstein and Norway joined the EU ETS from Phase II.

of the grid with the areas of NUTS regions, without altering the accuracy of the data. Gridded emissions were overlayed with the spatial polygons of NUTS regions[8] and, at each time point, the mean of the overlapping grid point values was calculated as the measure of fossil fuel emissions in each region.

#### 4.4.2.2 Climate variables

Monthly averaged gridded data on climate variables were obtained from the ERA5 dataset at a 0.25 degree ($\sim$27.75 km at the equator, for both longitude and latitude) spatial resolution throughout Europe, from 2000 to 2019. ERA5 is the fifth generation reanalysis[9] for the global climate and weather, produced by the Copernicus Climate Change Service (C3S) at the European Centre for Medium-Range Weather Forecasts (ECMWF) (Hersbach et al., 2020). Historical data on five climate variables, namely temperature of air at 2m above the surface (K), total sky direct solar radiation at surface ($Jm^{-2}$), total cloud cover (dimensionless), total precipitation (m) and surface pressure (Pa) were retrieved directly from the C3S. Wind speed values ($ms^{-1}$) were computed using the eastward and northward speed components of the 100m wind.[10] Relative humidity (%) was calculated from the 2m air and dew point temperatures (K) using the August-Roche-Magnus approximation (Alduchov and Eskridge, 1996). In the original data, monthly total precipitation values were provided as monthly sums. All other climate variables were provided as monthly averages. For each climate variable and at a given time point, the average value of the grid points that lied within the spatial polygon of a NUTS region was considered the measure of that variable in the region. The moderate size of NUTS regions guarantees little spatial variation in climate variables across each region, and justifies the use of mean values of climate variables as the proxy for regional climate.

#### 4.4.2.3 Economic activity

Data on total GVA at basic prices (million EUR) of NUTS regions were obtained from the Urban Data Platform Plus of European Commission's Knowledge Centre for Territorial Policies[11] for the period 2000-2019. Annual data were disaggregated[12] to monthly time series using the

[8]Spatial polygons of NUTS regions were retrieved from `https://ec.europa.eu/eurostat/web/gisco/geodata/reference-data/administrative-units-statistical-units/nuts`.

[9]Being extensively used in climate change and variability research (see Parker, 2016; Sheridan et al., 2020, for numerous examples), reanalysis data provide the most comprehensive picture presently attainable of past weather and climate worldwide (ECMWF, 2020b). Since most differences between reanalyses and observations are unreal or insignificant in many cases (Parker, 2016), the vast majority of research regards reanalysis and observational data as the same, or sufficiently indistinguishable for nearly all comparative or integrative purposes (Sheridan et al., 2020).

[10]The choice of the 100m wind over the 10m wind was motivated by the fact that the average hub height of wind turbines (an essential factor for determination of wind energy potential) is 90 meters (Wiser et al., 2020).

[11]`http://urban.jrc.ec.europa.eu`

[12]Temporal disaggregation is the process of obtaining high-frequency time series from low-frequency data (Chamberlin, 2010). Temporal disaggregation methods are extensively used across the European Statistical System

Denton-Cholette interpolation method (Dagum and Cholette, 2006) with temporal additivity constraint (i.e. preserving the movements of the original series and ensuring that the sum of monthly values of the resulting series was equal to the corresponding annual values of the original series) (Sax and Steiner, 2013). A similar temporal disaggregation method has been employed in a number of previous studies within the field of energy economics (see for example Sharif et al., 2020; Shahbaz et al., 2017).

The relationship between the explanatory variables and the response variable (fossil fuel $CO_2$ emissions) is not necessarily expected to be linear, and the choice of empirical modeling framework (see Section 4.4.3.1) is a reflection of this very fact. Hence, common measures of linear association between variables may not be the most appropriate statistical tools to describe such relationship. That being said, a preliminary correlation analysis using Pearson's product moment correlation coefficient shows that air temperature, solar radiation, relative humidity and total GVA have statistically significant linear correlation (at the 5% level of significance) with fossil fuel $CO_2$ emissions in the vast majority (respectively 235, 232, 220 and 223) of NUTS regions under study. The extent to which these four variables or the other ones have predictive usefulness for perfecting the response variable in each region is determined by means of an algorithm dedicated to the measurement of feature importance (see Section 4.4.3.1).

## 4.4.3 Methodology

### 4.4.3.1 Predictive modeling-based construction of counterfactual emissions

In order to estimate counterfactual emissions in each NUTS region, the present study adopts a predictive modeling framework based on the Extreme Gradient Boosting (XGBoost) algorithm (Chen and Guestrin, 2016). XGBoost is a pioneering, fast and high-performing gradient-boosted tree ensemble machine learning algorithm that can provide accurate predictions of a response variable by integrating the estimates obtained from a number of base models (trees). This predictive tool is theoretically appropriate for modeling complex, (potentially) nonlinear relationships between a number of variables in a regression-like setting, where the problem of interest is to learn how a set of predictors can affect the response variable.[13] XGBoost does not make strong assumptions about the data distribution, and is by nature immune to multicollinearity (Chen et al., 2018). The latter inherent feature makes such an algorithm particularly suitable for the present analysis, considering that some predictors (i.e. climate variables) might be lin-

in the production of official statistics (Buono et al., 2018). For example, in France and Italy quarterly figures of Gross Domestic Product (GDP) are derived from annual figures using temporal disaggregation methods (Sax and Steiner, 2013).

[13] As with any other predictive model, XGBoost does not in itself imply any causal relationship between variables. In this regard, by no means does the present modeling framework suggest that a change in climate variables (or economic activity) directly causes a change in fossil fuel $CO_2$ emissions. That being said, a change in climate conditions is expected to be associated with a change in $CO_2$ emissions from energy systems as the largest contributor to total $CO_2$ emissions.

early related.

The value of a response variable $y_i \in \mathbb{R}$ (where $i = 1,...N$, and $N$ is the number of data points) is estimated from predictors $x_i \in \mathbb{R}^p$ (with $p$ being the number of predictors) by the tree ensemble model of the XGBoost algorithm as

$$\hat{y}_i = \hat{f}(x_i) = \sum_{k=1}^{K} g_k(x_i) \quad g_k \in \mathscr{G} \tag{4.1}$$

where $K$ is the number of trained trees, $\mathscr{G} = \{g(x) = w_{q(x)}\}(q : \mathbb{R}^p \to J, w \in \mathbb{R}^J)$ is the space of regression trees, $q$ is the structure of each individual (independent) tree that associates an observation with the corresponding leaf score $w$, and $J$ is the total number of leaves in the tree (Chen and Guestrin, 2016).

The algorithm builds each tree from a single root node and grows it to a particular depth (i.e. the longest path from the root node to a leaf) by continually splitting the training data based on all or some of the predictors in the predictor space. The outcome of this process is a tree with a root node, a number of internal nodes (each of which split data points by one predictor), and some leaves to which prediction scores (weights) are assigned. The final predicted value of the response variable for a given observation is obtained by taking the sum of all the scores in the relevant leaves of individual trees. As proposed by Chen and Guestrin (2016), the selection of splitting points and the appointment of prediction scores in XGBoost are done with the help of an enhanced more regularized version of gradient boosting technique, in such a way as to minimize loss of an objective function that consists of training loss and regularization to avoid overfitting.[14] Mathematically speaking, the tree building algorithm is reliant upon the minimization of

$$\mathscr{L} = \sum_{i=1}^{N} L(\hat{y}_i, y_i) + \sum_{k=1}^{K} \Omega(g_k) \tag{4.2}$$

where

$$\Omega(g_k) = \gamma J_k + \frac{1}{2}\lambda \sum_{j=1}^{J_k} w_{j,k}^2$$

Here, $L$ is the squared error loss (cost) function, which measures the difference between original values of the response variable $y_i$ and the predicted values $\hat{y}_i$ (Chen and Guestrin, 2016). $J_k$ and $w_{j,k}$ are the number of leaves and the prediction score attributed to the $j$-th leaf of the $k$-th regression tree, respectively. The parameter $\gamma$ is one of the parameters that can be tuned to avoid overfitting, and is defined as the minimum loss reduction required to further split the

[14] Overfitting occurs when a model learns a great many details about the relationship between the input variables and the output of interest, hence failing to generalize to formerly unobserved data.

leaf node. $\lambda$ is the L2 norm on the prediction scores. These two, in conjunction with a number of tree-related parameters (together called hyperparameters of the model), cannot be estimated from data and need to be specified in advance.

For each phase of the EU ETS, tree-based ensemble models are trained to learn the contemporaneous relationship between regional fossil fuel $CO_2$ emssion and all its potential climatic predictors in the pre-intervention period, i.e. before the beginning of the phase. To obtain the most appropriate model specification for each NUTS region and keep overfitting at a minimum, the present study combines extensive grid search hyperparameter tuning with k-fold cross-validation ($k = 10$). K-fold cross-validation is a standard resampling method for assessing model performance in predicting new unobserved samples. This technique consists of splitting the training data into k roughly equal-sized partitions (folds), fitting a model using all data except each individual partition, and making out-of-sample forecasts on the held-out partition (Kuhn et al., 2013). The out-of-sample forecast performance in each fold is evaluated by a metric such as root-mean-square error (RMSE), and the summary (e.g. mean) of the k measures of performance are used to assess the overall predictive performance of the model.

In order to find optimal hyperparameter values, 576 variations in the hyperparameter search space are considered, each of which being evaluated using 10-fold cross validation. This results in a total number of $576 \times 10$ tree ensemble models to be trained and evaluated for each NUTS region. The hyperparameter configuration that results in the minimum average RMSE across all folds in a given region is selected as the best tune (i.e. the base model for statistical analyses and prediction purposes) for that region. Possible values of hyperparameters are selected, for the most part, on the basis of recommendations of Boehmke and Greenwell (2019) and Thakur (2020). Table (4.2) presents the hyperparameter configurations used for evaluating tree ensemble models in each NUTS region.

Table 4.2: Hyperparameter configurations used for evaluating tree ensemble models for each NUTS region.

| Hyperparameter | Range | Default Value | Selected Values for Tuning |
|---|---|---|---|
| $\gamma$ | [0,∞) | 0 | {0,0.1} |
| $\eta$ | [0,1] | 0.3 | {0.05,0.1,0.2,0.3} |
| Maximum Depth | {1..∞} | 6 | {3..8} |
| Minimum Child Weight | [0,∞) | 1 | {1,5} |
| Column Sample by Tree | (0,1] | 1 | $\{\frac{2}{9},\frac{3}{9},\frac{4}{9}\}$ |
| Sub-sample | (0,1] | 1 | {0.5,0.75} |

Here, $\gamma$ is the minimum loss reduction required to make a further split on a node of a given tree. Increasing $\gamma$ leads to a more conservative algorithm. $\eta$ is the learning rate, which shrinks prediction scores to prevent overfitting. The maximum depth parameter controls the number of

terminal nodes in a a tree and increasing its value makes the model more complex and more susceptible to overfitting. Minimum child weight determines the minimum sum of instance weight (hessian) needed in a terminal node of a tree. A higher minimum child weight provides more conservative results and makes the model less likely to overfit the data. The sub-sample parameter determines what proportion of the training data set should be used to build trees in every boosting iteration. Using values less than 1 for this parameter leads to "stochastic" boosting, distinguished from "regular" boosting (which makes use of all points to grow a tree). The column sample by tree parameter controls the fraction of columns (predictors) used for constructing each tree. Sub-sampling of columns takes place once for every tree constructed. Using values less than 1 for this parameter leads to a more conservative algorithm. The number of trees used for boosting, and the regularization term $\lambda$ are set to 100 and 1, respectively.

The variables used in the present study are of time series nature. Therefore, when developing an empirical model based on these data, attention should be given not only to the information contained in different features, but also the additional information that might be added by the time component–an aspect that is called temporal autocorrelation (or serial correlation). In this regard, it should be emphasized that the algorithm utilized in the present study is safeguarded against likely temporal autocorrelation in the data for two reasons. First, the data are divided, in a random manner, into training and validation data sets during the 10-fold cross-validation process. Second, using stochastic boosting (as opposed to regular boosting) makes the algorithm train trees on sub-samples of the training dataset at each iteration. Therefore, the likelihood of adjacent observations being used by the algorithm at each iteration is remote and inconsequential.

Like many other modern modeling techniques, XGBoost is data-demanding. The smaller the size of the training data, the higher the prospect that the model has a poor performance. That being the case, for each EU ETS phase, all available data prior to the beginning of the phase are used for model construction. This allows for drawing causal inferences about the effectiveness of each phase separately and independently from the previous phase(s) (in the case of Phase II and Phase III), presuming that fitted models already embody the impacts of the previous phase(s) on fossil fuel $CO_2$ emissions, if any. There is an underlying assumption in this approach to phase assessment that there exists no omitted relevant factor correlated with both the beginning of each EU ETS phase and variations in fossil fuel $CO_2$ emissions.

In addition to the climate variables and the measure of economic activity, a time-based feature (month of the year) is created with integer encoding and included in empirical models as a numerical control variable to account for possible month seasonality information in the data. The ultimate data set used for empirical modeling (in the pre-intervention period) and counterfactual estimation (in the post-intervention period) includes 96, 156 and 240 monthly observations for the first, second and third phases, respectively. Models are constructed with 9

independent variables (consisting of 7 climate variables, total GVA and the time-based feature), and the natural logarithm of fossil fuel $CO_2$ emissions[15] as the response variable.

Once the the model with the best tune for each NUTS region is obtained from hyperparameter optimization, the usefulness of climate variables for predicting $CO_2$ emissions is calculated using the permutation feature importance algorithm with the RMSE ratio as the importance measure (Breiman, 2001; Fisher et al., 2019; Molnar, 2020) and 1000 repetitions. The importance of a feature is measured by calculating the increase in the optimal model's prediction error (in terms of the RMSE ratio) at each repetition, when the values of that feature are shuffled (Molnar, 2020). For the sake of this study, the median of the distribution of feature importance values for a given climate variable (obtained from 1000 repetitions) in each region is taken as the predictive usefulness measure of the variable. A given climate variable has predictive usefulness for the prediction of emissions, if permuting its values increases the model RMSE (i.e. the model is reliant on the feature for the prediction). A climate variable is unimportant if permuting its values leaves the model RMSE unaltered (i.e. the feature is ignored by the model for the prediction). Since shuffling the values of a predictor breaks all its connections not only with the response variable but also with other predictors, the permutation feature importance algorithm innately accounts for all interactions among features(Molnar, 2020). As argued by Molnar (2020), a disadvantage to this attribute, however, is that in case there is interaction between any pair of variables, the importance of such interaction will be included in the importance measure of both variables.

All the analyses and data visualization in this study have been carried out in R software environment (R Core Team, 2020; Kuhn, 2008; Molnar et al., 2018).

#### 4.4.3.2 Causal inference based on counterfactual emissions

In order to draw causal inferences from counterfactual estimates across temporal and spatial scales, the launch of each phase of the EU ETS is regarded as an intervention. Broadly speaking, the main objective of this analysis is to compare real fossil fuel $CO_2$ emissions in NUTS regions over the course of each phase with the corresponding counterfactual emissions, and to verify whether the actual emissions were lower than what would have been realized if no such emissions reduction mechanism had been in place.

For each NUTS region $m$ (with $m$ ranging from 1 to 248), let $y_t^{(m)}$ and $y_t'^{(m)}$ denote the fossil fuel $CO_2$ emissions at time $t$ with and without the intervention, respectively. $y_t^{(m)}$ and $y_t'^{(m)}$ may not be observed simultaneously. Instead, what is observable at time $t$ is

$$y_t^{(m)} = \delta_t y_t^{(m)} + (1 - \delta_t) y_t'^{(m)} \tag{4.3}$$

[15]This transformation is necessary for empirical modeling purposes, i.e. to avoid potential negative predicted values of the response variable. Predicted emissions are back-transformed for the presentation and visualization of results.

where $\delta_t = 1$ if $t$ denotes a point in time after the intervention (beginning of the EU ETS phase), and $\delta_t = 0$ if $t$ is a time point before the intervention and

$$y_t'^{(m)} = \begin{cases} y_t^{(m)} & t = 1, ..., T_0 - 1 \\ \hat{y}_t^{(m)} & t = T_0, ..., T \end{cases} \tag{4.4}$$

where $\hat{y}_t^{(m)}$ is the estimated counterfactual emissions in region $m$ at time $t$ (resulting from tree ensemble models), and $T_0$ is the intervention point. For each phase of the EU ETS, the intervention effect is tested across all NUTS regions in each month succeeding the intervention (temporal analysis), and over all succeeding months for every NUTS region (spatial analysis) using the non-parametric Wilcoxon signed-rank test (Wilcoxon, 1992). The null hypothesis of this test is that the median[16] difference between pairs of actual and counterfactual emissions after the intervention is greater than or equal to zero (see McDonald, 2009). In mathematical terms, the null and alternative hypotheses for the temporal analysis are

$$\begin{aligned} H_0 &: \text{median}(y_t - \hat{y}_t) \geq 0 \\ H_1 &: \text{median}(y_t - \hat{y}_t) < 0 \end{aligned} \tag{4.5}$$

where $y_t = (y_t^{(1)}, ..., y_t^{(m)})$ and $\hat{y}_t = (\hat{y}_t^{(1)}, ..., \hat{y}_t^{(m)})$ are actual and counterfactual emissions in $m$ NUTS regions, respectively, at time $t$ ($t = T_0, ..., T$). The rejection of the null hypothesis for a given time point $t$ would lead to the conclusion that the intervention was effective in reducing fossil fuel $CO_2$ emissions at time $t$. In a similar vein, the null and alternative hypotheses for the spatial analysis are

$$\begin{aligned} H_0 &: \text{median}(y^{(m)} - \hat{y}^{(m)}) \geq 0 \\ H_1 &: \text{median}(y^{(m)} - \hat{y}^{(m)}) < 0 \end{aligned} \tag{4.6}$$

where $y^{(m)} = (y_{T_0}^{(m)}, ..., y_T^{(m)})$ and $\hat{y}^{(m)} = (\hat{y}_{T_0}^{(m)}, ..., \hat{y}_T^{(m)})$ are actual and counterfactual emissions in region $m$ at $T - T_0 + 1$ time points after the intervention. If the null hypothesis of this test is rejected for a NUTS region in a particular phase, it can be concluded that fossil fuel $CO_2$ emissions in that region had significantly decreased compared to what it would have been in the absence of the intervention.

As a sanity check and in order to quickly evaluate whether it is reasonable, from an empirical point of view, to expect any intervention effect in the proposed framework, emissions time series of all NUTS regions were tested for the presence of a structural break at the intervention points using the Chow test (Chow, 1960). For each phase, the two sub-intervals used for con-

[16]Given the rather broad temporal and geographical scope of the present study, median is less sensitive to extreme observations and is a better measure of the central tendency of the difference between actual and counterfactual emissions. On top of the advantages of using a non-parametric test over a parametric test, this is a reason why Wilcoxon signed-rank test was preferred to the classic parametric Student's t-test.

ducting this test are all available time points before the starting date of the phase (intervention point) and the period of time over which the respective phase runs. Furthermore, to rule out the possibility of incorrect estimation of counterfactuals and the true intervention effect, a similar test was carried out on air temperature time series–a predictor of fossil fuel $CO_2$ emissions that might be indirectly affected by the interventions and jeopardize the causal inference.

## 4.5 Results

Before proceeding with exploratory and counterfactual analyses and in order to test whether the starting dates of the EU ETS trading periods (phases) were practically sensible choices for drawing causal inferences about the effectiveness of this emissions reduction mechanism in the first place, the Chow test was conducted on longitudinal series of fossil fuel $CO_2$ emissions in all NUTS regions under study. The results of this test with a significance level of 0.05 indicated the presence of a structural break in January 2005 (the beginning of the first phase) in 57.66% of NUTS regions (143 out of 248). The starting date of the second phase (January 2008) proved to be a break point in 89.11% (221 out of 248) of NUTS regions. Finally, January 2013 (the beginning of the third phase) was found to be a structural break in emissions series in 94.75% (235 out of 248) of NUTS regions. According to these findings, empirically speaking, it seems well justified to consider phase launches as intervention points. To rule out the possibility that air temperature, as a potential predictor of fossil fuel $CO_2$ emissions, could be influenced by the interventions, a similar test was carried out on air temperature series, and no evidence of such influence was found[17]. Indeed, structural breaks in air temperature series at the starting dates of the EU ETS phases (January 2005, January 2008 and January 2013) were identified in no NUTS regions.

### 4.5.1 Exploratory results

#### 4.5.1.1 Predictive usefulness of climate variables

Through the use of the permutation feature importance algorithm, this study was able to assess the predictive usefulness of different climate variables and characterize the most important features for the prediction of $CO_2$ emissions at regional level. Figure 4.1 illustrates the predictive usefulness of each climate variable (as represented by the permutation feature importance measure) in predicting regional fossil fuel $CO_2$ emissions across the three phases of the EU ETS.

In every single NUTS region, the feature importance of all climate variables is greater than 1 in at least one phase. In other words, in no NUTS region a continual absence of predictive usefulness of a climate variable is observed. This provides the first empirical evidence of the

[17] Results available upon request.

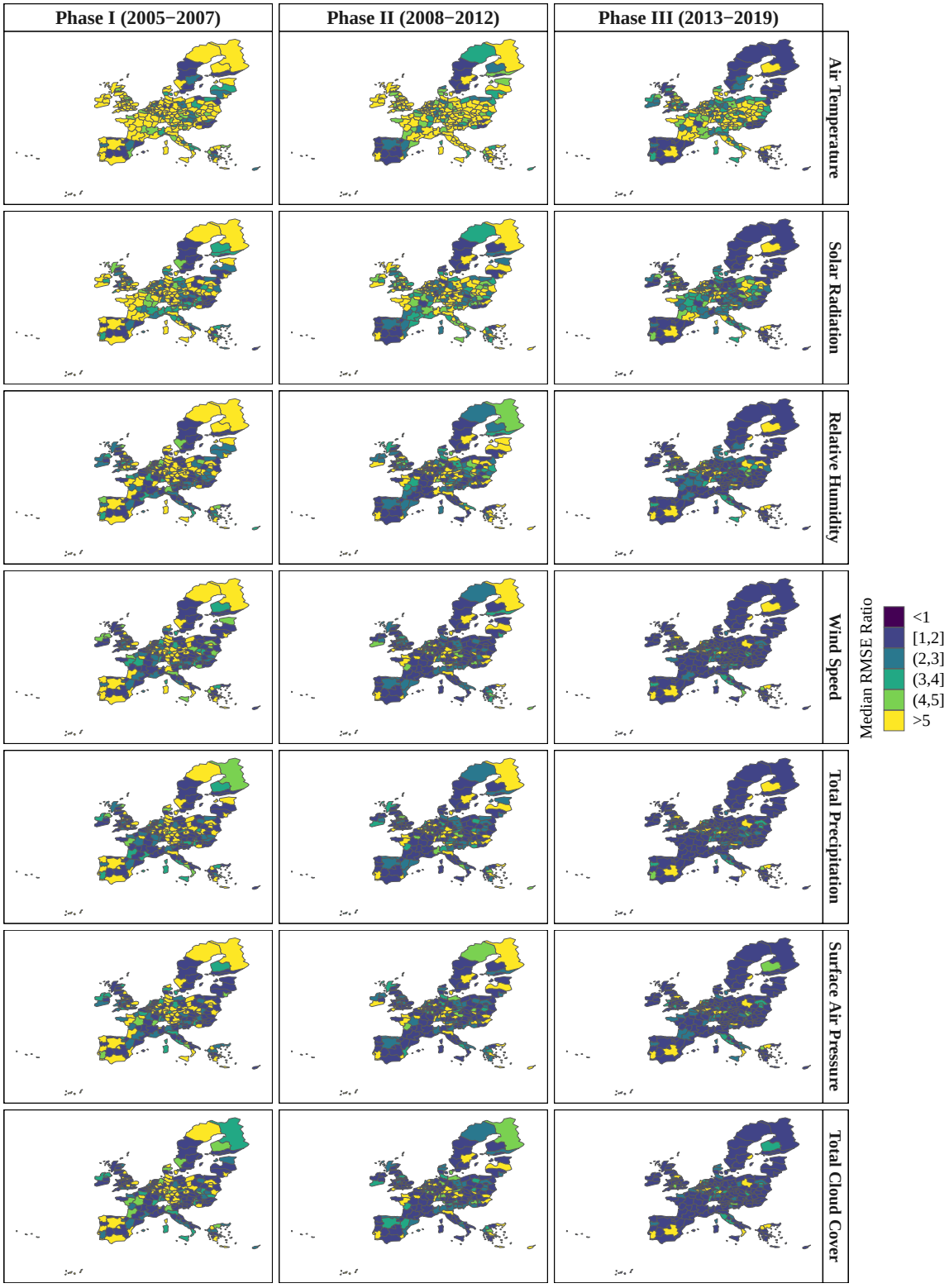


Figure 4.1: Permutation feature importance of climate variables in predicting regional fossil fuel $CO_2$ emissions across the three phases of the EU ETS. The feature importance measure is the median RMSE ratio and the number of repetitions is 1000).

appropriateness of the selected climate variables as predictors of regional $CO_2$ emissions. The feature importance value of air temperature, solar radiation and relative humidity is greater than 2 across all the three phases in 169, 103 and 29 NUTS regions, respectively. The predictive usefulness of the remaining four variables is less pronounced, with the feature importance of total precipitation, surface air pressure, total cloud cover and wind speed being greater than 2 across all the three phases in only 17, 16, 15 and 11 NUTS regions, respectively. These findings can prove critical in the understanding of the climatic predictors of fossil fuel $CO_2$ emissions at a regional scale, and can have important implications for energy management. For instance, comparatively low predictive usefulness of total precipitation and wind speed in a given region across the three phases may indicate underrepresentation of hydro and wind energy in the energy mix in that region, and call for attention to the development of these renewable energies.

To provide a general overview of the predictive usefulness of each climate variable at European level, regional importance measures are summarized by calculating the median feature importance over NUTS regions (Figure 4.2)

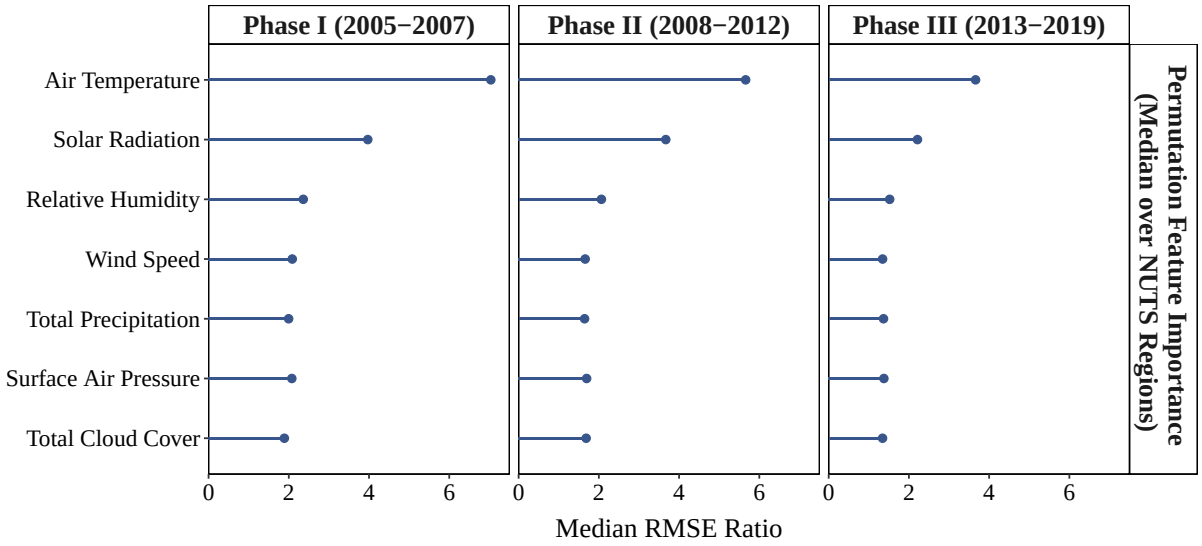


Figure 4.2: Permutation feature importance (median over NUTS regions) of climate variables in predicting fossil fuel $CO_2$ emissions across the three phases of the EU ETS. The feature importance measure is the median RMSE ratio and the number of repetitions is 1000).

From Figure 4.2, two key findings emerge. First, considering the whole study area and all the three phases of the EU ETS, the median feature importance over NUTS regions is greater than 1 for all climate variables. Indeed, despite the spatial variability in the predictive usefulness of climate variables (as seen in Figure 4.1), overall, all climate variables have proved to be important (useful) for the prediction of $CO_2$ emissions. Second, among different climate variables, air temperature proves to be the most important feature for predicting $CO_2$ emissions in all the three phases, followed by solar radiation and relative humidity. In general, total precipitation, surface air pressure, total cloud cover and wind speed have relatively lower importance

in predicting emissions across the EU ETS zone. A noteworthy observation here is that two out of the three most studied climatic drivers of carbon emissions in the existing literature, namely wind speed and total precipitation, have proved to be relatively less useful than some previously understudied variables such as solar radiation and relative humidity for the prediction of fossil fuel $CO_2$ emissions in Europe.

It must be reminded that decision tree ensemble methods such as Extreme Gradient Boosting are robust to highly (or perfectly) correlated explanatory variables. Likewise, the permutation feature importance algorithm can deal with correlated predictors. Nevertheless, if explanatory variables are strongly correlated, the permutation feature importance can be biased by unrealistic data instances and underestimate the importance of each of the two correlated variables by splitting the importance between them (Molnar, 2020). In light of this issue, comparatively low feature importance of total cloud cover can be explained in part by the possible high correlation between total cloud cover and solar radiation. The results shown in Figure 4.2 therefore need to be interpreted with caution.

#### 4.5.1.2 Emissions status

Figure 4.3 shows the percentage of NUTS regions in which monthly fossil fuel $CO_2$ emissions were reduced (not reduced) compared to counterfactual estimates during the course of each EU ETS phase. Over 36 months of the first phase (from January 2005 to December 2007), between 29.03% and 69.35% NUTS regions experienced a reduction in monthly emissions, with an average percentage of 48.28%. Over 60 months of the second phase (from January 2008 to December 2012), monthly actual emissions were lower than counterfactual emissions in 83.99% of NUTS regions on average, with a range between 60.88% and 99.59%. Finally, over 84 months of the third phase (from January 2013 to December 2019), between 57.25% and 96.37% of NUTS regions went through an emissions reduction against the counterfactual, with an average percentage of 86.59%. These results indicate that, in terms of the average percentage of regions with reduced monthly emissions across Europe, Phase III of the EU ETS has been the most effective trading period.

Figure 4.4 represents the spatial distribution of NUTS regions with emissions reduction in 0 to 100% of months in each phase of the EU ETS. As observed in this figure, the percentage of months in which fossil fuel $CO_2$ emissions were reduced compared to counterfactual estimates has increased from the first phase to the next two phases in several regions in England, France, Germany, Spain, Portugal and eastern Europe. Conversely, a number of regions in Scotland, Estonia and Republic of Cyprus went through a constant decrease in the percentage of months with emissions reduction from the first phase to the third phase.

As a complement to Figure 4.4 and in order to get a broader overview of the effectiveness of each trading period in terms of the fraction of months with emissions reduction at a regional

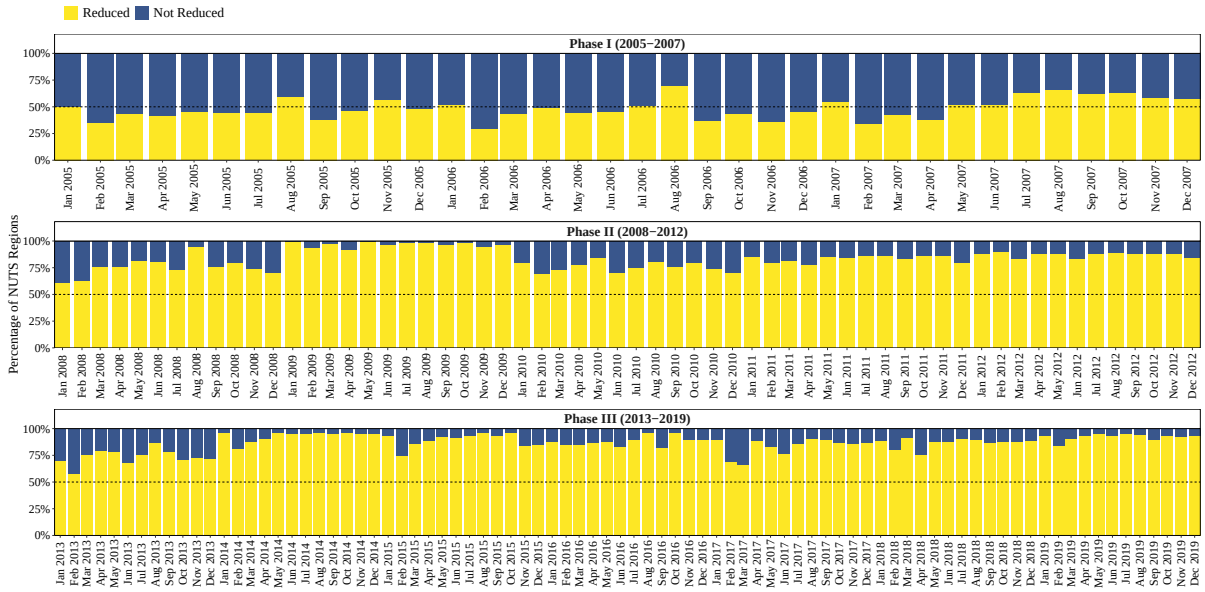


Figure 4.3: Percentage of NUTS regions with reduced (non-reduced) monthly fossil fuel $CO_2$ emissions against counterfactual estimates in each EU ETS phase

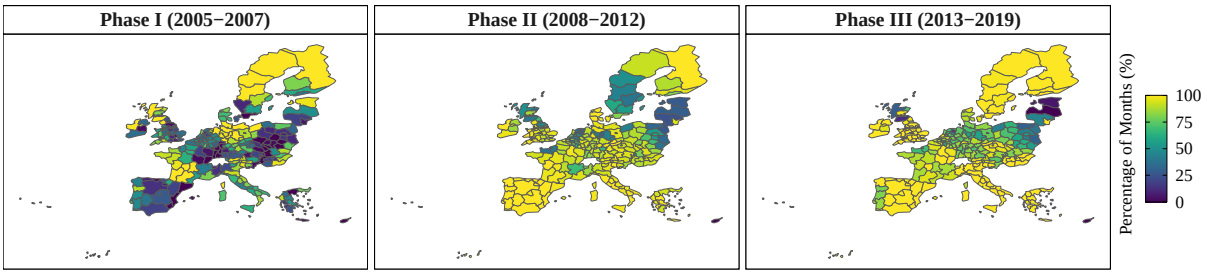


Figure 4.4: Spatial distribution of NUTS regions with reduced fossil fuel $CO_2$ emissions in 0 to 100% of months in each phase of the EU ETS.

level, the percentage of NUTS regions with emissions reduction or increase in all months as well as emissions reduction in more than 50% of months in each phase was calculated. The results are shown in Figure 4.5. Compared to the other two phases, Phase II exhibits the lowest percentage of regions with emissions increase in all months (0.4% of regions). However, when it comes to the percentage of regions with emissions reduction in all and more than 50% of months, Phase III stands out with 40.32% and 94.35% of regions, respectively.

One region in Ireland (Northern & Western Ireland) and one region in Finland (North & East Finland) experienced reduced emissions in all months from January 2005 to December 2019, and 105 regions underwent an emissions reduction in more than 50% of months in all the three phases. On the other side, five regions located in Republic of Cyprus, Greece (North Aegean), Lithuania (Central & Western region), and Poland (Lubelskie and Podlaskie) underwent an emissions increase in more than 50% of months in all the three phases. Only one region (Cyprus) experienced increased emissions over the whole period.

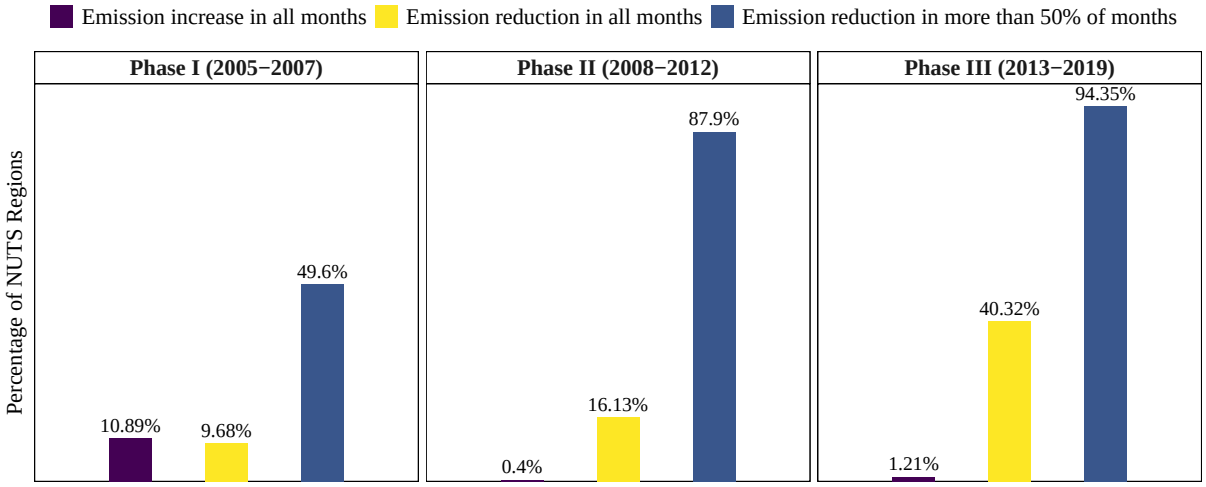


Figure 4.5: Percentage of NUTS regions with emissions reduction or increase in all months as well as emissions reduction in more than 50% of months in each phase of the EU ETS

In order to characterize the relationship between actual and counterfactual fossil fuel $CO_2$ emissions and its evolution over time, median monthly trajectories of actual (observed) and counterfactual (fitted) values of emissions for each phase of the EU ETS are plotted. To offer a more detailed overview of the intervention effect, pointwise and cumulative differences between median actual and counterfactual (fitted) values are also visualized. Figure 4.6 summarizes the effect of the launch of the first phase of the EU ETS on fossil fuel $CO_2$ emissions across Europe.

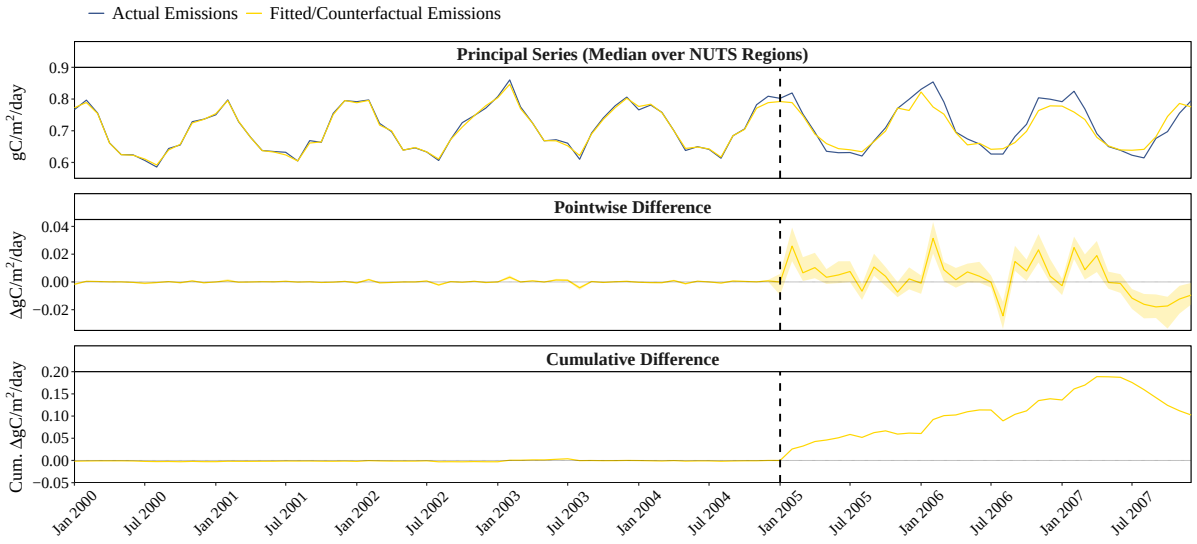


Figure 4.6: Median monthly trajectories of actual (observed) and counterfactual (fitted) values of emissions (top panel); pointwise deviation of median actual values from median counterfactual (fitted) estimates, accompanied by 95% bootstrap confidence intervals with 10000 samples (middle panel); cumulative median difference between actual and counterfactual (fitted) values (bottom panel) for the first phase of the EU ETS.

As observed in Figure 4.6, in the pre-intervention period (from January 2000 to December

2004), the median model-derived estimates fit the median actual (observed) data points pretty well, and the seasonal patterns are successfully captured by the tree ensemble models. Sensible preventative measures taken during the model estimation process guarantee this high goodness-of-fit against overfitting.[18]

During Phase I, actual monthly emissions were, in median, 0.79% higher than counterfactual estimates across all NUTS regions, with the range of change being from -4.85% (in August 2006) to 5.05% (in February 2006). A negative (positive) change is indicative of emissions reduction (increase). In terms of the pointwise difference between median actual and counterfactual series in the post-intervention period, no persistent emissions reduction was attained in the first 28 months (from January 2005 to April 2007). However, from May 2007 until the end of Phase I, median actual monthly emissions remained consistently lower than median counterfactual monthly estimates. Considering the temporal evolution of the cumulative difference between median actual and counterfactual values, an increasing trend could be observed from January 2005 to April 2007, followed by a decreasing trend starting in May 2007. For this phase, the cumulative difference between median actual and counterfactual emissions fluctuated around zero before the intervention, and its value at the intervention point is almost zero. This is indicative of no overall under or overestimation of emissions values in the pre-intervention period.

In a similar vein, the impact of the launch of Phase II on median monthly fossil fuel $CO_2$ emissions across Europe is demonstrated in Figure 4.7. During the second phase, actual monthly emissions were, in median, 9.1% lower than counterfactual emissions across all NUTS regions, with the range of change being from -14.39% (in October 2012) to -1.56% (in January 2008). As can be seen in Figure 4.7, pointwise difference between median actual and counterfactual series was negative in all months after the intervention. For this phase, the cumulative difference between median actual and counterfactual emissions at the intervention point was almost zero, indicating the absence of any remarkable overall under or overestimation in the pre-intervention period. The slight improvement in model performance compared to the first phase may be attributed to the increased size of the training data used for model estimation. The cumulative difference series was on a decreasing trend in all months following the intervention.

Ultimately, Figure 4.8 shows the paths of median actual and counterfactual emissions over the course of Phase III, accompanied by pointwise and cumulative differences between the two series. During the third phase, actual monthly emissions were, in median, 8.39% lower than counterfactual emissions across all NUTS regions, with the range of change being from

[18]That said, overfitting does not necessarily translate into poor prediction on new (unseen) data in the context of methods used in modern machine-learning (such as tree-based ensemble algorithms and neural networks). By reconciling modern machine-learning practice and the classical bias–variance trade-off, Belkin et al. (2019) show that models such as XGBoost may be trained to (almost) exactly fit the training data, while still performing well on unseen data. The interested reader is referred to the reference cited herein for more detailed description.

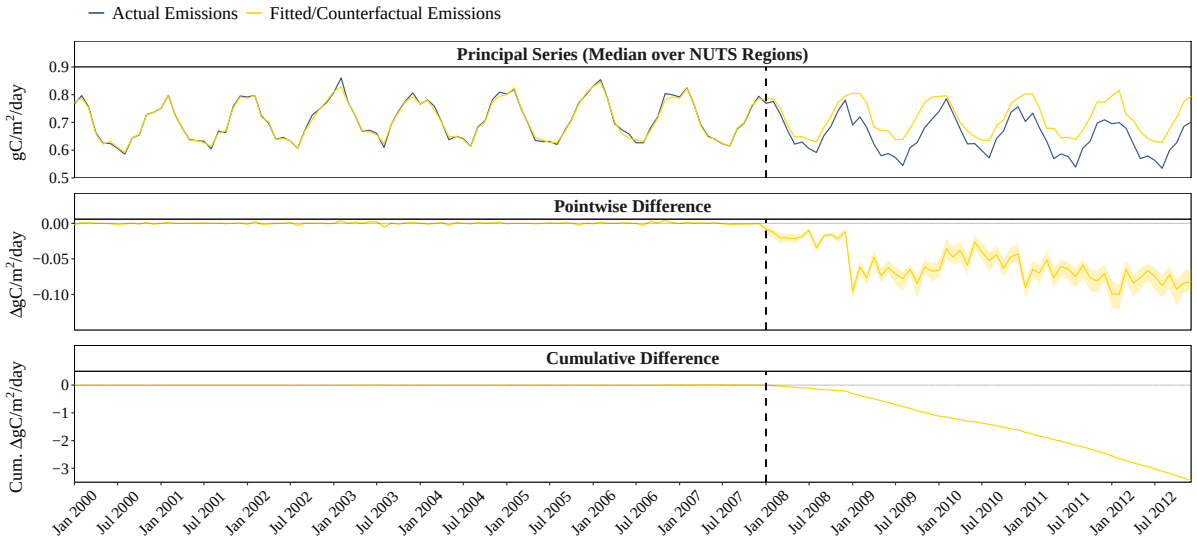


Figure 4.7: Median monthly trajectories of actual (observed) and counterfactual (fitted) values of emissions (top panel); pointwise deviation of median actual values from median counterfactual (fitted) estimates, accompanied by 95% bootstrap confidence intervals with 10000 samples (middle panel); cumulative median difference between actual and counterfactual (fitted) values (bottom panel) for the second phase of the EU ETS.

-14.66% (in August 2019) to -1.5% (in February 2013). As illustrated by Figure 4.7, pointwise difference between median actual and counterfactual series was negative in all months after the intervention, and the cumulative difference series was on a decreasing trend following the intervention. Similar to Phase II, no overall under or overestimation in the pre-intervention period was observed for Phase III. Owing to the highest level of data availability for training the models, predictions made for this phase are expected to be the most reliable.

### 4.5.2 Inferential results

Inferences about the causal impact of each phase of the EU ETS (i.e. intervention effect) were drawn based on a statistical test of the significance of difference between actual and counterfactual emissions. Causal inferences were made based on temporal and spatial analyses. From a temporal perspective, the present work tested whether the median difference between pairs of actual and counterfactual emissions across all NUTS regions was significantly greater than zero in each month following the intervention. Figure 4.9 illustrates the results of the temporal analysis. This analysis found evidence for the presence of a significant intervention effect in the second and third phases and 8 (out of 36) months of the first phase. An important observation is that the median difference between pairs of actual and counterfactual emissions across all NUTS regions was consistently negative from July 2007 to December 2019, indicating the effectiveness of the EU ETS in reducing fossil fuel $CO_2$ emissions during the mentioned period.

From a spatial point of view, it was tested whether the median difference between actual and counterfactual emissions in all months following the intervention was significantly greater

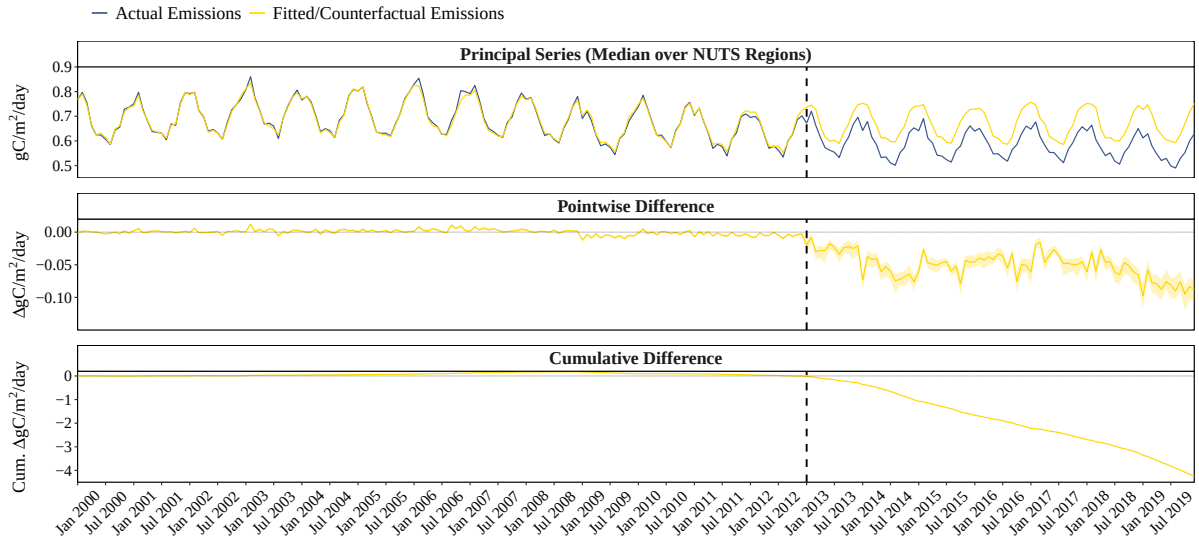


Figure 4.8: Median monthly trajectories of actual (observed) and counterfactual (fitted) values of emissions (top panel); pointwise deviation of median actual values from median counterfactual (fitted) estimates, accompanied by 95% bootstrap confidence intervals with 10000 samples (middle panel); cumulative median difference between actual and counterfactual (fitted) values (bottom panel) for the third phase of the EU ETS.

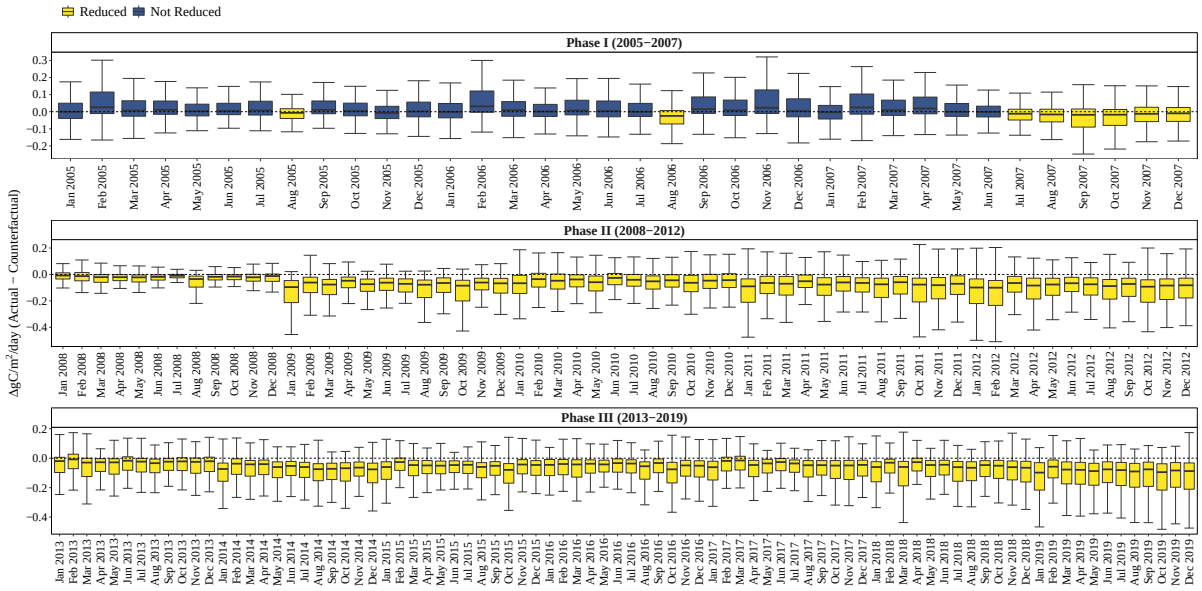


Figure 4.9: Distribution of the difference between actual and counterfactual emissions in NUTS regions in a given month during Phase I (top panel), Phase II (middle panel) and Phase III (bottom panel) of the EU ETS. Boxplots are color-coded based on the rejection (yellow) or non-rejection (blue) of the Wilcoxon signed-rank test's null hypothesis at a significance level of 0.05. Note: The upper (lower) whisker extends from the hinge to the largest (smallest) value no further than 1.5 times the interquartile range. Data points beyond the whiskers are removed from the plot for the sake of better visualization.

than zero in each NUTS regions. Figure 4.10 depicts the spatial distribution of NUTS regions where the intervention effect was significant (insignificant) over the course of each EU ETS phase. This figure provides a general overview of the effectiveness of the EU ETS in reducing

fossil fuel $CO_2$ emissions across European regions. The spatial analysis found evidence for significant emissions reduction in 84, 209 and 226 regions in the first, second and third phases, respectively. Results also demonstrated that 66 European regions went through significant emissions reduction over the course of all the first three phases. On the other side, emissions in the following nine NUTS regions were not significantly affected by any of the EU ETS phases: Cyprus, North Aegean (Greece), Central & Western Lithuania region, Latvia, Overijssel and Flevoland (the Netherlands), Lubelskie, Podlaskie and Mazowiecki regionalny (Poland).

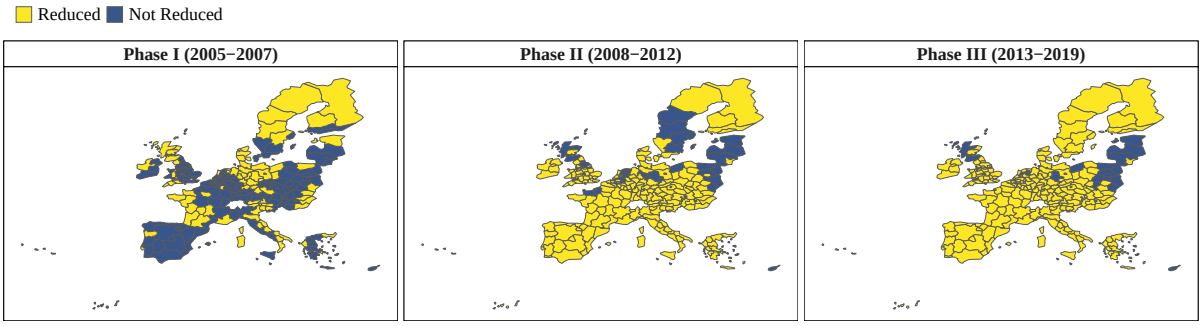


Figure 4.10: Spatial distribution of NUTS regions in which the intervention effect was significant (insignificant) during Phase I (left panel), Phase II (middle panel) and Phase III (right panel). Regions are color-coded based on the rejection (yellow) or non-rejection (blue) of the Wilcoxon signed-rank test's null hypothesis at a significance level of 0.05.

## 4.6 Discussion

With reference to the relative ineffectiveness of the first (pilot) phase of the EU ETS (from both temporal and spatial perspectives) from 2005 to 2007, the results of this study are consistent with what has been found in previous studies (see for example Bayer and Aklin, 2020; Ellerman, 2015). As highlighted by Ellerman (2015), such relative ineffectiveness may be attributed to the oversupply of emissions allowances in Phase I. For the period spanning from 2008 to 2019 the spatial analysis revealed that Phase II was only slightly less effective than Phase III (which included more sectors) in terms of the number of NUTS regions in which significant emissions reduction was realized. An argument could be made that this finding is justified by the difference in allowance allocation between the two phases. While in the first two phases the best part of allowances were freely allocated with grandfathering, a rather environmentally-ineffective output-based allocation approach was adopted for incumbent installations in Phase III, where allocations were associated with historical output of such plants (Economics, 2014). Although an output-based approach may reduce carbon leakage, it dilutes the effective carbon price for the recipient entities and minimizes the emissions reduction by those incumbent firms (Economics, 2014).

As is the case with the majority of studies, the findings of this paper have to be seen in light of some limitations. First, it is perhaps not entirely realistic to attribute all fossil fuel $CO_2$ emissions reduction from 2005 to 2019 to the EU ETS. Indeed, other policy packages at regional, national and EU levels, and the long-term tendency towards increased energy efficiency may also have contributed to emissions reduction across Europe (Ellerman et al., 2016). Nevertheless, as pointed out by Martin et al. (2016), isolating the impacts of emissions trading systems on emissions reduction from those of other factors is an extremely challenging, if not impossible, practice. Serving as the EU's foremost instrument for emissions reduction, the EU ETS already includes the biggest emitters of fossil fuel $CO_2$ (Jaraite-Kažukauske and Di Maria, 2016). In addition, as reported by the European Commission, overall emissions not covered by the EU ETS (emissions from non-ETS industries, transport, buildings, agriculture and waste) have been rather steady for several years (European Comission, 2021e). In view of these considerations, it appears perfectly legitimate to consider aggregate regional fossil fuel $CO_2$ emissions as the target variable in the effectiveness evaluation of the EU ETS. However, the possibility that the installations targeted by the EU ETS might not be present in all NUTS regions under study could not be ruled out. Although such possibility does not affect the results of the temporal analysis carried out in the current study, it can have detrimental effects on inferences made based on the spatial analysis. Through access to reliable data, future research might investigate this possibility and further improve this region-based study by intersecting sectoral or firm-level emissions data with regional boundaries to sort out net emissions from ETS-regulated facilities at regional scale. Second, the likelihood that some of the regional reductions may be due to outsourcing of carbon emissions to other regions within the EU (a situation referred to as carbon leakage) should be acknowledged. Such a possibility could potentially impact the interpretation of the findings from the spatial analysis in this paper, but not the temporal analysis. In any case, as reported by Economics (2014), empirical studies of carbon leakage in the EU ETS have failed to obtain conclusive evidence of significant leakage. Finally, this study considered only land fossil fuel $CO_2$ emissions and disregarded emissions from European aviation that has been included in the EU ETS since 2012. Examinations of the effectiveness of the EU ETS in reducing emissions from air travel have given mixed results (see Heiaas, 2021; Fageda and Teixidó, 2022; Anger and Köhler, 2010). Therefore, further research on the causal relationship between the EU ETS and aviation emissions issue is warranted.

## 4.7 Conclusion

As the cornerstone of the European Union's policy to address climate change and reduce $CO_2$ emissions, the EU ETS has attracted great attention of scholars since its launch in January 2005. However, despite widespread research attention to this trading scheme, comprehensive empirical evidence on achievement of its main target (i.e. emissions reduction) over the course of the

first three phases remains scarce. In an effort to fill this gap, this paper offered an innovative yet intuitive predictive modeling-based approach to the effectiveness evaluation of the the EU ETS with regard to reducing regional fossil fuel $CO_2$ emissions over the 2005-2019 period. The paper makes a link between two strands of the debate on carbon emissions by contributing to the literature on the environmental effectiveness of the EU ETS and climate-related explanatory factors for fossil fuel $CO_2$ emissions across Europe.

By means of temporal and spatial analyses, this study was able to verify whether each of the three phases of the EU ETS could reduce monthly fossil fuel $CO_2$ emissions across European socio-economic regions. The temporal analysis found support for significant emissions reduction over the course of the second and third phases and 8 (out of 36) months of the first phase. The results of the spatial analysis demonstrated significant emissions reduction in 84, 209 and 226 regions in the first, second and third phases, respectively. This work also examined the usefulness of an extensive set of climate variables for predicting fossil fuel $CO_2$ emissions in each region. As a result of this investigation, air temperature, solar radiation and relative humidity were identified as the most important predictors of fossil fuel $CO_2$ emissions in all the three phases. This is indeed an important finding in the understanding of climate-related explanatory factors for $CO_2$ emissions, and can have important implications for energy management at regional scale.

At the end, it should be emphasized that the primary purpose of this explorative study was to examine whether the EU ETS could attain its principal objective of cutting fossil fuel $CO_2$ emissions across Europe, and to identify all climate-related explanatory factors for such emissions across European socio-economic regions. Providing the full story behind the findings of this research necessitates an in-depth regional analysis based on sectoral and/or firm-level data–an exercise that goes beyond the scope of this paper and is left to future research.

CHAPTER 5

# European Union Emissions Trading System: Carbon Price Determinants

**Article Title:** ct carbon emissions allowances prices? Evidence from the first three phases of the EU ETS" (Eslahi and Mazza, 2022)

**Abstract:** This study examines the predictive impact of climate conditions and electricity demand on hourly spot prices of emissions allowances during the first three phases of the European Union Emissions Trading System (EU ETS) (2005-2019). We propose an original methodology for constructing European-scale electricity demand and climate indices and characterize the relationship between those indices and emissions allowances prices by means of an advanced predictive modeling technique (Extreme Gradient Boosting). Empirical findings assert that electricity demand and the climate factors under study were of importance for estimating EUA prices during the first three phases of the EU ETS, with air temperature and electricity demand being most relevant to emissions allowances prices. Conversely, total precipitation and relative humidity proved to be the least relevant variables to the outcome. The results also indicate that the relationship between emissions allowances prices and their climatic predictors was not linear in the studied period. The paper contributes to the growing body of literature on the structural determinants of carbon prices in the EU ETS and enhances our understanding of the impact of climate variability–in the provision of renewable energy production–on the most prominent market-based measure to reduce $CO_2$ emissions in Europe.

**Keywords:** The EU ETS, Emissions Allowances Prices, Electricity Demand, Climate Variables, Predictive Modeling

## 5.1 Introduction

In order to reduce greenhouse gas emissions, many countries worldwide have attempted to enact legislation or devise a mechanism for trading carbon contracts. The main argument for those considerations is that, excessive greenhouse gas emissions and their irreversible consequences for the environment cannot be prevented unless there are powerful (pecuniary) incentives for companies to promote emissions reductions. As such, application of the 'polluter pays' principle through putting a price on carbon dioxide ($CO_2$) and other greenhouse gases has found its place in the national and international environmental policies aimed at fighting global warming.

The European Union Emissions Trading System (hereinafter referred as the EU ETS) is the European Union's major market-based environmental scheme to combat climate change and its impacts under the Kyoto Protocol. Established in 2005, the EU ETS is the earliest and biggest international carbon market in the world, functioning on a cap and trade basis. The scheme is split into distinct trading periods or phases with their own specificities, of which three had drawn to a close by the end of 2020, and the fourth was well under way at the time of writing. $CO_2$ emissions allowances (also called carbon credits or emissions certificates) are a class of assets that represent the right to emit one tonne of $CO_2$ or the equivalent amount of other notorious greenhouse gases (referred to as $CO_2$ equivalent and denoted by $CO_2e$) over a specific period of time, and that can be traded by carbon market participants. Emissions allowances used in the EU ETS are commonly referred to as European Union Allowances (EUA).

The price of emissions allowances traded on a carbon market is frequently used as a measure of the effectiveness of the market. Carbon price provides an economic signal to emitters of $CO_2$, and enables them to decide whether to lower their emissions, or continue emitting and paying for their emissions (World Bank, 2022). Similar to other financial markets, the dynamics of carbon markets are largely driven by the underlying supply and demand fundamentals (Christiansen et al., 2005). The supply of carbon allowances in a cap and trade system like the EU ETS completely depends on the nation or Union-wide limit (cap), and on allocations of the cap to companies and installations covered by the system (Alberola et al., 2008; Batten et al., 2021). The total amount of $CO_2e$ that can be emitted by the sectors covered by the EU ETS is controlled by setting an annually-decreasing limit (cap) on the number of emissions permits. While in the first and second phases of the EU ETS (2005-2012), the cap was determined by each member state through the so-called National Allocation Plans (NAPs), since the beginning of phase three (2013-2020), the cap on emissions was set by the European Commission for the entire set of EU ETS Member States as a whole (European Comission, 2021a).

The allocation of carbon credits takes place in the primary market, where the emissions allowances are issued for free or at an auction-based cost. So as to establish auctioning as the default method for allocating emission allowances, free allocation has been decreasing each

year since the launch of the EU ETS, with free allowances being unavailable to power plants since the beginning of the third phase (European Comission, 2021c). Indeed, electricity producers have been obliged since 2013 to buy all the allowances they need to generate electricity either through auctions on the primary market, or on the secondary market[1] (European Comission, 2021d).

Previously issued emissions allowances can subsequently be traded on the secondary market as needed. Spot and derivatives trading of European Union Allowance are carried out over the counter or via intermediaries like exchanges. The spot market is of particular importance for traders of emission certificates and emitters of $CO_2$ for two major reasons: first, the valuation of potential derivatives is contingent upon understanding spot price dynamics; second, $CO_2$-emitting entities rely on spot prices in order to better assess their production costs and support emissions-related investment decisions (Seifert et al., 2008). The European Securities and Markets Authority (ESMA) confirms that, while the primary market is rather concentrated, the largest participants (i.e. emitters of $CO_2$) are active in the secondary market to ensure that auctioned or freely-allocated allowances are disseminated to other secondary market participants (ESMA, 2022).

The demand side of emissions trading in the European Union is in turn primarily based on the level of $CO_2$ production by the companies and installations covered by the emissions trading scheme. The level of $CO_2$ emissions itself is dependent on numerous factors such as economic growth, fuel (crude oil, natural gas and coal) and power (electricity) prices and climate conditions (Christiansen et al., 2005; Alberola et al., 2008; Creti et al., 2012; Batten et al., 2021). Among these factors, climate conditions have a substantial double effect since they can influence $CO_2$ emissions (hence the demand for carbon credits) both through their impact on energy demand (consumption) and through their impact on renewable and nonrenewable electricity and heat generation (see Christiansen et al., 2005; Amato et al., 2005; Benz and Trück, 2009; Chevallier, 2013; Batten et al., 2021; Ampudia et al., 2022).

Given the fact that the EU ETS is dominated by firms involved in electricity generation (Ahamada and Kirat, 2015), careful attention should be given to the impact of climate conditions on the electric power sector. Indeed, the electricity sector is one of the most sensitive sectors of the economy to climate variations, because the demand for and supply of electricity are closely linked with several climate variables (Valor et al., 2001; McFarland et al., 2015).

[1] With the aim of supporting the modernisation of the energy sector, Article 10c of the EU ETS Directive provides ten lower-income Member States (Bulgaria, Czech Republic, Estonia, Croatia, Latvia, Lithuania, Hungary, Poland, Romania, and Slovakia) with a derogation from the general rules on no free allocation for electricity production (European Comission, 2021d). The optional free allocation was initially planned to be available only during phase 3 of the EU ETS (2013-2020), but its availability was extended by the ETS Directive into the fourth phase (2021-2030). Not all the eligible Member States, however, decided to make use of the possibility to provide free allocation to installations for electricity generation during either phase.

Aside from electricity demand itself as a potential predictor of emissions allowances prices,[2] six climate variables are likely to influence $CO_2$ emissions through affecting electricity production and consumption, thus leading to a possible change in demand for emissions allowances: air temperature, wind speed, solar radiation, total precipitation, surface air pressure and relative humidity.

When it comes to its impact on $CO_2$ emissions, air temperature is often identified with its strong connection to the demand for energy, and most importantly electricity. The idea is that low (high) temperatures boost the need for heating (cooling), hence increasing electric and even non-electric (fossil fuel) energy consumption[3] and $CO_2$ emissions (see among others Mansanet-Bataller et al., 2007; Alberola et al., 2008; Benz and Trück, 2009; Hintermann, 2010; Yao, 2021). Rising temperatures can also influence the energy supply side either by increasing water temperatures, hence negatively affecting thermal power plants' cooling efficiency, or by reducing the efficiency of solar photovoltaic panels–in either case increasing emissions levels (Ebinger and Vergara, 2011). Wind speed, solar radiation and total precipitation affect the share of electricity generated by the most commonly-used non-emitting (clean) energy sources and thus emissions levels (Christiansen et al., 2005; Benz and Trück, 2009; Wei et al., 2020). Finally, surface air pressure and relative humidity are related to the generation cycle and cooling efficiency of fossil-fuel-fired power production, hence changing $CO_2$ emissions levels by affecting the efficiency and reliability of energy supplies from fossil energy sources (Wilbanks et al., 2008; Ebinger and Vergara, 2011; Loew et al., 2020).

Existing research acknowledges climate conditions, among other factors such as energy prices and fuel switching, as structural determinants of carbon prices.[4] Indeed, several attempts have been made to empirically explain the relationship between $CO_2$ prices and variations in some climate factors such as air temperature, rainfall and wind speed in the course of the first, second or third phase of the EU ETS (Mansanet-Bataller et al., 2007; Alberola et al., 2008; Redmond and Convery, 2008; Benz and Trück, 2009; Keppler and Mansanet-Bataller, 2010; Hintermann, 2010; Bredin and Muckley, 2011; Lutz et al., 2013; Rickels et al., 2015; Batten et al., 2021).

A closer look to the literature on the relationship between emissions allowances prices in the EU ETS and climatic determinants of those prices, nonetheless, reveals a number of gaps and shortcomings. First, research on the climatic predictors of EUA prices has been mostly restricted to the study of a limited set of climate variables (the foremost of which is air tem-

[2]By way of illustration, pressures from increases in electricity demand may result in the adoption of low-cost energy sources that are more carbon-intensive, hence changing emission levels in the electricity sector (Goh et al., 2018b).

[3]The impact of high temperatures on the use of fossil fuels for purposes other than electricity generation is less clear since air conditioning systems used for satisfying cooling demand are predominantly powered by electricity (Melillo et al., 2014).

[4]See Chevallier (2013) for a review of academic literature on carbon price drivers.

perature), and has paid little or no attention to other climate factors (such as wind speed, solar radiation, relative humidity and surface air pressure) that may as well have a predictive impact on emissions through affecting renewable and nonrenewable energy systems. In particular, the effect of climate variations on carbon prices in the provision of renewable energy production is understudied (Ampudia et al., 2022). This is of particular importance for regions like Europe that rely, to a significant extent, on renewable sources like wind, solar and hydropower[5].

Additionally, the effect of climate conditions on EUA price development has, by and large, been solely attributed to the demand for energy, most importantly electricity, for heating and cooling purposes (see Mansanet-Bataller et al., 2007; Alberola et al., 2008; Redmond and Convery, 2008; Benz and Trück, 2009; Hintermann, 2010). In a specific case, previous research has in fact treated air temperature as a proxy for energy consumption, rather than view it as a climate factor that may be correlated with the demand for electric and non-electric (fossil fuel) energy. Although air temperature can influence emissions on the demand side through increased heating or cooling-related needs, this is not the only way in which emissions can be affected by temperature. A rise in air temperature reduces the efficiency of power generation from solar photovoltaic panels, and that of fossil fuel (thermal) power stations in converting fuel into electricity (Ebinger and Vergara, 2011; Melillo et al., 2014), hence leading to increased emissions[6]. Given these considerations, isolating the effect of electricity demand on emissions allowances prices will advance the understanding of the effect of climate variables on $CO_2$ emissions and EUA prices via increasing non-electrical applications of fossil fuels (e.g. heating, in the case of air temperature) or through affecting renewable and/or nonrenewable electricity production (the case of air temperature, wind speed, solar radiation, total precipitation, surface air pressure and relative humidity).

Furthermore, the research to date has tended to rely on climate indicators that are unrepresentative of the broad spectrum of climate conditions across Europe, and mostly limited to one or few cities or countries.[7] European territory is, however, sufficiently large to cover a significant range of climatic conditions, from semi-arid Mediterranean to subarctic (boreal) cli-

[5]In 2020, renewable energy sources made up 37.5% of gross electricity consumption in the European Union (Eurostat, 2022).

[6]The reason for the latter is that fossil fuel power plants (as well as nuclear facilities) use water for cooling, and the higher the water temperature, the less efficient the power generation. There is strong large-scale empirical evidence that increase in water temperature is positively related to increase in air temperature (see for example Seyedhashemi et al., 2022).

[7]For example, Mansanet-Bataller et al. (2007) have utilized temperature and precipitation data from Germany; Alberola et al. (2008), Keppler and Mansanet-Bataller (2010) and Bredin and Muckley (2011) have relied on population-weighted temperature data from France, Germany, Spain and the United Kingdom; Hintermann (2010) has used a population-weighted temperature index based on data from a number of monitoring locations in Europe, and precipitation data from Norway, Sweden, Denmark and Finland; Lutz et al. (2013) have based their analysis on temperature data from France, Germany, Italy, and the United Kingdom (until September 2009) and 18 countries (since October 2009); Rickels et al. (2015) have made use of wind speed and precipitation data from Germany, Scandinavia and Spain; and Batten et al. (2021) have used temperatures in Munich, Germany as a proxy for the temperature in the whole Europe.

mate (Wasson et al., 2007). As a particular example, France itself hosts seven different types of climate–from Mediterranean to continental cold.[8]

Finally, the existing accounts fail to demonstrate what the specific relationships between climate variables and EUA prices look like. As emphasized by Chevallier (2013), characterization of possible nonlinearities in such relationships in an extensive European-scale study is called for.

To address these research gaps, the current study examines, within a predictive modeling framework, the observed association between EUA prices and a comprehensive set of European-scale electricity demand and climate indices during the first three phases of the EU ETS. The originality and significance of this research work lie in the following points. First, to the best of the authors' knowledge no study in the literature on climatic drivers of carbon prices has till date utilized data of comparable spatio-temporal granularity and scope. As concerns the spatial resolution and scope of the data, the use of country-level data on demand for electricity, in company with large-scale European gridded data sets on climate variables and fossil fuel $CO_2$ emissions, offers the possibility of constructing aggregate indicators that could summarize electricity demand and climate conditions across the EU ETS zone in the most precise manner. In regard to the temporal resolution and scope of the analysis, the use of data at hourly frequency over a 15-year period for empirical modeling allows for a better understanding of the climatic predictors of intraday emissions allowances prices during the first three phases of the EU ETS.

Second, the study takes advantage of the most extensive set of potential climatic predictors of carbon prices used to date in the literature on price determinants in the EU ETS. In particular, the analysis is enriched with the inclusion of all those climate variables that are directly related to electricity production from wind, solar, and run-of-river hydropower sources–altogether referred to as climate-related renewable energy (CRE) sources. This choice of variables provides new empirical insights into the interconnections between CRE production potential and the leading market mechanism to set a limit on $CO_2$ emissions in Europe.

Third, instead of relying on coarse proxies of electricity demand and climate conditions–as is common in the relevant academic literature, the present research puts forward a state-of-the-art intuitive methodology for constructing large-scale indices using data from the entire geographical scope of the EU ETS. In an attempt to investigate climatic predictors of emissions allowances prices, this is the first study to adopt an interdisciplinary approach to develop European-scale climate indicators by borrowing the concept of "hydro-ecoregions" from hydrology and environmental science. From a methodological standpoint, the proposed hydro-ecoregions-based approach to the construction of European-scale climate indicators can easily be reimagined for purposes other than the characterization of climatic predictors of emissions allowances prices.

[8]See Section 5.2.2.2 for more details.

Ultimately, by virtue of the properties of the empirical modeling framework, this study makes a major contribution to research on determinants of carbon prices by ranking explanatory factors based on their predictive importance. This will contribute to a deeper understanding of the extent to which each explanatory factor should be given consideration as regards the estimation of carbon prices. Moreover, the present research quantifies complicated, nonlinear predictive impact of explanatory factors on the price of carbon and explores, for the first time, how the pure effect of electricity demand and different climate variables on emissions allowances prices varies with the predictor's value. The paper departs from previous literature by analyzing such effect across the entire distribution of predictors (as opposed to the tails of the distribution, i.e. extreme climate conditions) while controlling for various types of seasonality.

The remaining part of the paper proceeds as follows. Section 5.2 describes the data sets utilized for the analysis, details the methods for constructing the population-weighted electricity demand index and emissions-weighted climate indices, sets out the approach to the empirical modeling of emissions allowances prices based on the electricity demand and climate indices, and delineates the framework for characterizing the predictive impact of such indices on EUA prices. The findings of the analysis are presented in Section 5.3. Section 5.4 is concerned with the explanation and interpretation of some major results and makes recommendations for further research work. The paper concludes by summarising the scope of the study and main results, and highlighting the significance of the findings and research implications (Section 5.5).

## 5.2 Materials and Methods

### 5.2.1 Data

The analysis is undertaken using data on the explained variable, i.e. European Union Allowance (EUA) prices,[9] along with the explanatory variables, namely population-weighted electricity demand index and emissions-weighted climate indices.[10] The data consist of five independent datasets that could be classified into three major groups: (1) Market data on European Union Allowance (EUA) prices; (2) Country-level electricity demand and population data, which are utilized in the construction of the population-weighted electricity demand index for the EU ETS zone; and (3) Gridded data on climate variables and fossil fuel $CO_2$ emissions, which are utilized in the construction of emissions-weighted climate indices for the EU ETS zone. After intersecting the data on the explained and explanatory variables, 33087 observations with hourly timestamps–from March 8, 2005 (20:00) to December 30, 2019 (10:00)–are retained for

[9] For methodological reasons, prices are log-transformed prior to the empirical modeling (see Section 5.2.2.3). This transformation is necessary to avoid potential negative predicted values of the response variable.

[10] In addition to explanatory variables, integer-encoded time-based features are created and included in the empirical model to account for possible seasonality information in the data. See Section 5.2.2.3 for more details on time-based features.

the empirical analysis.

#### 5.2.1.1 European Union Allowance (EUA) prices

Market data on hourly European Union Allowance (EUA) spot prices (in the unit of euros per tonne of $CO_2$) are sourced from Refinitiv Datascope. The original data consist of spot prices of emissions allowances from the combination of three major markets of the EU ETS over the 2005-2019 period, namely Powernext, BlueNext and the European Energy Exchange (EEX). Powernext (based in Paris, France) was the leading trading platform over the 2005-2008 period, accounting for the largest share of the spot market transactions of emissions allowances during the first phase of the EU ETS (Daskalakis et al., 2009). Despite being the the largest emissions secondary market for trading on a Spot basis during the second phase of the EU ETS, BlueNext (also headquartered in Paris, France) permanently shut down its trading operations in December 2012. Last but not least, the EEX (located in Leipzig, Germany) has been offering spot trading of the EU ETS allowances since 2005.[11]

When available, the last transaction price in the original dataset is used as the spot price in the present study. In the intervals where the last transaction price is not available, the quote midpoint, defined as the average of Closing Ask and Closing Bid prices, is used as a proxy for the spot price. The ultimate dataset used for the analysis contains 33087 hourly observations from March 8, 2005 (20:00) to December 30, 2019 (10:00). The use of sparse trading data with natural gaps–in lieu of populated data–is based on the consideration that assessing the predictive impact of climate factors and electricity demand on EUA transaction prices is pointless if time points with no real market activity are used. From a methodological point of view, including artificially-populated data points in the response variable would impede the interpretation of predictive modeling results. It cannot be denied, however, that the analysis would be improved with a completely continuous data set.

#### 5.2.1.2 Electricity demand

Data on daily electricity demand (the consumption of electricity) expressed as mean power in megawatts (MW) at the country level for the 2005-2019 period are obtained from the European Centre for Medium-Range Weather Forecasts (ECMWF)[12]. The Copernicus Climate Change Service (C3S) operational energy dataset (ECMWF, 2020a) includes electricity demand in 27 Member States of the EU ETS, namely post-Brexit EU countries excluding Cyprus and Malta, along with the United Kingdom and Norway.[13] However, in light of the late joining of Bulgaria, Romania, Norway and Croatia in the EU ETS, not all countries present in the dataset have been persistently used for the construction of electricity demand index over the study period (see

[11] Powernext activities were merged into EEX in January 2020.

[12] `https://cds.climate.copernicus.eu/`

[13] The dataset does not cover four Member States: Cyprus, Malta, Iceland and Lichtenstein.

Section 5.2.2.1). With the help of country-level hourly air temperature[14] as indicator series, the daily electricity demand series for each country are disaggregated[15] to hourly series using the regression-based Chow-Lin method (Chow and Lin, 1971) with temporal additivity constraint, i.e. ensuring that the sum of hourly values of the obtained series is equal to the corresponding daily values of the original series (see Sax and Steiner, 2013).

Several studies have emphasized the dependence of electricity demand on air temperature (see for example Henley and Peirson, 1997; Valor et al., 2001; Pardo et al., 2002; Amato et al., 2005; Thatcher, 2007; Hekkenberg et al., 2009), making the latter a natural candidate for such temporal disaggregation. With this in mind, before proceeding with the temporal disaggregation, a simple linear regression of the daily electricity demand series on daily averaged air temperature series for each country over the whole study period is conducted. This step allows to investigate, in the first place, the correlation between the two variables and to substantiate the empirical soundness of using hourly air temperature as indicator series in the disaggregation process. The analysis confirmed a significant relationship between electricity demand and air temperature at the daily level at 1% significance level for all countries (with the exception of Greece for which the significance level falls to 10%). The regression analysis is further accompanied by an Augmented Dickey-Fuller (ADF) test to examine the validity of choice of the temporal disaggregation method. The null hypothesis of no-cointegration between daily electricity demand and daily averaged air temperature series is rejected at the 1% significance level, supporting the choice of the Chow-Lin method. The results of these statistical tests are not shown since they are not central to the study's aims. Derived country-level hourly electricity demand series are then used to construct an electricity demand index (see Section 5.2.2.1), as a proxy for the consumption of electricity across the EU ETS zone.

#### 5.2.1.3 Population

Yearly population data for the 27 countries in the electricity demand dataset are obtained from the World Bank (`https://data.worldbank.org/indicator/SP.POP.TOTL`) for the 2005-2019 period. Total population of each country in a given year is the mid-year estimate of the number of all residents of the country.

[14]Country-level hourly air temperature series are calculated by taking the average of the gridded ambient air temperature at 2m above the surface provided by the ERA5 reanalysis (Hersbach et al., 2020) over the area of each country. These data are retrieved from the Copernicus Climate Change Service (C3S) at the European Centre for Medium-Range Weather Forecasts (ECMWF).

[15]The use of temporal disaggregation methods (Chamberlin, 2010) is common in the energy economics literature. Multiple previous studies have employed similar techniques to obtain high-frequency time series from low-frequency data (see for example Sharif et al., 2020; Shahbaz et al., 2017).

#### 5.2.1.4 Climate variables

The present study employs gridded data on climate variables obtained from the ERA5 dataset (Hersbach et al., 2020) at an hourly temporal resolution and a 0.25 degree ($\sim$27.75 km at the equator for both longitude and latitude) spatial resolution over the area of the EU ETS zone during the period under study. Produced by the Copernicus Climate Change Service (C3S) at the European Centre for Medium-Range Weather Forecasts (ECMWF), this dataset offers the most comprehensive picture currently available of the global climate and weather (ECMWF, 2020b). Data on temperature of air at 2m above the surface (K)[16], total sky direct[17] solar radiation at surface ($Jm^{-2}$), total precipitation (m) and surface air pressure (Pa) are obtained directly from the C3S. Wind speed ($ms^{-1}$) at each grid point is calculated from the eastward and northward wind vectors at a height of 100m[18]. Relative humidity (%) values are calculated using the August-Roche-Magnus approximation (Alduchov and Eskridge, 1996), based on the 2m air and dew point temperatures (K). The original data represent the mean area average of climate variables over each grid at a given time point (hour).

#### 5.2.1.5 Fossil fuel $CO_2$ emissions

Gridded data on fossil fuel $CO_2$ emissions at a monthly temporal resolution and a 1 degree ($\sim$111 km at the equator for both longitude and latitude) spatial resolution over the area of the EU ETS zone during the period under study are obtained from the Open-source Data Inventory for Anthropogenic $CO_2$ (ODIAC) (Oda and Maksyutov, 2011, 2015; Oda et al., 2018). Derived from multiple proxies such as point source emissions and satellite remote sensing of night lights, this database is one of the most temporally and spatially fine-grained data presently available on global fossil fuel $CO_2$ emissions. Emissions values are expressed as monthly mean of gram carbon/$m^2$/day.

### 5.2.2 Methodology

#### 5.2.2.1 Construction of population-weighted electricity demand index

Country-level hourly series of electricity consumption are summarized into a convex combination, using yearly country-level shares of the total population as the coefficients. Population shares represent the importance (weight) that should be assigned to electricity demand in each country under study. The resulting index, hereinafter referred to as population-weighted electricity demand index, is used as a proxy for the consumption of electricity across the EU ETS

[16]For easier interpretation, temperatures are converted to degrees Celsius before being used for the empirical modeling.

[17]Solar photovoltaic and solar thermal plants are most productive when exposed to direct solar radiation.

[18]100m is the nearest height to the average hub height of modern land-based wind turbines used for wind power generation (Wiser et al., 2020).

zone at a given hour. Mathematically speaking, the population-weighted electricity demand index at hour $t$ is calculated as follows:

$$\text{Electricity Demand Index}^{(t)} = \sum_{i_t} \left( \text{Population Share}_{i_t}^{(t)} \times \text{Electricity Demand}_{i_t}^{(t)} \right) \tag{5.1}$$

where

$$\text{Population Share}_{i_t}^{(t)} = \frac{\text{Population}_{i_t}^{(t)}}{\sum_{i_t} \text{Population}_{i_t}^{(t)}} \quad (\sum_{i_t} \text{Population Share}_{i_t}^{(t)} = 1)$$

Here, $t$ denotes the time period of interest (in the unit of hour), and the subscript $i_t$ runs over the countries that are members of the EU ETS at time $t$. It should be noted that not all the 27 countries in the electricity demand dataset were members of the EU ETS from 2005 to 2019. Bulgaria and Romania joined the European Union and the EU ETS in January 2007. Norway has been a part of the emissions trading scheme since January 2008. Finally, Croatia became an EU member country in July 2013. For this reason, in the construction of the population-weighted electricity demand index for a given time period (hour), only the data from the Member States of the EU ETS during the period concerned are used. This means that, for the periods spanning from March 8, 2005 (20:00) to December 31, 2006 (23:00), from January 1, 2007 (00:00) to December 31, 2007 (23:00), from January 1, 2008 (00:00) to June 30, 2013 (23:00), and from July 1, 2013 (00:00) to December 31, 2019 (23:00), data on 23, 25, 26 and 27 countries, respectively, are utilized for constructing the index. For a given hour $t$, population shares are calculated using population estimates for the year in which the time period $t$ lies. The weighting method is based on the assumption that the hourly population of a target country throughout the year corresponds to the country's annual population estimate. This assumption has its roots in the inherent limitation of the population data that are on an annual frequency.

#### 5.2.2.2 Construction of emissions-weighted climate indices

In order to construct aggregate indicators that could describe, as accurately as possible, climate conditions across the EU ETS zone, we capitalize on the notion of European hydro-ecoregions put forward by Wasson et al. (2007). Hydro-ecoregions (hereafter denoted as HER) are defined as geographical units that exhibit similar climatological, topographic, geological and lithological characteristics. Wasson et al. (2007) have identified a total of 133 HERs in Europe and Turkish Thrace, that are further classified into 9 distinct climate classes (aka homogeneous climate regions) based on several climatic factors: Alpin Mountain, Boreal, Continental Cold, Hyper Mediterranean, Mediterranean, Oceanic, Temperate, Temperate Mountain, and Temper-

ate Warm. The EU ETS zone covers 131 HERs that span across 29 countries[19] and embody all the above-mentioned climate classes. Figure 5.1 provides a map of these HERs and their corresponding climate classes.

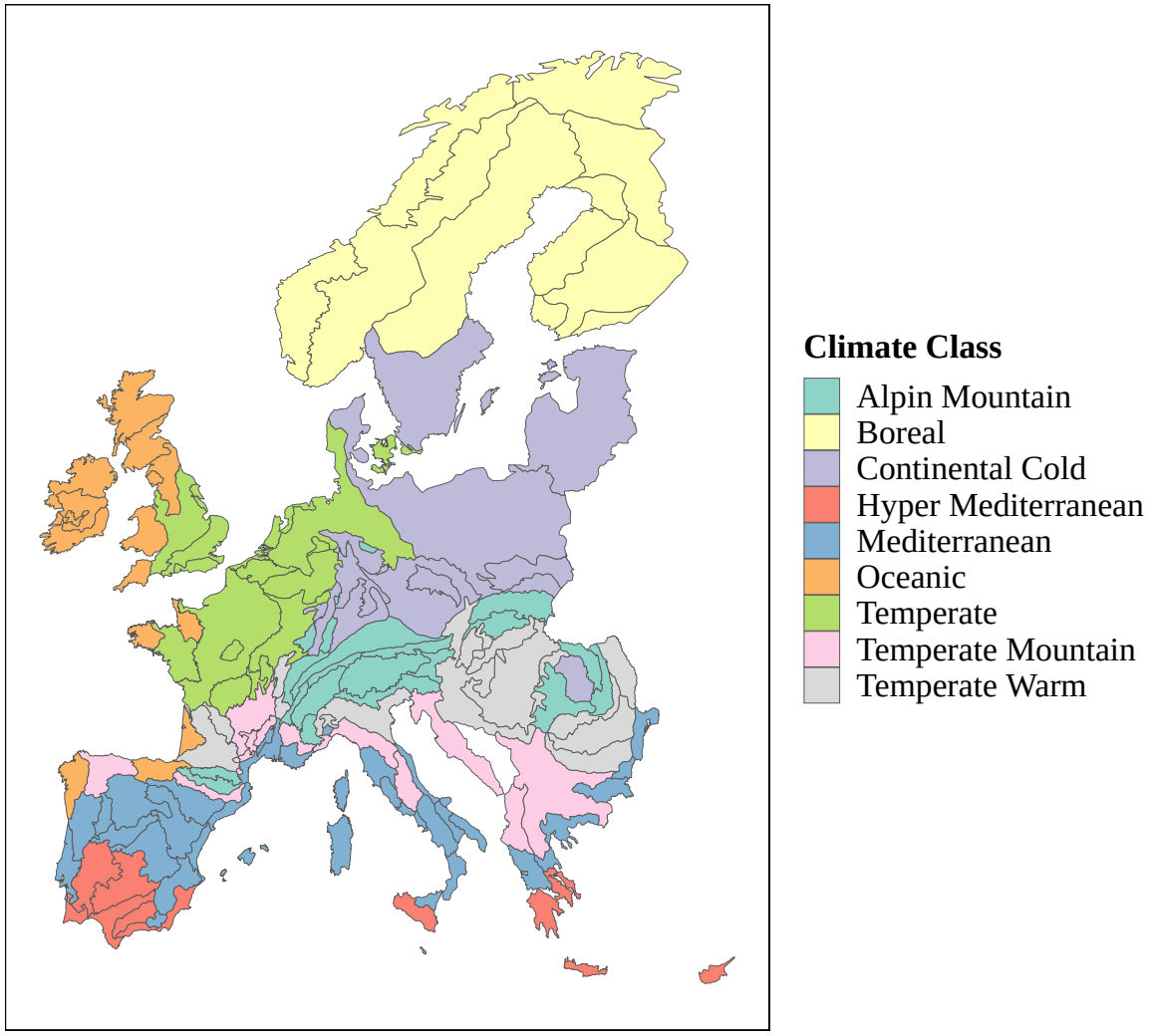


Figure 5.1: Hydro-ecoregions (HERs) and their corresponding climate classes across the EU ETS zone. Data used for plotting the map are sourced from Wasson et al. (2007).

Given the way the homogeneous climate regions are delineated (so as to minimize intra-regional and maximize inter-regional differences in terms of climate conditions) (for more details see Wasson et al., 2007), the present paper presumes that the selected climate variables (air temperature, solar radiation, relative humidity, wind speed, total precipitation and surface air pressure) show very little variation within the area of each climate class. In this regard, at a given time point (hour), the mean area average of climate variables over all the HERs belonging to the same climate class can well represent the climate conditions in those HERs at that point

[19] 27 post-Brexit EU member countries along with the United Kingdom and Norway. No HER is available for Iceland and Liechtenstein.

in time[20].

The first step in constructing European-scale emissions-weighted climate indices thus consists in summarizing climate conditions of the EU ETS zone at each hour by climate class. This is achieved by calculating the average value of each climate variable at the grid points lying within different homogeneous climate regions. The nine aggregate climate indicators at each hour are then weighted by the share of fossil fuel $CO_2$ emissions in the corresponding climate class to total emissions across all climate classes. Since carbon emissions are transmission channels through which climate variables can affect EUA prices, emissions shares are natural candidates to represent the importance (weight) that should be assigned to climate variables in each climate class. For each of the six climate variables, the emissions-weighted index at a given hour $t$ is constructed as follows:

$$\text{Climate Index}^{(t)} = \sum_j \left( \text{Emissions Share}_j^{(t)} \times \text{Climate Indicator}_j^{(t)} \right) \tag{5.2}$$

where

$$\text{Emissions Share}_j^{(t)} = \frac{\text{Emissions}_j^{(t)}}{\sum_j \text{Emissions}_j^{(t)}} \quad (\sum_j \text{Emissions Share}_j^{(t)} = 1)$$

Here, the subscript $j$ runs over the nine climate classes. For a given hour $t$, emissions shares are calculated using monthly estimates for fossil fuel $CO_2$ emissions, i.e. emissions in the month in which the time period $t$ lies. Calculation of emissions shares is performed in three steps. First, monthly gridded emissions are overlayed with the spatial boundaries of each climate class[21], and the mean area average of emissions estimates over all the HERs belonging to that climate class is used as the measure of emissions in the entire region. Second, emissions estimates (originally expressed in the unit of monthly mean of gram carbon/$m^2$/day) are multiplied by the total surface area of the climate classes (in $m^2$) to obtain the average monthly quantity of carbon released per day in the area belonging to each climate class. Finally, the quantity estimates of carbon released in different climate classes are summed up to provide the total quantity of carbon released per day (monthly mean) across the entire EU ETS zone. Emissions shares are obtained by calculating the proportion of emissions released over the area of each homogeneous climate region out of the total emissions across all homogeneous climate

[20]For the sake of comprehensiveness, the entire set of homogeneous climate regions–including those overlapping with Bulgaria, Romania, Norway and Croatia–are used for the construction of emissions-weighted climate indices over the entire period. Since no climate class is exclusive to these countries, such a choice is not expected to significantly influence the results.

[21]In order to match the the spatial resolution of the emissions data to that of the climate variables, the ODIAC data were disaggregated to $0.25 \times 0.25$ degree cells while maintaining values of the original cells. This adaptation was made to achieve a neatly arranged intersection of grid points with the areas of climate classes, without changing the accuracy of the data.

regions.

The underlying assumption of this weighting scheme is that the suggested emissions shares (calculated based on monthly averages of gram carbon per day) could be regarded as acceptable proxies for emissions shares at an hourly level. Ideally, the frequencies of emissions shares and aggregate climate indicators would match. Nonetheless, in the absence of more temporally fine-grained emissions data, it is well justified to make use of monthly based weighting coefficients. In view of the slight difference between regional time zones in Europe[22]–which could potentially lead to similar intraday patterns of $CO_2$ emissions–the above assumption seems on the whole to be warranted to hold.

Table 5.1 features summary statistics of the explained and explanatory variables (except time-based predictors) included in the empirical model (see Section 5.2.2.3), namely the constructed electricity demand and climate indices along with emissions allowances (EUA) spot prices.

Table 5.1: Summary statistics of hourly emissions allowances (EUA) spot prices, electricity demand index and climate indices from March 8, 2005 (20:00) to December 30, 2019 (10:00). The total number of observations is 33087.

| Variable | Mean | Max | Min | SD |
|---|---|---|---|---|
| EUA Price (€/tonne $CO_2$e) | 12.36 | 53.50 | 0.01 | 7.49 |
| Electricity Demand Index (MW) | 1395.40 | 1815.70 | 975.80 | 135.21 |
| Air Temperature Index (°C) | 12.30 | 31.22 | -10.94 | 7.51 |
| Solar Radiation Index ($Jm^{-2}$) | 627288 | 2273029 | 0 | 518677.10 |
| Relative Humidity Index (%) | 91.75 | 98.76 | 78.28 | 4.09 |
| Wind Speed Index ($ms^{-1}$) | 5.21 | 12.22 | 2.18 | 1.24 |
| Total Precipitation Index (m) | 0.0001 | 0.00061 | 0.0000015 | 0.000068 |
| Surface Air Pressure Index (Pa) | 98040 | 100020 | 95001 | 649.7647 |

#### 5.2.2.3 Empirical modeling of EUA prices based on electricity demand and climate indices

To characterize the predictive impact of climate factors and electricity demand on emissions allowances prices, the present study employs Extreme Gradient Boosting (Chen and Guestrin, 2016)–a pioneering tree ensemble supervised machine learning algorithm that can be used for regression predictive modeling. This algorithm can empirically establish (nonlinear) relation-

[22] 18 out of 29 countries under study (17 Member States of the EU together with Norway) share the same time zone, i.e. Central European Time (UTC+1). Ireland, Portugal and the United Kingdom use Western European Time (UTC). Lastly, 8 out of 29 countries under study (Finland, Estonia, Latvia, Lithuania, Romania, Bulgaria, Greece and Cyprus) use Eastern European Time (UTC+2).

ships between explanatory and response variables, without making any formal distributional assumptions nor being vulnerable to multicollinearity. As is the case with all predictive models, Extreme Gradient Boosting does not intrinsically indicate causal relationships between variables. That being so, the modeling approach proposed here does not imply that a change in climate conditions or electricity demand leads directly to a change in emissions allowances spot prices. Instead, we argue that a change in electricity demand and climate conditions is expected to be associated with a change in emissions, and consequently a change in the demand for emissions certificates. Therefore, evaluating the predictive association between EUA transaction prices and their explanatory factors is the first step towards establishing any causal relationship between those variables. The empirical modeling is carried out using log-transformed EUA spot prices as the explained variable, along with 11 explanatory variables: the electricity demand index, six climate indices (air temperature, solar radiation, relative humidity, wind speed, total precipitation and surface air pressure) and four time-based features (hour of the day, day of the week, month of the year and year).

The tree-based model of the Extreme Gradient Boosting algorithm is comprised of a number of regression decision trees that are trained for predicting a response variable based on the values of explanatory variables. This model can be expressed in the general form

$$\hat{y_i} = \hat{f}(x_i) = \sum_{k=1}^{K} g_k(x_i) \quad g_k \in \mathscr{F} \tag{5.3}$$

where the subscript $i$ indicates the set of $N$ data points used for modeling ($\{(x_i, y_i) \,|\, i = 1, ...N, x_i \in \mathbb{R}^p, y_i \in \mathbb{R}\}$, with $p$ being the number of explanatory variables), and $K$ is the number of trained regression decision trees utilized by the model. $\mathscr{F} = \{g(x) = w_{q(x)}\}$ ($q : \mathbb{R}^p \to J, w \in \mathbb{R}^J$) denotes the space of regression trees, where $q$ is the structure of each individual tree that maps a data point to the corresponding leaf score $w$, and $J$ is the total number of leaves in the tree (Chen and Guestrin, 2016). The tree growing process of the Extreme Gradient Boosting algorithm is described by Chen and Guestrin (2016) as follows. A regression tree starts with a single root node and is extended to a certain depth (i.e. the longest path between the root node and a leaf) by continually splitting the training data based on all or a subset of explanatory variables. The result is a tree with a root node, a set of intermediary nodes–that each split data points by one explanatory variable–and a number of leaves to which prediction scores are ascribed. The scores assigned to a given observation in the relevant leaves of individual trees are then added to obtain the ultimate prediction of the explained variable for that observation. The algorithm decides on splitting points and assigns prediction scores using an enhanced gradient boosting method, and with the aim of minimizing an objective function that consists of two parts, namely training loss and regularization:

$$\mathscr{L} = \sum_{i=1}^{N} L(\hat{y}_i, y_i) + \sum_{k=1}^{K} \Omega(g_k) \tag{5.4}$$

where

$$\Omega(g_k) = \gamma J_k + \frac{1}{2}\lambda \sum_{j=1}^{J_k} w_{j,k}^2$$

Here, the squared error loss function $L$ measures the difference between original values of the explained variable $y_i$ and the predicted values $\hat{y}_i$. $J_k$ and $w_{j,k}$ denote the number of leaves and the prediction score assigned to the $j^{\text{th}}$ leaf of the $k^{\text{th}}$ regression tree, respectively. The so-called hyperparameter $\gamma$ is the minimum loss reduction required to further split a leaf node of the tree, and $\lambda$ is the L2 regularization term on the prediction scores. The values of these two model hyperparameters, together with those of tree-specific parameters control the learning process of the algorithm and need to be designated in advance (Chen and Guestrin, 2016).

To avoid overfitting[23], hyperparameters of the Extreme Gradient Boosting algorithm are tuned using grid search, and each combination of model hyperparameters are evaluated using 5-fold cross-validation with 5 repetitions. The model performance metric for the evaluation of each hyperparameter combination is the root-mean-square error (RMSE), which measures the average prediction error made by the model in predicting the outcome of interest for an observation. More precisely, the hyperparameter combination that minimizes average RMSE across all folds is selected as the optimal tune, and the model with the optimal hyperparameter configuration is retained as the base model for further analysis.

Table 5.2 presents the domain of hyperparameters defined for the sake of the present analysis. The number of trees used for boosting, and the L2 regularization term ($\lambda$) are fixed at 100 and 1, respectively. The choice of possible hyperparameter values is motivated principally by recommendations of Boehmke and Greenwell (2019) and Thakur (2020). The discrete grid of hyperparameter values includes 1296 unique combinations of hyperparameter values. Each combination is evaluated $5 \times 5$ times during the model validation procedure. This leads to a total of $1296 \times 25$ tree ensemble models that are trained and evaluated to choose optimal hyperparameter values for the Extreme Gradient Boosting algorithm.

Altering hyperparameter values can affect the performance and training behavior of the Extreme Gradient Boosting algorithm in different ways. Lower values of the learning rate $\eta$ make the model more robust to overfitting. Increasing the the minimum loss reduction factor $\gamma$

[23] Although the present study adopts powerful preventative measures against overfitting, it should be noted that overfitting does not necessarily conduce to poor generalization when it comes to methods used in modern machine-learning (e.g. tree-based ensemble algorithms and neural networks). Belkin et al. (2019) provide empirical evidence on good generalization behavior of the families of "interpolating" functions explored by boosting with decision trees and random forests.

Table 5.2: Hyperparameter configurations used for evaluating tree ensemble models.

| Hyperparameter | Range | Default Value | Selected Values for Tuning |
|---|---|---|---|
| $\gamma$ | [0,∞) | 0 | {0.1,1,10} |
| $\eta$ | [0,1] | 0.3 | {0.05,0.1,0.2,0.3} |
| Maximum Depth | {1..∞} | 6 | {3..8} |
| Minimum Child Weight | [0,∞) | 1 | {7,10,20} |
| Column Sample by Tree | (0,1] | 1 | $\{\frac{3}{11},\frac{6}{11}\}$ |
| Sub-sample | (0,1] | 1 | {0.3,0.5,0.7} |

leads to a more conservative algorithm. The number of terminal nodes in a a tree is controlled by the maximum depth parameter, decreasing the value of which leads to a more conservative and so less vulnerable to overfitting model. Minimum child weight specifies the minimum sum of instance weight (hessian) needed in a child node. A smaller minimum child weight may lead to the learning of relationships that might relate uniquely to the sample used for tree construction, therefore increasing the complexity of trees and their susceptibility to overfitting. The fraction of explanatory variables used for constructing each tree is determined by a parameter called column sample by tree. The sub-sampling of explanatory variables occurs once for every tree built. By default this parameter is set to 1 meaning that all explanatory variables are used. A column sample by tree value less than 1 results in a more conservative algorithm. Finally, the fraction of data that is used to build trees in each boosting iteration is regulated by the sub-sample parameter. If this parameter is set to 1, all data points are utilized to grow a tree–an approach referred to as regular boosting. A sub-sample value less than 1, makes the model randomly sample a subset of training data prior to growing trees. The latter is referred to as stochastic boosting.

The empirical modeling framework used in the present study is not likely to suffer from serial correlation in the time series data for three reasons. First, during the repeated 5-fold cross-validation procedure used for identifying the optimal hyperparameter configuration, the data are divided into training and validation data sets in a random manner. Second, when training the tree ensemble models, we adopt a stochastic boosting approach (as contrasted with regular boosting), which makes the algorithm randomly select–without replacement–only a fraction of the training data at each iteration. Ultimately, the unpopulated times series of hourly data used for modeling present natural gaps and do not necessarily include adjacent observations. Thus, the odds of adjacent observations being used by the algorithm at each iteration is insignificant.

#### 5.2.2.4 Characterizing the predictive impact of electricity demand and climate indices on EUA prices

Characterization of the predictive impact of electricity demand and climate indices on EUA prices is carried out in two steps. The first step consists of computing permutation feature importance (Breiman, 2001; Fisher et al., 2019) of those indices, and ranking them based on their significance for the prediction of emissions allowances spot prices. The importance of a given index is measured by calculating the increase in the base model's prediction error (measured by RMSE ratio) after permuting–with repetition–the values of the index. The algorithm is based on the simple idea that shuffling the values of an index breaks the associations between the index and the true outcome of interest[24] (see Molnar, 2020). The larger the increase in prediction error (loss) after permuting an explanatory variable, the more important the variable is for predicting the response variable; correspondingly, if permuting the values of a variable leaves the base model's prediction error unaltered, the variable is considered unimportant since in such a case, the model disregards the variable for the prediction (Molnar, 2020). Permutation of indices is repeated 1000 times to construct the null distribution of importance measures. In formal terms, the feature importance measure of an explanatory variable $p$ is computed as

$$\text{Feature Importance}_p = \frac{L(y_i, \hat{f}(x_i^{perm:p}))}{L(y_i, \hat{f}(x_i))} \quad (i = 1, ...N; x_i \in \mathbb{R}^p; y_i \in \mathbb{R}) \tag{5.5}$$

where $L$ is the RMSE loss (error) function and $x_i^{perm:p}$ is the $i^{\text{th}}$ data point with the $p^{\text{th}}$ index replaced by a randomly sampled value, without replacement, from another data point. As the The permutation feature importance algorithm of Fisher et al. (2019) is based on resampling without replacement, a permutation test can be carried out with the null hypothesis that the feature importance of the explanatory variable $p$ is 1:

$$H_0 : \text{Feature Importance}_p = 1 \tag{5.6}$$

If the variable $p$ is not important in predicting the outcome of interest, one should expect that the values for feature importance measure of the variable fluctuate around 1. Indeed, the aforementioned permutation test offers a framework to construct confidence intervals and p-values from resampling without replacement, hence allowing for determining statistical significance of a variable's importance.

[24] As reminded by Molnar (2020), shuffling the values of an explanatory variable destroys its relationship not only with the outcome variable, but also with other explanatory variables. In this regard, all interactions among explanatory variables are naturally taken into account by the permutation feature importance algorithm. Due to this characteristic, the algorithm nevertheless suffers form the disadvantage of incorporating the importance of any interaction between a pair of variables into the importance measure of both variables. Moreover, not only can the permutation feature importance be biased by unrealistic data instances if explanatory variables are highly correlated, but also including two highly correlated variables can decrease the importance of each variable by splitting the importance between the two (Molnar, 2020).

In the second step, we describe how electricity demand and climate indices influence the predicted outcome of the base model on average. For this aim, mean-centered accumulated local effects (Apley and Zhu, 2020) are calculated and plotted for every single index. Accumulated Local Effects (ALE) are model-agnostic global explanation measures used for the evaluation of the relationship between explanatory variables and the response variable. According to Molnar (2020), the construction of the ALE plot of a numerical explanatory variable is conducted as follows. First, the distribution of the variable is divided into a number of intervals. For all the data points in each interval, the value of the explanatory variable of interest is replaced with the lower and upper bounds of the defined interval, and the difference in the model's predicted outcome for each data point is calculated. This difference in prediction is considered the "effect" of the explanatory variable for an individual data point that lies in the given interval[25]. The effects of all data points within the interval are then added up and divided by the number of data points that belong to the interval, resulting in an average that represents the "local" effect of the variable. Ultimately, to find the uncentered ALE of an explanatory variable value that corresponds to the interval, average effects across all previous intervals are "accumulated". In mathematical terms, the uncentered ALE of a numerical explanatory variable $p$ at a certain value $x$ is estimated as

$$\hat{\tilde{f}}_{p,ALE}(x) = \sum_{l=1}^{l_p(x)} \frac{1}{n_p(l)} \sum_{i:x_p^{(i)} \in N_p(l)} \left[ \hat{f}(z_{l,p}, x_{\setminus p}^{(i)}) - \hat{f}(z_{l-1,p}, x_{\setminus p}^{(i)}) \right] \tag{5.7}$$

where $N_p(l)$ denotes the $l^{\text{th}}$ interval (aka neighborhood) among the intervals into which the distribution of the variable $p$ is divided, and $n_p(l)$ is the number of data points whose value of the variable $p$ lies within the interval $N_p(l)$. Starting and end points of this interval are denoted by $z_{l-1,p}$ and $z_{l,p}$, respectively. The outer sum runs from the first interval up to and including the interval $l_p(x)$ to which $x$ belongs. In the last resort the uncentered ALE is mean-centered so that average effect over the data is zero (Apley and Zhu, 2020; Molnar, 2020):

$$\hat{f}_{p,ALE}(x) = \hat{\tilde{f}}_{p,ALE}(x) - \frac{1}{N} \sum_{i=1}^{N} \hat{\tilde{f}}_{p,ALE}(x_p^{(i)}) \tag{5.8}$$

As argued by Molnar (2020), the definition of intervals for calculating the ALE of an explanatory variable is rather subjective. Using a small number of intervals improves stability of the estimates but at the cost of compromising on the visualization of the real complexity of the prediction model. Increasing the number of intervals, on the other hand, results in more accurate albeit shaky ALE plots. For the sake of this study, we use the percentiles of the distribution

[25]The use of differences in the formula blocks the effect of other (possibly correlated) explanatory variables. Indeed, ALE estimates are able to determine the pure effect of a variable without mingling the effect with the effects of correlated features.

of explanatory variables to define ALE evaluation intervals. Such a choice guarantees that there is the same number of data points in each interval, with the disadvantage that the length of intervals can be dissimilar. In the case of extremely skewed variables, the latter attribute should warrant a cautious interpretation of interval-wise effects.

Data analysis, modeling and visualization in the present study have been performed using R programming language (R Core Team, 2020; Kuhn, 2008; Molnar et al., 2018).

## 5.3 Results

Amongst the 1296 unique combinations in the hyperparameter grid space (see Section 5.2.2.3), the hyperparameter values presented in Table 5.3 were selected as the optimal configuration (tune) since they minimized average RMSE across all folds.

Table 5.3: Optimal hyperparameter configuration (tune) of the tree ensemble model, used as the base model for further analysis (average RMSE $= 0.252$; average $R^2 = 0.963$)

| Hyperparameter | Best Tune |
|---|---|
| $\gamma$ | 0.1 |
| $\eta$ | 0.1 |
| Maximum Depth | 8 |
| Minimum Child Weight | 20 |
| Column Sample by Tree | $\frac{6}{11}$ |
| Sub-sample | 0.7 |

Permutation feature importance measures (based on 1000 repetitions) for the electricity demand and climate indices are illustrated in Figure 5.2. The importance of each index is measured by calculating the increase in the base model's prediction error (RMSE ratio) at each repetition, when the values of the index are permuted.

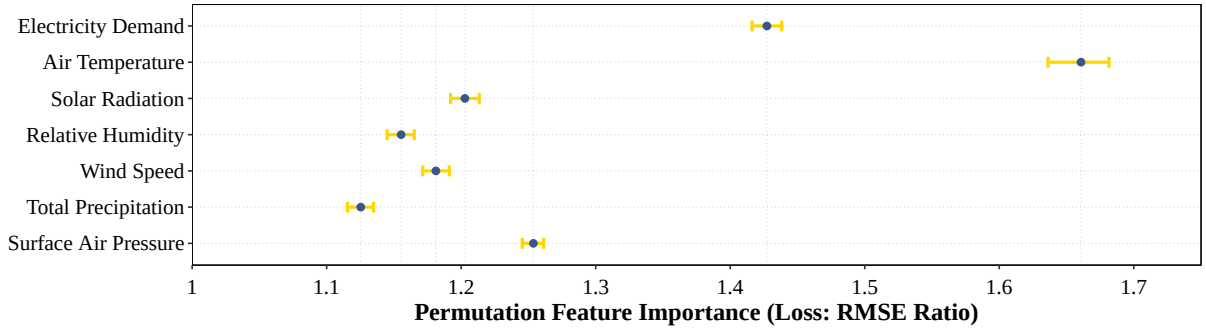


Figure 5.2: Permutation feature importance measures (RMSE ratios) for electricity demand and climate indices. I-shaped bars represent 5% to 95% inter-quantile ranges of importance values from 1000 repetitions. The solid dot within the interval signifies median importance.

From Figure 5.2, two key findings emerge. First, the null hypothesis of feature unimportance (as expressed in Equation 5.6) is rejected at a significance level of 0.1 for the electricity demand index and all climate indices. None of the 90% confidence intervals for feature importance estimates include 1, leading to the conclusion that climate factors and electricity demand are indeed of predictive importance within the proposed empirical modeling framework. This is an important finding in the understanding of the importance of explanatory factors for the prediction of emissions allowances prices. Second, among different indices, air temperature proves to be the most important feature for predicting emissions allowances prices, followed by electricity demand, surface air pressure and solar radiation. Wind speed, relative humidity and total precipitation are less important variables (in decreasing order of importance) when it comes to the prediction of emissions allowances prices.

The assessment of the predictive impact of electricity demand index and climate indices on EUA prices is complemented by the estimation of ALE values for each index. Figure 5.3 demonstrates ALE plots of the electricity demand and climate indices. Different panels of this figure show how the predicted outcome of the base model changes, compared to the average prediction, at different values of each index.

A major implication of Figure 5.3 is that the predictive relationship between emissions allowances prices and electricity demand and climate indices is nonlinear in nature. This is indicative of the inappropriateness of adopting a linear modeling framework for establishing the association between carbon price and its electricity demand-related and climatic explanatory factors.

The inspection of individual panels of the figure permits to identify the effect that each single index, isolated of all others, has on the output. Starting from the top panel, the ALE curve of electricity demand exhibits an overall increasing–yet non-monotonic–behavior from low to high index values. Given the method of calculation of ALE values, one should however be careful when interpreting this behavior on a non-local basis, i.e. across different intervals. The main effect of electricity demand is persistently lower than average prediction of the data at index values below 1382 MW (corresponding to the $55^{\text{th}}$ percentile). For the intervals in which the electricity demand index value is above 1591 MW (corresponding to the $90^{\text{th}}$ percentile), the model predicts higher values of log-transformed EUA prices with respect to the average prediction. This finding is in accordance with expectations and previous findings, indicating that in the short term and due to production rigidities, higher demand for electrical energy translates directly into an increase in demand for EUA credits and therefore into higher EUA prices (Ampudia et al., 2022). Model predictions for moderate values of the electricity demand index (i.e. from around 1382 to 1591 MW corresponding to the 55%-90% inter-quantile range) mainly correspond to mean prediction. Overall, the predictive impact of electricity demand on emissions allowances prices is more pronounced in the extremes of the distribution.

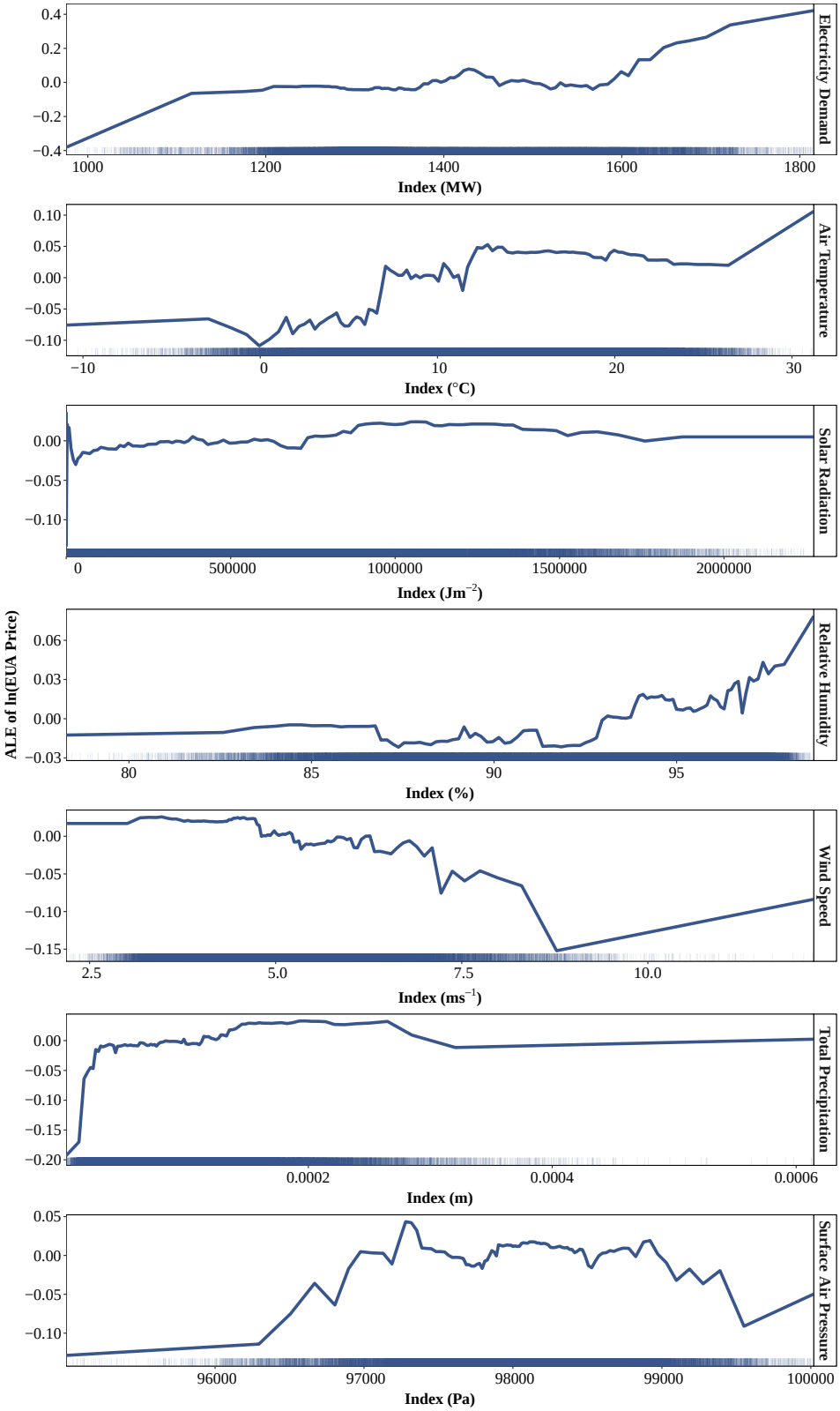


Figure 5.3: Mean-centered accumulated local effects (ALE) of electricity demand and climate indices in predicting EUA prices over the study period. The distribution of data points for each index is displayed on the margin of horizontal axis.

At temperatures below about 7°C (corresponding to the 29$^{th}$ percentile), the predicted values of (logarithmic) EUA prices are persistently lower than average prediction of the data. At index values above 11.5°C (corresponding to the 46$^{th}$ percentile), the model persistently predicts higher values of log-transformed EUA prices with respect to the average prediction. In cool temperatures (7-11.5°C, corresponding to the 29%-46% inter-quantile range), model predictions are mostly in line with the average prediction. When comparing these results to those of the existing literature, an important finding arises as to the main effect of extreme heat or extreme cold on carbon prices. While prior research suggests that both high and low temperatures positively influence carbon prices (see for example Mansanet-Bataller et al., 2007), the findings of the present study demonstrate that the effect of air temperature on predicted emissions allowances prices (unaccompanied by the potential simultaneous effect of electricity demand) is greater than average prediction of the data only in the upper half of the distribution. The positive pure effect of air temperature on emissions allowances prices in upper percentiles can be attributed to the reduced efficiency (increased emissions) of thermal (fossil fuel) power plants and, to a lesser extent, the reduced efficiency of solar photovoltaic panels in warmer climates. If any, the increase in non-electric (fossil fuel) energy consumption for cooling in high temperatures could only contribute to the intensification of the observed positive effect of air temperature on EUA prices in warm climates. Interestingly, however, the expected positive effect of low temperatures on EUA prices through increasing non-electric (fossil fuel) energy consumption for heating tend to be offset by the increased efficiency of thermal (fossil fuel) power plants in low temperatures–a phenomenon that allows such plants to produce the same amount of power with less fuel consumption, and hence emit less $CO_2$. Needless to say, the expected positive effect of both low and high air temperatures on the price of carbon through increasing the electricity demand for heating and cooling purposes has already been captured by the electricity demand index itself (note that both cold and hot climates are associated with a high demand for electricity (see Figure 5.4 in Section 5.4), with low temperatures pertaining to a relatively higher electricity demand compared to high temperatures).

The ALE curve of solar radiation does not exhibit a noteworthy overall increasing or decreasing behavior. Except for a few spikes observed in the intervals in which there is no or very little solar radiation (i.e. below 8,522 $Jm^{-2}$, corresponding to the the 8$^{th}$ percentile of the distribution), model predictions at different values of the solar radiation are close to the average prediction. At index values from 8,522 $Jm^{-2}$ to 713,290 $Jm^{-2}$ (corresponding to the 8%-60% inter-quantile range), the pure effect of solar radiation on the prediction is slightly negative in the majority of intervals. Above the 60$^{th}$ percentile of solar radiation index, model predictions are marginally greater than average prediction.

Up to the index value of 92.95% (corresponding to the 53$^{rd}$ percentile) for relative humidity, model predictions are always lower than average predictions, while exhibiting a non-monotonic

behavior. For the intervals with index values higher than 92.95%, the estimated pure effect of relative humidity on the prediction of EUA prices is persistently positive. These findings are in accordance with the premise that high atmospheric humidity has an adverse effect on the efficiency of cooling systems in the context of climate change (Wilbanks et al., 2008), possibly leading to higher $CO_2$ emissions and higher demand for emissions allowances.

In the intervals corresponding to relatively low wind speed values (below 5.24 $ms^{-1}$), predicted emissions allowances prices are constantly higher than average prediction. Above 5.24 $ms^{-1}$ (corresponding to the $56^{th}$ percentile of wind speed values), ALE estimates in all intervals are continuously non-positive, with the minimum value of the feature effect achieved at 8.77 $ms^{-1}$ (corresponding to the $98^{th}$ percentile). For extremely high wind speed values (above 8.77 $ms^{-1}$), the feature effect on the prediction of EUA prices becomes less pronounced, although it is still negative. These findings are consistent with expectations that higher (lower) potential for wind electricity generation is associated with lower (higher) $CO_2$ emissions, hence less (more) demand for for EUA certificates.

Below the index value of $1.12 \times 10^{-4}$ m (corresponding to the $59^{th}$ percentile), the ALE estimates for total precipitation are negative in almost all intervals. Above the total precipitation index of $1.12 \times 10^{-4}$ m, the model predicts slightly higher values of log-transformed EUA prices with respect to the average prediction in the majority of percentiles, with a level shift observed in the ALE curve at the $96^{th}$ percentile. These results indicate that, at least at an hourly scale, higher (lower) precipitation levels are not, as might be expected, associated with lower (higher) demand for EUA credits. This finding could be explained by the fact that hourly precipitation levels mainly affect small-scale run-of-river hydroelectricity, as a climate-related renewable energy (CRE). According to the European Rivers Network[26], although hydroelectric power accounts for about 80% of electricity generation from renewable resources and 19% of total electricity generation in Europe, the share of run-of-river hydroelectricity in Europe's electricity generation is only about 3%. As a consequence, the pure effect of this feature on the prediction at different values does not bear any practical significance in a real-world sense[27].

Ultimately, the ALE of surface air pressure exhibits an inverted U-shaped curve, with the main feature effect being consistently negative for the intervals with index values below 96896

[26] `https://www.ern.org/`

[27] As argued by Ebinger and Vergara (2011), the extent to which hydroelectric power is affected by variations of climate variables depends on (1) the availability of hydropower resources (which itself depends on several meteorological factors, including but not limited to precipitation levels) and (2) the complexity of hydropower systems. This latter could be identified with the relevance of hydropower generation for the whole power system in the specific region under study (whether hydroelectricity is complementary to (for example France) or complemented by (for example Norway) other power sources), as well as geographical dispersion and the level of integration of hydropower through transmission capacity (Ebinger and Vergara, 2011). A comprehensive analysis of climate impacts on the share of electricity production from hydropower (which could ultimately lead to a change in emission levels and consequently the demand for carbon credits) is beyond the scope of this paper and left for future research.

Pa (corresponding to the 5$^{th}$ percentile) and above 99029 Pa (corresponding to the 93$^{rd}$ percentile). In the 5%-93% inter-quantile range of surface air pressure values (from 96896 to 99029 Pa), the sequence of interval-wise feature effects oscillates between negative and positive values around zero, with the global maximum attained at 97279 Pa, or the 11$^{th}$ percentile of index values. This finding may be attributed to the potential impact of surface air pressure on the efficiency of fossil fuel–fired power plants. Nonetheless, given that previous empirical studies have been inconclusive on whether atmospheric pressure can exert a significant influence on net power plant efficiency (see Loew et al., 2020), further research is needed to describe the dynamics of the relationship between carbon emissions and surface air pressure.

## 5.4 Discussion

In contrast to many machine learning algorithms, decision tree algorithms (including Extreme Gradient Boosting) are extremely robust to correlated features. ALE estimates are likewise unbiased in the case of existence of high correlation among features. Nevertheless, if features are strongly correlated, the interpretation of ALE plots remains rather challenging. The reason is that, when two variables are highly dependent, it is only reasonable to analyze their joint simultaneous effect rather than the individual effect of each variable in isolation. This drawback does not relate uniquely to ALE estimates though; it is a general problem of using strongly correlated features for empirical modeling. In the particular case of ALE plots, and as argued by Molnar (2020), an interpretation of the effect across intervals (i.e. interpreting changes in the main effect of a feature for a data point (compared to the average prediction) for different values, with the assumption that the other feature values are fixed) is not permitted if the explanatory variables are strongly correlated. Indeed, although interval-level effects are accumulated to construct a smooth ALE curve, the effects are estimated locally using different data points. Therefore, in the presence of high correlation among variables, the interpretation of the effect can only be local (Molnar, 2020).

In light of the above-mentioned consideration and as a robustness check to validate the interpretations made in the context of the present study, we performed correlation analysis of electricity demand and climate indices. With four exceptions (see below for details), the correlation between any pair of indices was found to be weak–albeit statistically significant due to large sample size. In order to evaluate the practical significance of correlations for predictive purposes, a linear model was trained to predict each index based on each of the other indices, and the coefficient of determination was used as the measure of strength of association (aka effect size) between indices. Figure 5.4 demonstrates a pairwise scatter plot, along with density plots of the indices and a pairwise linear model-based variance explained, measuring how much of the variation in one of the indices is associated with variation in another index.

With the exception of four instances (Solar Radiation-Relative Humidity, Solar Radiation-

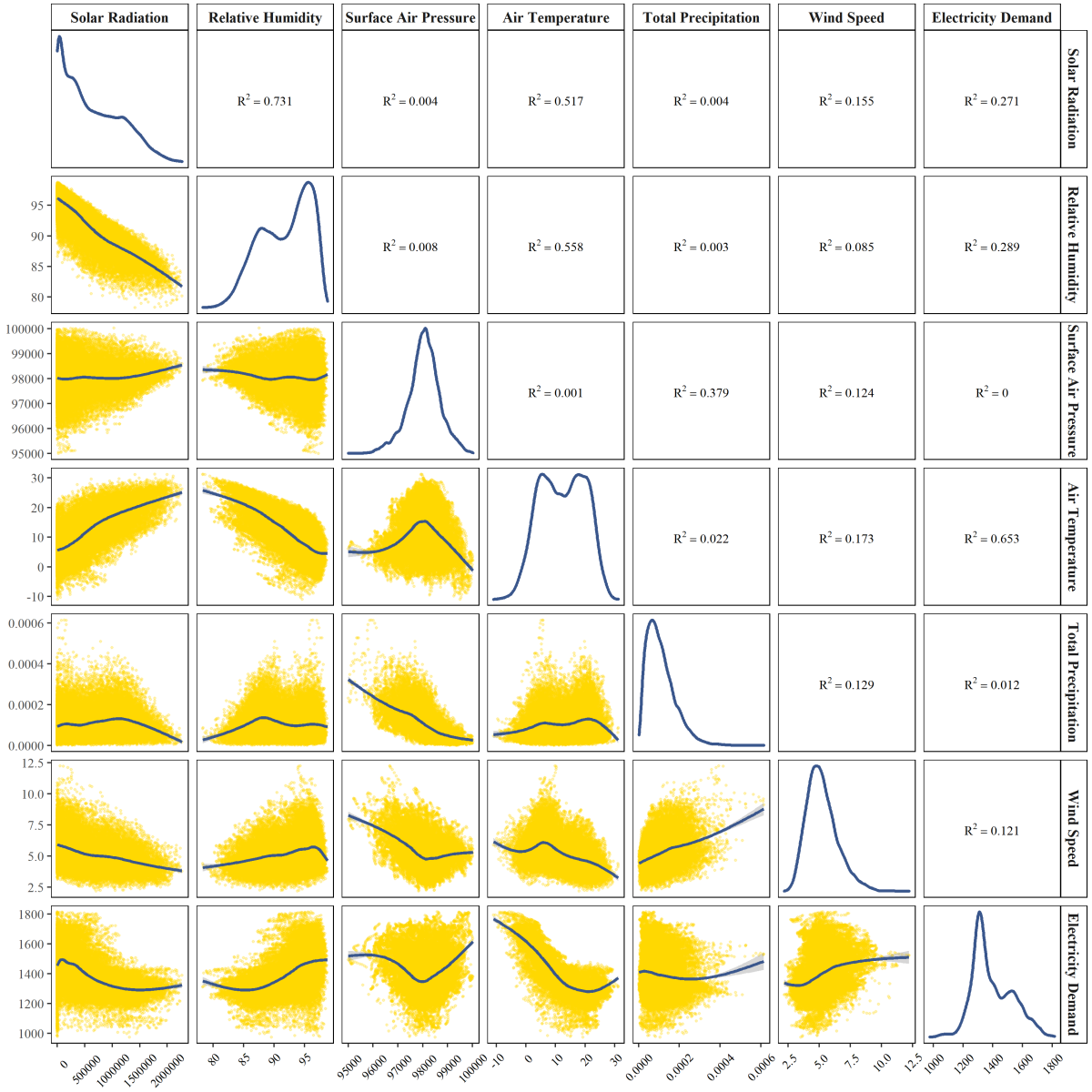


Figure 5.4: Pairwise scatter plot of electricity demand and climate indices, accompanied by smoothed conditional means using generalized additive model with integrated smoothness as the smoothing method (lower triangular portion of matrix); Density plots of electricity demand and climate indices (main diagonal of matrix); Pairwise coefficient of determination ($R^2$), or the proportion of variation in an index that is predictable from another index (upper triangular portion of matrix).

Air Temperature, Air Temperature-Relative Humidity[28] and Air Temperature-Electricity Demand), all combinations of variables exhibited very low values of variance explained. The coefficient of determination observed for any pair of indices reaches at the maximum 73%, a value that is reached for the Solar Radiation-Relative Humidity pair. Although these findings are not–in practical sense–significant enough to be cause for concern, special emphasis should

[28]Relative humidity is calculated based on air and dew point temperatures. Hence, a high (negative) association between relative humidity and air temperature is expected.

be put on the need to interpret with caution the permutation feature importance measures and the ALE estimates across intervals in the case of solar radiation, air temperature, relative humidity and electricity demand indices.

Considering the entire set of features used for empirical modeling in the present paper, the air temperature index exhibits the highest median importance (although accompanied by the widest 90% confidence interval among all features) for predicting emissions allowances prices. Such high importance can be partly explained by the presence of interaction effects between air temperature and other variables such as solar radiation and relative humidity. The importance of total precipitation in predicting emissions allowances prices is rather limited compared to all other indices, mainly to the modest share of small-scale run-of-river hydroelectricity in total electricity production across Europe (see Section 5.3). Among the three indices that directly affect climate-related renewable energies (wind, solar photovoltaics, and run-of-river hydroelectricity), solar radiation proves to be the most important feature for predicting emissions allowances prices, followed by wind speed. Total precipitation shows relatively lower importance. Despite the larger share of electricity production by wind than solar power in Europe (Eurostat, 2022), wind speed is slightly less important–in permutation feature importance sense–than solar radiation for the prediction of EUA prices. A possible explanation for this finding is that solar radiation perhaps interacts with other features (such as air temperature and relative humidity) and the interaction effects are included in the importance measurement of solar radiation. As discussed in Section 5.2.2.4, this is an inherent limitation of the permutation feature importance algorithm.

A venue for future research includes the investigation of the relationship between climate derivatives and the price of emissions allowances traded on the EU ETS. Climate derivatives are a class of financial contracts used for hedging against financial losses related to fluctuations in climate conditions (Jewson and Brix, 2005). Financial instruments associated with a variety of climate variables such as air temperature, rainfall, snowfall, sunshine, wind speed, etc. are traded in over-the-counter (OTC) and exchange weather markets across the globe, with the dominance of North American market in terms of development (Hess, 2012; Buckley et al., 2002). Previous research has found that there exists a close connection between energy and weather markets, in the sense that climate factors are correlated with energy prices (Hess, 2012). As a particular example, Considine (2000) argues that, in regions where there is a real need for heating (cooling) in winter (summer), electricity spot market prices are exceedingly sensitive to forecasts of unusually high or low temperatures. In a similar vein, it could be argued that weather forecasts–perhaps more importantly than contemporaneous weather conditions–can affect price formation in carbon spot (and derivatives) markets, hence implying a connection between climate derivatives markets and carbon emission trading. In the European context, the following two points should, however, be noted. First, although experiencing steady growth

over the last decades, the European climate derivatives market is not as developed as its American counterpart (Buckley et al., 2002), mainly because energy suppliers as well as consumers are relatively less concerned about climate risk. The reason may lie in less extreme variations in weather, less sharp differences between the seasons, and smaller temperature spread in Europe compared to North America–and the United States in particular. Second, the most common underlying of European climate derivatives is temperature, and the proportion of contracts related to other climate factors is rather limited (see Buckley et al., 2002). This sets a limit on the number of climate factors that could be studied in the context of carbon-climate markets relationship. In any case, future research should build on the initial empirical findings in the present study and further examine the effects of climate factors on the price of emissions allowances–especially those traded in the derivatives market[29]–by including climate forecasts.

Owing to the fact the analysis was carried out on a time period spanning across the first three phases of the EU ETS,[30] phase-wise characterization of the relationship between electricity demand and climate factors and emissions allowance prices is not possible in context of this study. Thanks to the inclusion of time-based features (hour of the day, day of the week, month of the year and year) in the predictive model that can control phase-specific effects, this, however, does not pose a serious limitation for the interpretation of the obtained results. That having been said, phase-wise analyzes could produce interesting findings that account more for specificities pertaining to individual phases, such as relatively generous allowance allocation in the first (pilot) phase of the scheme (Oberndorfer, 2009) as well as substantial uncertainty and high volatility associated with EUA prices during the first phase (Bredin and Muckley, 2011), or in the years corresponding to the COVID-19 crisis era (2020-2022). These are important issues to be explored in future research.

## 5.5 Conclusion

The aim of the present research was to examine the predictive impact of electricity demand and climate factors on spot prices of emissions allowances during the first three phases of the European Union Emissions Trading System (EU ETS). Capitalizing on the concept of hydro-ecoregions from hydrology and environmental science, six emissions-weighted climate indices

[29] As documented by Cludius and Betz (2020), electricity generators participate more actively in the carbon derivatives market than in the spot market with the aim of hedging power forward sales. That said, trade in allowances in the spot market was significant in the first three phases of the EU ETS, although the volumes on the spot market have been in decline since phase 2 (Bredin and Parsons, 2016).

[30] The bigger the size of the input data, the higher the likelihood that the Extreme Gradient Boosting algorithm has a good performance in learning the relationship between explained and explanatory variables. This explains why models were trained over the entire data period (2005-2019) instead of splitting the period into three sub-periods each applicable to one phase (i.e. 2005-2007 for the first phase; 2008-2012 for the second phase; and 2013-2019 for the third case). Moreover, the results obtained from separate models trained on data sets with heterogeneous data sizes (as would be the case with the three trading periods under study) could not be readily compared, hence limiting the generalizability of the findings.

were constructed to accurately represent climate conditions across the EU ETS zone. Those indices, along with a population-weighted electricity demand index were employed for the empirical estimation of emissions allowances prices within an advanced predictive modeling framework equipped with novel methodological approaches to results interpretation.

The most obvious finding to emerge from this study is that electricity demand and all climate factors proved to be important for estimating carbon credits transaction prices during the first three trading periods of the ETS, with air temperature and electricity demand being most relevant to emissions allowances prices, and total precipitation and relative humidity being the least relevant features to the target. The results also indicate that the relationship between emissions allowances prices and the explanatory factors for such prices was not linear.

The empirical findings in this study should enhance our understanding of the impact of climate fluctuations on the most prominent market-based measure to reduce $CO_2$ emissions in Europe. On a related note, the provision of renewable energy development–as a complementary tool to the emissions trading scheme–will be essential for addressing climate change on the part of the EU countries. Hence, careful examination of the relevance of climate factors directly related to renewable energy production (e.g. solar radiation, wind speed and total precipitation) to the formation of carbon prices offers some insight into the complex interplay between these two principal instruments for the reduction of $CO_2$ emissions.

Finally, it should be recalled that the present study did not try to induce causal relationships between carbon prices and electricity demand and climate factors. Instead of attempting to make an observation-based causal claim about such relationship, the paper proposed a predictive modeling framework for the estimation of emissions allowances prices based on the observed association between those prices and a set of European-scale electricity demand and climate indices. Determining whether this association is indicative of a causal relationship between carbon prices and electricity demand and climate variables is beyond the scope of any statistical analysis per se. Given the exploratory nature of this study, it is thus unquestionably worthwhile for future research to investigate further into the identification of the underlying mechanisms and processes through which electricity demand and climate factors can influence EUA transaction prices.

CHAPTER 6

# General Conclusion

There is a direct relationship between global warming and the emission of carbon dioxide ($CO_2$) and other greenhouse gases. As far as European countries are concerned, the development of renewable electricity production and the European Union Emissions Trading System (EU ETS) are two main tools for reducing $CO_2$ emissions and dealing with climate change. The main objective of this doctoral project was to examine climate variables as explanatory factors for $CO_2$ emissions, and to explore how the main tools mentioned above can help reduce emissions at French and European level. This principal objective was pursued in four related but distinct essays on the association between climate and carbon emissions–in the provision of climate change mitigation policies, each addressing one or multiple sub-objectives.

Key questions about the "future" of electricity generation and alternative power generation technologies need to be understood by innovative methods that would possibly allow for a careful evaluation of the "past". The first essay (see Chapter 2) aims to attain this clear goal by exploring possible emission outcomes that could have occurred under different conditions of electricity production in France over the 2013-2021 period. This essay attempts to characterize the predictive impact of climate-related renewable electricity generation (i.e. wind, solar photovoltaic, and small-scale run-of-river hydroelectric power) on daily $CO_2$ emissions in the French electric power system.

For this aim, the chapter presents a state-of-the-art three-step machine learning-based methodology that allows a detailed description of the link between climate-related renewable electricity production and $CO_2$ emissions per unit of electricity generated in France. In the first step, a tree-based ensemble model is trained to empirically learn the association between electricity sector emissions and the electric energy produced by different fuel types to the granularity of days over a nine-year period. With the help of cutting-edge post hoc interpretability methods, various forms of information on the nature of such relationship are then extracted from the learning model. Next, a statistically based counterfactual analysis framework is proposed to quantify, for the first time, the predictive impact of (unexploited) climate-related renewable electricity

production potential on $CO_2$ emissions over the period considered. Finally, four counterfactual scenarios of increased climate-related renewable electricity production in France over the study period are explored, and the optimal mix of renewable energy sources for minimizing counterfactual estimates of emissions and the intermittency of climate-related renewable electricity production under each scenario is identified.

It is expected that the first essay will prove useful for broadening our understanding of environmental impacts of electricity generation, and serve as a reference for subsequent research on implementation of sustainable energy policies. The study will hopefully appeal to scholars engaged with the debates surrounding economics and policy of renewable energy vis-à-vis climate change and variability.

Decarbonizion of the power sector, as a crucial factor in mitigating climate change, is an environmental challenge responding to which requires an in-depth understanding of explanatory factors behind electricity generation-related emissions. While electricity supply and demand are closely connected with climate conditions, there has been little empirical analysis of how and to what extent climate impacts on the demand and supply of electricity translate into greenhouse gas emissions in the electricity sector. To address this knowledge gap, the second essay (see Chapter 3) sets out a data-driven predictive modeling framework for investigating the observed association between hourly $CO_2$ emissions in the French electric power system and a comprehensive set of climate factors over the 2013-2020 period.

This chapter makes several noteworthy contributions to the debate on the relationship between electricity generation and climate. The study's methodological contribution lies in formulating a novel interdisciplinary approach to constructing electric power-weighted climate indices from gridded climate variables and regional power indicators, based on the principal mechanism through which each climate factor can affect emissions in the electricity sector. Complex nonlinear relationships between electricity sector emissions and their climatic predictors are characterized, for the first time, employing a cutting-edge regression predictive modeling technique. The empirical modeling framework is further equipped with advanced post hoc interpretability methods in machine learning, allowing the extraction of various forms of information on the nature of such relationships.

It is expected that the second essay will prove invaluable for expanding our understanding of the sensitivity of electricity sector emissions to climate change and variability, while offering a flexible methodological framework that can easily be re-imagined for the other purposes other than characterization of the determinants of emissions from electricity production. In this regard, study will hopefully appeal to scholars engaged with carbon emissions reduction in the power sector.

As the European Union's central tool for reducing greenhouse gas emissions in a cost-effective manner, the European Union Emissions Trading System (EU ETS) has attracted much

interest on the part of economics research community. The third essay (see Chapter 4) conducts a spatio-temporal evaluation of the environmental effectiveness of this scheme in its first three phases (2005-2019). The chapter puts forward an innovative predictive modeling framework for causal inference based on counterfactuals. The proposed approach capitalizes on the statistical structure of regional climate-emissions relationships to estimate counterfactual fossil fuel $CO_2$ emissions over the period following the beginning of each phase, and examines the impact of the EU ETS by comparing realized monthly emissions with counterfactual estimates across European socio-economic regions.

The third essay's methodological contribution lies in adopting a novel approach to counterfactual estimation of $CO_2$ emissions, at the finest possible temporal (monthly) and spatial (regional) scales, based on the most comprehensive set to date of climatic predictors of emissions that themselves are not influenced by policy instruments. Such an approach extends and enhances our understanding of determinants of regional fossil fuel carbon emissions across Europe while allowing for evaluating the environmental effectiveness of the EU ETS. In this regard, the study explores the intersection between two streams of environmental and energy economics literature by contributing to the debates on explicative factors behind $CO_2$ emissions and effectiveness evaluation of the European carbon market.

From a practical point of view, the region-based spatio-temporal analysis proposed in Chapter 4 may complement existing firm, sector, country and EU-level analyses of the effectiveness of the EU ETS in reducing anthropogenic carbon emissions throughout its first three phases. It is expected that this chapter will be of wide interest to scholars engaged with discussions surrounding climate change and emissions reduction via carbon markets. Thanks to the documentation of findings in clear and detailed writing, the study is readily accessible to climate policy-makers in Europe, who may seek ex-post empirical analyses that shed light on the achievement level of the trading system's main target (i.e. emissions reduction) in the previous trading periods.

Exploring climate-related predictors of carbon prices in the European carbon market was the topic of the fourth essay (see Chapter 5). The major objective of this chapter was to investigate the predictive impact of climate conditions and electricity demand on hourly spot prices of emissions allowances during the first three trading periods of the EU ETS (2005-2019). Relying on data of incomparable spatio-temporal granularity and scope in the existing literature, the study sets out an ensemble tree-based predictive modeling framework for estimating carbon emissions allowances prices based on the explanatory variables.

The fourth essay makes several noteworthy contributions to the empirical analysis of the EU ETS, and more particularly the determinants of emissions allowances prices in this carbon market. The study's methodological contribution lies in formulating an innovative interdisciplinary approach to constructing European-scale electricity demand and climate indicators that embrace the broad spectrum of climate conditions across the EU ETS zone. The complex non-

linear relationship between the price of carbon and the utilized predictors, namely electricity demand and climate conditions, is characterized, for the first time, using a cutting-edge statistical modeling framework. Various forms of information on the nature of such relationship are then extracted from the model by means of advanced post hoc interpretability methods.

From a policy application point of view, the inclusion of predictor variables that are directly related to electricity production from climate-related renewable energy (wind, solar, and run-of-river hydropower) sources provides new empirical insights into the interconnections between the potential for renewable electricity generation and the leading climate policy instrument in Europe. In this regard, the results of Chapter 5 will lead to a deeper understanding of the impact of climate variability on the most prominent mechanism for reducing $CO_2$ emissions in Europe. The study will hopefully appeal to scholars engaged with the dynamics of market-based environmental policies on a more specific level.

Despite the fact that the four studies in this dissertation significantly contribute to the discourse on the complex climate-emissions nexus and the functioning of climate change mitigation tools in Europe, some questions remain regarding the extension of research findings and conclusions to non-European contexts and/or future time periods. Indeed, the dissertation is concerned with ex post (backward-looking) and counterfactual analyses of the European carbon market and electricity generation-related emissions vis-à-vis climate change and variability based on historical data. There is ample opportunity to supplement and extend obtained promising results through entering the uncertainty dimension into the equation (e.g. by considering future energy scenarios and climate change projections), and analyze the challenges of the considered market and non-market mitigation mechanisms in the decades to follow.

# Bibliography


Abadie, A., Diamond, A., and Hainmueller, J. (2010). Synthetic control methods for comparative case studies: Estimating the effect of California's tobacco control program. *Journal of the American statistical Association*, 105(490):493–505.

Abadie, A. and Gardeazabal, J. (2003). The economic costs of conflict: A case study of the Basque Country. *American economic review*, 93(1):113–132.

Abrell, J., Ndoye Faye, A., and Zachmann, G. (2011). Assessing the impact of the EU ETS using firm level data. Technical report, Bruegel working paper.

Adams, S. and Nsiah, C. (2019). Reducing carbon dioxide emissions; Does renewable energy matter? *Science of the Total Environment*, 693:133288.

ADEME (2015). Un mix électrique 100% renouvelable ? Analyses et optimisations. Accessed on 14 February 2022.

ADEME (2018). Trajectoires d'évolution du mix électrique 2020-2060. Accessed on 14 February 2022.

ADEME (2021). ADEME - Bilans GES Site. `https://www.bilans-ges.ademe.fr/en/accueil/contenu/index/page/EU-ETS_/siGras/0`. (Accessed on 04/10/2021).

Adewuyi, A. O. and Awodumi, O. B. (2017). Renewable and non-renewable energy-growth-emissions linkages: Review of emerging trends with policy implications. *Renewable and Sustainable Energy Reviews*, 69:275–291.

Ahamada, I. and Kirat, D. (2015). The impact of phase II of the EU ETS on wholesale electricity prices. *Revue d'économie Politique*, 125(6):887–908.

Alberola, E., Chevallier, J., and Chèze, B. (2008). Price drivers and structural breaks in European carbon prices 2005–2007. *Energy policy*, 36(2):787–797.

Alduchov, O. A. and Eskridge, R. E. (1996). Improved Magnus form approximation of saturation vapor pressure. *Journal of Applied Meteorology and Climatology*, 35(4):601–609.

Amato, A. D., Ruth, M., Kirshen, P., and Horwitz, J. (2005). Regional energy demand responses to climate change: methodology and application to the commonwealth of Massachusetts. *Climatic Change*, 71(1):175–201.

Ampudia, M., Bua, G., Kapp, D., Salakhova, D., et al. (2022). The role of speculation during the recent increase in EU emissions allowance prices. *Economic Bulletin Boxes*, 3.

Anderson, B. and Di Maria, C. (2011). Abatement and Allocation in the Pilot Phase of the EU ETS. *Environmental and Resource Economics*, 48(1):83–103.

Ang, B. W. and Su, B. (2016). Carbon emission intensity in electricity production: A global analysis. *Energy Policy*, 94:56–63.

Ang, J. B. (2007). CO2 emissions, energy consumption, and output in France. *Energy policy*, 35(10):4772–4778.

Anger, A. and Köhler, J. (2010). Including aviation emissions in the EU ETS: Much ado about nothing? A review. *Transport Policy*, 17(1):38–46.

Apergis, N. and Payne, J. E. (2009). CO2 emissions, energy usage, and output in Central America. *Energy Policy*, 37(8):3282–3286.

Apergis, N. and Payne, J. E. (2014). Renewable energy, output, CO2 emissions, and fossil fuel prices in Central America: Evidence from a nonlinear panel smooth transition vector error correction model. *Energy economics*, 42:226–232.

Apergis, N. and Payne, J. E. (2015). Renewable energy, output, carbon dioxide emissions, and oil prices: evidence from South America. *Energy Sources, Part B: Economics, Planning, and Policy*, 10(3):281–287.

Apergis, N., Payne, J. E., Menyah, K., and Wolde-Rufael, Y. (2010). On the causal dynamics between emissions, nuclear energy, renewable energy, and economic growth. *Ecological Economics*, 69(11):2255–2260.

Apley, D. W. and Zhu, J. (2020). Visualizing the effects of predictor variables in black box supervised learning models. *Journal of the Royal Statistical Society: Series B (Statistical Methodology)*, 82(4):1059–1086.

Arrieta, F. R. P. and Lora, E. E. S. (2005). Influence of ambient temperature on combined-cycle power-plant performance. *Applied energy*, 80(3):261–272.

Bartos, M. D. and Chester, M. V. (2015). Impacts of climate change on electric power supply in the Western United States. *Nature Climate Change*, 5(8):748–752.

Batten, J. A., Maddox, G. E., and Young, M. R. (2021). Does weather, or energy prices, affect carbon prices? *Energy Economics*, 96:105016.

Bayer, P. and Aklin, M. (2020). The European Union emissions trading system reduced CO2 emissions despite low prices. *Proceedings of the National Academy of Sciences*, 117(16):8804–8812.

Behrens, P., Van Vliet, M. T., Nanninga, T., Walsh, B., and Rodrigues, J. F. (2017). Climate change and the vulnerability of electricity generation to water stress in the European Union. *Nature Energy*, 2(8):1–7.

Bel, G. and Joseph, S. (2015). Emission abatement: Untangling the impacts of the EU ETS and the economic crisis. *Energy Economics*, 49:531–539.

Bélaïd, F. and Youssef, M. (2017). Environmental degradation, renewable and non-renewable electricity consumption, and economic growth: Assessing the evidence from Algeria. *Energy policy*, 102:277–287.

Belkin, M., Hsu, D., Ma, S., and Mandal, S. (2019). Reconciling modern machine-learning practice and the classical bias–variance trade-off. *Proceedings of the National Academy of Sciences*, 116(32):15849–15854.

Beltrami, F., Fontini, F., and Grossi, L. (2021). The value of carbon emission reduction induced by renewable energy sources in the Italian power market. *Ecological Economics*, 189:107149.

Bento, J. P. C. and Moutinho, V. (2016). CO2 emissions, non-renewable and renewable electricity production, economic growth, and international trade in Italy. *Renewable and Sustainable Energy Reviews*, 55:142–155.

Benz, E. and Trück, S. (2009). Modeling the price dynamics of CO2 emission allowances. *Energy Economics*, 31(1):4–15.

Bersani, A. M., Falbo, P., and Mastroeni, L. (2022). Is the ETS an effective environmental policy? Undesired interaction between energy-mix, fuel-switch and electricity prices. *Energy Economics*, page 105981.

Bessec, M. and Fouquau, J. (2008). The non-linear link between electricity consumption and temperature in Europe: A threshold panel approach. *Energy Economics*, 30(5):2705–2721.

Bilgili, F., Koçak, E., and Bulut, Ü. (2016). The dynamic impact of renewable energy consumption on CO2 emissions: a revisited Environmental Kuznets Curve approach. *Renewable and Sustainable Energy Reviews*, 54:838–845.

Bloomfield, H., Brayshaw, D., Troccoli, A., Goodess, C., De Felice, M., Dubus, L., Bett, P., and Saint-Drenan, Y.-M. (2021). Quantifying the sensitivity of european power systems to energy scenarios and climate change projections. *Renewable Energy*, 164:1062–1075.

Boehmke, B. and Greenwell, B. (2019). *Hands-on machine learning with R*. Chapman and Hall/CRC.

Boontome, P., Therdyothin, A., and Chontanawat, J. (2017). Investigating the causal relationship between non-renewable and renewable energy consumption, CO2 emissions and economic growth in Thailand. *Energy Procedia*, 138:925–930.

Bredin, D. and Muckley, C. (2011). An emerging equilibrium in the EU emissions trading scheme. *Energy Economics*, 33(2):353–362.

Bredin, D. and Parsons, J. (2016). Why is spot carbon so cheap and future carbon so dear? The term structure of carbon prices. *The Energy Journal*, 37(3).

Breeze, P. (2019). Solar power. In *Power Generation Technologies*, pages 293–321. Newnes.

Breiman, L. (2001). Random forests. *Machine learning*, 45(1):5–32.

Brodersen, K. H., Gallusser, F., Koehler, J., Remy, N., Scott, S. L., et al. (2015). Inferring causal impact using Bayesian structural time-series models. *Annals of Applied Statistics*, 9(1):247–274.

Brouwer, A. S., van den Broek, M., Zappa, W., Turkenburg, W. C., and Faaij, A. (2016). Least-cost options for integrating intermittent renewables in low-carbon power systems. *Applied Energy*, 161:48–74.

Buckley, N., Hamilton, A., Harding, J., Roche, N., Ross, N., Sands, E., Skelding, R., Watford, N., and Whitlow, H. (2002). European weather derivatives. In *General Insurance Convention*.

Bull, S., Bilelo, D., Ekmann, J., Sale, M., and Schmalzer, D. (2007). Effects of climate change on energy production and distribution in the United States in Effects of Climate Change on Energy Production and Use in the United States. *A Report by the US Climate Change Science Program and the Subcommttee on Global Change Research: Washington DC*.

Bulut, U. (2017). The impacts of non-renewable and renewable energy on CO 2 emissions in Turkey. *Environmental Science and Pollution Research*, 24(18):15416–15426.

Buono, D., Elliott, D., Mazzi, G., Bikker, R., Frölich, M., Gatto, R., Guardalbascio, B., Hauf, S., Infante, E., Moauro, F., et al. (2018). ESS guidelines on temporal disaggregation, benchmarking and reconciliation. *Luxembourg: European Union*.

Chamberlin, G. (2010). Methods Explained: Temporal Disaggregation. *Economic & Labour Market Review*, 4(11):106–121.

Chen, T., Benesty, M., and He, T. (2018). Understand Your Dataset with Xgboost. *R Document*.

Chen, T. and Guestrin, C. (2016). XGBoost: A Scalable Tree Boosting System. In *Proceedings of the 22nd ACM SIGKDD International Conference on Knowledge Discovery and Data Mining*, KDD '16, pages 785–794, New York, NY, USA. ACM.

Chen, Y., Wang, Z., and Zhong, Z. (2019). CO2 emissions, economic growth, renewable and non-renewable energy production and foreign trade in China. *Renewable energy*, 131:208–216.

Chevallier, J. (2013). Carbon price drivers: an updated literature review. *International Journal of Applied Logistics (IJAL)*, 4(4):1–7.

Chèze, B., Chevallier, J., Berghmans, N., and Alberola, E. (2020). On the CO2 emissions determinants during the EU ETS Phases I and II: a plant-level analysis merging the EUTL and Platts power data. *The Energy Journal*, 41(4).

Chow, G. C. (1960). Tests of equality between sets of coefficients in two linear regressions. *Econometrica: Journal of the Econometric Society*, pages 591–605.

Chow, G. C. and Lin, A.-l. (1971). Best linear unbiased interpolation, distribution, and extrapolation of time series by related series. *The review of Economics and Statistics*, pages 372–375.

Christiansen, A. C., Arvanitakis, A., Tangen, K., and Hasselknippe, H. (2005). Price determinants in the EU emissions trading scheme. *Climate Policy*, 5(1):15–30.

Chrobak, P., Skovajsa, J., and Zalesak, M. (2016). Effect of cloudiness on the production of electricity by photovoltaic panels. In *MATEC Web of Conferences*, volume 76, page 02010. EDP Sciences.

Chu, C.-T. and Hawkes, A. D. (2020). Optimal mix of climate-related energy in global electricity systems. *Renewable Energy*, 160:955–963.

Cludius, J. and Betz, R. (2020). The role of banks in EU emissions trading. *The Energy Journal*, 41(2).

Conover, W. J. (1999). *Practical nonparametric statistics*, volume 350. john wiley & sons.

Considine, G. (2000). Introduction to weather derivatives. *Weather derivatives group, Aquila energy*, pages 1–10.

Creti, A., Jouvet, P.-A., and Mignon, V. (2012). Carbon price drivers: Phase I versus Phase II equilibrium? *Energy Economics*, 34(1):327–334.

Crook, J. A., Jones, L. A., Forster, P. M., and Crook, R. (2011). Climate change impacts on future photovoltaic and concentrated solar power energy output. *Energy & Environmental Science*, 4(9):3101–3109.

Cruz Rios, F., Naganathan, H., Chong, W. K., Lee, S., and Alves, A. (2017). Analyzing the impact of outside temperature on energy consumption and production patterns in high-performance research buildings in Arizona. *Journal of Architectural Engineering*, 23(3):C4017002.

Dagum, E. B. and Cholette, P. A. (2006). *Benchmarking, temporal distribution, and reconciliation methods for time series*, volume 186. Springer Science & Business Media.

Daskalakis, G., Psychoyios, D., and Markellos, R. N. (2009). Modeling CO2 emission allowance prices and derivatives: Evidence from the European trading scheme. *Journal of Banking & Finance*, 33(7):1230–1241.

de Perthuis, C., Ellerman, A. D., and Convery, F. J. (2010). *Le prix du carbone: Les enseignements du marché européen du CO2*. Village Mondial.

Dechezleprêtre, A., Nachtigall, D., and Venmans, F. (2018). The joint impact of the European Union emissions trading system on carbon emissions and economic performance.

Declercq, B., Delarue, E., and D'haeseleer, W. (2011). Impact of the economic recession on the European power sector's CO2 emissions. *Energy Policy*, 39(3):1677–1686.

del Río, P. (2017). Why does the combination of the European Union Emissions Trading Scheme and a renewable energy target makes economic sense? *Renewable and Sustainable Energy Reviews*, 74:824–834.

Dogan, E. and Seker, F. (2016). Determinants of CO2 emissions in the European Union: the role of renewable and non-renewable energy. *Renewable Energy*, 94:429–439.

Dong, K., Sun, R., and Hochman, G. (2017). Do natural gas and renewable energy consumption lead to less CO2 emission? Empirical evidence from a panel of BRICS countries. *Energy*, 141:1466–1478.

Débat national sur la transition énergétique (2013). Synthèse des travaux du débat national sur la transition énergétique de la France.

Ebinger, J. and Vergara, W. (2011). *Climate impacts on energy systems: key issues for energy sector adaptation*. The World Bank.

ECMWF (2020a). Climate and energy indicators for Europe from 1979 to present derived from reanalysis.

ECMWF (2020b). Fact sheet: Reanalysis. (Accessed on 05 February 2021).

Economics, V. (2014). Carbon leakage prospects under phase III of the EU ETS and beyond. *London, UK: DECC*.

Edelsbrunner, P. and Schneider, M. (2013). Modelling for Prediction vs. Modelling for Understanding: Commentary on Musso et al.(2013). *Frontline Learning Research*, 1(2):99–101.

Edenhofer, O. (2015). *Climate change 2014: mitigation of climate change*, volume 3. Cambridge University Press.

Egenhofer, C., Alessi, M., Georgiev, A., and Fujiwara, N. (2011). The EU Emissions Trading System and Climate Policy towards 2050: Real incentives to reduce emissions and drive innovation? *CEPS Special Reports*.

Ellerman, A. D. (2015). *The EU ETS: What we know and what we don't know*. MIT Press, Cambridge, MA.

Ellerman, A. D. and Buchner, B. K. (2008). Over-allocation or abatement? A preliminary analysis of the EU ETS based on the 2005–06 emissions data. *Environmental and Resource Economics*, 41(2):267–287.

Ellerman, A. D., Convery, F. J., and De Perthuis, C. (2010). *Pricing carbon: the European Union emissions trading scheme*. Cambridge University Press.

Ellerman, A. D., Marcantonini, C., and Zaklan, A. (2016). The European Union emissions trading system: ten years and counting. *Review of Environmental Economics and Policy*, 10(1):89–107.

Ellerman, A. D. and McGuinness, M. (2008). CO2 abatement in the UK power sector: evidence from the EU ETS trial period.

Engeland, K., Borga, M., Creutin, J.-D., François, B., Ramos, M.-H., and Vidal, J.-P. (2017). Space-time variability of climate variables and intermittent renewable electricity production–A review. *Renewable and Sustainable Energy Reviews*, 79:600–617.

Eslahi, M. (2022a). Climate-Related Renewable Energy Sources and Carbon Emissions: A Machine Learning-Based Investigation of Electricity Production in France. *Available at SSRN 4220899*.

Eslahi, M. (2022b). Identifying Climatic Drivers of Emissions From Electricity Production: Insights From a Predictive Modeling-Based Approach. *Available at SSRN 4221092*.

Eslahi, M. (2022c). Mission Accomplished? An Ex-post Predictive Evaluation of the Effectiveness of the EU ETS in Reducing Regional Fossil Fuel Carbon Emissions. *Available at SSRN 4221044*.

Eslahi, M. and Mazza, P. (2022). Can Climate Factors and Electricity Demand Predict Carbon Emissions Allowances Prices? Evidence From the First Three Phases of the EU ETS. *Available at SSRN 4220880*.

ESMA (2022). Final Report-Emission allowances and associated derivatives.

European Comission (2021a). Emissions cap and allowances. (Accessed on 05/31/2022).

European Comission (2021b). EU Emissions Trading System (EU ETS) - Climate Action. `https://ec.europa.eu/clima/policies/ets_en#tab-0-0`. (Accessed on 04/10/2021).

European Comission (2021c). Free allocation. (Accessed on 06/01/2022).

European Comission (2021d). Free allocation for the modernisation of the energy sector. (Accessed on 06/01/2022).

European Comission (2021e). Progress made in cutting emissions - Climate Action. `https://ec.europa.eu/clima/policies/strategies/progress_en`. (Accessed on 04/11/2021).

European Commission (2021). CO2 emissions from energy use clearly decreased in the EU in 2020. Accessed on 12 February 2022.

European Environment Agency (2022). Greenhouse gas emission intensity of electricity generation in Europe. `https://www.eea.europa.eu/ims/greenhouse-gas-emission-intensity-of-1`. (Accessed on 08/05/2022).

European Environment Agency (2020). CO2 Intensity of Electricity Generation. Accessed on 16 February 2021.

Eurostat (2008). Sectoral productivity at regional level. Accessed on 11 February 2021.

Eurostat (2022). Renewable energy statistics - Statistics Explained. (Accessed on 05/25/2022).

Fageda, X. and Teixidó, J. J. (2022). Pricing carbon in the aviation sector: Evidence from the European emissions trading system. *Journal of Environmental Economics and Management*, 111:102591.

Farhani, S. and Shahbaz, M. (2014). What role of renewable and non-renewable electricity consumption and output is needed to initially mitigate CO2 emissions in MENA region? *Renewable and Sustainable Energy Reviews*, 40:80–90.

Fisher, A., Rudin, C., and Dominici, F. (2019). All Models are Wrong, but Many are Useful: Learning a Variable's Importance by Studying an Entire Class of Prediction Models Simultaneously. *J. Mach. Learn. Res.*, 20(177):1–81.

François, B., Hingray, B., Raynaud, D., Borga, M., and Creutin, J. (2016). Increasing climate-related-energy penetration by integrating run-of-the river hydropower to wind/solar mix. *Renewable Energy*, 87:686–696.

Friedman, J. H. (2002). Stochastic gradient boosting. *Computational statistics & data analysis*, 38(4):367–378.

Gerlak, A. K., Weston, J., McMahan, B., Murray, R. L., and Mills-Novoa, M. (2018). Climate risk management and the electricity sector. *Climate risk management*, 19:12–22.

Gernaat, D. E., de Boer, H. S., Daioglou, V., Yalew, S. G., Müller, C., and van Vuuren, D. P. (2021). Climate change impacts on renewable energy supply. *Nature Climate Change*, 11(2):119–125.

Gilfillan, D. and Marland, G. (2020). CDIAC-FF: Global and National CO2 Emissions from Fossil Fuel Combustion and Cement Manufacture: 1751-2017. *Earth System Science Data Discussions*, pages 1–23.

Gloaguen, O. and Alberola, E. (2013). Assessing the factors behind CO2 emissions changes over the phases 1 and 2 of the EU ETS: an econometric analysis. *CDC Climat Research, Paris, France*.

Goh, T., Ang, B., Su, B., and Wang, H. (2018a). Drivers of stagnating global carbon intensity of electricity and the way forward. *Energy Policy*, 113:149–156.

Goh, T., Ang, B., and Xu, X. (2018b). Quantifying drivers of CO2 emissions from electricity generation–Current practices and future extensions. *Applied Energy*, 231:1191–1204.

González-Díaz, A., Alcaráz-Calderón, A. M., González-Díaz, M. O., Méndez-Aranda, Á., Lucquiaud, M., and González-Santaló, J. M. (2017). Effect of the ambient conditions on gas

turbine combined cycle power plants with post-combustion CO2 capture. *Energy*, 134:221–233.

Granger, C. W. J. and Newbold, P. (2014). *Forecasting economic time series*. Academic Press.

Green, J. F. (2021). Does carbon pricing reduce emissions? A review of ex-post analyses. *Environmental Research Letters*.

Gretszel, P., Gurgul, H., Lach, Ł., and Schleicher, S. (2020). Testing for economic and environmental impacts of EU Emissions Trading System: A panel GMM approach.

Grubb, M., Laing, T., Sato, M., and Comberti, C. (2012). *Analyses of the Effectiveness of Trading in EU-ETS*. Climate Strategies.

Hamilton, N. E. and Ferry, M. (2018). ggtern: Ternary diagrams using ggplot2. *Journal of Statistical Software*, 87(1):1–17.

Heiaas, A. M. (2021). The EU ETS and Aviation: Evaluating the Effectiveness of the EU Emission Trading System in Reducing Emissions from Air Travel. *Review of Business and Economics Studies*, (1).

Hekkenberg, M., Benders, R., Moll, H., and Uiterkamp, A. S. (2009). Indications for a changing electricity demand pattern: The temperature dependence of electricity demand in the Netherlands. *Energy Policy*, 37(4):1542–1551.

Helm, C. and Sprinz, D. (2000). Measuring the effectiveness of international environmental regimes. *Journal of Conflict Resolution*, 44(5):630–652.

Henley, A. and Peirson, J. (1997). Non-linearities in electricity demand and temperature: parametric versus non-parametric methods. *Oxford bulletin of economics and statistics*, 59(1):149–162.

Hersbach, H., Bell, B., Berrisford, P., Hirahara, S., Horányi, A., Muñoz-Sabater, J., Nicolas, J., Peubey, C., Radu, R., Schepers, D., et al. (2020). The ERA5 global reanalysis. *Quarterly Journal of the Royal Meteorological Society*, 146(730):1999–2049.

Hess, M. (2012). *Pricing energy, weather and emission derivatives under future information*. PhD thesis, PhD dissertation, University Duisburg-Essen, Germany, 2013.

Hijmans, R. J. (2020). *raster: Geographic Data Analysis and Modeling*. R package version 3.4-5.

Hintermann, B. (2010). Allowance price drivers in the first phase of the EU ETS. *Journal of Environmental Economics and Management*, 59(1):43–56.

Ho, L. T., Dubus, L., De Felice, M., and Troccoli, A. (2020). Reconstruction of multidecadal country-aggregated hydro power generation in Europe based on a random forest model. *Energies*, 13(7):1786.

International Energy Agency (2021). France 2021 Energy Policy Review.

International Energy Agency (IEA) (2020). European Union 2020 Energy Policy Review. Accessed on 13 February 2022.

Iwata, H., Okada, K., and Samreth, S. (2012). Empirical study on the determinants of CO2 emissions: evidence from OECD countries. *Applied Economics*, 44(27):3513–3519.

Jaforullah, M. and King, A. (2015). Does the use of renewable energy sources mitigate CO2 emissions? A reassessment of the US evidence. *Energy Economics*, 49:711–717.

Jaraite-Kažukauske, J. and Di Maria, C. (2016). Did the EU ETS make a difference? An empirical assessment using Lithuanian firm-level data. *The Energy Journal*, 37(1).

Jebli, M. B. and Youssef, S. B. (2015). The environmental Kuznets curve, economic growth, renewable and non-renewable energy, and trade in Tunisia. *Renewable and Sustainable Energy Reviews*, 47:173–185.

Jebli, M. B. and Youssef, S. B. (2017). The role of renewable energy and agriculture in reducing CO2 emissions: Evidence for North Africa countries. *Ecological indicators*, 74:295–301.

Jebli, M. B., Youssef, S. B., and Ozturk, I. (2016). Testing environmental Kuznets curve hypothesis: The role of renewable and non-renewable energy consumption and trade in OECD countries. *Ecological Indicators*, 60:824–831.

Jewson, S. and Brix, A. (2005). *Weather derivative valuation: the meteorological, statistical, financial and mathematical foundations*. Cambridge University Press.

Karmellos, M., Kopidou, D., and Diakoulaki, D. (2016). A decomposition analysis of the driving factors of CO2 (Carbon dioxide) emissions from the power sector in the European Union countries. *Energy*, 94:680–692.

Keppler, J. H. and Mansanet-Bataller, M. (2010). Causalities between CO2, electricity, and other energy variables during phase I and phase II of the EU ETS. *Energy Policy*, 38(7):3329–3341.

Khan, M. T. I., Ali, Q., and Ashfaq, M. (2018). The nexus between greenhouse gas emission, electricity production, renewable energy and agriculture in Pakistan. *Renewable Energy*, 118:437–451.

Kim, K. (2019). Elasticity of substitution of renewable energy for nuclear power: Evidence from the Korean electricity industry. *Nuclear Engineering and Technology*, 51(6):1689–1695.

Klemetsen, M. E., Rosendahl, K. E., and Jakobsen, A. L. (2016). The impacts of the EU ETS on Norwegian plants' environmental and economic performance. Technical report, Discussion Papers.

Kuhn, M. (2008). Building Predictive Models in R Using the caret Package. *Journal of Statistical Software, Articles*, 28(5):1–26.

Kuhn, M., Johnson, K., et al. (2013). *Applied predictive modeling*, volume 26. Springer.

Kumar, S., Fujii, H., and Managi, S. (2015). Substitute or complement? Assessing renewable and nonrenewable energy in OECD countries. *Applied Economics*, 47(14):1438–1459.

Laing, T., Sato, M., Grubb, M., Comberti, C., et al. (2013). *Assessing the effectiveness of the EU Emissions Trading System*, volume 126. Grantham Research Institute on Climate Change and the Environment London, UK.

Leamer, E. E. (1985). Vector autoregressions for causal inference? In *Carnegie-rochester conference series on Public Policy*, volume 22, pages 255–304. Elsevier.

Lee, C.-C. and Chiu, Y.-B. (2011). Electricity demand elasticities and temperature: Evidence from panel smooth transition regression with instrumental variable approach. *Energy Economics*, 33(5):896–902.

Lehner, B., Czisch, G., and Vassolo, S. (2005). The impact of global change on the hydropower potential of Europe: a model-based analysis. *Energy Policy*, 33(7):839–855.

Leitão, N. C. (2014). Economic growth, carbon dioxide emissions, renewable energy and globalization. *International Journal of Energy Economics and Policy*, 4(3):391–399.

Liu, X., Zhang, S., and Bae, J. (2017a). The impact of renewable energy and agriculture on carbon dioxide emissions: investigating the environmental Kuznets curve in four selected ASEAN countries. *Journal of cleaner production*, 164:1239–1247.

Liu, X., Zhang, S., and Bae, J. (2017b). The nexus of renewable energy-agriculture-environment in BRICS. *Applied energy*, 204:489–496.

Liu, Z., Ciais, P., Deng, Z., Lei, R., Davis, S. J., Feng, S., Zheng, B., Cui, D., Dou, X., Zhu, B., et al. (2020). Near-real-time monitoring of global CO2 emissions reveals the effects of the COVID-19 pandemic. *Nature communications*, 11(1):1–12.

Loew, A., Jaramillo, P., Zhai, H., Ali, R., Nijssen, B., Cheng, Y., and Klima, K. (2020). Fossil fuel–fired power plant operations under a changing climate. *Climatic Change*, 163(1):619–632.

Long, X., Naminse, E. Y., Du, J., and Zhuang, J. (2015). Nonrenewable energy, renewable energy, carbon dioxide emissions and economic growth in China from 1952 to 2012. *Renewable and Sustainable Energy Reviews*, 52:680–688.

Lutz, B. J., Pigorsch, U., and Rotfuß, W. (2013). Nonlinearity in cap-and-trade systems: The EUA price and its fundamentals. *Energy Economics*, 40:222–232.

Mansanet-Bataller, M., Pardo, A., and Valor, E. (2007). CO2 prices, energy and weather. *The Energy Journal*, 28(3).

Martin, R., Muûls, M., and Wagner, U. J. (2016). The impact of the European Union Emissions Trading Scheme on regulated firms: What is the evidence after ten years? *Review of environmental economics and policy*, 10(1):129–148.

Matuszko, D. (2012). Influence of the extent and genera of cloud cover on solar radiation intensity. *International Journal of climatology*, 32(15):2403–2414.

McDonald, J. H. (2009). *Handbook of biological statistics*, volume 2. sparky house publishing Baltimore, MD.

McFarland, J., Zhou, Y., Clarke, L., Sullivan, P., Colman, J., Jaglom, W. S., Colley, M., Patel, P., Eom, J., Kim, S. H., et al. (2015). Impacts of rising air temperatures and emissions mitigation on electricity demand and supply in the United States: a multi-model comparison. *Climatic Change*, 131(1):111–125.

Meckling, J., Sterner, T., and Wagner, G. (2017). Policy sequencing toward decarbonization. *Nature Energy*, 2(12):918–922.

Melillo, J. M., Richmond, T., Yohe, G., et al. (2014). Climate change impacts in the United States. *Third national climate assessment*, 52.

Menyah, K. and Wolde-Rufael, Y. (2010). CO2 emissions, nuclear energy, renewable energy and economic growth in the US. *Energy policy*, 38(6):2911–2915.

Milly, P. C., Dunne, K. A., and Vecchia, A. V. (2005). Global pattern of trends in streamflow and water availability in a changing climate. *Nature*, 438(7066):347–350.

Ministère de la Transition écologique (2019). l'Assemblée nationale inscrit la neutralité carbone et l' « urgence écologique et la crise climatique » dans la loi. (Accessed on 14 February 2022).

Molnar, C. (2020). *Interpretable machine learning*. Lulu. com.

Molnar, C., Casalicchio, G., and Bischl, B. (2018). iml: An R package for interpretable machine learning. *Journal of Open Source Software*, 3(26):786.

Moral-Carcedo, J. and Vicéns-Otero, J. (2005). Modelling the non-linear response of Spanish electricity demand to temperature variations. *Energy economics*, 27(3):477–494.

Möst, D. and Fichtner, W. (2010). Renewable energy sources in European energy supply and interactions with emission trading. *Energy Policy*, 38(6):2898–2910.

Moutinho, V., Varum, C., and Madaleno, M. (2017). How economic growth affects emissions? An investigation of the environmental Kuznets curve in Portuguese and Spanish economic activity sectors. *Energy Policy*, 106:326–344.

Oberndorfer, U. (2009). EU emission allowances and the stock market: evidence from the electricity industry. *Ecological Economics*, 68(4):1116–1126.

Oda, T. and Maksyutov, S. (2011). A very high-resolution (1 km× 1 km) global fossil fuel CO 2 emission inventory derived using a point source database and satellite observations of nighttime lights. *Atmospheric Chemistry and Physics*, 11(2):543–556.

Oda, T. and Maksyutov, S. (2015). ODIAC fossil fuel CO2 emissions dataset (version name: ODIAC2020). *Center for Global Environmental Research, National Institute for Environmental Studies.*

Oda, T., Maksyutov, S., and Andres, R. J. (2018). The Open-source Data Inventory for Anthropogenic CO 2, version 2016 (ODIAC2016): a global monthly fossil fuel CO 2 gridded emissions data product for tracer transport simulations and surface flux inversions. *Earth System Science Data*, 10(1):87–107.

OECD (2008). *OECD glossary of statistical terms*. Organisation for Economic Co-operation and Development.

Owusu, P. A. and Asumadu-Sarkodie, S. (2016). A review of renewable energy sources, sustainability issues and climate change mitigation. *Cogent Engineering*, 3(1):1167990.

Özbuğday, F. C. and Erbas, B. C. (2015). How effective are energy efficiency and renewable energy in curbing CO2 emissions in the long run? A heterogeneous panel data analysis. *Energy*, 82:734–745.

Paramati, S. R., Sinha, A., and Dogan, E. (2017). The significance of renewable energy use for economic output and environmental protection: evidence from the Next 11 developing economies. *Environmental Science and Pollution Research*, 24(15):13546–13560.

Pardo, A., Meneu, V., and Valor, E. (2002). Temperature and seasonality influences on Spanish electricity load. *Energy Economics*, 24(1):55–70.

Parker, W. S. (2016). Reanalyses and observations: What's the difference? *Bulletin of the American Meteorological Society*, 97(9):1565–1572.

Percebois, J. and Pommeret, S. (2019). Storage cost induced by a large substitution of nuclear by intermittent renewable energies: The French case. *Energy Policy*, 135:111067.

Perera, A., Nik, V. M., Chen, D., Scartezzini, J.-L., and Hong, T. (2020). Quantifying the impacts of climate change and extreme climate events on energy systems. *Nature Energy*, 5(2):150–159.

Petrick, S. and Wagner, U. J. (2014). The impact of carbon trading on industry: Evidence from German manufacturing firms. *Available at SSRN 2389800*.

Pryor, S. C., Scavia, D., Downer, C., Gaden, M., Iverson, L., Nordstrom, R., Patz, J., and Robertson, G. P. (2014). Midwest. Climate change impacts in the United States: The third national climate assessment. *In: Melillo, JM; Richmond, TC; Yohe, GW, eds. National Climate Assessment Report. Washington, DC: US Global Change Research Program: 418-440.*, pages 418–440.

Qi, T., Zhang, X., and Karplus, V. J. (2014). The energy and CO2 emissions impact of renewable energy development in China. *Energy Policy*, 68:60–69.

Qin, P., Xu, H., Liu, M., Xiao, C., Forrest, K. E., Samuelsen, S., and Tarroja, B. (2020). Assessing concurrent effects of climate change on hydropower supply, electricity demand, and greenhouse gas emissions in the Upper Yangtze River Basin of China. *Applied Energy*, 279:115694.

R Core Team (2020). *R: A Language and Environment for Statistical Computing*. R Foundation for Statistical Computing, Vienna, Austria.

Rafaty, R., Dolphin, G., and Pretis, F. (2020). Carbon pricing and the elasticity of CO2 emissions.

Redmond, L. and Convery, F. (2008). Determining the Price of Carbon in the EU ETS.

Rickels, W., Görlich, D., and Peterson, S. (2015). Explaining european emission allowance price dynamics: Evidence from phase ii. *German Economic Review*, 16(2):181–202.

Rodrigues, J. F., Wang, J., Behrens, P., and de Boer, P. (2020). Drivers of CO2 emissions from electricity generation in the European Union 2000–2015. *Renewable and Sustainable Energy Reviews*, 133:110104.

Rogelj, J., Shindell, D., Jiang, K., Fifita, S., Forster, P., Ginzburg, V., Handa, C., Kheshgi, H., Kobayashi, S., Kriegler, E., et al. (2018). Mitigation pathways compatible with 1.5 C in the context of sustainable development. In *Global warming of 1.5 C*, pages 93–174. Intergovernmental Panel on Climate Change.

RTE-Réseau de Transport d'Électricité (2021). Production – Hydraulique : RTE Bilan électrique 2021. `https://bilan-electrique-2021.rte-france.com/production_hydraulique/`. (Accessed on 07/26/2022).

Réseau de Transport d'Électricité (RTE) (2020). Bilan des émissions de CO2. Accessed on 13 February 2022.

Sadorsky, P. (2009). Renewable energy consumption, CO2 emissions and oil prices in the G7 countries. *Energy Economics*, 31(3):456–462.

Sadorsky, P. (2020). Energy related CO2 emissions before and after the financial crisis. *Sustainability*, 12(9):3867.

Saidi, K. and Mbarek, M. B. (2016). Nuclear energy, renewable energy, CO2 emissions, and economic growth for nine developed countries: Evidence from panel Granger causality tests. *Progress in Nuclear Energy*, 88:364–374.

Saint-Drenan, Y.-M., Wald, L., Ranchin, T., Dubus, L., and Troccoli, A. (2018). An approach for the estimation of the aggregated photovoltaic power generated in several European countries from meteorological data. *Advances in Science and Research*, 15:51–62.

Salazar-Núñez, H. F., Venegas-Martínez, F., and Lozano-Díez, J. A. (2021). Assessing the interdependence among renewable and non-renewable energies, economic growth, and CO2 emissions in Mexico. *Environment, Development and Sustainability*, pages 1–17.

Sax, C. and Steiner, P. (2013). Temporal disaggregation of time series.

Scarlat, N., Prussi, M., and Padella, M. (2022). Quantification of the carbon intensity of electricity produced and used in Europe. *Applied Energy*, 305:117901.

Schaeffer, R., Szklo, A. S., de Lucena, A. F. P., Borba, B. S. M. C., Nogueira, L. P. P., Fleming, F. P., Troccoli, A., Harrison, M., and Boulahya, M. S. (2012). Energy sector vulnerability to climate change: A review. *Energy*, 38(1):1–12.

Sebri, M. and Ben-Salha, O. (2014). On the causal dynamics between economic growth, renewable energy consumption, CO2 emissions and trade openness: Fresh evidence from BRICS countries. *Renewable and Sustainable Energy Reviews*, 39:14–23.

Seifert, J., Uhrig-Homburg, M., and Wagner, M. (2008). Dynamic behavior of CO2 spot prices. *Journal of Environmental Economics and Management*, 56(2):180–194.

Seyedhashemi, H., Hingray, B., Lavaysse, C., and Chamarande, T. (2021). The Impact of Low-Resource Periods on the Reliability of Wind Power Systems for Rural Electrification in Africa. *Energies*, 14(11):2978.

Seyedhashemi, H., Vidal, J.-P., Diamond, J. S., Thiéry, D., Monteil, C., Hendrickx, F., Maire, A., and Moatar, F. (2022). Regional, multi-decadal analysis on the Loire River basin reveals that stream temperature increases faster than air temperature. *Hydrology and Earth System Sciences*, 26(9):2583–2603.

Shafiei, S. and Salim, R. A. (2014). Non-renewable and renewable energy consumption and CO2 emissions in OECD countries: a comparative analysis. *Energy Policy*, 66:547–556.

Shahbaz, M., Van Hoang, T. H., Mahalik, M. K., and Roubaud, D. (2017). Energy consumption, financial development and economic growth in India: New evidence from a nonlinear and asymmetric analysis. *Energy Economics*, 63:199–212.

Sharif, A., Mishra, S., Sinha, A., Jiao, Z., Shahbaz, M., and Afshan, S. (2020). The renewable energy consumption-environmental degradation nexus in Top-10 polluted countries: Fresh insights from quantile-on-quantile regression approach. *Renewable Energy*, 150:670–690.

Sheridan, S. C., Lee, C. C., and Smith, E. T. (2020). A comparison between station observations and reanalysis data in the identification of extreme temperature events. *Geophysical Research Letters*, 47(15):e2020GL088120.

Shirizadeh, B., Perrier, Q., and Quirion, P. (2022). How sensitive are optimal fully renewable power systems to technology cost uncertainty? *The Energy Journal*, 43(1).

Shirizadeh, B. and Quirion, P. (2021). Low-carbon options for the French power sector: What role for renewables, nuclear energy and carbon capture and storage? *Energy Economics*, 95:105004.

Sinha, A., Shahbaz, M., and Sengupta, T. (2018). Renewable energy policies and contradictions in causality: a case of Next 11 countries. *Journal of cleaner production*, 197:73–84.

Solaun, K. and Cerdá, E. (2019). Climate change impacts on renewable energy generation. A review of quantitative projections. *Renewable and sustainable energy Reviews*, 116:109415.

Tarroja, B., AghaKouchak, A., and Samuelsen, S. (2016). Quantifying climate change impacts on hydropower generation and implications on electric grid greenhouse gas emissions and operation. *Energy*, 111:295–305.

Thakur, A. (2020). *Approaching (almost) any machine learning problem*. Abhishek Thakur.

Thatcher, M. J. (2007). Modelling changes to electricity demand load duration curves as a consequence of predicted climate change for Australia. *Energy*, 32(9):1647–1659.

Valor, E., Meneu, V., and Caselles, V. (2001). Daily air temperature and electricity load in Spain. *Journal of applied Meteorology*, 40(8):1413–1421.

Van Vliet, M. T., Yearsley, J. R., Ludwig, F., Vögele, S., Lettenmaier, D. P., and Kabat, P. (2012). Vulnerability of US and European electricity supply to climate change. *Nature Climate Change*, 2(9):676–681.

Wagner, U. J., Muûls, M., Martin, R., and Colmer, J. (2014). The causal effects of the European Union Emissions Trading Scheme: evidence from French manufacturing plants. In *Fifth World Congress of Environmental and Resources Economists, Instanbul, Turkey*. Citeseer.

Waheed, R., Chang, D., Sarwar, S., and Chen, W. (2018). Forest, agriculture, renewable energy, and CO2 emission. *Journal of Cleaner Production*, 172:4231–4238.

Waisman, H., De Coninck, H., and Rogelj, J. (2019). Key technological enablers for ambitious climate goals: insights from the IPCC special report on global warming of 1.5 C. *Environmental Research Letters*, 14(11):111001.

Wasson, J., Chandesris, A., Bautista, A. G., Pella, H., and Villeneuve, B. (2007). *REBECCA, Relationships between ecological and chemical status of surface waters. European Hydro-Ecoregions*. PhD thesis, irstea.

Wasson, J.-G., Chandesris, A., Pella, H., and Blanc, L. (2002). Typology and reference conditions for surface water bodies in. *Typology and ecological classification of lakes and rivers*, 566:37.

Wei, L., Jiheng, L., Junhong, G., Zhe, B., Lingbo, F., and Baodeng, H. (2020). The effect of precipitation on hydropower generation capacity: a perspective of climate change. *Frontiers in Earth Science*, 8:268.

Wilbanks, T., Bhatt, V., Bilello, D., Bull, S., Ekmann, J., Horak, W., Huang, Y. J., Levine, M. D., Sale, M. J., Schmalzer, D., et al. (2008). Effects of climate change on energy production and use in the United States. *US Department of Energy Publications*, page 12.

Wilcoxon, F. (1992). Individual comparisons by ranking methods. In *Breakthroughs in statistics*, pages 196–202. Springer.

Wiser, R. H., Bolinger, M., Hoen, B., Millstein, D., Rand, J., Barbose, G. L., Darghouth, N. R., Gorman, W., Jeong, S., Mills, A. D., et al. (2020). Wind energy technology data update: 2020 edition.

World Bank (2022). What is Carbon Pricing? | Carbon Pricing Dashboard. (Accessed on 06/03/2022).

World Nuclear Association (2022). Nuclear Power in France. Accessed on 13 February 2022.

Yalew, S. G., van Vliet, M. T., Gernaat, D. E., Ludwig, F., Miara, A., Park, C., Byers, E., De Cian, E., Piontek, F., Iyer, G., et al. (2020). Impacts of climate change on energy systems in global and regional scenarios. *Nature Energy*, 5(10):794–802.

Yao, J. (2021). *Electricity Consumption and Temperature: Evidence from Satellite Data*. International Monetary Fund.

Zeb, R., Salar, L., Awan, U., Zaman, K., and Shahbaz, M. (2014). Causal links between renewable energy, environmental degradation and economic growth in selected SAARC countries: progress towards green economy. *Renewable energy*, 71:123–132.

University of Lille
SESAM Doctoral School
LEM – Lille Économie Management – UMR 9221
IÉSEG School of Management

# Essays on Climate and Carbon Emissions: The EU Emissions Trading System and Renewable Energies

Dissertation Submitted in Partial Fulfillment of the Requirements
for the Degree of Doctor of Philosophy (Ph.D.) in Economics

**Mohammadehsan Eslahi**

Doctoral Advisor:

Dr. Paolo Mazza, HDR

December 12, 2022

**Thesis Examination Committee Members**

- **Doctoral Advisor:**

Dr. Paolo Mazza, HDR – Associate Professor, IÉSEG School of Management

- **Referees:**

Dr. Anna Creti, HDR – Full Professor, Paris Dauphine University-PSL

Dr. Maria-Eugenia Sanin, HDR – Associate Professor, University of Évry–Paris-Saclay University

- **Examiners:**

Dr. Jean-Philippe Boussemart*, HDR – Full Professor, University of Lille (*Committee Chair)

Dr. Julien Chevallier, HDR – Full Professor, Paris 8 University

Dr. Corrado Di Maria – Professor, University of East Anglia